10-24-2018

CALCULATION GUIDED RATIONAL DESIGN AND SYNTHESIS OF NOVEL CATIONIC FLUORESCENT meso–PYRIDINIUM BODIPYS FOR BIO-IMAGING

Daniel J. LaMaster
Louisiana State University and Agricultural and Mechanical College

CALCULATION GUIDED RATIONAL DESIGN AND SYNTHESIS OF NOVEL CATIONIC FLUORESCENT *meso*–PYRIDINIUM BODIPYS FOR BIO-IMAGING

A Dissertation

Submitted to the Graduate Faculty of the
Louisiana State University
Agricultural and Mechanical College
in partial fulfillment of the
requirements for the degree of
Doctor of Philosophy

in

The Department of Chemistry

by
Daniel J. LaMaster
B.S., McKendree University, 2013
December 2018

In loving memory of Jean Clausius.
February 17, 1953 – March 17, 2012

Acknowledgements

To start off, I would like to thank Dr. Graça Vicente for her overwhelming support throughout my graduate studies. The research freedom and mentoring she provides her students allows us to develop our scientific creativity and our own individual projects which is a rare opportunity that I know everyone in the group, past and present, appreciates.

Next up, I'd like to thank Dr. Ken Lopata for his mentoring and willingness to explain things in various ways until you understand. I greatly appreciate his patience for my copious use of his office hours. I would not have been successful in his course or in several research projects without his support.

I would also like to thank Dr. Kevin Smith along with my past and present group members–Dr. Haijun Wang, Dr. Jaime Hayes, Dr. Ning Zhao, Dr. Sunting Xuan, Dr. Qianli Meng, Dr. Elizabeth Okoth, Dr. Tyrslai Williams, Dr. Holden Smith, Dr. Adam Bruner, Adonnay Sissay, Alex Meyer, Maodie Wang, Guanyu Zhang, and Nichole Kaufman–for always indulging my curiosity about both their chemistry and mine.

I am grateful to several faculty and staff within the department for all of the valuable discussions, both professional and personal, over the years and their assistance with anything relevant to the discussions at hand. I know I would not have made it through my first semester if not for Dr. Kartika and Dr. Ragains. Dr. Crowe's willingness to spend hours on end talking and sharing his insight into both chemistry and life helped me develop my perspective on life and new directions in my research. Mrs. Connie David's training on ESI-MS will be an invaluable skill and her assistance with interpreting the slew of confounding data over the years is much appreciated.

Lastly, I'd like to thank Ms. Kim Mollere and Dr. Gretchen Schneider for being such an awesome support system over the years, especially when I didn't even know I needed one.

Table of Contents

List of Abbreviations

^{1}H	Proton NMR
^{13}C	Carbon NMR
^{11}B	Boron NMR
δ	Chemical shift
ε	Extinction coefficient
λ_{max}	Wavelength of maximum absorbance
λ_{em}	Wavelength of maximum fluorescence emission
ϕ_F	Fluorescence quantum yield
ACN	Acetonitrile
BODIPY	Boron dipyrromethene
$CDCl_3$	Deuterated chloroform
CT	Charge transfer
d	Doublet
dd	Doublet of doublets
ddd	Doublet of doublets of doublets
dt	Doublet of triplets
d-PeT	donor-Photoinduced electron transfer
DCM	Dichloromethane
DDQ	2,3-Dichloro-5,6-dicyano-p-benzoquinone
DFT	Density Functional Theory
DIPEA	Diisopropylethylamine
DMSO-d6	Deuterated dimethylsulfoxide

EtOAc	Ethyl acetate
EDG	Electron donating group
ES	Excited state
ESI-MS TOF	Electro-spray ionization mass spectroscopy time of flight
EWG	Electron withdrawing group
HOMO	Highest occupied molecular orbital
HRMS	High resolution mass spectroscopy
Hz	Hertz
IC_{50}	Half maximal inhibitory concentration
ICT	Intramolecular charge transfer
ISC	Intersystem crossing
LUMO	Lowest unoccupied molecular orbital
m	Multiplet
MeOD	Deuterated methanol
mg	Milligram
mL	Milliliter
MO(s)	Molecular orbital(s)
MS	Mass Spectra
m/z	Mass to charge ratio
NIR	Near Infrared
nm	Nanometer
NMR	Nuclear magnetic resonance
NCS	N-Chlorosuccinimide

NBS	N-Bromosuccinimide
PES	Potential energy surface
ppm	Parts per million
s	Singlet
t	Triplet
td	Triplet of doublets
TCCA	Trichloroisocyanuric acid
TDDFT	Time-Dependent Density Functional Theory
TEA	Triethylamine
TFA	Trifluoroacetic acid
THF	Tetrahydrofuran
VEE	Vertical excitation energy
VIP	Vertical Ionization Potential

List of Tables

List of Figures

List of Schemes

Abstract

Chapter 1 contains a brief overview of the history, synthesis, and properties of BODIPY dyes as well as that of the biomedical applications of bio-imaging and photodynamic therapy. Additionally, an overview of the theoretical framework of density functional theory and its time-dependent variant are provided. In Chapter 2, the effects of structural modification on the electronic structure and electron dynamics of cationic meso-(4-pyridyl)-BODIPYs were investigated. A library of 2,6-difunctionalized *meso*-(4-pyridyl)-BODIPYs bearing various electron-withdrawing substituents was designed and DFT calculations were used to model the redox properties, while TDDFT was used to determine the effects of functionalization on the excited states. Structural modification was able to restructure the low lying molecular orbitals to effectively inhibit d-PeT. A new *meso*-(4-pyridyl) BODIPY bearing 2,6-dichloro groups was synthesized and shown to exhibit enhanced charge recombination fluorescence. The fluorescence enhancement was determined to be the result of functionalization modulating the kinetics of the excited state dynamics. The syntheses employed in the preparation of several additional derivatives from the previously designed meso-(4-pyridyl)-BODIPY library are reported in Chapter 3. The dyes were then characterized photophysically and biologically. The photophysical properties were found to follow the expected trend. The ionic derivatives all displayed decreased cellular uptake and the only derivatives exhibiting high phototoxicity were the neutral dyes containing heavy atoms. Chapter 4 presents a comparative study of the differences in the photophysical and biological properties of the series of meso-pyridinium BODIPY isomers through an experimental and computational investigation. The three structural isomers were synthesized and

photophysically characterized revealing differences in both absorption and emission wavelengths as well as fluorescence quantum yields. TDDFT calculations were used to model the dyes' electronic structure and excited states to evaluate the impact of pyridine orientation on the optical properties. The dyes' biological activity was evaluated in human epithelial type-2 (HEp-2) cancer cells. Decreasing cellular uptake from 4-Py > 2-Py > 3-Py was observed for both neutral and ionic derivatives. All three derivatives, both neutral and ionic, displayed equivalent phototoxicity (IC_{95} = 100 μM) with the exception of 4-Py^{+} (IC_{90} = 100 μM).

Chapter 1. Introduction

1.1. BODIPY Dyes

1.1.1. Fundamental Properties of BODIPYs

While the aza-BODIPY was first synthesized in 1943 as a pigment by Rogers and coworkers[1,2], the BODIPY was not synthesized until the late 1960's by Treibs and Kruezer.[3] However, it received relatively little attention until the mid-1980's[4-6] when Monsma and co-workers[7] recognized the boron dipyrromethenes' (4,4-difluoro- 4-bora-3a,4a-diaza-s-indacene, henceforth referenced as BODIPY) potential as a biological label. Since then, BODIPYs have found application as bio-labels,[5,6,8-29,] laser dyes,[5,6,8,30-38] light harvesting chromophores,[6,8,33,39-51] fluorescent probes,[5,6,8,12,13,33,52-60] and photosensitizers for photodynamic therapy.[61-65]

Although the BODIPY is commonly referred to as "porphyrin's little sister", it actually falls into a different class of dyes. Porphyrins, azaporphyrins, phthalocyanines, and their derivatives (i.e. chlorins, bacteriochlorins, isobacteriochlorins, isoporphyrins, etc…) are aromatic macrocycles similar to systems like coronene. BODIPYs, on the other hand, can be viewed as having a rigidified monomethine structure and as such have been classified as cyanine dyes, Figure 1.1. The cyanine family is a class of polymethine dyes characterized by having two nitrogen atoms conjugated via an odd number of methylene groups. However, unlike the traditional cyanine platform in which

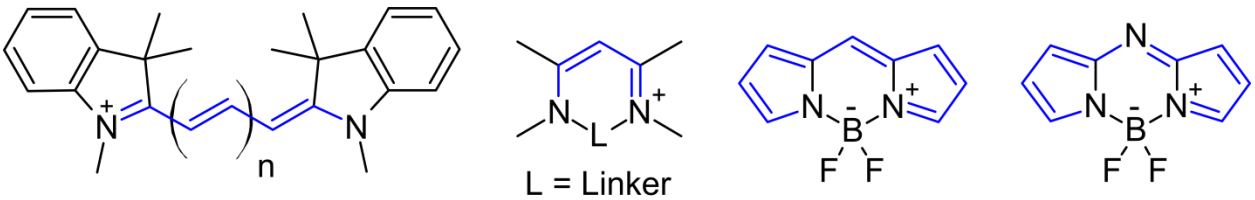

Cy3, n = 1 Rigidified Cyanine BODIPY aza-BODIPY

Figure 1.1. Structures of nitrogen-containing dyes.

the nitrogens have three and four covalent bonds respectively, the nitrogens in the BODIPY platform each only have three covalent bonds and one forms an additional dative bond with the boron linker resulting in an overall neutral species.

The common numbering system used in BODIPY nomenclature follows the system used for the structural analog s-indacene, instead of that used for dipyrromethenes (Figure 1.2), hence the BODIPY core is also referred to as bora-diazaindacene. However, the 8- position is commonly referred to as the meso- position which is consistent with the porphyrin system.

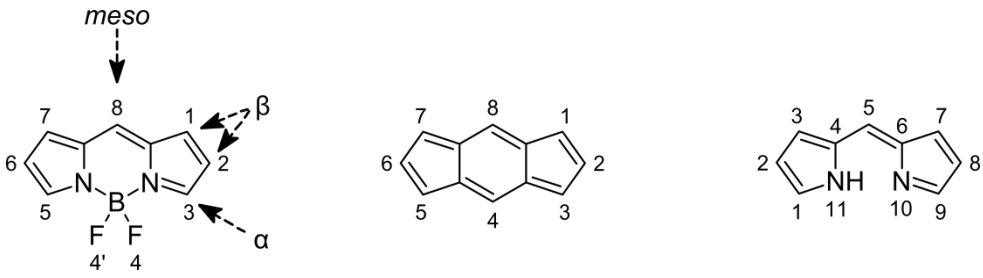

Figure 1.2. BODIPY numbering system based on s-indacene.

Looking at the BODIPY in terms of its physical structure, it can be broken down into two parts: a bidentate dipyrromethene ligand complexed with an electron deficient Lewis acid (boron). In preparation, the dipyrromethene is typically complexed with a BF_2 unit supplied by boron trifluoride diethyl etherate. This complexation results in a fused tricyclic structure where the pyrrolic nitrogens, α-carbons, the BF_2 unit, and the methine bridge form a central six-membered ring flanked by the two pyrroles. The BF_2 constrains the freely rotatable dipyrromethene preventing *cis/trans* isomerization, rigidifying the core, and resulting in high fluorescence quantum yields. Dipyrromethene salts have intense absorption peaks in the visible spectrum causing nanomolar concentrations to produce a black solution, yet the fluorescence intensity is quite low.[66]

The structural constraint from the boron complexation results in a dramatic increase in fluorescence intensity. The X-ray crystallographic analysis of single crystal BODIPYs shows the π-electron delocalization across the nine carbon, two nitrogen backbone. The boron center possesses a nearly tetrahedral geometry with two perpendicular planes of symmetry, one through the F_1–B–F_2 plane and one through the N_1–B–N_2 plane. The N_1–C_1 and N_1–C_4 bond lengths are characteristic of double and single bonds, respectively, indicating the strong delocalization along the backbone and the lack of pyrrolic aromaticity. This delocalization, depicted in Figure , along with the nitrogens' electronegativity, gives rise to the BODIPY's experimentally observed regioselective carbon reactivity.

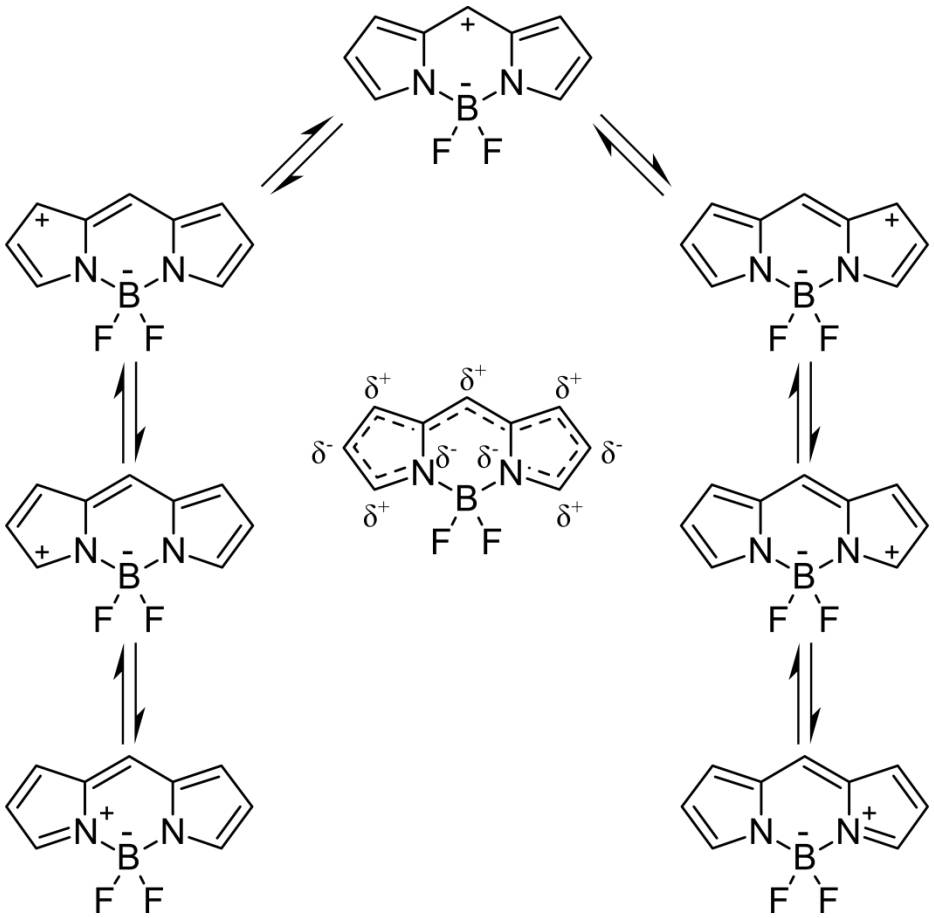

Figure 1.3. BODIPY resonance structures and partial charges.

The BODIPY core undergoes electrophilic aromatic substitution at 2/6-, 3/5-, and 1/7- positions as well as nucleophilic addition/elimination reactions at the 8- and 3/5-positions, in order of decreasing reactivity.[67] The selective and regiospecific reactivity on a single platform gives the BODIPY unsurpassed potential for diverse derivatization and preparation of complex dyes for various applications. Despite the resonance structures' capacity to explain the observed carbon reactivity, quantum calculations of the atomic charges have shown the boron center to have the greatest positive charge.

Similar to their tetrapyrrolic older sister, BODIPYs also exhibit sharp absorption and emission bands in the visible spectrum, small Stoke's shifts, high molar absorption coefficients (typically 40,000 $M^{-1}cm^{-1} < \varepsilon <$ 110,000 $M^{-1}cm^{-1}$), and high fluorescence quantum yields (usually $0.50 < \phi_F < 0.90$).[4,5,13,14,62,64,68,] Additional desirable properties include high thermal and photostability, negligible triplet state formation, high solubility in common solvents (due to a lack of aggregation), and minimal sensitivity to the polarity and pH of their environment making them reasonably stable to physiological conditions, and reduced toxicity.[4,9,13,16,52,55,69,70,]

The BODIPY has a strong $S_0 \rightarrow S_1$ transition resulting in the experimentally observed sharp absorption peak.[70,71] The shoulder generally seen on the main absorption peak has been attributed to the $0 \rightarrow 1$ vibrational mode transition. This shoulder is also seen in the emission spectra.

With the large dependence of the BODIPYs' optical properties on the structure, there is an ever increasing need for effective rational design of new dyes. Electronic structure elucidation through quantum calculations is a powerful tool for both explaining predicting properties and experimental phenomena. The insight provided by

calculations modelling known systems can be applied in the development of new fluorescent scaffolds with desirable properties far surpassing what is already known.

1.1.2. Electronic Properties

One of the most important properties of BODIPYs that has garnered them so much attention is the ease in which their optical properties can be altered with simple functionalization (Figure 1.4). Essential to effectively utilize this property is an understanding of the relationship between the BODIPYs physical and electronic structures. Figure 1.5 shows the molecular orbitals that were calculated for the 8-pyridyl-1,3,5,7-tetramethylBODIPY platform. The optical properties of the common BODIPY core are typically confined to the 470-530 nm region.[5,17,26,52]

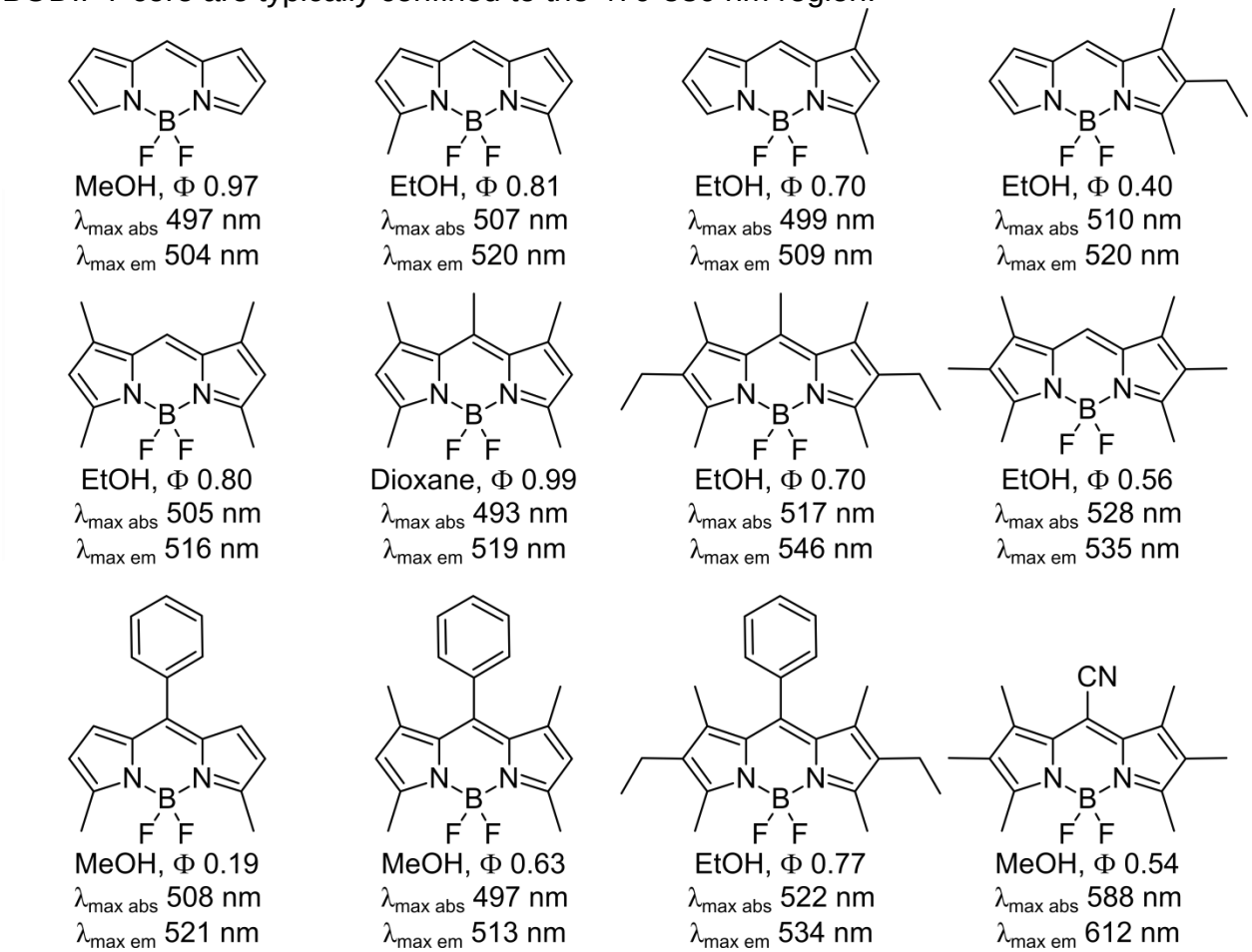

Figure 1.4. The substituent effects on the optical properties of simple BODIPYs.[68,72]

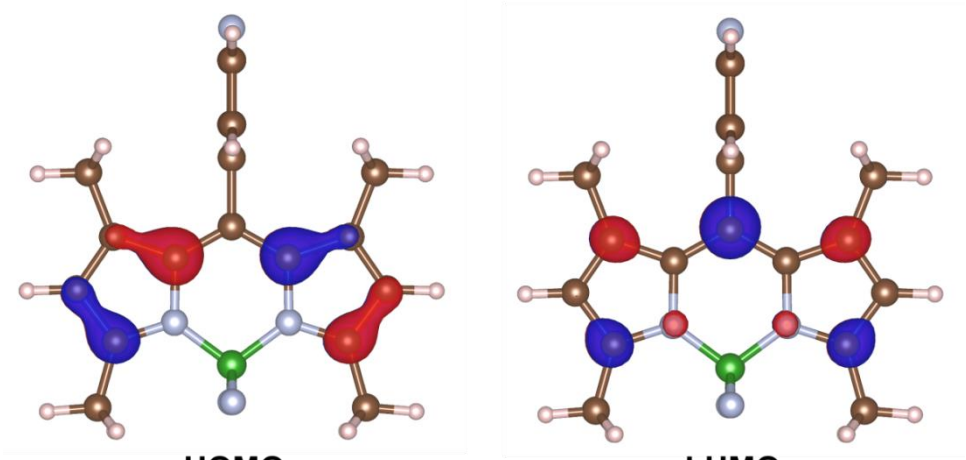

Figure 1.5. Calculated molecular orbitals of 8-pyridyl-1,3,5,7-tetramethylBODIPY core.

The molecular orbital (MO) plots show that the highest occupied molecular orbital (HOMO) is functionally localized on the 2-, 3-, 5-, and 6- positions while the lowest unoccupied molecular orbital (LUMO) is mainly located on the 8- position and to a smaller extent the 1-, 3-, 5-, and 7- positions. Looking at both reveals that meso-functionalization will have the greatest effect on the LUMO and 1,7-functionalization will have a similar effect, just to a lesser extent, while it is more difficult to qualitatively determine the extent of the effect functionalization at the 3,5- will have compared to 2,6- due to the overlap of the HOMO and LUMO at the 3,5- positions.

Several strategies exist for tuning the BODIPYs optical properties, but most involve decreasing the HOMO-LUMO gap.[73], The push-pull strategy involves raising the energy of the HOMO by installing electron-donating groups on the positions where it is localized and lowering the energy of the LUMO by using electron-withdrawing groups on the 1-, 7-, and 8- positions. Individually, both of these alterations will decrease the HOMO-LUMO gap, however, in combination, the effect is amplified.

Another method involves extending the conjugation to achieve the same overall result. This can be accomplished a few different ways, the first of which is aromatic ring

fusion. With ring fused systems, extending the conjugation through the β-positions has a stronger effect than that produced by fusion through the 2,3-/5,6- positions. The expansion of the π-system can also be done by incorporating styryl, ethynyl, ethynyl aryl, and (to a lesser extent) aryl groups at the 1-, 3-, 5-, and 7- positions. Introduction of styryl groups at the 3,5- positions has a stronger effect than at the 2,6-.[5,74] Extending the π-conjugation through the meso- position can have a significant effect on the absorption, however, sterics play a large part in limiting the impact on the electronics.

While small groups such as 3/5-styryl and global ethynyl moieties can lie planar to the BODIPY core, *meso*-aromatic groups typically maintain a 45° dihedral angle to the BODIPY core when the 1- and 7- positions are unsubstituted. If the dye has 1,7-functionalities, the *meso*-aromatic ring will stand perpendicular to the BODIPY core, minimizing the orbital overlap between the two and consequently impacting the BODIPY's electronics. It is important to note, though, that 1,7-functionalization does rigidify the structure, effectively eliminating the meso- group's free rotation which increases the fluorescence quantum yield.

The last method is a well-established tactic with porphyrins, cyanines, and other dyes. Replacing a methine bridge (i.e. the meso- carbon) with a nitrogen atom can produce, on average, an 80 nm red-shift in the absorption spectra. While these nitrogen-bridged BODIPYs, dubbed aza-BODIPYs, are highly desirable targets, their synthetic difficulty and limited functionalizability of currently reported platforms restricts the feasibility for their practical application, although there are a few in clinical trials.

Orbital overlap and hybridization are other important factors to consider when designing dyes and explaining observed trends. In systems where the orbital overlap

between two groups is poor, there can be poor transmission of electronic effects through sigma induction/donation.

1.1.3. Synthesis of the BODIPY Core

BODIPYs with meso-substituents are the most frequently reported BODIPY platform in the literature due to their greater stability than their meso-free counterparts. The meso-free derivatives are susceptible to degradation by molecular oxygen, which is depicted in Figure 1.6. When larger moieties are present on the meso-position, access to the 8- carbon is sterically hindered and the oxidation process is significantly retarded.

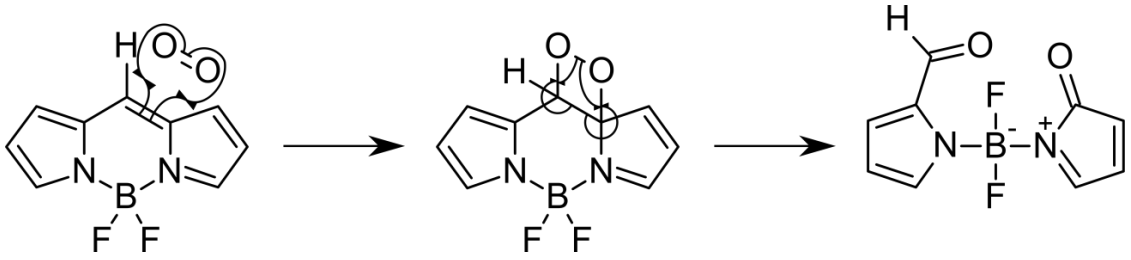

Figure 1.6. Mechanism of oxidative degradation of meso-free BODIPY.

The synthesis of the dyes generally starts with preparation of the dipyrromethene which can be accomplished several different ways (Scheme). Most commonly reported syntheses of symmetric, meso-substituted BODIPYs employ a standard three step, one-pot procedure which begins with the condensation of two equivalents of an α-free pyrrole with an aldehyde (usually aromatic) using an acid catalyst. Subsequent oxidation, with a mild oxidant such as 2,3-dichloro-4,5-dicyanobenzoquinone (DDQ) or p-chloranil, produces the fully conjugated dipyrromethene. The dipyrromethene ligand can then be complexed with a boron center to form the BODIPY by reacting with $BF_3{\cdot}OEt_2$ in the presence of a tertiary amine. The rather mild reaction conditions involved well tolerate a large variety of functional groups and allow for the preparation of a diverse library of BODIPY platforms.

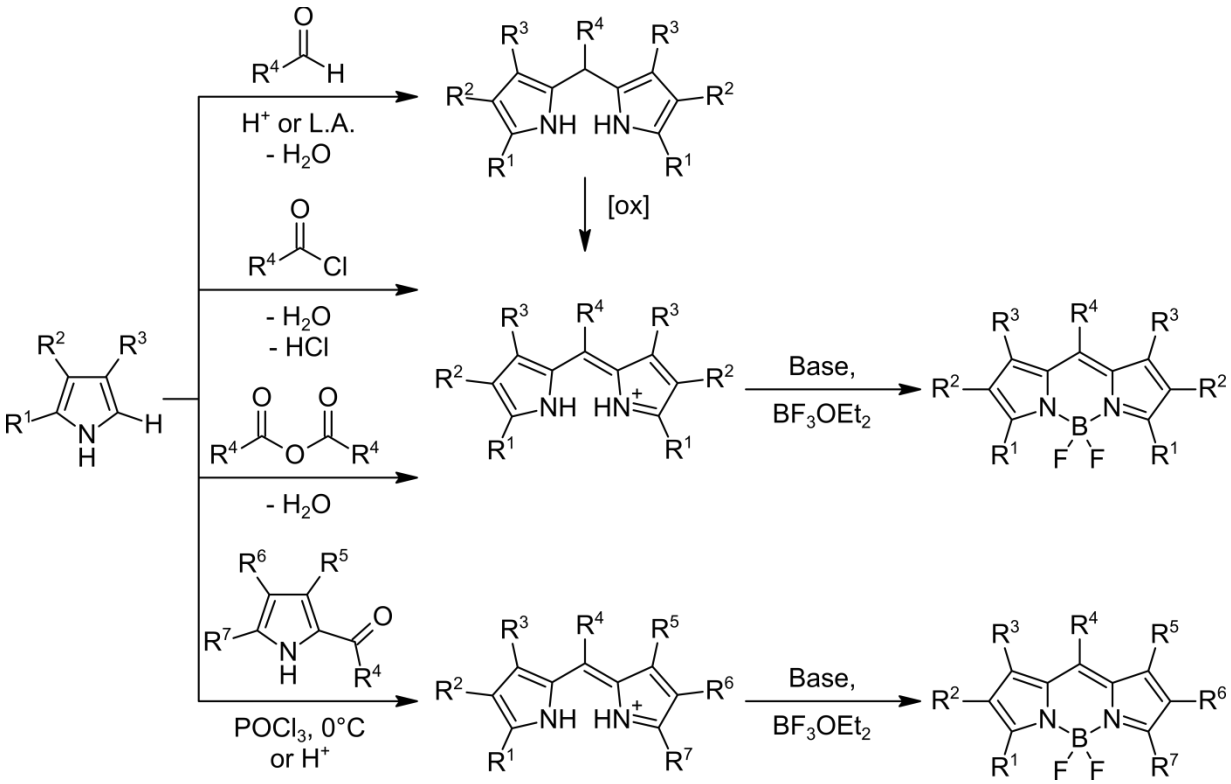

Scheme 1.1. General strategies for synthesis of BODIPYs via condensation reactions of an α-free pyrrole with activated carbonyl compounds.

When utilizing the previously described standard procedure, there are several points that should be noted. With pyrroles, the α-positions are the most reactive as the nitrogen's lone pair resonates over pushing one π-bond back and the second π-bond out at an α-position to act as a nucleophilic lone pair. To minimize the formation of poly-pyrroles and maximize the yield of the desired product, the pyrroles should only have one α-free position. Following aldehyde condensations, an additional oxidation step is required to transform the dipyrromethane to the required dipyrromethene. The oxidations typically employ mild oxidizing agents because the pyrrole rings are electron rich and the dipyrromethanes can yield multiple oxidation products. Furthermore, stronger oxidants lead to greater amounts of meso-unsubstituted BODIPY in the final reaction mixture and even the commonly used oxidizing agents still create byproducts which require tedious chromatography to remove.

Another commonly used method involves pyrrole condensation with an acid chloride or an anhydride. These condensations directly afford the dipyrromethene and do not require subsequent oxidation which often leads to increased yields and easier purification. Reactions with anhydrides, and analogously with esters and amides, can prove difficult so often times the pyrrole is "activated" first with the Grignard of a volatile hydrocarbon prior to reaction with the carbonyl compound or the carbonyl compound is activated with catalytic amounts of a Lewis or Brønsted acid.

When preparing unsymmetric BODIPYs, two different pyrroles are need and one must be functionalized with the meso-carbon-to-be, otherwise a mixture of three unique dipyrromethanes will be formed. One of the pyrroles must be α-free or pseudo-α-free (i.e. pyrroles with an unprotected carboxylic acid on the 2-position). The second pyrrole will have either a carbonyl or a methylene leaving group such as a protonated alcohol, quaternary amine, or acetate. In general, the preparation of symmetrical BODIPYs is simpler than that for asymmetric dyes, though both have their own pros and cons.

1.1.4. Boron Functionalization

Functionalization at the boron center can allow further modification with minimal effects on the maximum absorption and emission wavelengths.[68,75] Introduction of additional chromophores to the boron center can be used to create energy transfer cassettes and tune the fluorescence quantum yields (Figure 1.7), while other functionalities can alter the solubility and stability. Aryl and ethynylaryl groups have been shown to be efficient at transferring their excitation energy to the BODIPY core with the resulting fluorophore possessing efficient emission from the BODIPY core, so long as the functional group has a high molar extinction coefficient.

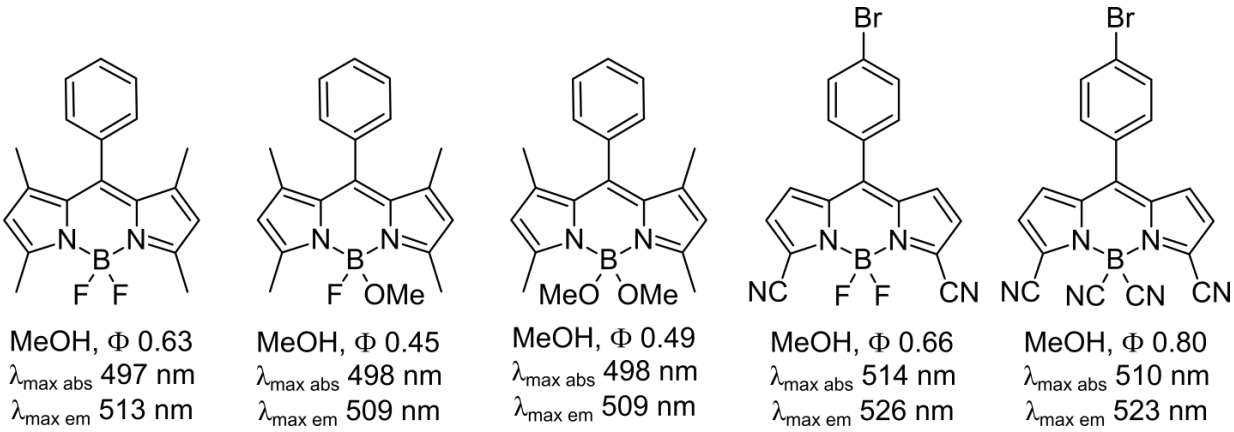

Figure 1.7. Effects of boron-functionalization on photophysical properties.

General methods for boron functionalization include the use of strong nucleophiles, such as Grignards and alkoxides, and using Lewis acids, such as aluminum(III) chloride and boron trichloride, to activate the boron center for nucleophilic attack by weak nucleophiles to produce various C- and O-BODIPYs.

1.1.5. Water Solubility

Despite great strides in the research surrounding BODIPY synthesis and application over the past 30 years, relatively little work on the development of small water soluble BODIPYs and other NIR absorbing/emitting fluorophores has been fruitful.[76-86] A BODIPY that absorbs at 848 nm has been prepared[5] by extending the conjugation and fusing two BODIPYs together, but the increased size of the π system prevents water-solubility and ignores part of the BODIPYs structural potential.[19,13] One large, ironically, advantage the BODIPY has over porphyrins and phthalocyanines is their smaller size. Porphyrins and phthalocyanines have large conjugated π systems which leads to greater hydrophobicity and aggregation.[87] The smaller size of the BODIPYs generally minimizes aggregation and increases solubility. Within the last 10 years, a variety of water-soluble derivatives have been reported bearing water-solubilizing groups including: polyethylene glycols,[12,56,88-93] amines,[94] hydroxyls,[94,95]

sulfonamides,[95] carboxylates,[12,56,88,95-97] sulfonates,[12,97-104] phosphonates,[12,88,105] quaternary ammonium salts,[12,68,98,102,106-108] carbohydrates,[109,110,111] peptides,[28,29] and boron functionalization.[94,111,112] Courtis and co-workers reported[94] greatly improved water solubility of small BODIPY fluorophores after transformation of F-BODIPYs to monoalkoxy O-BODIPYs (Figure 1.8). The greatest solubility enhancement was achieved by functionalizing the boron center with ethanolamine and the second best used ethylene glycol. However, these substitutions producing O- and C- BODIPYs diminish the boron center's electron deficiency resulting in a decreased stability limiting the usefulness of this method of solubilization.

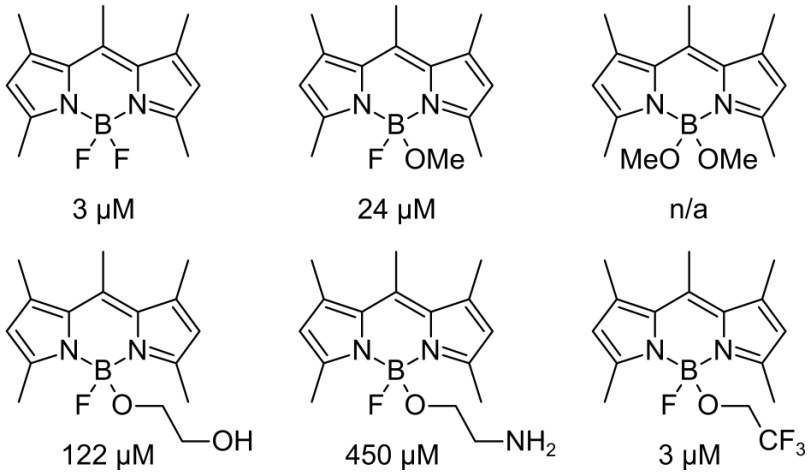

Figure 1.8. Water soluble alkoxy BODIPYs and their water solubilities.[94]

1.1.6. Stability

Recently, de la Moya et al[113] reported a series of stable N-BODIPYs, Figure 1.9, that retain their fluorescence quantum yields. Previous attempts to functionalize the boron center with nitrogen failed due to the nitrogen lone pairs quenching the boron's Lewis acidity and causing it to fall out. This work reported successful functionalization using electron-deficient (tosylated) amines.

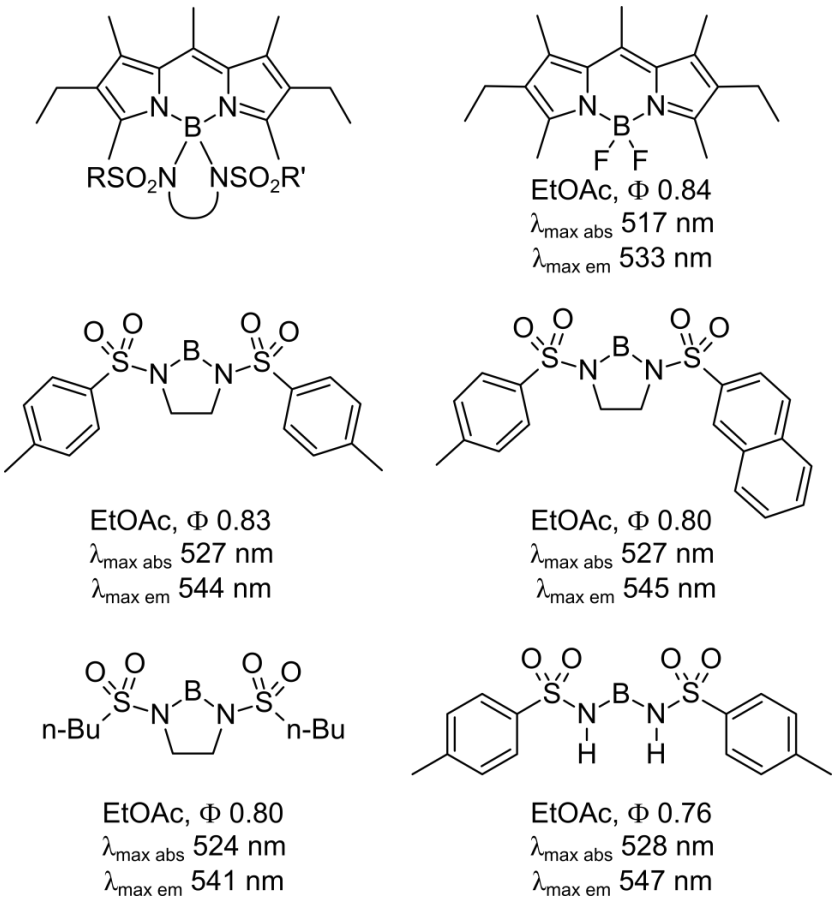

Figure 1.9. Structures and photophysical properties of recently reported N-BODIPYs[113]

Depending on the electronics of the functional group, the stability of the BODIPY to environmental factors can be greatly altered. Looking at the dipyrromethene as a Lewis base and the boron center as a Lewis acid, an electron rich dipyrromethene and electron deficient boron would have the strongest binding and greatest stability. Our group has recently reported[75] on the stability of a series of boron functionalized BODIPYs and found that the stability towards acid (TFA) increases in the order of BMe_2 and $B(OMe)_2 < BPh_2 < BF_2 < B(CN)_2$ with the dimethyl and dimethoxy derivatives being quite unstable while the dicyano derivative showed no sign of degradation after three days in solution with ten equivalents of TFA.

1.1.7.Medical Applications of BODIPY Dyes

1.1.7.1. Bio-Imaging

To detect cancer at early stages (i.e. stage 0 or stage 1, Figure 1.10), the imaging method employed should meet four basic criteria. It must be sensitive enough to detect an imaging agent at physiological (nanomolar) concentrations, have high spatial and temporal resolution, be non- or minimally invasive, and utilize common or relatively inexpensive instruments.[11] Common medical imaging techniques can be separated into three classifications: X-ray radiography and computed tomography, or CT fall under anatomic imaging; magnetic resonance imaging (MRI) and ultrasonography (US) are forms of functional imaging; and molecular imaging which includes radionuclide imaging (i.e. positron emission tomography, PET, and single photon computed tomography, SPECT) and optical imaging.[10,114] While X-ray, MRI, and ultrasound imaging can use contrast agents to provide additional information, molecular imaging has been defined

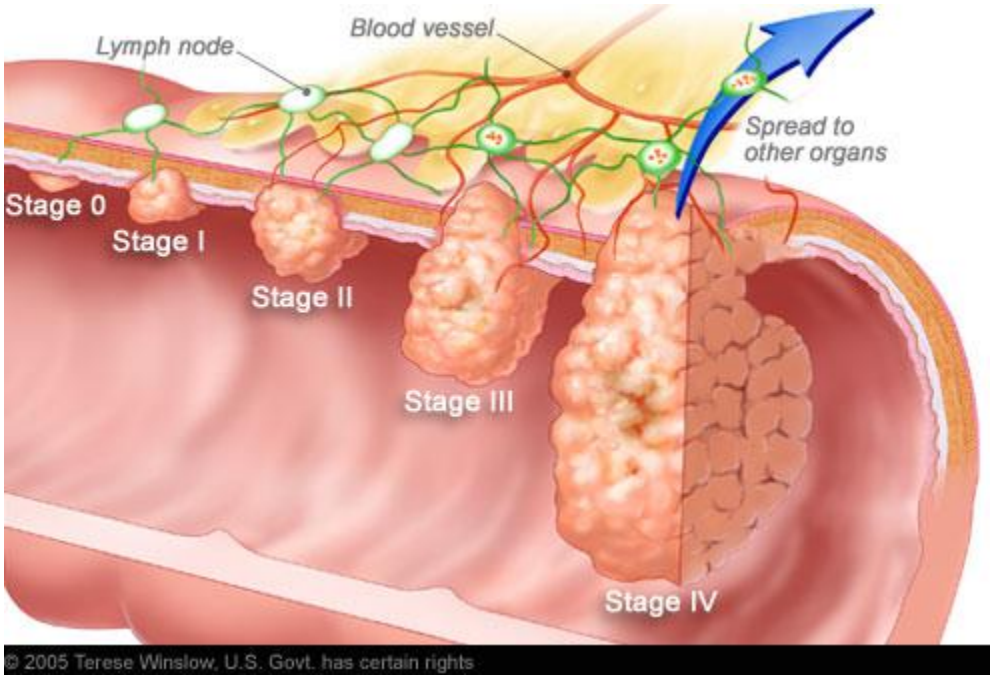

Figure 1.10. Development stages of colorectal cancer.[115]

as “as a technique to directly or indirectly monitor and record the spatiotemporal distribution of molecular or cellular processes for biochemical, biological, diagnostic, or therapeutic application.”[10,116] Radionuclide imaging is a highly sensitive and quantitative technique that can be used for whole body scans. However, it suffers from poor spatial and temporal resolution.[114] On the other hand, optical imaging has similar sensitivity, can target specific tissues, there is a wide variety of imaging agents each with their own pros and cons, and has an added benefit of its capacity to be used in real-time during surgery[117,118] or endoscopy.[119]

1.1.7.2. Imaging Agents

While the first report of a fluorescent organic molecule goes back to the identification of quinine sulfate in 1845 by Sir John Herschel,[120,121] the term “fluorescence” was first coined seven years later in 1852 in a publication on the subject by George Stokes.[122] Fluorescence microscopy was invented several decades after the initial development of organic fluorophores and subsequently applied to biological research with what can be considered the first fluorescence microscope yielding satisfactory work being reported in 1910 by H. Lehmann.[123] The firms of Reichert[124] and Zeiss[125] then reported their independent developments of ultraviolet microscopes in 1911 with Lehmann following suit in 1913.[126] The first considerable advancement came from Derrien’s report in 1924 of successfully localizing porphyrins in different animal tissues.[127,128] Despite this long history, the US Food and Drug Administration had only approved two fluorophores for medical use as of 2010.[10]

Fluorophores for optical imaging can be divided into three general classes: fluorescent nanocrystals (e.g. nanoparticles and quantum dots), genetically encoded

fluorophores (ex. Green fluorescent protein, GFP), and small molecule synthetic fluorophores. Some of the properties that must be considered when designing new imaging agents are the absorption and emission wavelengths, brightness, stability, pharmacokinetics, and solubility. Irradiation with high energy ultraviolet light causes tissue damage while on the other end the use of infrared light results in heating which also damages the tissues. Dyes that use blue and green light are good for surface imaging, however those wavelengths have poor tissue penetration so these dyes are only good for superficial imaging. The use of yellow and red light destroys the signal to noise ratio due to the autofluorescence of endogenous fluorophores, mainly hemoglobin.[114] To maximize tissue penetration, maintain a high signal to noise ratio, and avoid tissue damage, imaging agents should \absorb and emit in the deep red to near-infrared region in the range of 650 – 900 nm (i.e. the biological window).[16]

When it comes to brightness, the brighter fluorophores provide higher signal to noise ratios and greater depth penetration. The brightness is taken as the multiplicative product of a dye's molar extinction coefficient (ε) and fluorescence quantum yield (Φ_f), which means that greater quantum yields allow for less excitation light to be used. Stability on the other hand, applies to both the fluorophore and the conjugate. They must be stable both in vitro and in vivo and the latter is usually compromised after intracellular localization. While rhodamine derivatives can remain fluorescent for over one week, fluorescein, BODIPY, & cyanine dye derivatives lose fluorescence within days of intracellular localization[129,130] Another common problem is photobleaching resulting from excited state redox reactions or production of reactive oxygen species.

The pharmacokinetics is intimately intertwined with the solubility. To start off, most small molecule fluorophores can alter pharmacokinetics of the bio-molecule to which they are conjugated. The size of the dye relative to the bio-molecule is important. When a small molecule fluorophore is conjugated to an amino acid or sugar, the fluorophore will significantly alter the pharmacokinetics of the latter. The same is true when an antibody is conjugated to a quantum dot. However, when a small fluorophore is conjugated to a large peptide or protein, the bio-molecule will dominate the pharmacokinetics, although the dye will still alter them. The imaging agent also need to have minimal, if any, non-specific tissue accumulation.

With regard to solubility, the small molecule synthetic fluorophore needs to be amphiphilic, or have a balance between hydrophilicity and lipophilicity, to have a high cell membrane permeability for intracellular imaging. (Bio-conjugates targeting cell membrane receptors need to be soluble in physiological media, but do not necessarily need high cell membrane permeability.) If the dye is too hydrophobic, it will aggregate/precipitate from the physiological environment, but if it is too hydrophilic, its ability to pass through lipid membranes will be decreased. The BODIPY platform is neutral with high cellular uptake, but its highly hydrophobic nature is problematic for imaging biological samples limiting its practical use. It is also worth noting that BODIPYs lacking hydrophilic moieties have cell membrane permeability, but also have an affinity for localizing in the intracellular membrane resulting in an increased non-specific background signal. Introduction of bulky PEG groups and ionic moieties have been shown to increase BODIPY water solubility, but generally at the cost of its cell membrane permeability. This balance was first reported on by Wu et al[131] where two

distyrylBODIPYs each bearing an anionic carboxylate and a tetraethylene glycol moiety differed greatly in their cell membrane permeability. The derivative containing styryl PEGylated benzenes had no cellular uptake, but the analogous derivative containing naphthalenes instead of benzenes exhibited restored cell membrane permeability.

Despite the large variety of organic fluorophores, the structural scaffolds that absorb and emit in the lower energy visible region are still rather limited (Figure 1.11). The fluorescein scaffold has proven to be quite versatile with much work having been done on functionalizing fluorescein itself, TokyoGreens (TGs), rhodamines,

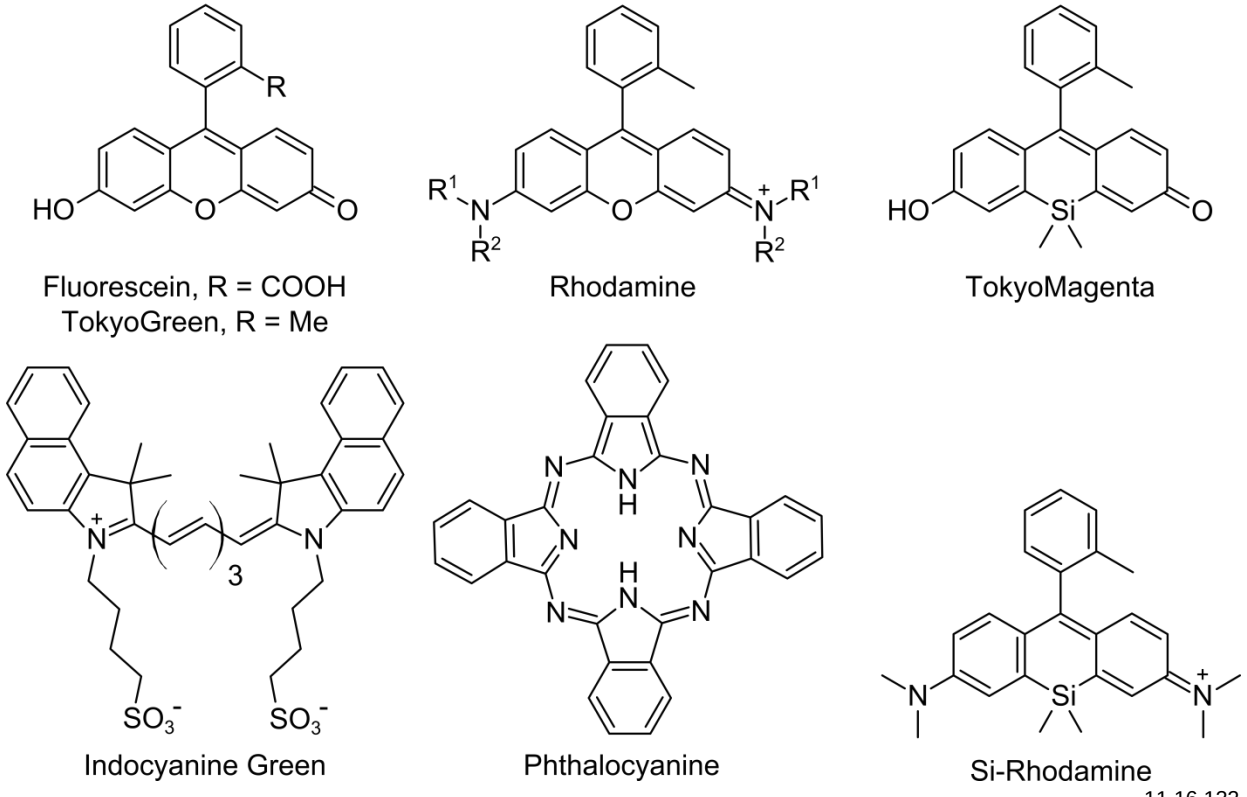

Figure 1.11. Fluorescent scaffolds, excluding BODIPY, employed in bioimaging.[11,16,132]

TokyoMagentas (TMs), Si-rhodamines, cyanine dyes including BODIPYs, and to a lesser extent phthalocyanines.[11,132-135] While there are hundreds of reports demonstrating the use of the BODIPY platform as an imaging agent owing to its easily tunable optics and stability under physiological conditions, the primary advantage

BODIPYs have over other scaffolds is the marked decrease in toxicity which is the foundation of the BODIPY's bright future as a clinical imaging agent.

1.1.7.3. **Photodynamic Therapy (PDT)**

Photodynamic therapy (PDT) is a minimally invasive ternary medical treatment employing a photosensitizer drug, light, and molecular oxygen to produce a cytotoxic effect in a targeted tissue. In clinical application, a patient is kept in a dark room while the photosensitizer is injected and given 24 to 48 hours to accumulate in the tumor after which a fiber-optic cable is inserted through a small incision and then used to irradiate the diseased tissue. The dose of light applied must be carefully regulated because the amount of light needs to be both great enough to induce a phototoxic response and small enough to minimize damaging surrounding healthy tissue. Since light is diffracted in random directions after entering biological tissues, it can incidentally excite the PSs in neighboring healthy tissue.

Despite the relative youth of the term PDT, use of this treatment dates back to antiquity where over 4,000[136] years ago the ancient Egyptians would treat vitiligo by consuming the Ammi majus growing along the Nile riverbanks, which contains psoralens, followed by exposure to sunlight. In 1900, Oscar Raab's report[137] on the cytotoxic effects in Paramecia, resulting from exposure to light after treatment with acridine orange, can be considered the starting point for modern PDT. The first report of skin cancer being treated with PDT was published three years later.[138] The transition to employing porphyrins in PDT can be traced back to 1913 when a German physician, Friedrich Meyer-Benz, self-administered a 200 mg dose of hematoporphyrin. He observed no adverse effects to the injection until exposure to sunlight after which he

experienced a large amount of swelling and this photosensitivity persisted for several months.[139] The ability of porphyrins to produce phototoxic effects was examined in detail by Policard[140] in 1925 and their use in PDT has continued into modern times.

1.1.7.3.1. Photosensitizers (PS)

For a PS to be a viable candidate to move forward to clinical trials, there are several desirable properties that need to be evaluated which include: low to negligible dark toxicity, good pharmacokinetics, strong absorption at long wavelengths, low quantum yields for photobleaching, high intersystem crossing efficiency, high singlet oxygen quantum yield, option for facile derivatization, facile synthesis from readily available starting materials, and simple drug formulation with a long shelf life. The pharmacokinetics of the PDT agent should show low side-effect profiles with rapid clearance from the body and high selectivity for accumulation in tumor cells. The first PDT agent to be approved in the US, Canada, Japan, and various European countries due to its enigmatic low dark-toxicity and accumulation in solid tumors[141] is Photofrin ®. It is a hematoporphyrin oligomeric mixture of dimers through nonamers. The major drawbacks of this drug are its absorption at 630 nm, which limits the depth of tissue penetration, and its systemic clearance, which can take up to six weeks leaving the patient photosensitive during that time.[142]

While photobleaching does inhibit the PS from absorbing light, it is problematic in that it permanently deactivates the agent and the photobleaching quantum yield can be increased by an order of magnitude by simply changing the solvent from pure water to serum.[143] Another issue arising from this change is the significantly reduced fluorophore response frequently observed in the cellular environment.

From a clinical standpoint, the exact mechanism of cell death can be of minor importance since PDT targets tissues on a cellular level and depending on the agent's subcellular localization, different parts of the cell biology will be disrupted, all of which converge on cell death.[62,144-146] Complete tumor death is not always an absolute necessity for effective PDT with animal studies having found residual viable tumor cells following treatment became necrotic when the cascade of biological responses following irradiation resulted in complete vascular shutdown.[147-149] This shutdown induced oxidative stress in the remaining tumor cells which can lead to apoptosis and eventual total tumor necrosis.[150] However, from the viewpoint of basic scientists, the exact mechanism is quite important as it is the means by which more effective therapeutic agents are rationally designed and specific pathways towards cell death are targeted.

Unlike imaging agents, PSs have high intersystem crossing (ISC) rate constants causing them to switch from the singlet to the triplet state after irradiation and resulting in diminished fluorescence quantum yields (Φ_f), depicted in Figure 1.12. From here, the PS can either radiatively phosphoresce or non-radiatively relax via triplet annihilation. During the course of the latter, the triplet state PS can undergo two types of processes to produce cytotoxic reactive oxygen species.[151,152] In the Type I process, a photochemical electron transfer reaction occurs between the excited PS and a non-molecular oxygen substrate forming free radicals which can undergo subsequent reaction to produce peroxides, superoxides, and hydroxyl radicals. The Type II process varies in that reacts with molecular oxygen ($^3O_2$) in essentially a simple energy transfer. The triplet state PS* and molecular oxygen (naturally in the triplet state) undergo a triplet annihilation returning the PS to its singlet ground state and converting the triplet

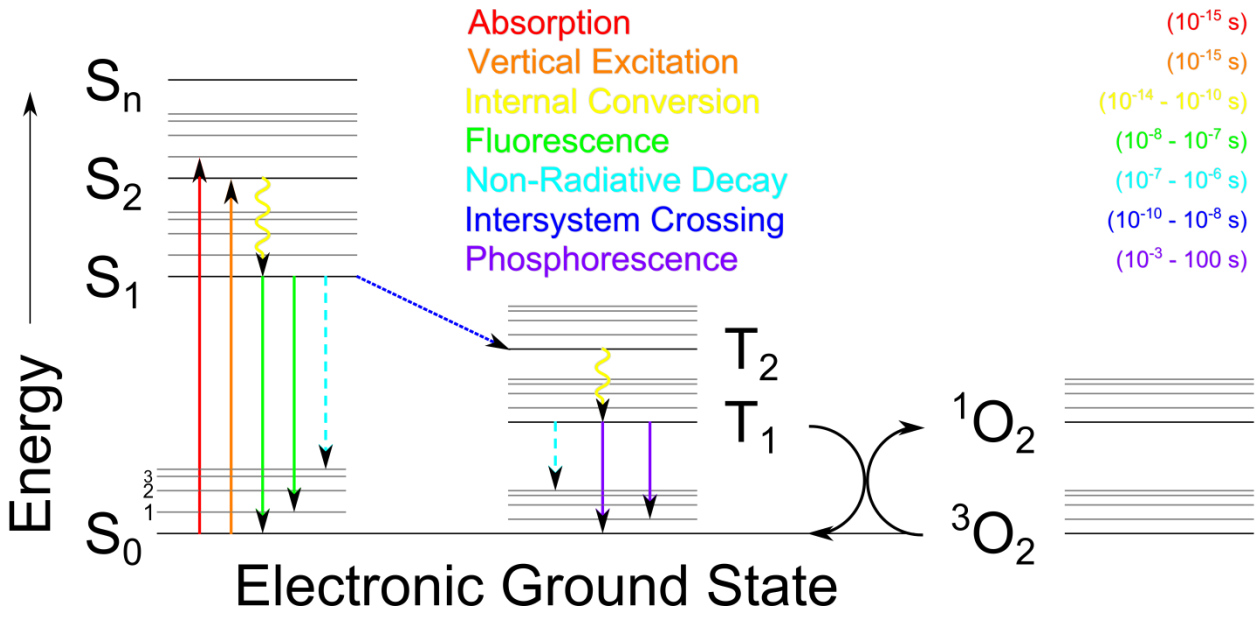

Figure 1.12. Light absorption and PDT activity in a simplified Jablonski diagram. molecular oxygen to excited singlet through a transfer of the PSs spin angular momentum.

Overall, the main difference between fluorophores for imaging and photosensitizers for PDT is the need for high fluorescence quantum yields (ϕ_F) for imaging versus high singlet oxygen quantum yields (Φ_{SO}) for PDT. The same property problems encountered with imaging agents have been encountered with PSs and, again, BODIPYs have shown promise. There are several strategies for effectively converting fluorophores for imaging into PSs for PDT, the easiest of which is through the heavy-atom effect by placing bromine or iodine on the 2,6- positions.[61,62,64,65,153,154]

1.1.7.3.2. Intersystem Crossing (ISC)

Intersystem crossing is a spin forbidden transition from the singlet to triplet spin state for pure spins states. With regard to quantum chemistry, spin is an intrinsic property of elementary particles that gives rise to the Pauli exclusion principle which states that two electrons with identical spin may not occupy the same space at the

same time, but electrons with opposite spins may do so. Here, the term “singlet” (S) refers to a system with all electrons being spin paired where as “triplet” (T) refers to a system with spin unpaired electrons. It occurs when a system contains impure singlet and triplet states that are close in energy. This mixing of states results from spin-orbit coupling, the interaction between the spin magnetic moment of an electron and the magnetic field produced by the relative motion of the electron around the nucleus. The aforementioned magnetic field is directly proportional to the nuclear charge (i.e. atomic number), hence it was dubbed the heavy-atom effect (H-A). In the field of organic dyes, ISC is most commonly induced via the H-A effect.

The carbonyl group, however, is an unusual exception. Despite not having heavy atoms, it can still undergo competitive ISC. This is a result of the oxygen lone pairs behaving in an unexpected way. Instead of occupying degenerate sp^2 orbitals, one lone pair occupies the empty p orbital and the second occupies a low lying sp hybridized orbital. The result is an $S_1(n\rightarrow\pi^*)$ transition that is very close in energy to its $T_2(\pi\rightarrow\pi^*)$ which is higher in energy than the $T_1(n\rightarrow\pi^*)$. The non-radiative decay from T_2 to T_1 is much faster than the ISC, occurring on the order of 10^{-12} to 10^{-10} timescales compared to 10^{-10} to 10^{-8}, effectively inhibiting the reverse process.

Another noteworthy method is the incorporation of fullerenes. The large size of the molecule and the π-conjugated system, along with the high degree of molecular symmetry, results in small splitting among the singlet and triplet states and rather large spin-orbit coupling. The triplet quantum yields are near 1.00 and the singlet oxygen quantum yields are nearly quantitative for both C_{60} and C_{70}.[152]

In looking at the physical mechanism of how the ISC occurs, the Jablonski diagram provides an incomplete picture and looking at the simplified Franck-Condon energy well diagram (Figure 1.13) can provide a more accurate depiction. The total electronic energy of a molecular system (i.e. ground state, S_0, energy) is less than the lowest energy state the system can achieve due to vibrational modes. The atoms within the molecules are constantly in motion so the lowest achievable energy the system can reach is the zero-point energy (ZPE). In Figure 1.13, the horizontal grey lines represent the vibrational modes of the system with the lowest lying line on the S_0 curve being the ZPE. After the system is excited with light, it moves to a vibrational mode in the first excited state (S_1) and undergoes non-radiative vibrational relaxation (i.e. internal conversion, IC) down the S_1 equilibrium geometry. The system shown can return to its ground state by two pathways: 1) fluorescence/non-radiative decay (NRD) or 2)

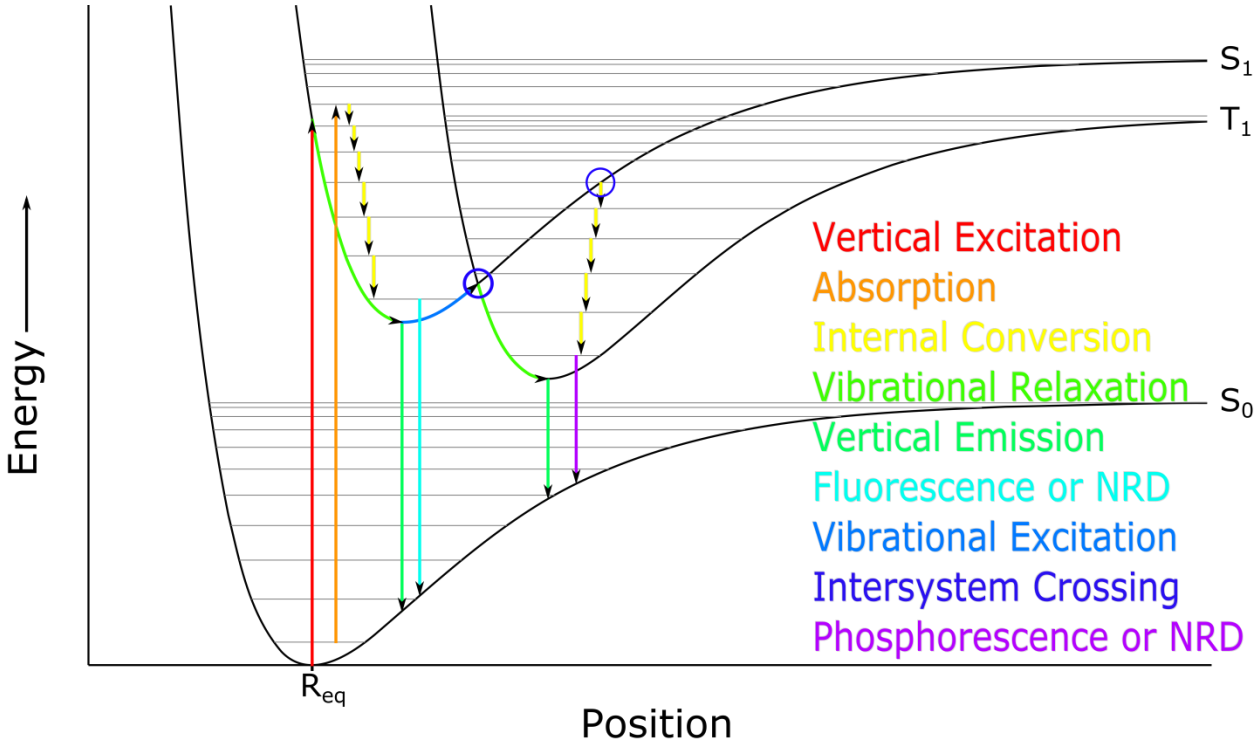

Figure 1.13. Simplified Franck-Condon energy well diagram.

vibrational excitation to achieve ISC followed by relaxation to the triplet state (T_1) equilibrium geometry prior to phosphorescence/NRD.

1.2. Computational Chemistry

1.2.1. Density Functional Theory

The field of computational chemistry is broad and growing. The wide variety of computational methods can be grouped into six main types: ab initio (wavefunction methods), density functional theory (DFT), semi-empirical and empirical, molecular mechanics (MM), molecular dynamics (MD), and quantum mechanics/molecular mechanics (QM/MM). Density functional theory (DFT) is a method that offers a balance of accuracy with computational expense and it's relatively low expense (time scaling factor of N^4 for N basis functions) has made it one of the most popular computational methods currently used. DFT side steps the many body problem of interacting electrons in a static external potential by calculating electronic structure as a function of electron density instead of solving the wavefunction,[155] which means the calculations can be solved exactly and, in principle, perfectly match experiment when supplied with an accurate electron density. However, if the electron density is constructed from linear combinations of atomic orbitals, the method runs back into the many-body problem. Kohn-Sham DFT[156] addresses this with a mean-field approximation which reduces the problem down to non-interacting particles moving in an effective potential (a combination of the static external potential and the Coulombic interactions between the other electrons present in the system). This approach divides the DFT energy ($E_{DFT}[\rho]$) into four terms (as shown below): the Kohn-Sham kinetic energy (of the electrons, $T_S[\rho]$), the electron-nuclear attraction and electron-field interactions ($V_{ext}[\rho]$), and the

electron-electron interaction term which is split into a known Coulomb potential ($J[\rho]$) and an exchange-correlation energy ($E_{XC}[\rho]$).

$$E_{DFT}[\rho] = T_S[\rho] + V_{ext}[\rho] + J[\rho] + E_{XC}[\rho] \quad \text{(eq. 1.1)}$$

Compensation for the assumption of non-interacting particles, in application, requires the use of an exchange-correlation functional to factor these interactions in to the energy of the system. The perfect functional would allow the calculation of properties that would exactly match experimental results every time. Unfortunately, the exact functional does not exist (to current knowledge). Since there is no known generally applicable exact functional, a variety of different flavors of functionals have been developed, most of which are built empirically (i.e. from fitting parameters to experimental results for a specific set of properties). These functionals, however, are thus not truly "ab initio" but rather a best fit to experimental results for a given library of compounds.

1.2.1.1. Time Dependent Density Functional Theory (TD-DFT)

When studying the dynamics and properties of a system in the presence of a time-dependent potential, time-dependent DFT (TDDFT) must be used. There are two main recipes for TDDFT: linear response TDDFT (LR-TDDFT) and real time TDDFT (RT-TDDFT). Both of these methods begin by converting the time-dependent Schrodinger equation to the time-dependent Kohn-Sham equation (TDKS) (time-dependent electronic density). LR-TDDFT iteratively solves the TDKS equations for the ground state system to obtain the eigenvalues from which transition energies (i.e. vertical excitation energies) and oscillator strengths can be extracted.[157] In more physical terms, the eigenvalues are the frequencies to which the electronic structure of

the system has a dramatic response, which equates to the frequencies of light that the system can absorb. This dependence on the ground state reference means that LR-TDDFT works well for small perturbations that do not completely destroy it ground state density (i.e. weak field excitations).

RT-TDDFT, on the other hand, hits the system with a user defined time-dependent potential (e.g. laser pulse) and propagates the electron density through time providing a full time-resolved result, instead of a frequency domain solution.[158,159,160] The time-resolved solution can include both linear and non-linear transitions, as well as both time and spatially resolved electronic responses (i.e. electron dynamics). For the purposes of obtaining absorption spectra, the conversion of the time-resolved data to the frequency domain is usually achieved through a Fourier transform though faster alternatives have been reported.[161]

An important point regarding the use of (TD)DFT is that it was designed to study compounds in the ground state and pure DFT functionals fail if the density deviates significantly from the ground state density. This is a direct result of the inclusion of the Coulomb potential in the KS energy equation. The mean field approximation employed in KS DFT describes the electrons moving in an effective potential (i.e. the Kohn-Sham potential). The KS potential ($v_{eff}(r)$), (eq. 1.2, is the sum of the electron-nuclei attraction potential ($v_{ext}(r)$), the exchange-correlation potential ($v_{XC}(r)$), and the Coulomb potential for the non-interacting particles ($v_J(r)$), which is defined below in (eq. 1.3) where the electron density, $\rho(r)$, over ϕ_i (KS) orbitals for an N-particle system is defined as:

$$v_{eff}(r) = v_{ext}(r) + v_J(r) + v_{XC}(r) \qquad \text{(eq.1.2)}$$

$$v_J(r) = e^2 \int \frac{\rho(r)}{|r - r'|} dr' \ , \quad e = 1 \, Hartree \qquad \text{(eq.1.3)}$$

$$\rho(r) = \sum_i^N |\phi_i(r)|^2 \qquad \text{(eq. 1.4)}$$

The Coulomb potential's dependence on $\frac{1}{r}$ means that regardless of the distance between two particles, there will always be long-range interactions which results in DFT failing to accurately describe electrons further from the nuclei as it always overestimates their interactions. To compensate for this, hybrid functionals were developed that mix a set amount of DFT character with a small amount of Hartree-Fock (HF) character.[162] HF is a computational method that fully accounts for exchange correlation, but neglects the Coulomb correlation. In the grand scheme of things, this allows for the accurate description of systems with uneven charge distribution. These hybrid functionals provide quality ground state descriptions while also yielding more accurate calculations of properties–such as reaction barriers, geometries, dipole moments, etc…– involving electrons further from the nuclei of the atoms in the system, for example vertical excitation energies (VEEs).

While the development of these functionals did greatly improve the accuracy of DFT calculations, they do still have their limits. For example, they still fail to accurately describe charge separated systems and even VEEs for various systems.[163] Thus, range separated functionals were born to address these issues. Range-separated functionals, like CAM-B3LYP,[164] employ a normal hybrid functional to describe the system close to the nuclei and gradually increase the amount of HF as the space of interest moves further away, which gives the correct long range asymptotic form of the potential. In general, the rule of thumb with regard to the choice of DFT functional type

is that GGA (Generalized Gradient Approximation) and LDA (Local Density Approximation) functionals should be used for metals, hybrid functionals work well for modeling reactions, and range-separated functionals are good at capturing long-range interactions, such as charge transfer.

1.3. References

1. Rogers, M. A. T., Tetra-Arylazadipyrromethines: A New Class of Synthetic Colouring Matter. *Nature* **1943,** *151*, 504.

2. Rogers, M. A. T., 2 : 4-Diarylpyrroles. Part I. Synthesis of 2 : 4-Diarylpyrroles and 2 : 2' : 4 : 4'-Tetra-Arylazadipyrromethines. *J. Chem. Soc.* **1943,** (0), 590-596.

3. Treibs, A.; Kreuzer, F. H., Difluorboryl-Komplexe Von Di- Und Tripyrrylmethenen. *Justus Liebigs Ann. Chem.* **1968,** *718*(1), 208-223.

4. Ulrich, G. Z., Raymond; Harriman, Anthony, The Chemistry of Fluorescent Bodipy Dyes: Versatility Unsurpassed. *Angew. Chem. Int. Ed.* **2008,** *47*(7), 1184-1201.

5. Lu, H.; Mack, J.; Yang, Y.; Shen, Z., Structural Modification Strategies for the Rational Design of Red/NIR Region BODIPYs. *Chem. Soc. Rev.* **2014,** *43*(13), 4778-4823.

6. Bañuelos, J., BODIPY Dye, the Most Versatile Fluorophore Ever? *Chem. Rec.* **2016,** *16*(1), 335-348.

7. Monsma, F. J.; Barton, A. C.; Kang, H. C.; Brassard, D. L.; Haugland, R. P.; Sibley, D. R., Characterization of Novel Fluorescent Ligands with High Affinity for D1 and D2 Dopaminergic Receptors. *J. Neurochem.* **1989,** *52*(5), 1641-1644.

8. Lakshmi, V.; Rajeswara Rao, M.; Ravikanth, M., Halogenated Boron-Dipyrromethenes: Synthesis, Properties and Applications. *Org. Biomol. Chem.* **2015,** *13*(9), 2501-2517.

9. Han, J.; Burgess, K., Fluorescent Indicators for Intracellular Ph. *Chem. Rev.* **2010,** *110*(5), 2709-2728.

10. Kobayashi, H.; Ogawa, M.; Alford, R.; Choyke, P. L.; Urano, Y., New Strategies for Fluorescent Probe Design in Medical Diagnostic Imaging. *Chem. Rev.* **2010,** *110*(5), 2620-2640.

11. Terai, T.; Nagano, T., Small-Molecule Fluorophores and Fluorescent Probes for Bioimaging. *Pflüg. Arch. Eur. J. Physiol.* **2013,** *465*(3), 347-359.

12. Fan, G.; Yang, L.; Chen, Z., Water-Soluble BODIPY and Aza-BODIPY Dyes: Synthetic Progress and Applications. *Front. Chem. Sci. Eng.* **2014,** *8*(4), 405-417.

13. Ni, Y.; Wu, J., Far-Red and near Infrared BODIPY Dyes: Synthesis and Applications for Fluorescent Ph Probes and Bio-Imaging. *Org. Biomol. Chem.* **2014,** *12*(23), 3774-3791.

14. Ziessel, R.; Ulrich, G.; Harriman, A., The Chemistry of Bodipy: A New El Dorado for Fluorescence Tools. *New J. Chem.* **2007,** *31*(4), 496-501.

15. Yuan, L.; Lin, W.; Zheng, K.; He, L.; Huang, W., Far-Red to near Infrared Analyte-Responsive Fluorescent Probes Based on Organic Fluorophore Platforms for Fluorescence Imaging. *Chem. Soc. Rev.* **2013,** *42*(2), 622-661.

16. Kowada, T.; Maeda, H.; Kikuchi, K., BODIPY-Based Probes for the Fluorescence Imaging of Biomolecules in Living Cells. *Chem. Soc. Rev.* **2015,** *44*(14), 4953-4972.

17. Lavis, L. D.; Raines, R. T., Bright Ideas for Chemical Biology. *ACS Chem. Biol.* **2008,** *3*(3), 142-155.

18. Wysocki, L. M.; Lavis, L. D., Advances in the Chemistry of Small Molecule Fluorescent Probes. *Curr. Opin. Chem. Biol.* **2011,** *15*(6), 752-759.

19. Umezawa, K.; Citterio, D.; Suzuki, K., New Trends in near-Infrared Fluorophores for Bioimaging. *Anal. Sci.* **2014,** *30*(3), 327-349.

20. Qian, X.; Xiao, Y.; Xu, Y.; Guo, X.; Qian, J.; Zhu, W., "Alive" Dyes as Fluorescent Sensors: Fluorophore, Mechanism, Receptor and Images in Living Cells. *Chem. Commun.* **2010,** *46*(35), 6418-6436.

21. Li, Z.; Zheng, M.; Guan, X.; Xie, Z.; Huang, Y.; Jing, X., Unadulterated BODIPY-Dimer Nanoparticles with High Stability and Good Biocompatibility for Cellular Imaging. *Nanoscale* **2014,** *6*(11), 5662-5665.

22. Su, D.; Teoh, C. L.; Sahu, S.; Das, R. K.; Chang, Y.-T., Live Cells Imaging Using a Turn-on Fret-Based BODIPY Probe for Biothiols. *Biomaterials* **2014,** *35*(23), 6078-6085.

23. Mikhalyov, I.; Gretskaya, N.; Johansson, L. B. Å., Fluorescent BODIPY-Labelled G_{M1} Gangliosides Designed for Exploring Lipid Membrane Properties and Specific Membrane-Target Interactions. *Chem. Phys. Lipids* **2009,** *159*(1), 38-44.

24. Lee, J.-S.; Kang, N.-y.; Kim, Y. K.; Samanta, A.; Feng, S.; Kim, H. K.; Vendrell, M.; Park, J. H.; Chang, Y.-T., Synthesis of a BODIPY Library and Its Application to the Development of Live Cell Glucagon Imaging Probe. *J. Am. Chem. Soc.* **2009,** *131*(29), 10077-10082.

25. Escobedo, J. O.; Rusin, O.; Lim, S.; Strongin, R. M., NIR Dyes for Bioimaging Applications. *Curr. Opin. Chem. Biol.* **2010,** *14*(1), 64-70.

26. Luo, S.; Zhang, E.; Su, Y.; Cheng, T.; Shi, C., A Review of NIR Dyes in Cancer Targeting and Imaging. *Biomaterials* **2011,** *32*(29), 7127-7138.

27. Terai, T.; Nagano, T., Fluorescent Probes for Bioimaging Applications. *Curr. Opin. Chem. Biol.* **2008,** *12*(5), 515-521.

28. Zhao, N.; Williams, T. M.; Zhou, Z.; Fronczek, F. R.; Sibrian-Vazquez, M.; Jois, S. D.; Vicente, M. G. H., Synthesis of BODIPY-Peptide Conjugates for Fluorescence Labeling of Egfr Overexpressing Cells. *Bioconjugate Chem.* **2017,** *28*(5), 1566-1579.

29. Williams, T. M.; Sable, R.; Singh, S.; Vicente, M. G. H.; Jois, S. D., Peptide Ligands for Targeting the Extracellular Domain of Egfr: Comparison between Linear and Cyclic Peptides. *Chem. Biol. Drug Des.* **2018,** *91*(2), 605-619.

30. Costela, A.; García-Moreno, I.; Pintado-Sierra, M.; Amat-Guerri, F.; Sastre, R.; Liras, M.; Arbeloa, F. L.; Prieto, J. B.; Arbeloa, I. L., New Analogues of the BODIPY Dye Pm597: Photophysical and Lasing Properties in Liquid Solutions and in Solid Polymeric Matrices. *The Journal of Physical Chemistry A* **2009,** *113*(28), 8118-8124.

31. Costela, A.; Garcia-Moreno, I.; Sastre, R., Polymeric Solid-State Dye Lasers: Recent Developments. *Phys. Chem. Chem. Phys.* **2003,** *5*(21), 4745-4763.

32. Duran-Sampedro, G.; Agarrabeitia, A. R.; Garcia-Moreno, I.; Costela, A.; Bañuelos, J.; Arbeloa, T.; López, A. I.; Chiara, J. L.; Ortiz, M. J., Chlorinated BODIPYs: Surprisingly Efficient and Highly Photostable Laser Dyes. *Eur. J. Org. Chem.* **2012,** *2012*(32), 6335-6350.

33. Ge, Y.; O'Shea, D. F., Azadipyrromethenes: From Traditional Dye Chemistry to Leading Edge Applications. *Chem. Soc. Rev.* **2016,** *45*(14), 3846-3864.

34. Mula, S.; Ray, A. K.; Banerjee, M.; Chaudhuri, T.; Dasgupta, K.; Chattopadhyay, S., Design and Development of a New Pyrromethene Dye with Improved Photostability and Lasing Efficiency: Theoretical Rationalization of Photophysical and Photochemical Properties. *J. Org. Chem.* **2008,** *73*(6), 2146-2154.

35. Rahn, M. D.; King, T. A., Comparison of Laser Performance of Dye Molecules in Sol-Gel, Polycom, Ormosil, and Poly(Methyl Methacrylate) Host Media. *Appl. Opt.* **1995,** *34*(36), 8260-8271.

36. Rahn, M. D.; King, T. A.; Gorman, A. A.; Hamblett, I., Photostability Enhancement of Pyrromethene 567 and Perylene Orange in Oxygen-Free Liquid and Solid Dye Lasers. *Appl. Opt.* **1997,** *36*(24), 5862-5871.

37. Shah, M.; Thangaraj, K.; Soong, M. L.; Wolford, L. T.; Boyer, J. H.; Politzer, I. R.; Pavlopoulos, T. G., Pyrromethene–BF_2 Complexes as Laser Dyes:1. *Heteroat. Chem.* **1990,** *1*(5), 389-399.

38. Zhang, D.; Martin, V.; Garcia-Moreno, I.; Costela, A.; Perez-Ojeda, M. E.; Xiao, Y., Development of Excellent Long-Wavelength BODIPY Laser Dyes with a Strategy That Combines Extending π-Conjugation and Tuning Ict Effect. *Phys. Chem. Chem. Phys.* **2011,** *13*(28), 13026-13033.

39. Kostereli, Z.; Ozdemir, T.; Buyukcakir, O.; Akkaya, E. U., Tetrastyryl-BODIPY-Based Dendritic Light Harvester and Estimation of Energy Transfer Efficiency. *Org. Lett.* **2012,** *14*(14), 3636-3639.

40. Singh, S. P.; Gayathri, T., Evolution of BODIPY Dyes as Potential Sensitizers for Dye-Sensitized Solar Cells. *Eur. J. Org. Chem.* **2014,** *2014*(22), 4689-4707.

41. Benniston, A. C.; Copley, G., Lighting the Way Ahead with Boron Dipyrromethene (Bodipy) Dyes. *Phys. Chem. Chem. Phys.* **2009,** *11*(21), 4124-4131.

42. Bessette, A.; Hanan, G. S., Design, Synthesis and Photophysical Studies of Dipyrromethene-Based Materials: Insights into Their Applications in Organic Photovoltaic Devices. *Chem. Soc. Rev.* **2014,** *43*(10), 3342-3405.

43. Wan, C. W.; Burghart, A.; Chen, J.; Bergström, F.; Johansson, L. B. Å.; Wolford, M. F.; Kim, T. G.; Topp, M. R.; Hochstrasser, R. M.; Burgess, K., Anthracene–BODIPY Cassettes: Syntheses and Energy Transfer. *Chem. Eur. J.* **2003,** *9*(18), 4430-4441.

44. D'Souza, F.; Smith, P. M.; Zandler, M. E.; McCarty, A. L.; Itou, M.; Araki, Y.; Ito, O., Energy Transfer Followed by Electron Transfer in a Supramolecular Triad Composed of Boron Dipyrrin, Zinc Porphyrin, and Fullerene: A Model for the Photosynthetic Antenna-Reaction Center Complex. *J. Am. Chem. Soc.* **2004,** *126*(25), 7898-7907.

45. Bozdemir, O. A.; Cakmak, Y.; Sozmen, F.; Ozdemir, T.; Siemiarczuk, A.; Akkaya, E. U., Synthesis of Symmetrical Multichromophoric Bodipy Dyes and Their Facile Transformation into Energy Transfer Cassettes. *Chem. Eur. J.* **2010,** *16*(21), 6346-6351.

46. Ziessel, R.; Harriman, A., Artificial Light-Harvesting Antennae: Electronic Energy Transfer by Way of Molecular Funnels. *Chem. Commun.* **2011,** *47*(2), 611-631.

47. Iehl, J.; Nierengarten, J.-F.; Harriman, A.; Bura, T.; Ziessel, R., Artificial Light-Harvesting Arrays: Electronic Energy Migration and Trapping on a Sphere and between Spheres. *J. Am. Chem. Soc.* **2012,** *134*(2), 988-998.

48. Fan, J.; Hu, M.; Zhan, P.; Peng, X., Energy Transfer Cassettes Based on Organic Fluorophores: Construction and Applications in Ratiometric Sensing. *Chem. Soc. Rev.* **2013,** *42*(1), 29-43.

49. Goeb, S.; Ziessel, R., Convenient Synthesis of Green Diisoindolodithienylpyrromethene−Dialkynyl Borane Dyes. *Org. Lett.* **2007,** *9*(5), 737-740.

50. Brizet, B.; Eggenspiller, A.; Gros, C. P.; Barbe, J.-M.; Goze, C.; Denat, F.; Harvey, P. D., B,B-Diporphyrinbenzyloxy-BODIPY Dyes: Synthesis and Antenna Effect. *J. Org. Chem.* **2012,** *77*(7), 3646-3650.

51. Lazarides, T.; Kuhri, S.; Charalambidis, G.; Panda, M. K.; Guldi, D. M.; Coutsolelos, A. G., Electron Vs Energy Transfer in Arrays Featuring Two Bodipy Chromophores Axially Bound to a Sn(Iv) Porphyrin Via a Phenolate or Benzoate Bridge. *Inorg. Chem.* **2012,** *51*(7), 4193-4204.

52. Boens, N.; Leen, V.; Dehaen, W., Fluorescent Indicators Based on BODIPY. *Chem. Soc. Rev.* **2012,** *41*(3), 1130-1172.

53. Culzoni, M. J.; Munoz de la Pena, A.; Machuca, A.; Goicoechea, H. C.; Babiano, R., Rhodamine and BODIPY Chemodosimeters and Chemosensors for the Detection of Hg^{2+}, Based on Fluorescence Enhancement Effects. *Anal. Methods* **2013,** *5*(1), 30-49.

54. Golovkova, T. A.; Kozlov, D. V.; Neckers, D. C., Synthesis and Properties of Novel Fluorescent Switches. *J. Org. Chem.* **2005,** *70*(14), 5545-5549.

55. Hou, J.-T.; Ren, W. X.; Li, K.; Seo, J.; Sharma, A.; Yu, X.-Q.; Kim, J. S., Fluorescent Bioimaging of Ph: From Design to Applications. *Chem. Soc. Rev.* **2017,** *46*(8), 2076-2090.

56. Li, X.; Gao, X.; Shi, W.; Ma, H., Design Strategies for Water-Soluble Small Molecular Chromogenic and Fluorogenic Probes. *Chem. Rev.* **2014,** *114*(1), 590-659.

57. Mei, Y.; Bentley, P. A.; Wang, W., A Selective and Sensitive Chemosensor for Cu^{2+} Based on 8-Hydroxyquinoline. *Tetrahedron Lett.* **2006,** *47*(14), 2447-2449.

58. Sun, W.; Guo, S.; Hu, C.; Fan, J.; Peng, X., Recent Development of Chemosensors Based on Cyanine Platforms. *Chem. Rev.* **2016,** *116*(14), 7768-7817.

59. Sunahara, H.; Urano, Y.; Kojima, H.; Nagano, T., Design and Synthesis of a Library of BODIPY-Based Environmental Polarity Sensors Utilizing Photoinduced Electron-Transfer-Controlled Fluorescence on/Off Switching. *J. Am. Chem. Soc.* **2007,** *129*(17), 5597-5604.

60. Ueno, T.; Urano, Y.; Kojima, H.; Nagano, T., Mechanism-Based Molecular Design of Highly Selective Fluorescence Probes for Nitrative Stress. *J. Am. Chem. Soc.* **2006,** *128*(33), 10640-10641.

61. Kamkaew, A.; Lim, S. H.; Lee, H. B.; Kiew, L. V.; Chung, L. Y.; Burgess, K., BODIPY Dyes in Photodynamic Therapy. *Chem. Soc. Rev.* **2013,** *42*(1), 77-88.

62. Awuah, S. G.; You, Y., Boron Dipyrromethene (BODIPY)-Based Photosensitizers for Photodynamic Therapy. *RSC Adv.* **2012,** *2*(30), 11169-11183.

63. Turan, I. S.; Cakmak, F. P.; Yildirim, D. C.; Cetin-Atalay, R.; Akkaya, E. U., Near-Ir Absorbing BODIPY Derivatives as Glutathione-Activated Photosensitizers for Selective Photodynamic Action. *Chem. Eur. J.* **2014,** *20*(49), 16088-16092.

64. Gibbs, J. H.; Zhou, Z.; Kessel, D.; Fronczek, F. R.; Pakhomova, S.; Vicente, M. G. H., Synthesis, Spectroscopic, and in Vitro Investigations of 2,6-Diiodo-BODIPYs with Pdt and Bioimaging Applications. *J. Photochem. Photobiol., B* **2015,** *145*, 35-47.

65. Yogo, T.; Urano, Y.; Ishitsuka, Y.; Maniwa, F.; Nagano, T., Highly Efficient and Photostable Photosensitizer Based on BODIPY Chromophore. *J. Am. Chem. Soc.* **2005,** *127*(35), 12162-12163.

66. Falk, H.; Grubmayr, K.; Neufingerl, F., Zur Photochemischen (Z)⇆(E)-Isomerisierung Von Gallenpigment-Partialstrukturen. *Monatshefte für Chemie / Chemical Monthly* **1977,** *108*(5), 1185-1188.

67. Zhao, N.; Xuan, S.; Fronczek, F. R.; Smith, K. M.; Vicente, M. G. H., Stepwise Polychlorination of 8-Chloro-BODIPY and Regioselective Functionalization of 2,3,5,6,8-Pentachloro-BODIPY. *J. Org. Chem.* **2015,** *80*(16), 8377-8383.

68. Loudet, A.; Burgess, K., BODIPY® Dyes and Their Derivatives: Syntheses and Spectroscopic Properties. In *Handbook of Porphyrin Science*, World Scientific Publishing Company: 2012; Vol. Open-Chain Oligopyrrole Systems, 1-164.

69. Nepomnyashchii, A. B.; Bard, A. J., Electrochemistry and Electrogenerated Chemiluminescence of BODIPY Dyes. *Acc. Chem. Res.* **2012,** *45*(11), 1844-1853.

70. Gräf, K.; Korzdorfer, T.; Kummel, S.; Thelakkat, M., Synthesis of Donor-Substituted Meso-Phenyl and Meso-Ethynylphenyl BODIPYs with Broad Absorption. *New J. Chem.* **2013,** *37*(5), 1417-1426.

71. Karlsson, J. K. G.; Harriman, A., Origin of the Red-Shifted Optical Spectra Recorded for Aza-BODIPY Dyes. *J. Phys. Chem. A* **2016,** *120*(16), 2537-2546.

72. Liu, C.-L.; Chen, Y.; Shelar, D. P.; Li, C.; Cheng, G.; Fu, W.-F., Bodipy Dyes Bearing Oligo(Ethylene Glycol) Groups on the Meso-Phenyl Ring: Tuneable Solid-State Photoluminescence and Highly Efficient Oleds. *J. Mater. Chem. C* **2014,** *2*(28), 5471-5478.

73. Xuan, S.; Zhao, N.; Ke, X.; Zhou, Z.; Fronczek, F. R.; Kadish, K. M.; Smith, K. M.; Vicente, M. G. H., Synthesis and Spectroscopic Investigation of a Series of Push–Pull Boron Dipyrromethenes (BODIPYs). *J. Org. Chem.* **2017,** *82*(5), 2545-2557.

74. Loudet, A.; Burgess, K., BODIPY Dyes and Their Derivatives: Syntheses and Spectroscopic Properties. *Chem. Rev.* **2007,** *107*(11), 4891-4932.

75. Wang, M.; Vicente, M. G. H.; Mason, D.; Bobadova-Parvanova, P., Stability of a Series of BODIPYs in Acidic Conditions: An Experimental and Computational Study into the Role of the Substituents at Boron. *ACS Omega* **2018,** *3*(5), 5502-5510.

76. Jiao, C.; Zhu, L.; Wu, J., BODIPY-Fused Porphyrins as Soluble and Stable near-Ir Dyes. *Chem. Eur. J.* **2011,** *17*(24), 6610-6614.

77. Collado, D.; Vida, Y.; Najera, F.; Perez-Inestrosa, E., Pegylated Aza-BODIPY Derivatives as NIR Probes for Cellular Imaging. *RSC Adv.* **2014,** *4*(5), 2306-2309.

78. Fischer, G. M.; Daltrozzo, E.; Zumbusch, A., Selective NIR Chromophores: Bis(Pyrrolopyrrole) Cyanines. *Angew. Chem. Int. Ed.* **2011,** *50*(6), 1406-1409.

79. Fischer, G. M.; Ehlers, A. P.; Zumbusch, A.; Daltrozzo, E., Near-Infrared Dyes and Fluorophores Based on Diketopyrrolopyrroles. *Angew. Chem. Int. Ed.* **2007,** *46*(20), 3750-3753.

80. Fischer, G. M.; Isomäki-Krondahl, M.; Göttker-Schnetmann, I.; Daltrozzo, E.; Zumbusch, A., Pyrrolopyrrole Cyanine Dyes: A New Class of near-Infrared Dyes and Fluorophores. *Chem. Eur. J.* **2009,** *15*(19), 4857-4864.

81. Fischer, G. M.; Jungst, C.; Isomaki-Krondahl, M.; Gauss, D.; Moller, H. M.; Daltrozzo, E.; Zumbusch, A., Asymmetric Ppcys: Strongly Fluorescing NIR Labels. *Chem. Commun.* **2010,** *46*(29), 5289-5291.

82. Fischer, G. M.; Klein, M. K.; Daltrozzo, E.; Zumbusch, A., Pyrrolopyrrole Cyanines: Effect of Substituents on Optical Properties. *Eur. J. Org. Chem.* **2011,** *2011*(19), 3421-3429.

83. Li, L.; Han, J.; Nguyen, B.; Burgess, K., Syntheses and Spectral Properties of Functionalized, Water-Soluble BODIPY Derivatives. *J. Org. Chem.* **2008,** *73*(5), 1963-1970.

84. Nakamura, M.; Tahara, H.; Takahashi, K.; Nagata, T.; Uoyama, H.; Kuzuhara, D.; Mori, S.; Okujima, T.; Yamada, H.; Uno, H., π-Fused Bis-BODIPY as a Candidate for NIR Dyes. *Org. Biomol. Chem.* **2012,** *10*(34), 6840-6849.

85. Wu, G.; Zeng, F.; Wu, S., A Water-Soluble and Specific BODIPY-Based Fluorescent Probe for Hypochlorite Detection and Cell Imaging. *Anal. Methods* **2013,** *5*(20), 5589-5596.

86. Zeng, L.; Jiao, C.; Huang, X.; Huang, K.-W.; Chin, W.-S.; Wu, J., Anthracene-Fused BODIPYs as near-Infrared Dyes with High Photostability. *Org. Lett.* **2011,** *13*(22), 6026-6029.

87. Würthner, F.; Kaiser, T. E.; Saha-Möller, C. R., J-Aggregates: From Serendipitous Discovery to Supramolecular Engineering of Functional Dye Materials. *Angew. Chem. Int. Ed.* **2011,** *50*(15), 3376-3410.

88. Bura, T.; Ziessel, R., Water-Soluble Phosphonate-Substituted BODIPY Derivatives with Tunable Emission Channels. *Org. Lett.* **2011,** *13*(12), 3072-3075.

89. Zhu, S.; Zhang, J.; Vegesna, G.; Luo, F.-T.; Green, S. A.; Liu, H., Highly Water-Soluble Neutral BODIPY Dyes with Controllable Fluorescence Quantum Yields. *Org. Lett.* **2011,** *13*(3), 438-441.

90. Zhu, S.; Dorth, N.; Zhang, J.; Vegesna, G.; Li, H.; Luo, F.-T.; Tiwari, A.; Liu, H., Highly Water-Soluble Neutral near-Infrared Emissive BODIPY Polymeric Dyes. *J. Mater. Chem. B* **2012,** *22*(6), 2781-2790.

91. Zhu, S.; Zhang, J.; Janjanam, J.; Vegesna, G.; Luo, F.-T.; Tiwari, A.; Liu, H., Highly Water-Soluble BODIPY-Based Fluorescent Probes for Sensitive Fluorescent Sensing of Zinc(Ii). *J. Mater. Chem. B* **2013,** *1*(12), 1722-1728.

92. Zhu, Y.; Lin, W.; Zhang, W.; Feng, Y.; Wu, Z.; Chen, L.; Xie, Z., Pegylated BODIPY Assembling Fluorescent Nanoparticles for Photodynamic Therapy. *Chin. Chem. Lett.* **2017,** *28*(9), 1875-1877.

93. Vegesna, G. K.; Sripathi, S. R.; Zhang, J.; Zhu, S.; He, W.; Luo, F.-T.; Jahng, W. J.; Frost, M.; Liu, H., Highly Water-Soluble BODIPY-Based Fluorescent Probe for Sensitive and Selective Detection of Nitric Oxide in Living Cells. *ACS Appl. Mater. Interfaces* **2013,** *5*(10), 4107-4112.

94. Courtis, A. M.; Santos, S. A.; Guan, Y.; Hendricks, J. A.; Ghosh, B.; Szantai-Kis, D. M.; Reis, S. A.; Shah, J. V.; Mazitschek, R., Monoalkoxy BODIPYs—a Fluorophore Class for Bioimaging. *Bioconjugate Chem.* **2014,** *25*(6), 1043-1051.

95. Takeda, A.; Komatsu, T.; Nomura, H.; Naka, M.; Matsuki, N.; Ikegaya, Y.; Terai, T.; Ueno, T.; Hanaoka, K.; Nagano, T.; Urano, Y., Unexpected Photo-Instability of 2,6-Sulfonamide-Substituted BODIPYs and Its Application to Caged Gaba. *ChemBioChem* **2016,** *17*(13), 1233-1240.

96. Komatsu, T.; Urano, Y.; Fujikawa, Y.; Kobayashi, T.; Kojima, H.; Terai, T.; Hanaoka, K.; Nagano, T., Development of 2,6-Carboxy-Substituted Boron Dipyrromethene (BODIPY) as a Novel Scaffold of Ratiometric Fluorescent Probes for Live Cell Imaging. *Chem. Commun.* **2009,** *45*(45), 7015-7017.

97. Dilek, Ö.; Bane, S. L., Synthesis, Spectroscopic Properties and Protein Labeling of Water Soluble 3,5-Disubstituted Boron Dipyrromethenes. *Bioorg. Med. Chem. Lett.* **2009,** *19*(24), 6911-6913.

98. Niu, S.-L.; Ulrich, G.; Ziessel, R.; Kiss, A.; Renard, P.-Y.; Romieu, A., Water-Soluble BODIPY Derivatives. *Org. Lett.* **2009,** *11*(10), 2049-2052.

99. Li, L.; Han, J.; Nguyen, B.; Burgess, K., Syntheses and Spectral Properties of Functionalized, Water-Soluble BODIPY Derivatives. *J. Org. Chem.* **2008,** *73*(5), 1963 - 1970.

100. Yao, H.-W.; Zhu, X.-Y.; Guo, X.-F.; Wang, H., An Amphiphilic Fluorescent Probe Designed for Extracellular Visualization of Nitric Oxide Released from Living Cells. *Anal. Chem.* **2016,** *88*(18), 9014 - 9021.

101. Kim, J.; Kim, Y., A Water-Soluble Sulfonate-BODIPY Based Fluorescent Probe for Selective Detection of Hocl/Ocl^- in Aqueous Media. *Analyst* **2014,** *139*(12), 2986-2989.

102. Niu, S.-L.; Massif, C.; Ulrich, G.; Ziessel, R.; Renard, P.-Y.; Romieu, A., Water-Solubilisation and Bio-Conjugation of a Red-Emitting BODIPY Marker. *Org. Biomol. Chem.* **2011,** *9*(1), 66-69.

103. Marfin, Y. S.; Aleksakhina; Merkushev; Rumyantsev; Tomilova, Interaction of BODIPY Dyes with the Blood Plasma Proteins. *J. Fluoresc.* **2016,** *26*(1), 255 - 261.

104. Wu, L.; Loudet, A.; Barhoumi, R.; Burghardt, R. C.; Burgess, K., Fluorescent Cassettes for Monitoring Three-Component Interactions in Vitro and in Living Cells. *J. Am. Chem. Soc.* **2009,** *131*(26), 9156 - 9157.

105. Wories, H. J.; Koek, J. H.; Lodder, G.; Lugtenburg, J.; Fokkens, R.; Driessen, O.; Mohn., G. R., A Novel Water-Soluble Fluorescent Probe: Synthesis, Luminescence and Biological Properties of the Sodium Salt of the 4-Sulfonato-3,3',5,5'-Tetramethyl-2,2'-Pyrromethen-1,1'-BF_2 Complex. *Recl. Trav. Chim. Pays-Bas* **1985,** *104*(11), 288 - 291.

106. Zhu, H.; Fan, J.; Mu, H.; Zhu, T.; Zhang, Z.; Du, J.; Peng, X., D-Pet-Controlled "Off-on" Polarity-Sensitive Probes for Reporting Local Hydrophilicity within Lysosomes. *Sci. Rep.* **2016,** *6*, 35627.

107. Niu, S. L.; Massif, C.; Ulrich, G.; Renard, P. Y.; Romieu, A.; Ziessel, R., Water-Soluble Red-Emitting Distyryl-Borondipyrromethene (BODIPY) Dyes for Biolabeling. *Chem. Eur. J.* **2012,** *18*(23), 7229-7242.

108. Niu, S.-L.; Ulrich, G.; Retailleau, P.; Harrowfield, J.; Ziessel, R., New Insights into the Solubilization of BODIPY Dyes. *Tetrahedron Lett.* **2009,** *50*(27), 3840-3844.

109. Isaad, J.; El Achari, A., A Water Soluble Fluorescent BODIPY Dye with Azathia-Crown Ether Functionality for Mercury Chemosensing in Environmental Media. *Analyst* **2013,** *138*(13), 3809-3819.

110. Lu, Z.; Mei, L.; Zhang, X.; Wang, Y.; Zhao, Y.; Li, C., Water-Soluble BODIPY-Conjugated Glycopolymers as Fluorescent Probes for Live Cell Imaging. *Polym. Chem.* **2013,** *4*(24), 5743-5750.

111. Nguyen, A. L.; Griffin, K. E.; Zhou, Z.; Fronczek, F. R.; Smith, K. M.; Vicente, M. G. H., Syntheses of 1,2,3-Triazole-BODIPYs Bearing up to Three Carbohydrate Units. *New J. Chem.* **2018,** *42*(10), 8241-8246.

112. Nguyen, A. L.; Bobadova-Parvanova, P.; Hopfinger, M.; Fronczek, F. R.; Smith, K. M.; Vicente, M. G. H., Synthesis and Reactivity of 4,4-Dialkoxy-BODIPYs: An Experimental and Computational Study. *Inorg. Chem.* **2015,** *54*(7), 3228-3236.

113. Ray, C.; Díaz-Casado, L.; Avellanal-Zaballa, E.; Bañuelos, J.; Cerdán, L.; García-Moreno, I.; Moreno, F.; Maroto, B. L.; López-Arbeloa, Í.; de la Moya, S., N-BODIPYs Come into Play: Smart Dyes for Photonic Materials. *Chem. Eur. J.* **2017,** *23*(39), 9383-9390.

114. Schaeffter, T., Imaging Modalities: Principles and Information Content. In *Imaging in Drug Discovery and Early Clinical Trials*, Springer Science: Boston, 2005; Vol. 62, 15-82.

115. Martin, L. J. What You Need to Know About Colorectal Cancer. https://www.webmd.com/colorectal-cancer/ss/slideshow-colorectal-cancer-overview; (accessed June 22, 2018).

116. Thakur, M.; Lentle, B. C., Report of a Summit on Molecular Imaging. *Radiology* **2005,** *236*(3), 753-755.

117. Hama, Y.; Urano, Y.; Koyama, Y.; Kamiya, M.; Bernardo, M.; Paik, R. S.; Krishna, M. C.; Choyke, P. L.; Kobayashi, H., In Vivo Spectral Fluorescence Imaging of Submillimeter Peritoneal Cancer Implants Using a Lectin-Targeted Optical Agent. *Neoplasia* **2006,** *8*(7), 607-IN602.

118. Sheth, R. A.; Upadhyay, R.; Stangenberg, L.; Sheth, R.; Weissleder, R.; Mahmood, U., Improved Detection of Ovarian Cancer Metastases by Intraoperative Quantitative Fluorescence Protease Imaging in a Pre-Clinical Model. *Gynecol. Oncol.* **2009,** *112*(3), 616-622.

119. Marten, K.; Bremer, C.; Khazaie, K.; Sameni, M.; Sloane, B.; Tung, C. H.; Weissleder, R., Detection of Dysplastic Intestinal Adenomas Using Enzyme-Sensing Molecular Beacons in Mice. *Gastroenterology* **2002,** *122*(2), 406-414.

120. Herschel, J. F. W., On a Case of Superficial Colour Presented by a Homogeneous Liquid Internally Colourless. *Philos. Trans. R. Soc. Lond.* **1845,** *135*, 143-145.

121. Herschel, J. F. W., On the Epipölic Dispersion of Light. *Philos. Trans. R. Soc. Lond.* **1845,** *135*, 147-153.

122. Stokes, G. G., On the Change of Refrangibility of Light. *Philos. Trans. R. Soc. Lond.* **1852,** *142*, 463-562.

123. Lehmann, H., Über Ein Filter Für Ultra-Violette Strahlen Und Seine Anwendungen. *Phys. Z.* **1910,** *11*, 1039.

124. Reichert, K., Das Fluoreszenzmikroskop. *Phys. Z.* **1911,** *12*, 1010.

125. Heimstädt, O., Das Fluoreszenzmikroskop. *Z. Wiss. Mikrosk.* **1911,** *28*, 330.

126. Lehmann, H., Das Lumineszenzmikroskop, Seine Grundlagen Und Seine Anwendungen. *Z. Wiss. Mikrosk.* **1913,** *30*, 417.

127. Derrien, E., Note Prèliminaire Sur Quelques Faits Nouveaux Pour L'histoire Naturelle Des Porphyrines Animales. *C. R. Seances Soc. Biol. Fil.* **1924,** *91*(2), 634-636.

128. Derrien, E., Sur L'accumulation D'une Porphyrine Dans La Glande De Harder Des Rongeurs Du Genre Mus Et Sur Son Mode D'excrètion. *C. R. Seances Soc. Biol. Fil.* **1924,** *91*(2), 637-639.

129. Hama, Y.; Urano, Y.; Koyama, Y.; Bernardo, M.; Choyke, P. L.; Kobayashi, H., A Comparison of the Emission Efficiency of Four Common Green Fluorescence Dyes after Internalization into Cancer Cells. *Bioconjugate Chem.* **2006,** *17*(6), 1426-1431.

130. Longmire, M. R.; Ogawa, M.; Hama, Y.; Kosaka, N.; Regino, C. A. S.; Choyke, P. L.; Kobayashi, H., Determination of Optimal Rhodamine Fluorophore for in Vivo Optical Imaging. *Bioconjugate Chem.* **2008,** *19*(8), 1735-1742.

131. Ni, Y.; Zeng, L.; Kang, N. Y.; Huang, K. W.; Wang, L.; Zeng, Z.; Chang, Y. T.; Wu, J., Meso-Ester and Carboxylic Acid Substituted BODIPYs with Far-Red and near-Infrared Emission for Bioimaging Applications. *Chem. Eur. J.* **2014,** *20*(8), 2301-2310.

132. Fu, M.; Xiao, Y.; Qian, X.; Zhao, D.; Xu, Y., A Design Concept of Long-Wavelength Fluorescent Analogs of Rhodamine Dyes: Replacement of Oxygen with Silicon Atom. *Chem. Commun.* **2008,** (15), 1780-1782.

133. Egawa, T.; Hanaoka, K.; Koide, Y.; Ujita, S.; Takahashi, N.; Ikegaya, Y.; Matsuki, N.; Terai, T.; Ueno, T.; Komatsu, T.; Nagano, T., Development of a Far-Red to near-Infrared Fluorescence Probe for Calcium Ion and Its Application to Multicolor Neuronal Imaging. *J. Am. Chem. Soc.* **2011,** *133*(36), 14157-14159.

134. Koide, Y.; Urano, Y.; Hanaoka, K.; Terai, T.; Nagano, T., Development of an Si-Rhodamine-Based Far-Red to near-Infrared Fluorescence Probe Selective for Hypochlorous Acid and Its Applications for Biological Imaging. *J. Am. Chem. Soc.* **2011,** *133*(15), 5680-5682.

135. Koide, Y.; Urano, Y.; Hanaoka, K.; Terai, T.; Nagano, T., Evolution of Group 14 Rhodamines as Platforms for near-Infrared Fluorescence Probes Utilizing Photoinduced Electron Transfer. *ACS Chem. Biol.* **2011,** *6*(6), 600-608.

136. Edelson, R. L., Light Activated Drugs. *Sci. Am. Libr. Ser.* **1988,** *259*(2), 68-75.

137. Raab, O., Ueber Die Wirkung Fluorescierenden Stoffe Auf Infusorien. *Z. Biol.* **1900,** *39*, 524–546.

138. yon Tappeiner, H. M., *Dtsch. Med. Wochenschr.* **1903,** *47*, 2024.

139. Meyer-Betz, F., Untersuchungen Uber Die Biologische (Photodynamische) Wirkung Des Hamatoporphyrins Und Anderer Derivative Des Blut-Und Gallenfarbstoffs. *Dtsch. Arch. Klin. Med.* **1913,** *112*, 476-503.

140. Policard, A., Etude Sur Les Aspects Offerts Par Des Tumeurs Experimentales Examinees a La Lumikre De Wood. *C. R. Soc. Biol.* **1924,** *91*, 1423-1428.

141. Bellineier, D. A.; Ho, Y.-K.; Pandey, R. K.; Missert, J. R.; Dougherty, T. J., Distribution and Elimination of Photofrin Ii in Mice. *Photochem. Photobiol.* **1989,** *50*(2), 221-228.

142. Henderson, B. W.; Dougherty, T. J., How Does Photodynamic Therapy Work? *Photochem. Photobiol.* **1992,** *55*(1), 145-157.

143. Aveline, B.; Hasan, T.; Redmond Robert, W., Photophysical and Photosensitizing Properties of Benzoporphyrin Derivative Monoacid Ring a (Bpd-Ma)*. *Photochem. Photobiol.* **2008,** *59*(3), 328-335.

144. Ehud, B.-H.; R., D. T. M. A., Cytoplasmic Free Calcium Changes as a Trigger Mechanism in the Response of Cells to Photosensitization. *Photochem. Photobiol.* **1993,** *58*(6), 890-894.

145. Dougherty, T. J., *In Advances in Photochemistry*. Interscience: New York, 1992; Vol. 17.

146. Ringel, I.; Gottfried, V.; Levdansky, L.; Winkelman, J. W.; Kimel, S., Photochemotherapy: Photodynamic Therapy and Other Modalities. In *Proceeding of Spie*, Ehrenberg, B.; Jori, G.; Moan, J., Eds. 1996; Vol. 2625, 156-163.

147. Fields, P. E.; Gajewski, T. F.; Fitch, F. W., Blocked Ras Activation in Anergic $CD4^+$ T Cells. *Science* **1996,** *271*(5253), 1276-1278.

148. H., F. V.; R., P. W.; W., H. B., Drug and Light Dose Dependence of Photodynamic Therapy: A Study of Tumor Cell Clonogenicity and Histologic Changes. *Photochem. Photobiol.* **1987,** *45*(5), 643-650.

149. W., L. H.; D., P.; Marcus, A. J., Generation of Eicosanoids from Mast Cells Exposed to Protoporphyrin and Irradiation. *Clin. Res.* **1986,** *34*, 763.

150. Barr, H.; Brown, S. G., In Photodynamic Therapy. *Marcel Dekker: New York* **1992**, 201-218.

151. Foote, C. S., Definition of Type I and Type Ii Photosensitized Oxidation. *Photochem. Photobiol.* **1991,** *54*(5), 659-659.

152. Foote, C. S., Photophysical and Photochemical Properties of Fullerenes. In *Electron Transfer I*, Mattay, J., Ed. Springer: Berlin, Heidelberg, 1994; Vol. 169, 347-363.

153. Bartelmess, J.; Francis, A. J.; El Roz, K. A.; Castellano, F. N.; Weare, W. W.; Sommer, R. D., Light-Driven Hydrogen Evolution by BODIPY-Sensitized Cobaloxime Catalysts. *Inorg. Chem.* **2014,** *53*(9), 4527-4534.

154. Rey, Y. P.; Abradelo, D. G.; Santschi, N.; Strassert, C. A.; Gilmour, R., Quantitative Profiling of the Heavy-Atom Effect in BODIPY Dyes: Correlating Initial Rates, Atomic Numbers, and 1o2 Quantum Yields. *Eur. J. Org. Chem.* **2017,** *2017*(15), 2170-2178.

155. Hohenberg, P.; Kohn, W., Inhomogeneous Electron Gas. *Physical Review* **1964,** *136*(3B), B864-B871.

156. Kohn, W.; Sham, L. J., Self-Consistent Equations Including Exchange and Correlation Effects. *Physical Review* **1965,** *140*(4A), A1133-A1138.

157. Casida, M. E., Time-Dependent Density Functional Response Theory for Molecules. In *Recent Advances in Density Functional Methods*, Chong, D. P., Ed. 1995; Vol. 1, 155-192.

158. Theilhaber, J., Ab Initio Simulations of Sodium Using Time-Dependent Density-Functional Theory. *Phys. Rev. B* **1992,** *46*(20), 12990-13003.

159. Yabana, K.; Bertsch, G. F., Time-Dependent Local-Density Approximation in Real Time. *Phys. Rev. B* **1996,** *54*(7), 4484-4487.

160. Lopata, K.; Govind, N., Modeling Fast Electron Dynamics with Real-Time Time-Dependent Density Functional Theory: Application to Small Molecules and Chromophores. *J. Chem. Theory Comput.* **2011,** *7*(5), 1344-1355.

161. Bruner, A.; LaMaster, D.; Lopata, K., Accelerated Broadband Spectra Using Transition Dipole Decomposition and Padé Approximants. *J. Chem. Theory Comput.* **2016,** *12*(8), 3741-3750.

162. Becke, A. D., Density-Functional Thermochemistry. Iii. The Role of Exact Exchange. *J. Chem. Phys.* **1993,** *98*(7), 5648-5652.

163. Dreuw, A.; Head-Gordon, M., Failure of Time-Dependent Density Functional Theory for Long-Range Charge-Transfer Excited States: The Zincbacteriochlorin−Bacteriochlorin and Bacteriochlorophyll−Spheroidene Complexes. *J. Am. Chem. Soc.* **2004,** *126*(12), 4007-4016.

164. Yanai, T.; Tew, D. P.; Handy, N. C., A New Hybrid Exchange–Correlation Functional Using the Coulomb-Attenuating Method (Cam-B3lyp). *Chem. Phys. Lett.* **2004,** *393*(1), 51-57.

Chapter 2. Structure Based Modulation of Electron Dynamics in meso-(4-Pyridyl)-BODIPYs: A Computational and Synthetic Approach

2.1. Introduction

Over the past 30 years, there has been a considerable amount of research focused on exploring the chemistry, properties, versatility, and applications of BODIPY dyes that range from tunable laser dyes to probes for biological fluorescence imaging.[1-9] One aspect that has been under explored is the development of low molecular weight water-soluble BODIPY derivatives. The first report of a small water-soluble BODIPY was by Worries et al. in 1985 which used sulfonate groups to solubilize the fluorophore,[10] but by 2007 only a handful of water-soluble BODIPYs had been reported.[6] Since then, the main strategy used for water-solubilization of BODIPY derivatives consists on the introduction of water-solubilizing groups, particularly at the boron center, including: polyethylene glycols,[9,11-18] hydroxyls and ethers,[19-21] amines,[19] sulfonamides,[21] carboxylates,[9,11,17,21-23] sulfonates,[9,23-30] phosphonates,[9-11] quaternary ammonium salts,[8,9,24,28,31,32] carbohydrates,[33-35] and peptides.[24,28,32,36,37] Most of these groups increase the size of the dye, decrease its stability,[38,39] or utilize negative charges which tend to decrease the cell membrane permeability. On the other hand cationic dyes such as rhodamine[7] and (poly)cationic porphyrins[40] are able to electrostatically interact with the negative charges present on cell membranes, increasing their permeability. Therefore, the investigation of small, cationic, and electron-deficient BODIPYs such as *meso*-pyridylBODIPYs is of interest, particularly the 1,3,5,7-tetramethyl-8-(4-pyridyl)-BODIPY which has C_2 symmetry and is readily available from

This chapter is reprinted and adapted with permission from LaMaster, D. J., Kaufman, N. E. M., Bruner, A. S., Vicente, M. G. H., Structure Based Modulation of Electron Dynamics in meso-(4-Pyridyl)-BODIPYs: A Computational and Synthetic Approach. Journal of Physical Chemistry A **2018**, *122(31)*, 6372-6380.

the condensation of 2,4-dimethylpyrrole with 4-pyridylcarboxyaldehyde, followed by oxidation and boron complexation. Previous studies on *meso*-(4-pyridyl)-BODIPY using transient absorption spectroscopy found that following BODIPY excitation, the dye undergoes donor-photoinduced electron transfer (d-PeT) to a charge transfer state, which is quenched by subsequent intersystem crossing (ISC),[41] and the fluorescence quantum yield drops from 0.30 to <0.001.[42] Hence, these pyridinium BODIPYs have found applications as non-fluorescent heavy-atom free singlet oxygen generators, and several groups have reported on their ISC enhancement, via bromination and iodination.[42-48]

However, for bio-imaging applications, the aforementioned electronic properties of *meso*-pyridinium BODIPYs are undesirable, and no studies have been reported so far on the manipulation of the electronic structure of BODIPYs to restore the fluorescent properties of this type of dye. Herein, we describe the synthetic and computational studies on restoring the fluorescence of *meso*-pyridinium BODIPYs by inhibiting either the d-PeT process or the ISC. In other BODIPY platforms, there are reports of d-PeT inhibition achieved by installation of electron-withdrawing groups at the 2,6- positions.[49-51] Using a similar strategy, a small library of BODIPYs bearing various electron-withdrawing groups at the 2,6-positions was designed (shown in Figure 2.1). This library can be broken down into three groups: the weakly electron deficient halogenated BODIPYs **2A** – **5A**, the moderately electron deficient carbonylated BODIPYs **6A** – **10A**, and the strongly electron deficient ditrifluoromethyl and dicyano BODIPYs **11A** and **12A**. The mechanism of the potential fluorescence enhancement was also of interest and was expected to occur for one, or both, of two reasons. The first was that making the

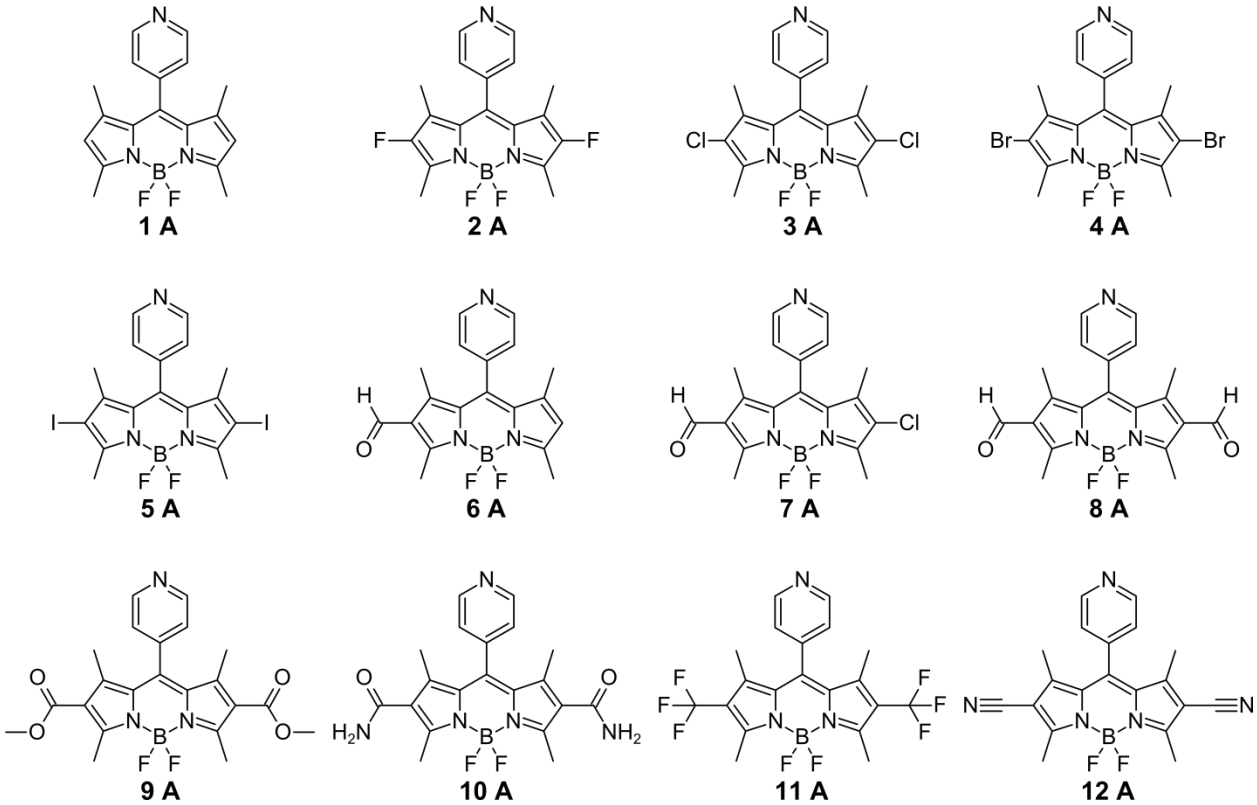

Figure 2.1. Structure of the A series BODIPYs used in quantum calculations. The corresponding N-methylated BODIPY cations are denoted “cat”.

BODIPY core electron deficient (i.e. increasing its oxidation potential) would make it less willing to give up the electron for the charge transfer and the second was that doing so would destabilize the charge transfer state, shortening its excited state lifetime, and inhibiting the ISC. A combination of density functional theory (DFT) and time-dependent DFT (TDDFT) calculations were used to determine whether the reported methodology applies to the *meso*-pyridinium BODIPY dyes and how the fluorescence is enhanced.

2.2. Results and Discussion

2.2.1. Quantum Chemical Calculations.

When evaluating orbital energy levels, molecular orbitals are calculated for the whole system to illustrate which parts of the molecular are involved in electronic transitions (e.g., BODIPY core or pyridinium ring). This shows how functionalization

affects transitions without the need to partition the molecule into fragments, which can introduce artifacts into the calculations.[50,52-54] It is worth noting that these calculations do not take into account spin-orbit coupling. Derivatives **4A** and **5A** both include large halogens known to induce the heavy-atom effect quenching their fluorescence.[45] They are included in this study for the difference in the halogens' electronegativities which will alter the vertical ionization potentials and add additional data points for potential results. In discussing the LUMOs of the cationic derivatives, the LUMOs localized on the pyridinium and BODIPY cores are denoted as $LUMO_{Py}$ and $LUMO_{BDP}$ respectively.

2.2.2. Calculated Oxidation Potentials.

The vertical ionization potentials used to calculate the oxidation potentials for the neutral library with the linear correlation relationship (eq. 2.1 for experimental and calculated vertical ionization potentials (VIPs) reported by Zhan and co-workers[55] from their systematic evaluation of calculated molecular properties from DFT calculations using B3LYP/6-31+G* (results summarized in Table 2.1). Within the framework of exact Kohn-Sham (KS) DFT, the energy of the highest occupied orbital is equivalent to the negative of the exact ionization potential; however, the negative of the HOMO energy calculated from most commonly used functionals deviates from the exact ionization potential. It has been reported that KS orbital energies can empirically corrected with a constant shift to reproduce experimental IPs.

$$IP_{calc} = 1.3124(-\varepsilon_{HOMO}) + 0.51414\ eV \qquad \text{(eq 2.1)}$$

Since their analysis showed that the VIPs were fairly insensitive to the choice of basis set and the 6-31+G** basis set varies only slightly from 6-31+G*, polarization functions also applied to hydrogen, their linear correlation was used.

The results in Table 2.1 show that the VIPs increase as the BODIPYs become more electron deficient. To show how the VIP changes with the functionalization, the ΔVIPs are also shown, given by the difference between the VIP of a given molecule and that of **1A**. In the halogenated systems **3A**-**5A**, the VIPs decreased with the halogen electronegativity, as expected. However, while the difluoro- derivative (**2A**) gave the smallest VIP increase, this can be explained by looking at the molecular orbital compositions. Fluorine is quite small, having high electronegativity and relatively stable valence electrons (i.e. low energy). In **2A**, the highest energy orbital involving the fluorine atoms is the HOMO-7, which is 3.281 eV lower in energy than the HOMO. The chlorines in **3A** contribute to the HOMO-1 while the halogens in **4A** and **5A** contribute to the HOMO. Since **3A**-**5A** halogens contribute to orbitals near the HOMO, they have a larger influence on respective VIPs.

Table 2.1. Calculated Orbital Energies and Vertical Ionization Potentials, in eV, for Neutral BODIPYs.

BODIPY	ε_{HOMO}	VIP	ΔVIP(**XA**–**1A**)
1A	-5.814	8.144	
2A	-6.034	8.433	0.289
3A	-6.072	8.483	0.339
4A	-6.051	8.456	0.312
5A	-6.043	8.444	0.300
6A	-6.170	8.611	0.467
7A	-6.487	9.027	0.883
8A	-6.276	8.751	0.607
9A	-6.319	8.807	0.663
10A	-6.240	8.704	0.560
11A	-6.566	9.131	0.987
12A	-6.742	9.363	1.218

The carbonyl derivatives are also included in Table 2.1. Unlike the halogenated systems, this group of carbonyl derivatives (**6A**–**10A**) does not show a direct correlation

to the strength of the withdrawing group. Instead, the VIP depends more on how electrons contribute to higher energy orbitals. Since several electrons are involved in these functional groups, VIP values can be close in energy. As such, ΔVIPs are also calculated to better capture the energy differences (Table 2.1). For the carbonyl systems, the chloro-formyl (**7A**) had the largest increase, followed by diamide (**9A**), dialdehyde (**8A**), diester (**10A**), and monoaldehyde (**6A**). If these had been ranked by decreasing electron withdrawing strength, the expected order would be **10A**, **9A**, **8A**, **7A**, and **6A**. The large increase in the chloro-formyl (**7A**) is best explained by the contributions of the chlorine to the HOMO, which shifts the VIP by +0.416 eV relative to **6A** monoaldehyde. The other outlier **10A** (diester) has no contributions to the HOMO, HOMO-1, or HOMO-2 orbitals, both of which had significant contributions from other withdrawing groups. Since the ester groups do not participate in the high energy orbitals of the valence, they have a small impact on the VIP. Continuing with the remaining derivatives (**11A** and **12A**), the values increased consistent with electron withdrawing strength. This trend is expected with the dicyano derivative (**12A**) giving the largest overall increase of 1.218 eV.

2.2.3. Time-Dependent DFT Calculations.

As a sanity to check help ensure the systems are being modelled properly, the first two excitations in the TDDFT analysis of the neutral library were checked and the results are summarized in Appendix A Table A1. These results show the HOMO→LUMO transition to be the first excitation with a strong oscillator strength (*f*) for all twelve dyes. The second excitation was HOMO-1 to LUMO, with noted exceptions.

The TDDFT analysis of the first few cationic derivatives modeled, summarized in Appendix A Table A2, revealed that the B3LYP hybrid functional is insufficient to accurately describe their excited states. DFT is known to fail for charge transfer in molecules and range-separated functionals have been developed to address this.[56] The typical BODIPY is known to have a strong $S_0 \rightarrow S_1$ transition and adding the pyridinium with a low lying LUMO should only introduce a single electronic transition that is lower in energy than the HOMO→LUMO transition of the BODIPY core.[57-59] The failure can be seen in both the degeneracy of the $LUMO_{BDP}$ and $LUMO_{Py+1}$ as well as the extra transitions from sub-HOMO orbitals that appeared between the HOMO→LUMO and HOMO→LUMO+1 transitions. In these cases, the lowest energy transition was HOMO→LUMO with the LUMO being localized on the pyridinium ring. The second lowest energy transition should have corresponded to the BODIPY core excitation (HOMO→LUMO+1), however, this transition was calculated to be the fifth transition with a much higher energy. Since the B3LYP functional proved to be insufficient for describing the long range interactions, the range-separated functional CAM-B3LYP was used instead.[59] The vertical excitation energy (VEE), oscillator strength (*f*), and predominant transition character (e.g., mostly HOMO→LUMO) were then calculated and the results for the first two transitions, summarized in Table 2.2, are consistent with experimental results for these fluorophores[42,59,60] showing the lowest energy transition as the HOMO→$LUMO_{Py}$ and the second lowest energy transition as the BODIPY absorption (HOMO→$LUMO_{BDP}$).

Table 2.2. Calculated CAM-B3LYP S_1 and S_2 Vertical Excitation Energy (VEE, eV), Oscillator Strengths (*f*, arbitrary units), and Predominant Transition Character for Cationic BODIPYs.

	S_1			S_2		
BODIPY	VEE	*f*	Trans.	VEE	*f*	Trans.
1catA	1.9148	0.00024	H → L	2.8746	0.55350	H → L+1
2catA	2.0246	0.00037	H → L	2.7642	0.47242	H → L+1
3catA	2.0216	0.00045	H → L	2.7234	0.57025	H → L+1
4catA	2.0089	0.00034	H → L	2.7113	0.60764	H → L+1
5catA	1.9881	0.00016	H → L	2.6823	0.67528	H → L+1
6catA	2.0170	0.00032	H → L	2.8712	0.66292	H → L+1
7catA	2.0949	0.00043	H → L	2.8465	0.78719	H → L+1
8catA	2.0628	0.00045	H → L	2.7969	0.67844	H → L+1
9catA	2.2614	0.00068	H → L	2.8505	0.68369	H → L+1
10catA	2.1953	0.00065	H → L	2.8657	0.80877	H → L+1
11catA	2.2759	0.00015	H → L	2.9184	0.68027	H → L+1
12catA	2.3255	0.00008	H → L	2.8084	0.72367	H → L+1

Figure 2.2 shows the HOMO, LUMO, and LUMO+1 orbitals, localized on the BODIPY, pyridinium, and BODIPY respectively for all cationic 12 dyes which means that none of the functionalizations were able to re-order the low laying virtual orbitals.. The first transition was found to be a strictly HOMO→$LUMO_{Py}$ dark state, while the second transition was HOMO→$LUMO_{BDP}$ with a strong oscillator strength. These results indicate that the BODIPYs' strong absorption will decay to the charge-transfer state. As such, it can be concluded that the BODIPY core oxidation potential has a negligible impact on the d-PeT charge transfer state for this BODIPY platform.

These results can be explained in two ways: by looking at the molecular orbitals of the BODIPY core (Figure 2.2) and by looking at the excited state potential energy surface. In the generic BODIPY platform, the HOMO is partially localized on the 2,6-positions, thus, the functionalizations employed decrease the energy of the HOMO. With the BODIPY and pyridinium orbitals orthogonal to each other, changes to the

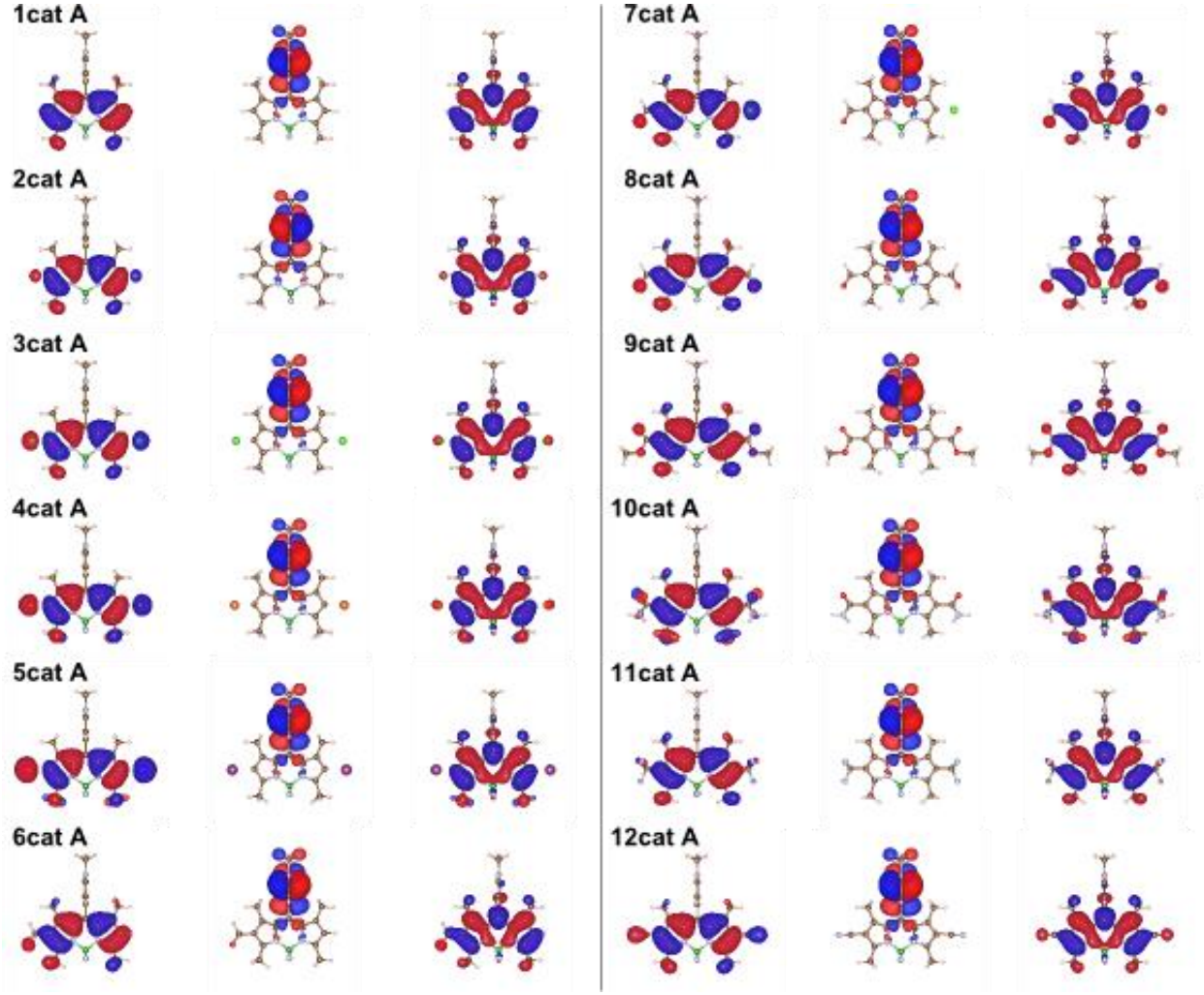

Figure 2.2. HOMO (left), LUMO (center), and LUMO+1 (right) of BODIPYs **1cat A** – **12cat A**.

BODIPY core orbitals due to functionalization do not significantly affect the orbitals on the pyridinium, which explains the minimal impact on the $LUMO_{Py}$. The excited state potential energy surface can depict the BODIPY as a donor-acceptor system. Once the electron is excited to the $LUMO_{BDP}$ (i.e. LUMO+1), the structure will relax to the S_2 equilibrium geometry and the electron will non-radiatively decay to the $LUMO_{Py}$ (i.e. LUMO) so the excitation itself can be viewed as the donation. As long as the $LUMO_{Py}$ is lower in energy than the $LUMO_{BDP}$, the donation will always occur. Therefore, the only way to inhibit the d-PeT is to re-order the orbitals, which can be accomplished by raising

the energy of the undesired acceptor ($LUMO_{Py}$), lowering the energy of the desired acceptor ($LUMO_{BDP}$), or a combination thereof.

Since it is of interest to raise the energy of $LUMO_{Py}$, methoxy groups were used to donate electron density into the ring. Although dimethylamino groups are stronger electron donors, their large size would have sterically hindered the pyridine methylation during synthesis and their basic nature could lead to their methylation to ammonium salts instead of the pyridine. To evaluate the best positions for the methoxy groups, the orbitals of the N-methylpyridinium cation (without the BODIPY) were calculated and plotted to determine where the LUMO is localized using DFT and the CAM-B3LYP functional. From this, the $LUMO_{Py}$ is located primarily on the 2,3- and 5,6-positions shown in Figure . The 2,-6 positions were selected for functionalization because functionalization at the 3,5- positions has already been reported to decrease synthetic yields and 2,6-dimethoxypyridyl BODIPY can be prepared from commercially available starting materials (2,4-dimethylpyrrole and methyl 2-chloro-6-methoxypyridine-4-carboxylate) with minimal additional work. The orbitals of the radical cation were also plotted to confirm they do not change upon population with an electron. The HOMO and LUMO of the radical cation matched the LUMO and LUMO+1 of the cation and the functionalization did not alter the localization in the proposed derivatives. Proof of concept for this strategy was then obtained via a test case by modelling the N-methylpyridinium (**N-MePy$^+$, A**), 2-methoxy- N-methylpyridinium (**2-OMe-N-MePy$^+$, B**), and 2,6-dimethoxy-N-methylpyridinium (**2,6-DiOMe-N-MePy$^+$, C**) cations (Appendix A

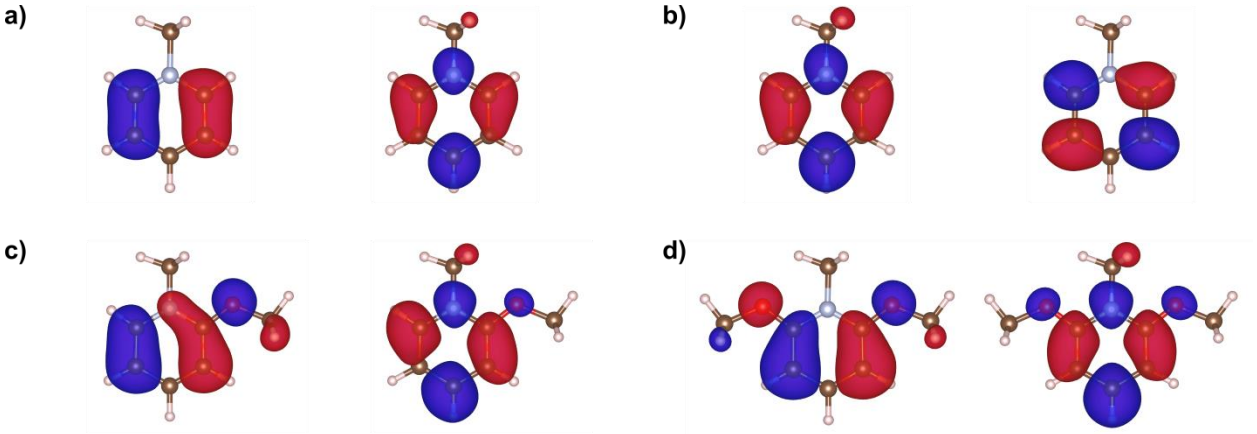

Figure 2.3. MO plots of the HOMO (left) and LUMO of a) N-methylpyridinium **(N-MePy^{+}**), b) N-methylpyridinium radical (**N-MePy$^{+\bullet}$**), c) 2-methoxy-N-methylpyridinium (**2-OMe-N-MePy^{+}),** and d) 2,6-dimethoxy-N-methylpyridinium (**2,6-DiOMe-N-MePy^{+}**) cations.

Table A3). It was found that one methoxy group could increase the LUMO energy by 0.509 eV and a second could raise it by an additional 0.488 eV with an overall increase of 1.003 eV.

In addition to raising the energy of the $LUMO_{Py}$ to reorder the states, we can also consider lowering the energy of $LUMO_{BDP}$. The $LUMO_{BDP}$ is largely localized on the meso-position and to a smaller extent on the 1,7-positions. Since the 2,6-dicyano-BODIPY (**12**) had the largest oxidation potential increase, it has the greatest shift in the orbital energy. Thus, the 1,7-dicyanoBODIPY (**13A**) was chosen to model the effects of lowering the $LUMO_{BDP}$. The new additions to the original library and their calculated VIPs are shown in Figure 2.4 and Table 2.3, respectively.

Moving the cyano groups from HOMO (**12catA**) to LUMO (**13catA**) structural positions decreased the VIP by 0.227 eV, but was able to effectively re-order the $LUMO_{Py}$ and $LUMO_{BDP}$, providing a 0.273 eV energy gap. The addition of methoxy groups to the pyridine unit slightly decreased the overall oxidation potential of the dyes by 0.025 eV per OMe. It should be noted that for series **12A-C**, each OMe group

decreased the VIP by ~0.03 eV. However, for series **13A-C**, there was an additive effect where the first OMe caused a 0.057 eV decrease while the second caused an additional 0.191 eV decrease.

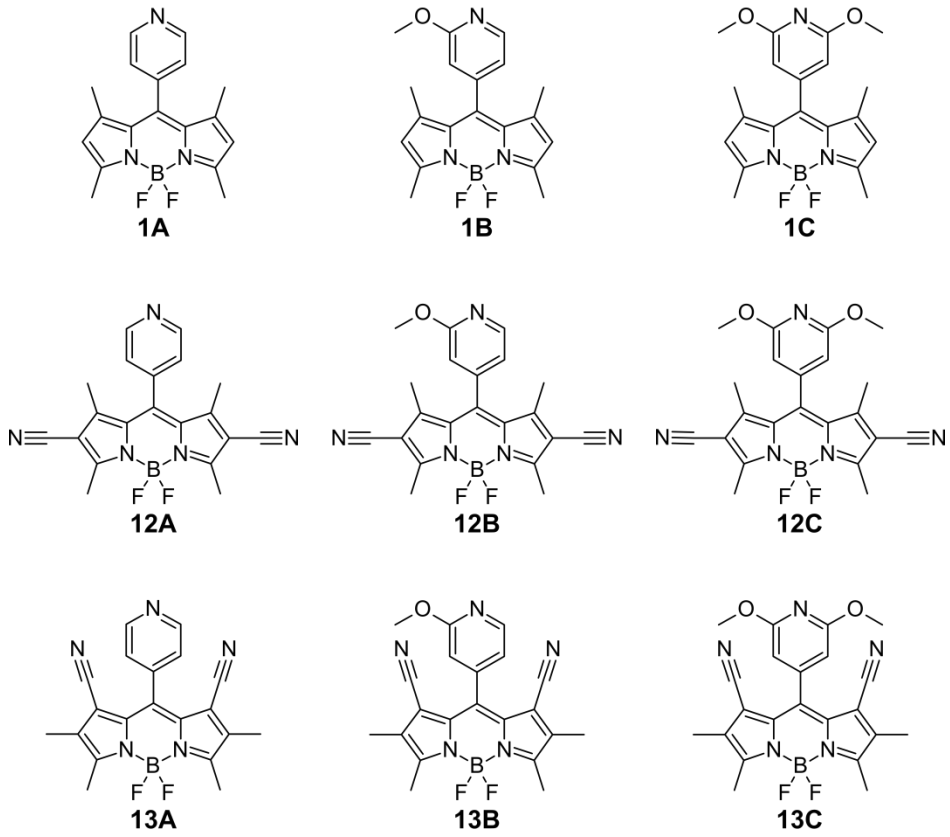

Figure 2.4: Structures of the Py'-BODIPY series **A–C** used in quantum calculations.

Table 2.3. Calculated Neutral Py'-BODIPY Orbital Energies and Vertical Ionization Potentials in eV.

BODIPY	ε_{HOMO}	VIP	ΔVIP(**X–1A**)
1A	-5.814	8.144	
1B	-5.795	8.119	-0.025
1C	-5.775	8.094	-0.050
12A	-6.742	9.363	1.218
12B	-6.719	9.333	1.188
12C	-6.693	9.298	1.154
13A	-6.569	9.135	0.991
13B	-6.525	9.078	0.934
13C	-6.380	8.888	0.743

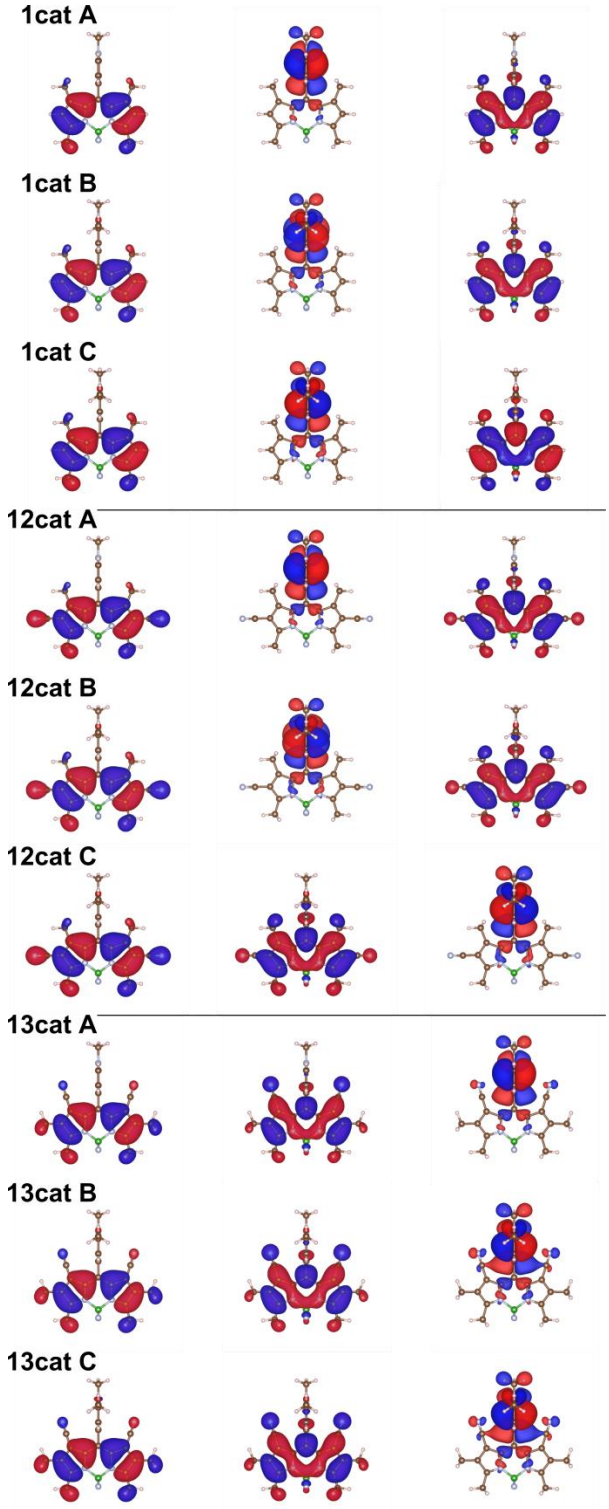

Figure 2.5. HOMO (left), LUMO (center), and LUMO+1 (right) of BODIPYs **1cat A-C**, **12cat A-C**, & **13cat A-C**.

The orbital energies and MO plots of BODIPYs **1catA-C**, **12catA-C**, and **13catA-C** (collectively referenced as Py'-BODIPYs) are summarized, and compared, in Table 2.4 and Figure 2.5 respectively, while the TDDFT results are summarized in Appendix A Table A4.

The molecular orbital plots show alteration of the $LUMO_{Py}$ alone to be an ineffective strategy by the lack of change in the orbitals of **1catA-C**. The lack of change in **12cat B** indicates that the combination of increasing the oxidation potential along with the energy of $LUMO_{Py}$ via a single methoxy group is also ineffective. However, the combination of the most effective $LUMO_{Py}$ increase and BODIPY VIP increase functionalizations (**12catC**) was able to raise the $LUMO_{Py}$ energy above that of the $LUMO_{BDP}$, though the energy difference is rather small at 0.080 eV and as such, d-PeT is still possible due to vibrational excitation. Adjusting the $LUMO_{BDP}$ (**13catA**–**C**), on the other hand, effectively re-ordered the orbitals and separated them by energy differences of 0.273 eV, 0.793 eV, and 1.115 eV respectively, which prevents d-PeT from occurring. The TDDFT calculations also show this with the first transition being HOMO→LUMO for **12catC** and **13catA-C** both having a strong oscillator strength and corresponding to the typical BODIPY excitation.

Table 2.4. Calculated Cationic Py'-BODIPY Orbital Energies in eV.

BODIPY	Orbital Energies (ε_X)			ΔE(**Xcat – XcatA**)		
	HOMO	$LUMO_{Py}$	$LUMO_{BDP}$	HOMO	$LUMO_{Py}$	$LUMO_{BDP}$
1catA	-9.472	-5.420	-4.545			
1catB	-9.399	-4.983	-4.464	+0.072	+0.437	+0.081
1catC	-9.332	-4.561	-4.383	+0.140	+0.858	+0.162
12catA	-10.298	-5.889	-5.449			
12catB	-10.139	-5.609	-5.149	+0.159	+0.280	+0.300
12catC	-10.227	-5.359	-5.439	+0.071	+0.530	+0.010
13catA	-10.162	-5.001	-5.274			
13catB	-10.073	-4.737	-5.530	+0.089	+0.264	-0.256
13catC	-10.010	-4.340	-5.455	+0.152	+0.661	-0.181

With the success from 1,7-functionalization, the effects were further studied to determine if weaker electron withdrawing groups would have similar results by modeling the 1,7-difluoro (**14A**) and 1,7-dichloro (**15A**) derivatives. It is worth noting that modeling the 1,7-di(trifluoromethyl) derivative was attempted, but the $-CF_3$ groups are sufficiently large that the steric interactions with the *meso*-pyridyl group would eliminate synthetic feasibility. The VIPs of the neutral dyes and the orbital energies of the cationic derivatives are shown in Table 2.5 with the data for **1A** and **13A** included for comparison. The VIPs follow the same trend observed in for the 2,6-difluoro (**2A**) and 2,6-dichloro (**3A**) derivatives as expected. The orbital energies of **14catA** and **15catA** both show that neither derivative is able to re-order the low laying orbitals as is observed in **13catA**. The TDDFT results, summarized in Table 2.6 also show this.

Table 2.5. Calculated Vertical Ionization Potentials, in eV, for Neutral BODIPYs **1A** and **13-15A** and the Orbital Energies, in eV, of the Respective Cations.

BODIPY	VIP	ΔVIP (**XA**–**1A**)	Orbital Energies (ε_X)			ΔE(**XcatA – 1catA**)		
			HOMO	$LUMO_{Py}$	$LUMO_{BDP}$	HOMO	$LUMO_{Py}$	$LUMO_{BDP}$
1A	8.144		-9.472	-5.420	-4.545			
14A	8.450	0.306	-9.661	-5.192	-4.690	-0.189	+0.228	-0.145
15A	8.465	0.320	-9.677	-5.174	-4.860	-0.205	+0.246	-0.315
13A	9.135	0.991	-10.139	-5.609	-5.149	-0.667	-0.189	-0.604

Table 2.6. Calculated S_1 and S_2 Vertical Excitation Energy (VEE, eV), Oscillator Strengths (*f*, arbitrary units), and Predominant Transition Character for Cationic BODIPYs **1A** and **13-15A**.

BODIPY	S_1			S_2		
	VEE	*f*	Trans.	VEE	*f*	Trans.
1catA	1.9148	0.00024	H→L	2.8746	0.55350	H→L+1
14catA	2.3690	0.00026	H→L	2.9101	0.58256	H→L+1
15catA	2.4106	0.00013	H→L	2.7732	0.60880	H→L+1
13catA	2.5747	0.62108	H→L	2.9304	0.00008	H→L+1

2.2.4. Inter-System Crossing (ISC).

Since most of the BODIPYs studied will still undergo d-PeT, the effects of 2,6-difunctionalization on ISC are of interest. To this end, **1catA** and **12catA** were studied further. Both structures were optimized along their S_1 excited states first using B3LYP and then with CAM-B3LYP. The B3LYP functional has a smaller computational expense than CAM-B3LYP so it was used to generate a more accurate input structure to feed in to the range-separated functional optimization. The energies of the S_1 and the triplet excitation with the same transition character (T_2 for both dyes) were then compared. The results, summarized in Table 2.7, show that the nature of the transitions, the orbital populations, the states involved, and the singlet-triplet energy gaps are identical for both dyes. These results indicate that the electronic possibility of ISC is unchanged in the 2,6-difunctionalized derivatives.

Table 2.7. Calculated S_1 and analogous triplet state excitations for S_1 relaxed structures of BODIPYs **1catA** and **12catA**.

BODIPY	Excitation	VEE (eV)	Trans.	Population	$\Delta(S_1\text{-}T_2)$ (eV)
1catA	S_1	1.4688	H → L	0.984261	0.0319
	T_2	1.4369	H → L	0.980000	
12catA	S_1	1.8740	H → L	0.974631	0.0319
	T_2	1.8421	H → L	0.973013	

2.2.5. Synthesis and Spectroscopic Properties.

BODIPYs **1A** and **1catA** were synthesized using the previously reported methodology.[61] In summary, 2,4-dimethylpyrrole reacted with 4-pyridylcarboxaldehyde in the presence of TFA to afford the dipyrromethane, which after DDQ oxidation and BF_3 complexation produced BODIPY **1A** in 46% yield. Chlorination of **1A** using trichloroisocyanuric acid[62] in dichloromethane at room temperature, gave BODIPY **3A** in

68% yield. The cationic BODIPYs **1catA** and **3catA** were obtained by methylation using methyl iodide in acetonitrile, as previously reported.[44]

The absorption and emission spectra of BODIPYs **1A** and **3A** were obtained in acetonitrile and dichloromethane at room temperature as were the spectra for **1Acat** and **3Acat** in addition to water and the results are shown in Table 2.8, Figure 2.6, and Figure 2.7. The absorption spectra displayed the characteristic BODIPY profile with a sharp peak due to the $S_0 \rightarrow S_1$ ($\pi \rightarrow \pi^*$) transition with a higher energy shoulder corresponding to the first vibrational mode. The absorption and emission spectra of **1catA** and **3catA** did not change upon switching the solvent from acetonitrile to water. In both cases, methylation caused about 10 nm bathochromic shift in the absorption while the emission shifted substantially to about 600 nm in both acetonitrile and water, and exhibited a broad, poorly resolved profile characteristic of luminescent charge recombination. These results are in agreement with previous observations of the spectroscopic behavior of **1A** and **1catA** in dichloromethane.[41,44]

Table 2.8. Photophysical properties of synthesized BODIPYs in different solvents.

Solvent	BODIPY	λ_{max} (nm)		Stokes Shift (nm)	Φ_f*	ε (M^{-1} cm^{-1})
		abs	em			
CH_2Cl_2	**1A**	505	533	28	–	80700
	1catA	515	531/646	16/131	–	34800
	3A	534	563	29	–	53800
	3catA	548	570/645	22/97	–	40500
CH_3CN	**1A**	501	515	14	0.31[a]	72100
	1catA	509	596	87	0.019[b]	26000
	3A	528	546	18	0.58[a]	50800
	3catA	538	600	62	0.048[b]	23400
H_2O	**1catA**	509	600	91	0.004[b]	31600
	3catA	540	605	65	0.038[b]	4100

*Relative quantum yields determined using: (a) rhodamine-6G (Φ_f = 0.86) in methanol as the standard, λ_{ex} = 473 nm [63] and (b) $Ru(bpy)_3Cl_2$ in water as the standard (Φ_f = 0.028), λ_{ex} = 436 nm.[64]

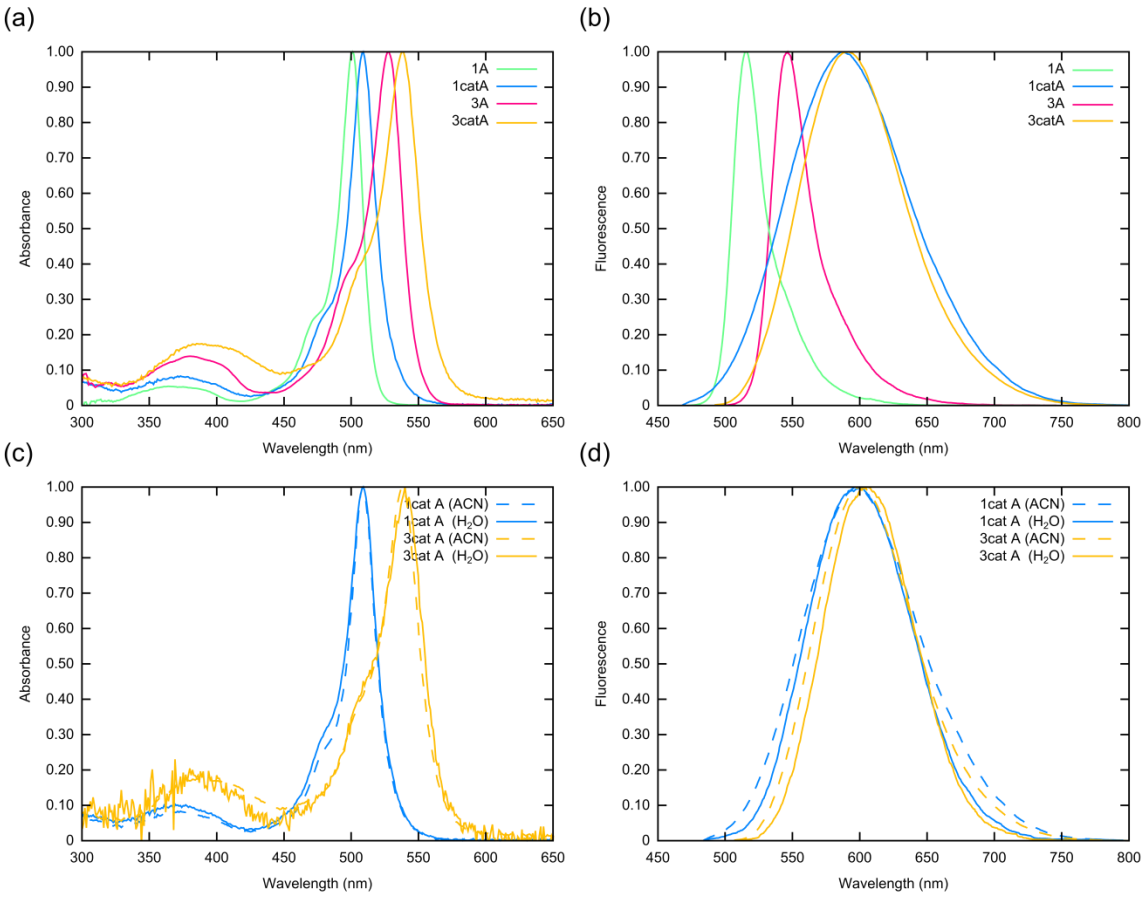

Figure 2.6. Normalized (a) absorption and (b) emission spectra of **1A** (green), **1catA** (blue), **3A** (red), and **3catA** (yellow) in acetonitrile along with the normalized (c) absorption and (d) emission spectra of **1catA** (blue) and **3catA** (yellow) in acetonitrile (dashed) and water (solid) at room temperature.

With the chlorines on the 2,6-positions being mildly electron-withdrawing groups, they had a small to moderate impact on the fluorescence quantum yield of both the neutral and ionic derivatives in acetonitrile, resulting in a two-fold increase for **3A** and about a 2.5-fold increase for **3catA**. The quantum yield has been previously observed to increase upon 2,6-dichlorination of *meso*-arylBODIPYs.[2,62,65,] After accounting for the two-fold increase in Φ_f from **1A** to **3A**, **3catA** had an additional 26% increase from **1catA**. When switching the solvent to water, the fluorescence quantum yields decreased due to the increased solvent polarity stabilizing the charge transfer state

which facilitated the subsequent deactivation by ISC, however, this led to an order of magnitude increse from **1catA** to **3catA**. With the d-PeT acceptor orbitals being unaffected by the functionalization, the fluorescence enhancement observed for **3catA** is attributed to an alteration of the excited state lifetime resulting from the higher BODIPY oxidation potential increasing the rate of charge recombination by magnifying the electron-hole electrostatic interaction.

Relative to acetonitrile and water, the spectra in dichloromethame displayed bathochromic shifts in both the absorption and emission wavelengths in all four cases.

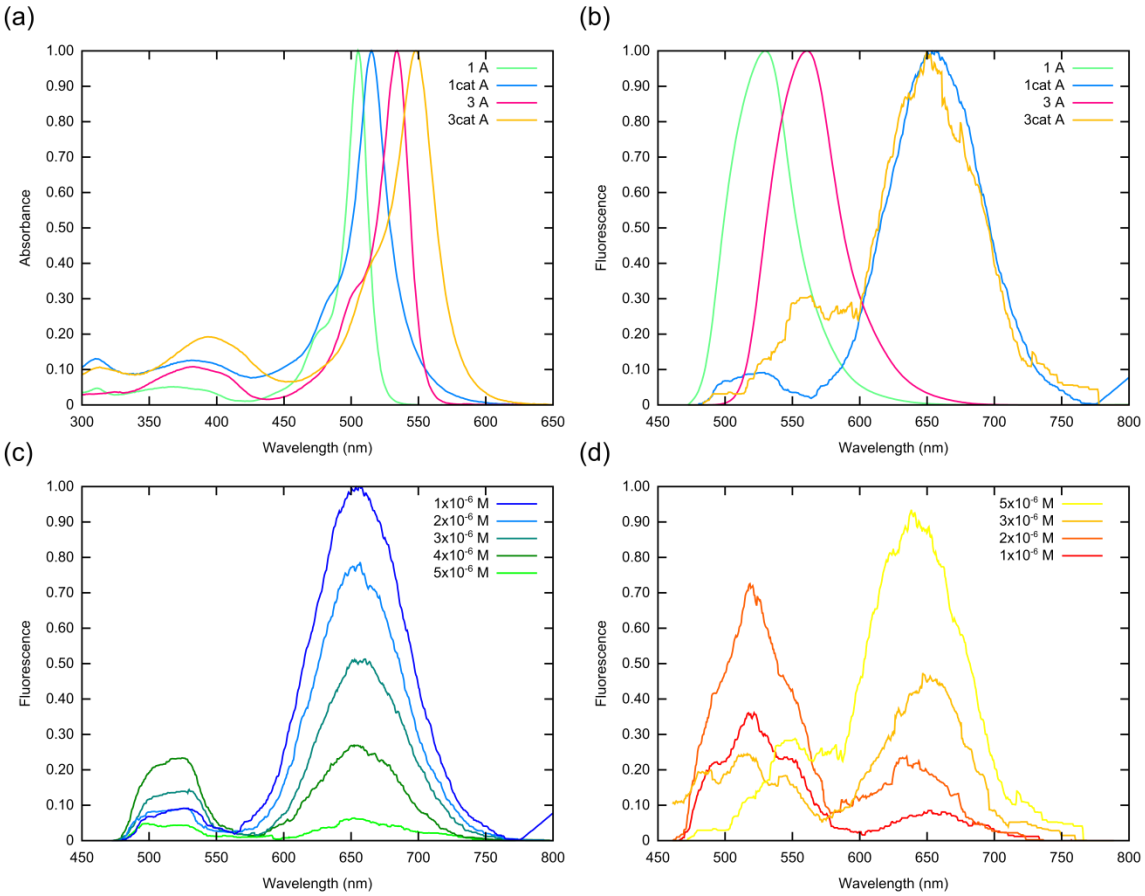

Figure 2.7. Normalized (a) absorption and (b) emission spectra of **1A** (green), **1catA** (blue), **3A** (red), and **3catA** (yellow) in dichloromethane and the emission profiles as a function of the concentration for **1catA** (c) and **3catA** (d).

The emission profile for **1catA**, upon excitation at 486 nm, shows two peaks. The first peak, corresponding to emission from the BODIPY core, at 531 nm lines up with emission from **1A** at 533 nm. The second peak, at 646 nm, is emission from the charge recombination. At both 1.0 and 2.0 μM, the peak intensities are equivalent, but the intensity of the higher energy peak decreases when the concentration is increased to 3.0 μM and again at 4.0 μM, but then it remains constant when going up to 5.0 μM. The spectra of **3catA** exhibits analogous features with the higher energy peak at 570 nm corresponding to the emission of **3A** and the lower energy peak at 645 nm resulting from charge recombination, however, the BODIPY emission predominates the spectrum at 1.0 and 2.0 μM concentrations and decreases when the concentration is increased. The enhanced BODIPY emission is attributed to the increased oxidation potential retarding the d-PeT process in dilute solutions of non-polar solvent allowing for increased BODIPY emission. At greater concentrations, the highly polar nature of **3catA** itself begins to change the effective dielectric constant of the solvent facilitating a restoration of the d-PeT process kinetics. Recalling the calculated VIPs, the dichlorination only resulted in a 0.339 eV increase while installation of the 2,6-dicyano groups resulted in a 1.218 eV increase. This suggests that **12A** should display photophysical properties with a dramatic improvement over **3A**. The synthesis of such a derivative is currently underway in our laboratories.

2.3. Conclusions

Several electronic structure-based molecular properties for a library of *meso*-(4-pyridyl) BODIPYs have been calculated and shown that the combination of increasing the BODIPY core oxidation potential as well as increasing the pyridinium reduction

potential, can re-order the low lying excited states which inhibits d-PeT; however, decreasing the BODIPY core reduction potential has a greater capacity for both re-ordering those states and sufficiently separating them. The states involved in the ISC were found to be unaffected by the 2,6-functionalization with various electron-withdrawing groups. Additionally, a new water soluble fluorescent *meso*-(4-pyridium)-BODIPY was synthesized, and a novel mechanism of fluorescence enhancement was demonstrated. In our work, structure based modulation of excited state electron dynamics was demonstrated and manipulation of fluorescence behavior was observed.

2.4. Methodology

2.4.1. Computational

All calculations were performed using the NWChem 6.5 software package.[66] Molecular properties were calculated for gas phase structures at 0 Kelvin. The ground state structures were optimized using density functional theory with the hybrid B3LYP[67,68] functional, the 6-31+G** basis set, and confirmed by subsequent frequency calculations. The energies of the HOMO were then used to calculate the vertical ionization potentials (VIPs) as a means of evaluating the electron deficiency of the BODIPY, which influences the d-PeT to the pyridinium ring. Furthermore, these VIPs can be used to then calculate the experimental oxidation potentials as shown by Zhan and co-workers.[55] Electronic transitions were calculated for each optimized structure using TDDFT with the B3LYP and the range-separated CAM-B3LYP[56] functionals. Here, the range-separated functional is used to describe the long-range interactions necessary to capture transitions between the BODIPY and the pyridinium ring. To evaluate the effect of functionalization on the quenching of the charge transfer state, structures were

optimized on their first singlet excited state (S_1). This yields the singlet-triplet energy gap involved in the intersystem crossing.

2.4.2. Experimental

1.3.1.1 General

All solvents and reagents were obtained from Sigma-Aldrich, Tokyo Chemical Industry, and Honeywell International Incorporated. The solvents were dried over 4Å molecular sieves as needed. The reagents were used as received without purification. Reactions were monitored using 0.2 mm silica gel plates (with indicator, polyester backed, 60 Å, pre-coated) and UV lamp. Liquid chromatography was performed on preparative TLC plates or via silica gel column chromatography (60 Å, 230−400 mesh) and all solvent systems were buffered with 0.1% triethylamine. NMR spectra were obtained on 400 (^{1}H) and 500 MHz (^{13}C) spectrometers at room temperature. Chemical shifts (δ) are given in parts per million (ppm) in $CDCl_3$ (7.27 ppm for ^{1}H NMR, 77.0 ppm for ^{13}C NMR) or C_2D_6SO (2.50 ppm for ^{1}H NMR, 39.5 ppm for ^{13}C NMR); coupling constants (J) are given in hertz. High-resolution mass spectra were measured on an ESI-TOF mass spectrometer in positive mode. All absorption spectra were recorded on a Varian Cary 50 Bio and emission spectra were recorded on a Perkin Elmer LS 55 Luminescence Spectrophotometer, at room temperature. Spectrophotometric grade solvents and quartz cuvettes (10 mm path length) were used. For the determination of the optical density (ε), solutions with absorbance at λ_{max} between 0.5 and 1 were used. For the determination of quantum yields, dilute solutions with absorbance between 0.03 and 0.05 at the particular excitation wavelength (462, 473, 488, 496 nm for **1A**, **1catA**, **3A**, and **3catA** respectively) were used and all measurements were taken within 8 hours

after solution preparation.[63,69] The external standards employed were rhodamine 6G in methanol and $Ru(bpy)_3Cl_2$ in water. BODIPY **1A** was prepared following a reported procedure[61] with a modified purification using 1:4 EtOAc/dichloromethane and 4% EtOAc/dichloromethane instead of 1:1 EtOAc/hexanes due to the increased solubility. BODIPY **1catA** was prepared in the same way as **3catA** and its physical data matched literature reports.[41]

2.4.3. Synthesis

2,6-Dichloro-8-(4-pyridyl)-1,3,5,7-tetramethyl-BODIPY (3A). To an oven dried flask charged with BODIPY **1A** (0.0118 g, 0.04 mmol) in dichloromethane (10.0 mL) was dropwise added trichloroisocyanuric acid (0.0076 g, 0.03 mmol, 2.62 eq) in dichloromethane (4.0 mL) and the mixture was stirred at room temperature under a nitrogen atmosphere. After TLC showed consumption of the starting material (about 30 minutes) the solution was purified over silica by column chromatography eluting with 2% methanol/dichloromethane yielding 10 mg, 69% yield (red solid): ^{1}H NMR (400 MHz, $CDCl_3$): δ = 8.85-8.84 (dd, J = 5.9 and 1.5 Hz, 2H), 7.31-7.30 (dd, J = 5.9 and 1.6 Hz, 2H), 2.61 (s, 6H), 1.42 (s, 6H); ^{13}C NMR (500 MHz,$CDCl_3$): δ = 153.7, 150.9, 142.8, 138.2, 137.5, 128.6, 123.3, 123.1, 12.5, 12.2 ppm; HRMS (ESI): *m/z* calcd (%) for $C_{18}H_{19}BF_2N_3Cl_2$: 393.0891[M+H]+; found: 393.0902; UV/Vis (CH_3CN): λ_{max}= 518, λ_{em}= 546 nm; (CH_2Cl_2): λ_{max}= 534, λ_{em}= 563 nm.

2,6-Dichloro-8-(N-methyl-4-pyridyl)-1,3,5,7-tetramethylBODIPY (3catA). In a 10 mL round bottom flask wrapped in foil, BODIPY **3A** (0.0111 g, 0.028 mmol) was dissolved in anhydrous MeCN (2.0 mL) and methyl iodide (2.0 mL). After refluxing for 1 hour, TLC showed consumption of starting material and the solvent was removed under

reduced pressure. Yield 15 mg, 100% (greenish-gray solid): ^{1}H NMR (400 MHz, DMSO-d_6): δ = 9.24-9.23 (d, J = 6.6 Hz, 2H), 8.44-8.42 (d, J = 6.7 Hz, 2H), 4.47 (s, 3H), 2.55 (s, 6H), 1.30 (s, 6H); ^{13}C NMR (500 MHz, DMSO-d_6): δ = 154.0, 149.6, 147.5, 138.0, 136.7, 128.2, 128.1, 123.0, 49.0, 13.2, 12.9 ppm; HRMS (ESI): *m/z* calcd (%) for $C_{19}H_{19}BF_2N_3Cl_2$: 407.1048[M*]+; found: 407.1048; UV/Vis (CH_3CN): λ_{max}= 530, λ_{em}= 596 nm; (CH_2Cl_2): λ_{max}= 548, λ_{em}= 570, 645 nm.

2.5. References

1. Bañuelos, J., BODIPY Dye, the Most Versatile Fluorophore Ever? *Chem. Rec.* **2016,** *16*(1), 335-348.

2. Duran-Sampedro, G.; Agarrabeitia, A. R.; Garcia-Moreno, I.; Costela, A.; Bañuelos, J.; Arbeloa, T.; López, A. I.; Chiara, J. L.; Ortiz, M. J., Chlorinated BODIPYs: Surprisingly Efficient and Highly Photostable Laser Dyes. *Eur. J. Org. Chem.* **2012,** *2012*(32), 6335-6350.

3. Ulrich, G. Z., Raymond; Harriman, Anthony, The Chemistry of Fluorescent Bodipy Dyes: Versatility Unsurpassed. *Angew. Chem. Int. Ed.* **2008,** *47*(7), 1184-1201.

4. Hou, J.-T.; Ren, W. X.; Li, K.; Seo, J.; Sharma, A.; Yu, X.-Q.; Kim, J. S., Fluorescent Bioimaging of Ph: From Design to Applications. *Chem. Soc. Rev.* **2017,** *46*(8), 2076-2090.

5. Terai, T.; Nagano, T., Small-Molecule Fluorophores and Fluorescent Probes for Bioimaging. *Pflüg. Arch. Eur. J. Physiol.* **2013,** *465*(3), 347-359.

6. Loudet, A. B., K., BODIPY Dyes and Their Derivatives: Syntheses and Spectroscopic Properties. *Chem. Rev.* **2007,** *107*(11), 4891–4932.

7. Kowada, T.; Maeda, H.; Kikuchi, K., BODIPY-Based Probes for the Fluorescence Imaging of Biomolecules in Living Cells. *Chem. Soc. Rev.* **2015,** *44*(14), 4953-4972.

8. Zhu, H.; Fan, J.; Mu, H.; Zhu, T.; Zhang, Z.; Du, J.; Peng, X., D-Pet-Controlled "Off-on" Polarity-Sensitive Probes for Reporting Local Hydrophilicity within Lysosomes. *Sci. Rep.* **2016,** *6*, 35627.

9. Fan, G.; Yang, L.; Chen, Z., Water-Soluble BODIPY and Aza-BODIPY Dyes: Synthetic Progress and Applications. *Front. Chem. Sci. Eng.* **2014,** *8*(4), 405-417.

10. Wories, H. J.; Koek, J. H.; Lodder, G.; Lugtenburg, J.; Fokkens, R.; Driessen, O.; Mohn., G. R., A Novel Water-Soluble Fluorescent Probe: Synthesis, Luminescence and

Biological Properties of the Sodium Salt of the 4-Sulfonato-3,3',5,5'-Tetramethyl-2,2'-Pyrromethen-1,1'-BF_2 Complex. *Recl. Trav. Chim. Pays-Bas* **1985,** *104*(11), 288 - 291.

11. Bura, T.; Ziessel, R., Water-Soluble Phosphonate-Substituted BODIPY Derivatives with Tunable Emission Channels. *Org. Lett.* **2011,** *13*(12), 3072-3075.

12. Zhu, S.; Zhang, J.; Vegesna, G.; Luo, F.-T.; Green, S. A.; Liu, H., Highly Water-Soluble Neutral BODIPY Dyes with Controllable Fluorescence Quantum Yields. *Org. Lett.* **2011,** *13*(3), 438-441.

13. Zhu, S.; Dorth, N.; Zhang, J.; Vegesna, G.; Li, H.; Luo, F.-T.; Tiwari, A.; Liu, H., Highly Water-Soluble Neutral near-Infrared Emissive BODIPY Polymeric Dyes. *J. Mater. Chem. B* **2012,** *22*(6), 2781-2790.

14. Zhu, S.; Zhang, J.; Janjanam, J.; Vegesna, G.; Luo, F.-T.; Tiwari, A.; Liu, H., Highly Water-Soluble BODIPY-Based Fluorescent Probes for Sensitive Fluorescent Sensing of Zinc(Ii). *J. Mater. Chem. B* **2013,** *1*(12), 1722-1728.

15. Zhu, Y.; Lin, W.; Zhang, W.; Feng, Y.; Wu, Z.; Chen, L.; Xie, Z., Pegylated BODIPY Assembling Fluorescent Nanoparticles for Photodynamic Therapy. *Chin. Chem. Lett.* **2017,** *28*(9), 1875-1877.

16. Vegesna, G. K.; Sripathi, S. R.; Zhang, J.; Zhu, S.; He, W.; Luo, F.-T.; Jahng, W. J.; Frost, M.; Liu, H., Highly Water-Soluble BODIPY-Based Fluorescent Probe for Sensitive and Selective Detection of Nitric Oxide in Living Cells. *ACS Appl. Mater. Interfaces* **2013,** *5*(10), 4107-4112.

17. Li, X.; Gao, X.; Shi, W.; Ma, H., Design Strategies for Water-Soluble Small Molecular Chromogenic and Fluorogenic Probes. *Chem. Rev.* **2014,** *114*(1), 590-659.

18. Brizet, B.; Bernhard, C.; Volkova, Y.; Rousselin, Y.; Harvey, P. D.; Goze, C.; Denat, F., Boron Functionalization of BODIPY by Various Alcohols and Phenols. *Org. Biomol. Chem.* **2013,** *11*(44), 7729-7737.

19. Courtis, A. M.; Santos, S. A.; Guan, Y.; Hendricks, J. A.; Ghosh, B.; Szantai-Kis, D. M.; Reis, S. A.; Shah, J. V.; Mazitschek, R., Monoalkoxy BODIPYs—a Fluorophore Class for Bioimaging. *Bioconjugate Chem.* **2014,** *25*(6), 1043-1051.

20. Nguyen, A. L.; Bobadova-Parvanova, P.; Hopfinger, M.; Fronczek, F. R.; Smith, K. M.; Vicente, M. G. H., Synthesis and Reactivity of 4,4-Dialkoxy-BODIPYs: An Experimental and Computational Study. *Inorg. Chem.* **2015,** *54*(7), 3228-3236.

21. Takeda, A.; Komatsu, T.; Nomura, H.; Naka, M.; Matsuki, N.; Ikegaya, Y.; Terai, T.; Ueno, T.; Hanaoka, K.; Nagano, T.; Urano, Y., Unexpected Photo-Instability of 2,6-Sulfonamide-Substituted BODIPYs and Its Application to Caged Gaba. *ChemBioChem* **2016,** *17*(13), 1233-1240.

22. Komatsu, T.; Urano, Y.; Fujikawa, Y.; Kobayashi, T.; Kojima, H.; Terai, T.; Hanaoka, K.; Nagano, T., Development of 2,6-Carboxy-Substituted Boron Dipyrromethene (BODIPY) as a Novel Scaffold of Ratiometric Fluorescent Probes for Live Cell Imaging. *Chem. Commun.* **2009,** *45*(45), 7015-7017.

23. Dilek, Ö.; Bane, S. L., Synthesis, Spectroscopic Properties and Protein Labeling of Water Soluble 3,5-Disubstituted Boron Dipyrromethenes. *Bioorg. Med. Chem. Lett.* **2009,** *19*(24), 6911-6913.

24. Niu, S.-L.; Ulrich, G.; Ziessel, R.; Kiss, A.; Renard, P.-Y.; Romieu, A., Water-Soluble BODIPY Derivatives. *Org. Lett.* **2009,** *11*(10), 2049-2052.

25. Li, L.; Han, J.; Nguyen, B.; Burgess, K., Syntheses and Spectral Properties of Functionalized, Water-Soluble BODIPY Derivatives. *J. Org. Chem.* **2008,** *73*(5), 1963 - 1970.

26. Yao, H.-W.; Zhu, X.-Y.; Guo, X.-F.; Wang, H., An Amphiphilic Fluorescent Probe Designed for Extracellular Visualization of Nitric Oxide Released from Living Cells. *Anal. Chem.* **2016,** *88*(18), 9014 - 9021.

27. Kim, J.; Kim, Y., A Water-Soluble Sulfonate-BODIPY Based Fluorescent Probe for Selective Detection of Hocl/Ocl^- in Aqueous Media. *Analyst* **2014,** *139*(12), 2986-2989.

28. Niu, S.-L.; Massif, C.; Ulrich, G.; Ziessel, R.; Renard, P.-Y.; Romieu, A., Water-Solubilisation and Bio-Conjugation of a Red-Emitting BODIPY Marker. *Org. Biomol. Chem.* **2011,** *9*(1), 66-69.

29. Marfin, Y. S.; Aleksakhina; Merkushev; Rumyantsev; Tomilova, Interaction of BODIPY Dyes with the Blood Plasma Proteins. *J. Fluoresc.* **2016,** *26*(1), 255 - 261.

30. Wu, L.; Loudet, A.; Barhoumi, R.; Burghardt, R. C.; Burgess, K., Fluorescent Cassettes for Monitoring Three-Component Interactions in Vitro and in Living Cells. *J. Am. Chem. Soc.* **2009,** *131*(26), 9156 - 9157.

31. Niu, S. L.; Massif, C.; Ulrich, G.; Renard, P. Y.; Romieu, A.; Ziessel, R., Water-Soluble Red-Emitting Distyryl-Borondipyrromethene (BODIPY) Dyes for Biolabeling. *Chem. Eur. J.* **2012,** *18*(23), 7229-7242.

32. Niu, S.-L.; Ulrich, G.; Retailleau, P.; Harrowfield, J.; Ziessel, R., New Insights into the Solubilization of BODIPY Dyes. *Tetrahedron Lett.* **2009,** *50*(27), 3840-3844.

33. Nguyen, A. L.; Griffin, K. E.; Zhou, Z.; Fronczek, F. R.; Smith, K. M.; Vicente, M. G. H., Syntheses of 1,2,3-Triazole-BODIPYs Bearing up to Three Carbohydrate Units. *New J. Chem.* **2018,** *42*(10), 8241-8246.

34. Lu, Z.; Mei, L.; Zhang, X.; Wang, Y.; Zhao, Y.; Li, C., Water-Soluble BODIPY-Conjugated Glycopolymers as Fluorescent Probes for Live Cell Imaging. *Polym. Chem.* **2013,** *4*(24), 5743-5750.

35. Isaad, J.; El Achari, A., A Water Soluble Fluorescent BODIPY Dye with Azathia-Crown Ether Functionality for Mercury Chemosensing in Environmental Media. *Analyst* **2013,** *138*(13), 3809-3819.

36. Zhao, N.; Williams, T. M.; Zhou, Z.; Fronczek, F. R.; Sibrian-Vazquez, M.; Jois, S. D.; Vicente, M. G. H., Synthesis of BODIPY-Peptide Conjugates for Fluorescence Labeling of Egfr Overexpressing Cells. *Bioconjugate Chem.* **2017,** *28*(5), 1566-1579.

37. Williams, T. M.; Sable, R.; Singh, S.; Vicente, M. G. H.; Jois, S. D., Peptide Ligands for Targeting the Extracellular Domain of Egfr: Comparison between Linear and Cyclic Peptides. *Chem. Biol. Drug Des.* **2018,** *91*(2), 605-619.

38. Lincoln, R.; Greene, L. E.; Krumova, K.; Ding, Z.; Cosa, G., Electronic Excited State Redox Properties for BODIPY Dyes Predicted from Hammett Constants: Estimating the Driving Force of Photoinduced Electron Transfer. *J. Phys. Chem. A* **2014,** *118*(45), 10622-10630.

39. Wang, M.; Vicente, M. G. H.; Mason, D.; Bobadova-Parvanova, P., Stability of a Series of BODIPYs in Acidic Conditions: An Experimental and Computational Study into the Role of the Substituents at Boron. *ACS Omega* **2018,** *3*(5), 5502-5510.

40. Jensen, T. J.; Vicente, M. G. H.; Luguya, R.; Norton, J.; Fronczek, F. R.; Smith, K. M., Effect of Overall Charge and Charge Distribution on Cellular Uptake, Distribution and Phototoxicity of Cationic Porphyrins in Hep2 Cells. *J. Photochem. Photobiol., B* **2010,** *100*(2), 100-111.

41. Harriman, A.; Mallon, L. J.; Ulrich, G.; Ziessel, R., Rapid Intersystem Crossing in Closely-Spaced but Orthogonal Molecular Dyads. *ChemPhysChem* **2007,** *8*(8), 1207-1214.

42. Ulrich, G.; Ziessel, R., Convenient and Efficient Synthesis of Functionalized Oligopyridine Ligands Bearing Accessory Pyrromethene-BF_2 Fluorophores. *J. Org. Chem.* **2004,** *69*(6), 2070-2083.

43. Kolemen, S.; Işık, M.; Kim, G. M.; Kim, D.; Geng, H.; Buyuktemiz, M.; Karatas, T.; Zhang, X. F.; Dede, Y.; Yoon, J.; Akkaya, E. U., Intracellular Modulation of Excited-State Dynamics in a Chromophore Dyad: Differential Enhancement of Photocytotoxicity Targeting Cancer Cells. *Angew. Chem. Int. Ed.* **2015,** *54*(18), 5340-5344.

44. Bartelmess, J.; Weare, W. W., Preparation and Characterization of Multi-Cationic BODIPYs and Their Synthetically Versatile Precursors. *Dyes Pigm.* **2013,** *97*(1), 1-8.

45. Bartelmess, J.; Francis, A. J.; El Roz, K. A.; Castellano, F. N.; Weare, W. W.; Sommer, R. D., Light-Driven Hydrogen Evolution by BODIPY-Sensitized Cobaloxime Catalysts. *Inorg. Chem.* **2014,** *53*(9), 4527-4534.

46. Caruso, E.; Banfi, S.; Barbieri, P.; Leva, B.; Orlandi, V. T., Synthesis and Antibacterial Activity of Novel Cationic BODIPY Photosensitizers. *J. Photochem. Photobiol., B* **2012,** *114*(3), 44-51.

47. Frath, D.; Yarnell, J. E.; Ulrich, G.; Castellano, F. N.; Ziessel, R., Ultrafast Photoinduced Electron Transfer in Viologen-Linked BODIPY Dyes. *ChemPhysChem* **2013,** *14*(14), 3348-3354.

48. Barba-Bon, A.; Costero, A. M.; Gil, S.; Harriman, A.; Sancenón, F., Highly Selective Detection of Nerve-Agent Simulants with BODIPY Dyes. *Chem. Eur. J.* **2014,** *20*(21), 6339-6347.

49. Sunahara, H.; Urano, Y.; Kojima, H.; Nagano, T., Design and Synthesis of a Library of BODIPY-Based Environmental Polarity Sensors Utilizing Photoinduced Electron-Transfer-Controlled Fluorescence on/Off Switching. *J. Am. Chem. Soc.* **2007,** *129*(17), 5597-5604.

50. Lu, H.; Zhang, S.; Liu, H.; Wang, Y.; Shen, Z.; Liu, C.; You, X., Experimentation and Theoretic Calculation of a BODIPY Sensor Based on Photoinduced Electron Transfer for Ions Detection. *J. Phys. Chem. A* **2009,** *113*(51), 14081-14086.

51. Ueno, T.; Urano, Y.; Kojima, H.; Nagano, T., Mechanism-Based Molecular Design of Highly Selective Fluorescence Probes for Nitrative Stress. *J. Am. Chem. Soc.* **2006,** *128*(33), 10640-10641.

52. Bañuelos, J.; López Arbeloa, F.; Arbeloa, T.; Salleres, S.; Amat-Guerri, F.; Liras, M.; López Arbeloa, I., Photophysical Study of New Versatile Multichromophoric Diads and Triads with BODIPY and Polyphenylene Groups. *J. Phys. Chem. A* **2008,** *112*(43), 10816-10822.

53. McCarroll, M. E.; Shi, Y.; Harris, S.; Puli, S.; Kimaru, I.; Xu, R.; Wang, L.; Dyer, D. J., Computational Prediction and Experimental Evaluation of a Photoinduced Electron-Transfer Sensor. *J. Phys. Chem. B* **2006,** *110*(46), 22991-22994.

54. Kennedy, D. P.; Kormos, C. M.; Burdette, S. C., Ferribright: A Rationally Designed Fluorescent Probe for Redox Active Metals. *J. Am. Chem. Soc.* **2009,** *131*(24), 8578-8586.

55. Zhan, C.-G.; Nichols, J. A.; Dixon, D. A., Ionization Potential, Electron Affinity, Electronegativity, Hardness, and Electron Excitation Energy: Molecular Properties from Density Functional Theory Orbital Energies. *J. Phys. Chem. A* **2003,** *107*(20), 4184-4195.

56. Yanai, T.; Tew, D. P.; Handy, N. C., A New Hybrid Exchange–Correlation Functional Using the Coulomb-Attenuating Method (Cam-B3lyp). *Chem. Phys. Lett.* **2004,** *393*(1), 51-57.

57. Lu, H.; Mack, J.; Yang, Y.; Shen, Z., Structural Modification Strategies for the Rational Design of Red/NIR Region BODIPYs. *Chem. Soc. Rev.* **2014,** *43*(13), 4778-4823.

58. Karlsson, J. K. G.; Harriman, A., Origin of the Red-Shifted Optical Spectra Recorded for Aza-BODIPY Dyes. *J. Phys. Chem. A* **2016,** *120*(16), 2537-2546.

59. Nithya, R.; Kolandaivel, P.; Senthilkumar, K., Understanding the Absorption and Emission Spectra of Borondipyrromethene Dye and Its Substituted Analogues. *Mol. Phys.* **2012,** *110*(8), 445-456.

60. Gräf, K.; Korzdorfer, T.; Kummel, S.; Thelakkat, M., Synthesis of Donor-Substituted Meso-Phenyl and Meso-Ethynylphenyl BODIPYs with Broad Absorption. *New J. Chem.* **2013,** *37*(5), 1417-1426.

61. Bartelmess, J.; Weare, W. W.; Latortue, N.; Duong, C.; Jones, D. S., Meso-Pyridyl BODIPYs with Tunable Chemical, Optical and Electrochemical Properties. *New J. Chem.* **2013,** *37*(9), 2663-2668.

62. Zhao, N.; Xuan, S.; Fronczek, F. R.; Smith, K. M.; Vicente, M. G. H., Stepwise Polychlorination of 8-Chloro-BODIPY and Regioselective Functionalization of 2,3,5,6,8-Pentachloro-BODIPY. *J. Org. Chem.* **2015,** *80*(16), 8377-8383.

63. Olmsted, J., Calorimetric Determinations of Absolute Fluorescence Quantum Yields. *J. Phys. Chem* **1979,** *83*(20), 2581-2584.

64. Katsumi, N., Synthesis, Luminescence Quantum Yields, and Lifetimes of Trischelated Ruthenium(Ii) Mixed-Ligand Complexes Including 3,3′-Dimethyl-2,2′-Bipyridyl. *Bull. Chem. Soc. Jpn.* **1982,** *55*(9), 2697-2705.

65. Dhokale, B.; Jadhav, T.; Mobin, S. M.; Misra, R., Meso Alkynylated Tetraphenylethylene (Tpe) and 2,3,3-Triphenylacrylonitrile (Tpan) Substituted BODIPYs. *J. Org. Chem.* **2015,** *80*(16), 8018-8025.

66. Valiev, M.; Bylaska, E. J.; Govind, N.; Kowalski, K.; Straatsma, T. P.; Van Dam, H. J. J.; Wang, D.; Nieplocha, J.; Apra, E.; Windus, T. L.; de Jong, W. A., Nwchem: A Comprehensive and Scalable Open-Source Solution for Large Scale Molecular Simulations. *Comput. Phys. Commun.* **2010,** *181*(9), 1477-1489.

67. Becke, A. D., Density-Functional Thermochemistry. Iii. The Role of Exact Exchange. *J. Chem. Phys.* **1993,** *98*(7), 5648-5652.

68. Lee, C.; Yang, W.; Parr, R. G., Development of the Colle-Salvetti Correlation-Energy Formula into a Functional of the Electron Density. *Phys. Rev. B* **1988,** *37*(2), 785-789.

69. Williams, A. T. R.; Winfield, S. A.; Miller, J. N., Relative Fluorescence Quantum Yields Using a Computer-Controlled Luminescence Spectrometer. *Analyst* **1983,** *108*(1290), 1067-1071.

Chapter 3. Synthesis and Characterization of the meso-Pyridinium BODIPY Library

3.1. Introduction

After computationally modelling the effects of functionalization on the excited states of a small library of meso-pyridylBODIPYs (Figure 3.1) with various electron-withdrawing groups on the 2,6- positions in Chapter 2, efforts were made to synthesize several members of this library so the photophysical properties could be experimentally measured and compared with the computational results. The work reported herein describes these efforts and the difficulties encountered, as well as the measured photophysical properties of the successfully prepared derivatives. The main synthetic routes to BODIPYs were described in Chapter 1, section 1.1.3. In summary, symmetric BODIPY 1A can be prepared from the condensation of 2,4-dimethylpyrrole (**14**) and pyridine-4-carboxaldehyde (**15**). Functionalization of the 2,6-positions can be achieved by electrophilic aromatic substitution or metal-mediated coupling reactions.

Following the synthesis and spectroscopic characterization, the biological properties of these dyes were evaluated in in human HEp-2 cells as they have not previously been reported. Of particular interest are the cellular uptake and cytotoxicity in the dark and light as they are important for subsequent applications.

3.2. Synthesis

The synthesis of **1A** (Scheme 3.1) has been reported in the literature with widely varying yields ranging from 13%[1] to 46%.[2] The best results were obtained when the aldehyde condensation was run in a 14:1 DCM/EtOH mixture. This solvent has been previously shown to improve the yields in dipyrromethane syntheses.[3] The condensation reaction time can be decreased from 3 days to overnight by using a larger

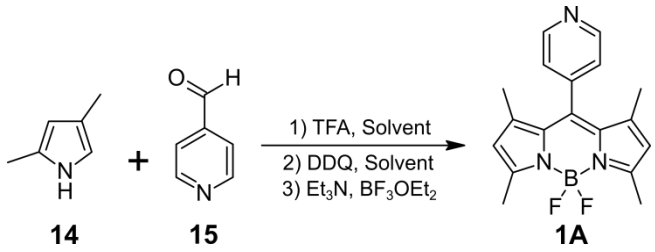

14 **15** **1A**

Scheme 3.1. General synthesis of BODIPY **1A**.

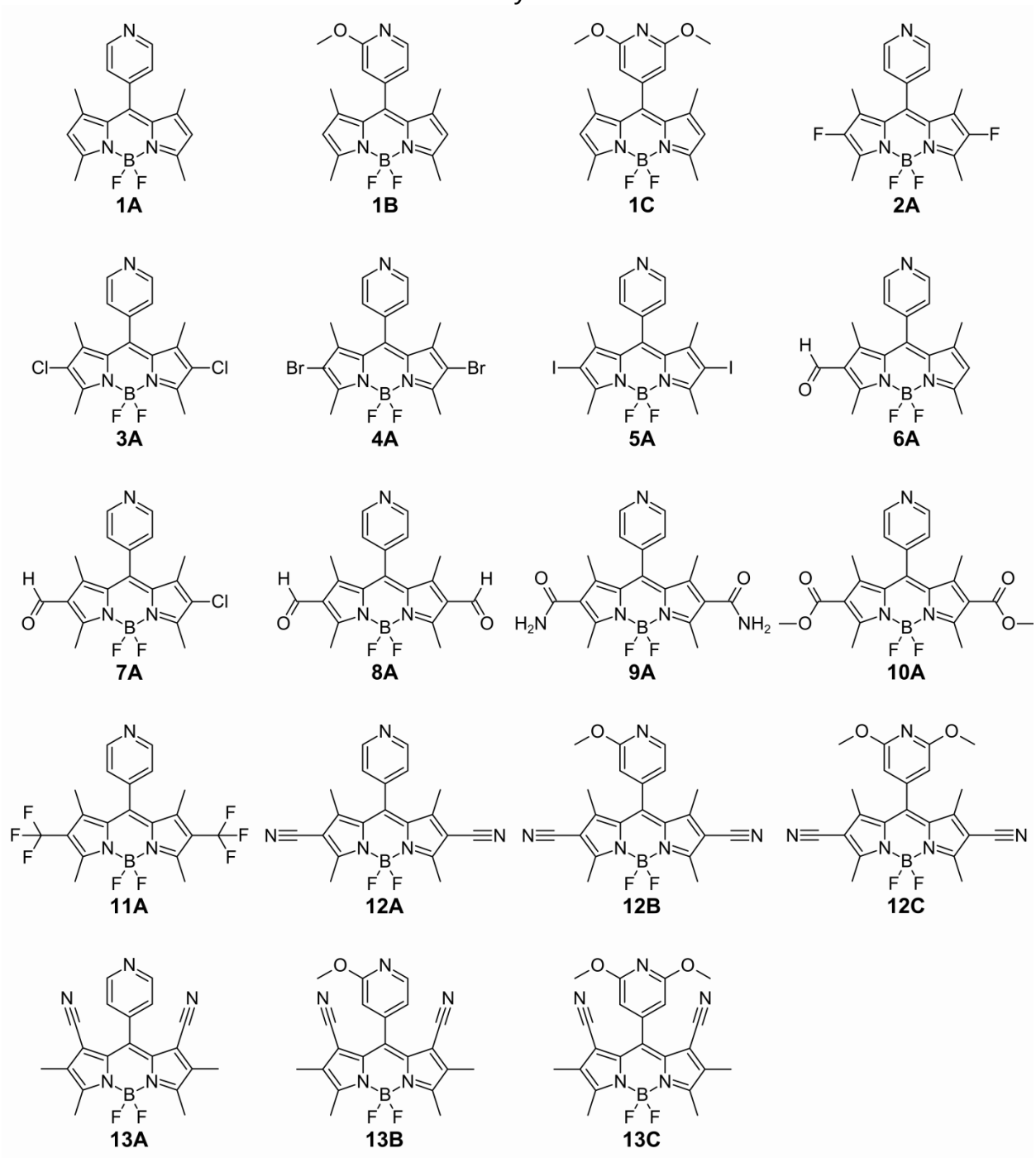

Figure 3.1. Structures of BODIPYs computationally studied in Chapter 2.

amount of TFA (2 drops in 30 mL solvent). Using 2 drops of TFA with 30 mL 14:1 DCM/MeOH and chloranil as the oxidant, BODIPY 1A was obtained in 34% yield. Owing to its basic nature, purification of this BODIPY platform can be temperamental. Flash column chromatography should be avoided as a portion of the product will stick on the column. Band streaking and product loss, resulting from the acid-base interactions between the product and the silica, can be minimized by buffering the solvent used to pack and elute the column with 0.1% TEA. Purification has been reported with the use of 1:1 EtOAc/hexanes which does give good separation on TLC, but the solubility of the product and crude reaction mixture in this solvent system is rather poor and significantly decreases the amount of product that can be collected from each column. Mixtures of 1:4 EtOAc/DCM, 2% and 4% EtOAc in DCM work well for this purification. Monofluorination at the 2- position of a BODIPY has been reported, albeit in 6% yield,[4] but the 2,6-difluoroBODIPY is a greater challenge. Instead of attempting to fluorinate **1A**, it was decided that preparation of **2A** from a fluorinated pyrrole (Scheme 3.2) would be a better synthetic route. Arene fluorination through diazonium reactions, but the preparation of aminopyrroles and diaminoBODIPYs would not be more trouble than a single data point is worth, so it was not considered a viable option. Attempts to fluorinate **16** using Selectfluor™ only resulted in oxidation of the pyrrole.[5] Since the pyrrole fluorination failed, pyrrole synthesis from fluorinated precursors was attempted (Scheme 3.3). The Knorr pyrrole synthesis using fluoroacetone was considered, but the zinc dust used to reduce the oxime would also be able to defluorinate the substrate. Alternative methods of reducing the oxime were attempted including the tin(II) chloride reduction that had been reported for an analogous oximinoacylacetate, but was

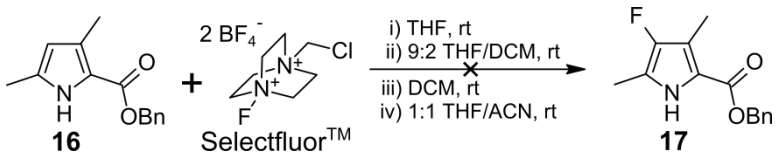

Scheme 3.2. Reaction conditions for pyrrole fluorination using Selectfluor™.[5]

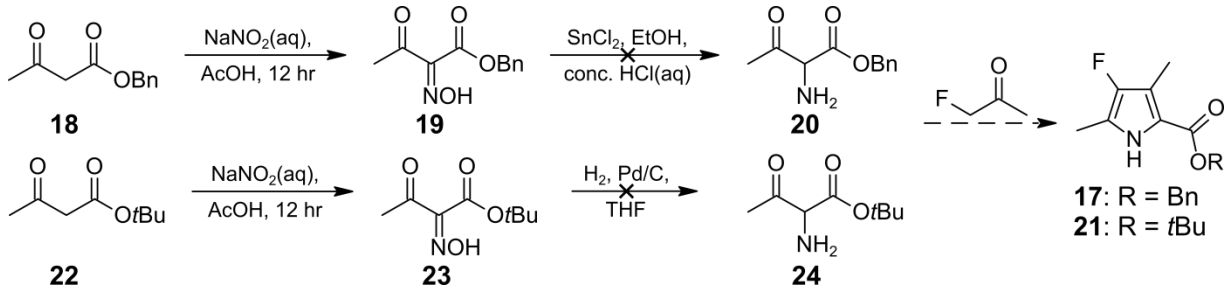

Scheme 3.3. Synthetic schemes for α-amino-β-dicarbonyl substrates to prepare fluorinated pyrroles **17** and **21**.

unsuccessful and no further attempts using this method were attempted due to the difficulty in removing the tin salts. Switching from benzyl acetoacetate **18** to the tert-butyl derivative **22** allowed for the attempted catalytic hydrogenation[6] to yield **24**, but no product was detectable by ESI-MS. The cyclized dimer was also not detected. A report of pyrrole synthesis from 2,4-pentandione and a glycine ester[7] was found along with a protocol for 2-fluorination of various 1,3-diketones using Selectfluor™.[8] However, 2,4-pentanedione was not included in this report and the attempt at fluorination failed (Scheme 3.4). While additional routes to 3-fluoropyrroles have been reported, they require the use of either expensive or non-commercially available starting materials. Seeing as the development of methodology for readily preparing the desired fluorinated pyrrole starting materials **17** and **21** is outside the scope of the current project, further endeavors to prepare **2A** were not made.

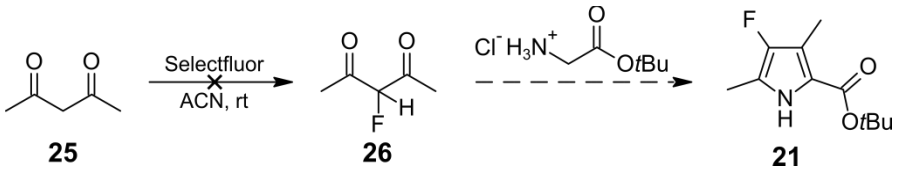

Scheme 3.4. Synthetic scheme for preparing pyrrole **21** from 2,4-pentanedione.

Employing the chlorination protocol previously developed by our group,[9] TCCA in AcOH, resulted in decomposition and formation of a complex reaction mixture from which the product **3A** could not be isolated. The other reaction conditions for the preparation of **3A** (Scheme 3.5) are fairly straight forward, however, the techniques involved can be challenging. Adding solvent after charging a flask with BODIPY **1A** and NCS does not work as the solubility of NCS in DCM is rather poor and the reagent never fully dissolves. This method requires the use of at least 8 equivalents of NCS, which can be difficult to completely remove by washing and result in three TLC spots becoming about 15 bands on a preparative TLC plate, and still no reaction is observed after stirring for several days without heating the mixture for several hours above 35°C. It was decided to attempt making **3A** from a chlorinated pyrrole (Scheme 3.6). Since the 5-position must be blocked to direct the chlorination to the 3-position, pyrrole **27** was prepared from 2,4-dimethylpyrrole and trichloromethylacyl chloride in 94% yield.[10,11] Preparation of pyrrole **28** from **27** using NCS in DCM was not a clean reaction and did not produce an efficient transformation. When employing TCCA in ACOH, the colorless solution of **27** in AcOH immediately turned black when the TCCA was added. The mass spectrum did not find any trace of the desired product and the TCC revealed multiple spots with fluorescence around 510 nm (qualitatively looked like standard BODIPY fluorescence). The solvent was then switched to DCM in order to retard the activity of

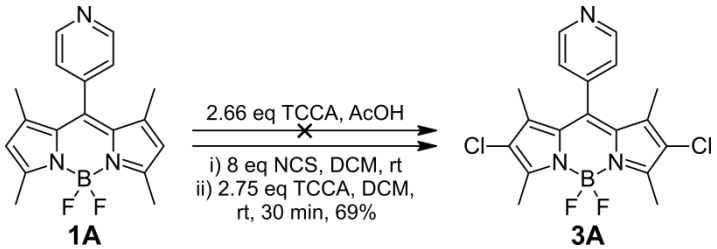

1A **3A**

Scheme 3.5. Synthetic scheme for preparing **3A** from **1A**.

TCCA. Upon addition of the TCCA solution, the colorless solution began turning orange, but further color change was not observed when the rate of addition was decreased. The mass spectrum confirmed product formation and oxidation products. Seeing that the oxidation reaction can be controlled by the solvent and rate of addition, **3A** was prepared by dissolving **1A** in DCM and slowly adding a dilute solution of 2.75

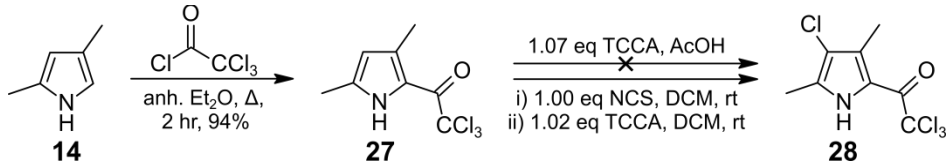

14 **27** **28**

Scheme 3.6. Synthetic scheme for preparing 5-protected-3-chloropyrrole **28**. [10]

equivalents TCCA in DCM at room temperature. As the reaction proceeded, the cyanuric acid produced, as the TCCA was consumed, precipitated out and the transparent solution became cloudy/opaque. When TLC showed complete consumption of the starting material, the crude reaction mixture was loaded onto a column and purified. BODIPY **3A** had been previously purified using 2% methanol in DCM, but this was not the best choice for this column as it dissolved the cyanuric acid. The use of 4% EtOAc in DCM would be a better choice and a higher yield would have been obtained if the column had been properly buffered as it was packed. That aside, the purification was relatively simple and the previously observed formation of additional bands, when NCS was used, was not observed.

Preparation of **4A** using conditions i) in Scheme 3.7 has been reported in high yield, [12] however, in my hands freshly recrystallized N-halosuccinimides produced complex mixtures that required several chromatography separations. However, treatment of **1A** with a dilute solution of bromine in DCM in the dark produced a very high yielding (98%) and clean transformation that was easily purified with a single

column. The production of 2,6-diiodoBODIPYs is commonly achieved using iodine and iodic acid in ethanol, but reaction times and temperatures can vary widely. The use of iodine monochloride is preferable due to its high reactivity and short reaction times,

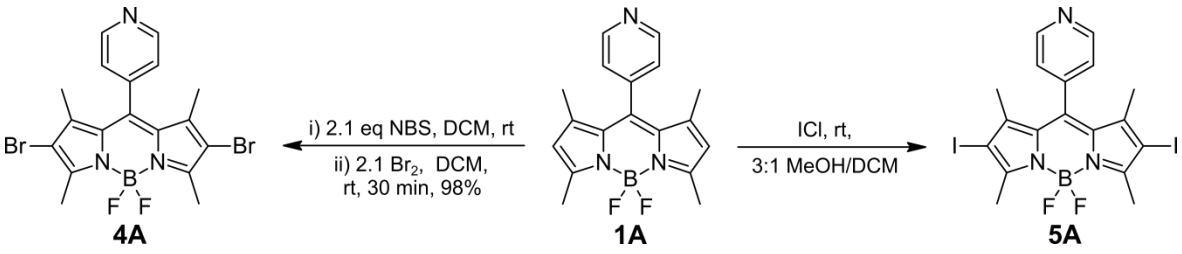

4A **1A** **5A**

Scheme 3.7. Synthetic schemes for the preparation of **4A** and **5A**.

typically 5-30 minutes, at room temperature. The reaction is moisture sensitive so anhydrous conditions should be maintained or a large excess of ICl will be needed.

BODIPY **6A** was prepared from **1A** by the standard Vilsmeier formylation, Scheme 3.8, using DMF and phosphorous oxychloride.[13,14] Attempts at further formylation **6A** to **8A** were made before realizing there was a problem with the $POCl_3$. Phosphorous oxychloride is not the most reliable reagent as it usually contains varying amounts of HCl and it cannot be kept anhydrous without a glovebox since it is not commercially available with a septum. Using freshly distilled $POCl_3$ can bypass these problems, but the vacuum distillation must be used with high temperature and extreme care to ensure none of it passes through the vacuum.

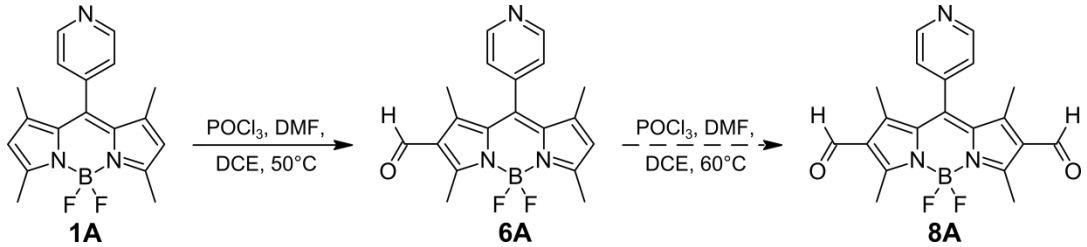

1A **6A** **8A**

Scheme 3.8. Synthetic scheme for the preparation of BODIPYs **6A** and **8A**.

The preparation of **9A** was attempted from functionalized pyrrole (Scheme 3.9). The Knorr pyrrole synthesis from **18** and acetoacetamide **29** to produce pyrrole **30** was

a facile transformation, however, a yield could not be determined due to the very poor solubility of the product. Typically the pyrrole precipitates out of the acetic acid and is collected by filtration and the excess zinc is then removed by dissolving the pyrrole

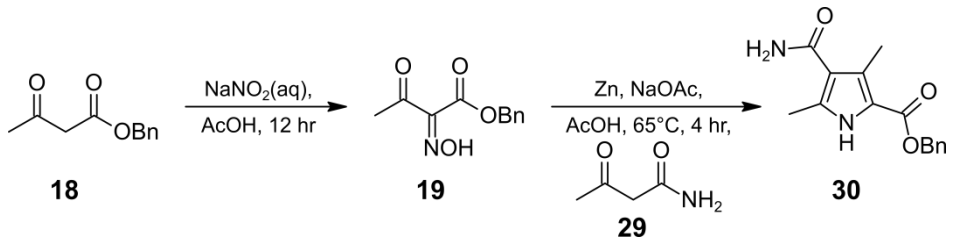

Scheme 3.9. Synthetic scheme used to prepare amide pyrrole **30**.

and filtering. Pyrrole **30** was insoluble in DCM, EtOAc, MeOH, EtOH, THF, ACN, acetone, ethylene glycol, toluene, and water. It was partially soluble in DMF, however it would have required at least 500 mL of DMF to dissolve the sample which would have proved too problematic to remove. Attempts at removing the residue it left on the glassware using DMF, concentrated hydrochloric acid, concentrated sulfuric acid, 50/50 concentrated sulfuric and chromic acids with a 7% oleum, and potassium isopropoxide have so far been futile. Since the NH_2 of the amide made pyrrole **30** insoluble, an N-protected amide was desired. The ideal protecting group would be readily removed under neutral conditions since BODIPYs can be sensitive to very acidic/basic conditions so the benzyl group was chosen and the acetoacetate was switched from the benzyl ester to the tert-butyl ester so an orthogonally diprotected amide pyrrole, **34**, could be prepared. N-benzylacetoacetamide **33** is not commercially available but was expected to be obtainable from the protected dioxinone **31** with benzylamine (Scheme 3.10). The transformation proceeded rapidly, but produced the stabilized enamine **32** instead. Decreasing the amount of benzylamine did not inhibit formation of **32**. It was interesting to find that the two sets of benzylic protons gave close, but unique signals. Several

attempts were made to convert **32** to **33** by hydrolyzing with water, aqueous weak acid, aqueous strong acid, and biphasic conditions using aqueous strong acid and toluene, but the acetoacetamide **33** was never detected by ESI-MS or TLC. An attempt was made to synthesize pyrrole **34** from **32** (Scheme 3.11) and was successful, although the reaction was problematic. Part way through, a thick gum-like substance accumulated around the solvent level and at the bottom, engulfing the stir bar. The flask had to be manually shaken and stirred, after additional solvent was added, for approximately 10 to

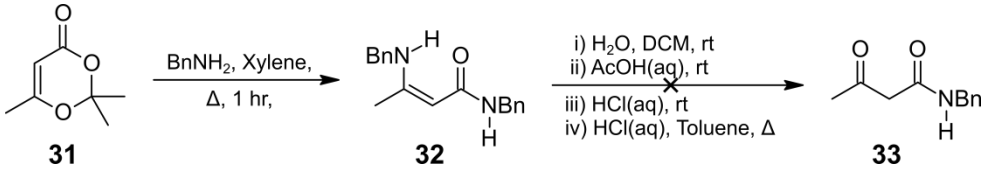

Scheme 3.10. Synthetic scheme for preparing N-benzylacetacetamide **33**.[15,6]

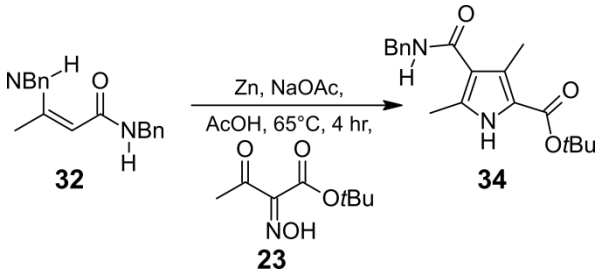

Scheme 3.11. Synthetic scheme for preparing N-protected amide pyrrole **34**.

15 minutes every 30 minutes for 3.5 hours. The MS of the solvent and the gum showed product in both and dissolution of the gum in DCM, MeOH, and acetone under sonication took at least 1 hour. Since the reaction was difficult, messy, and gave an overall poor yield, it was decided to aim for the diprotected amide. The diprotected acetoacetamide **35** was obtained in nearly quantitative yield since dibenzylamine is unable to form the imine that tautomerizes to the enamine as benzylamine did, though chromatography was still required as **31** from the fresh stock bottle was a black solution (Scheme 3.12). The acetoacetamide **35** presented a problem in that it was an oil that

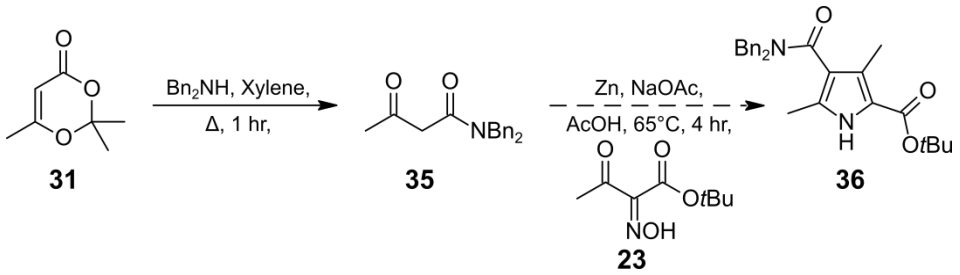

Scheme 3.12. Synthetic scheme for preparing di-N-protected amide pyrrole **36**.

slowly formed some crystals, but never completely crystallized making it difficult to work with so further attempts to prepare the diamide BODIPY **9A** were not made. The preparation of pyrrole **38** from benzyl and methyl acetoacetates **18** and **37**, respectively, (Scheme 3.13), proceeded readily as did the benzyl ester deprotection to afford the carboxylic acid pyrrole **39**. Decarboxylation with TFA should have been a facile and rapid transformation, however, It was difficult to tell if any transformation had occurred as the carboxylic acid pyrrole **39** had poor solubility, but should have gradually

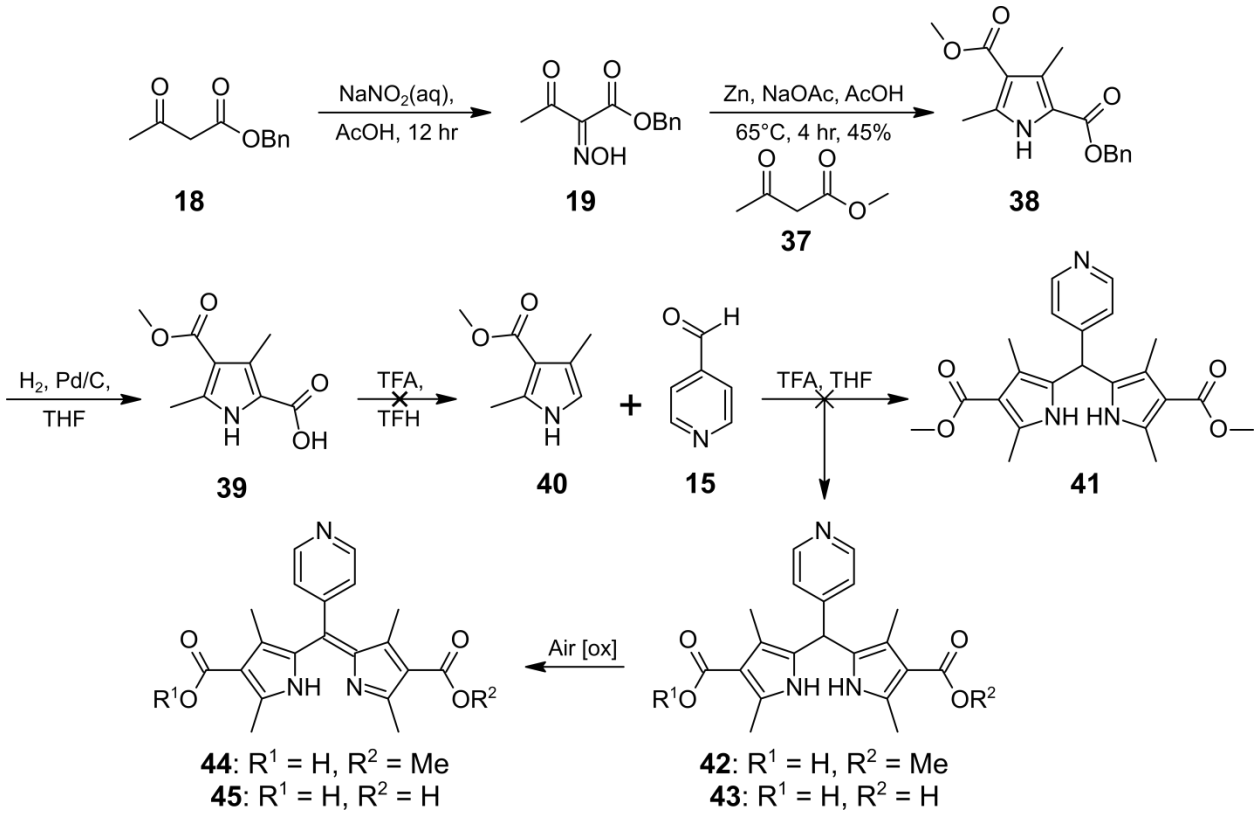

Scheme 3.13. Synthetic scheme for preparing dimethyl ester dipyrromethane **41**.

dissolved as the decarboxylation produced pyrrole **40**. Since there was no observable change in the amount of undissolved material and TLC showed the carboxylic acid pyrrole was still present even after several hours, the necessary amount of 4-formylpyridine **15** was added with the expectation that the activated form of **15** would be able to facilitate the decarboxylation during the condensation reaction to produce the dipyrromethane **41**. No change was observed even after 24 hours so it was assumed that the sample had degraded at some point, but allowing the solid exposed to air under ambient conditions for an extended amount of time resulted in the sample changing color from white to red. When TEA was added to a small amount of the red solid, the sample turned yellow indicating the dipyrromethane had been formed and undergone an air oxidation to form the dipyrromethene. Since the sample had such poor solubility, it is reasonable to expect that some or both of the esters had been hydrolyzed to give a mixture of **42** and **43**, which can expected to follow the aldehyde condensation which produces water as a byproduct in the presence of a strong acid.

In designing a retrosynthetic approach to prepare **11A**, the report by Huynh and co-workers[4] demonstrating BODIPY monofluorination as well as both mono- and di-trifluoromethylation was followed (Scheme 3.14). BODIPYs **52**, **53**, and **54** were obtained in 45%, 93%, and 81%, respectively, but only from **46**, **49**, and **50**. The brominated derivatives **48** and **51** were unreactive, as was the diiodopentamethyl derivative **47**, at both 25°C and 90°C under these conditions and the starting material was recovered in each case. This transformation was further reviewed to see if it could be used at a different stage in the synthesis, but attempts to obtain the 3-trifluoromethylpyrrole starting material have not been successful.[16]

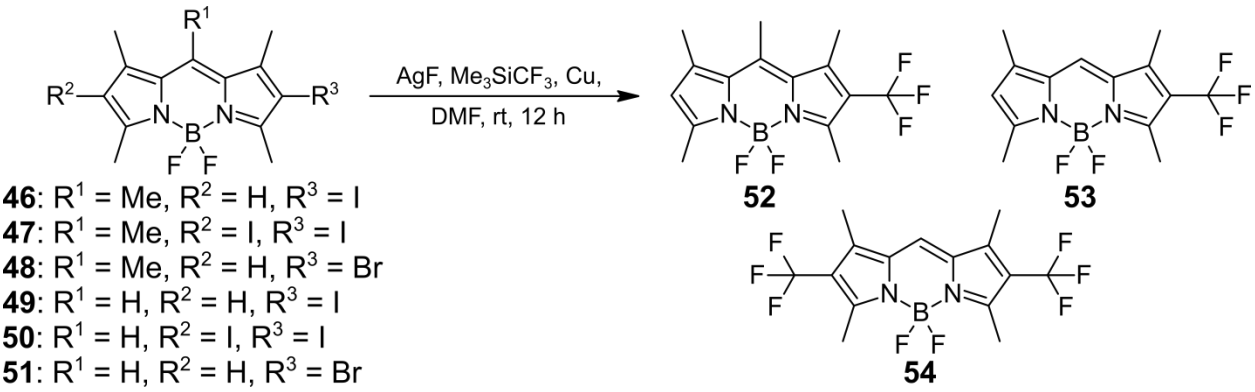

Scheme 3.14. Synthetic scheme reported for BODIPY trifluoromethylation.[4]

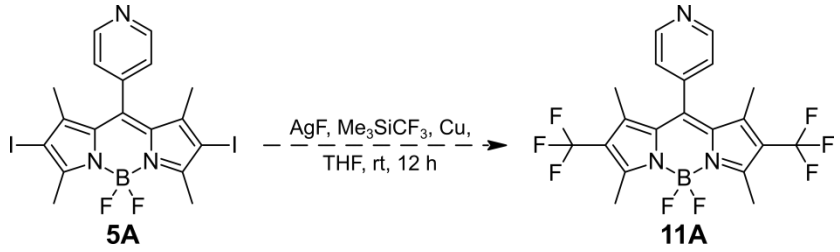

Scheme 3.15. Synthetic scheme proposed for preparation of **11A**.

In preparing BODIPY **12A**, post boron complexation functionalization of the BODIPY platform **1A**, **4A**, or **5A** would be preferable. Considering the protocol for trifluoromethylation using $CuCF_3$, an attempt to prepare **12A** from **4A** using CuCN in DMF was made, but after 20 hours at room temperature, TLC showed barely any product formation. The mixture was heated to 54°C for 4 hours at which point what appeared to be decomposition products had appeared so the mixture was removed from the heat and stirring was continued for an additional 24 hours before the starting material had been consumed. In the end, the desired product was not obtained, but a polar fluorescent band stuck to the column and could not be eluted off, but the method would be in poor yield if it did form the product. Another attempt using a catalytic amount of CuCN and an excess of NaCN in THF, starting with **4A** or **5A**, will be made to see if reducing the amount of copper(I) improves the yield since it can undergo single electron transfer reactions to produce the more stable Cu^{+2} ion (Scheme 3.16). An

alternative method is to start from a cyanopyrrole. Pyrrole functionalization and subsequent reactivity with a β-cyano group was explored in depth by former group member Dr. Waruna Jinadasa[17] and decarboxylation of 3-cyano-2,4-dimethylpyrrole-5-carboxylic acid was not achievable so preparation of 3-cyano-2,4-dimethylpyrrole **60** was sought. Several groups have reported use of the same protocol,[18,19] depicted in Scheme 3.17, starting with a Boc protected glycine derivative **55**. The procedure is fairly easy; however, the purification of **58** is troublesome due to poor solubility of the material in most common solvents. It should be noted that the melting point of 3-aminocrotononitrile is very close to the boiling point of ethanol which most likely results in the excess reagent melting on the rotovap resulting in the residue becoming a single insoluble mass. Portions of the product 58 could be removed from the mixture by EtOAc after sonication and standing for several hours. Once these solutions were drawn off, the residue left behind, after solvent removal, were quite soluble in common solvents supporting the idea that **57** had melted to form a single mass. In collaboration with a group member, **58** was successfully transformed to **59** and **60**. Attempts to prepare **12A** from **60** and 4-formylpyridine (**15**) by acid catalyzed condensation have been unsuccessful so far as the intermediate carbinol precipitates out of solution. Gentle heating and running the reaction in THF did not allow the transformation to proceed, but using $BF_3 \cdot OEt_2$ instead of TFA effectively facilitated the transformation and greatly decreased the reaction time. Subsequent oxidation and complexation are currently underway.

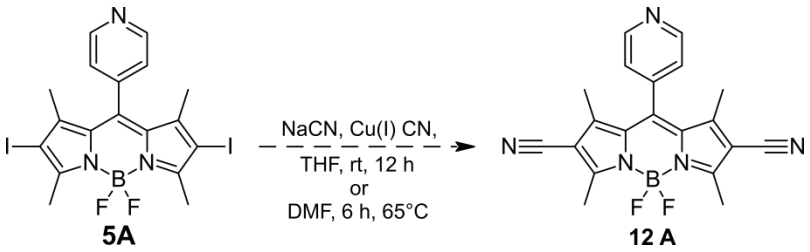

5A **12 A**

Scheme 3.16. Synthetic scheme proposed for preparation of **12A**.

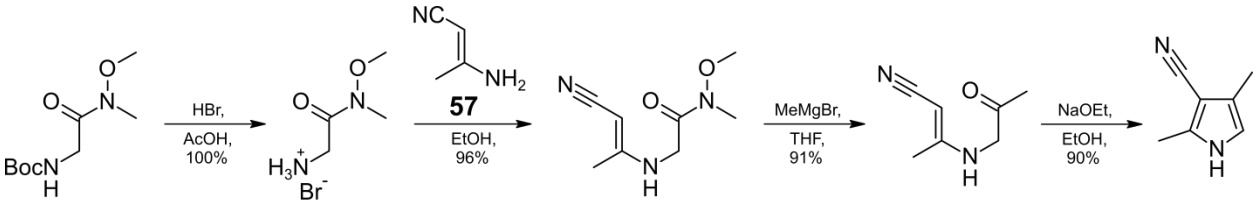

55 **56** **58** **59** **60**

Scheme 3.17. Synthetic scheme for preparation of cyanopyrrole **60**.

To prepare the promising BODIPYs in series C, the methyl 2,6-dimethyoxy-pyridine-4-carboxylate **62** was desired to bypass the subsequent oxidation step. The transformation proceeds through an addition-elimination process so simple nucleophilic substitution conditions were attempted. A transformation did occur as the physical properties of the material changed, most notably the solubility, however the ^{1}H NMR still showed two separate peaks in the aromatic region, but they were different from the starting material. Following patent reports for its preparation from methyl 2,6-dichloro-pyridine-4-carboxylate by refluxing with NaOMe in DMF, the starting material was consumed in under an hour and the N,N-dimethylamide **63** was produced in high yield. Attempts to prepare the dipyrromethene **65** from **63** with the Grignard pyrrole **64** were unsuccessful. The transformation of **63** to **62** was achieved by refluxing with methanol in sulfuric acid, but this procedure was not pursued due to its intrinsic hazards. The next step is to repeat the reaction to produce **63** with the exception of extending the reaction time to 16 hours as the patent reports. It is expected that the extended reaction time will result in the excess NaOMe converting the DMF to methyl formate and

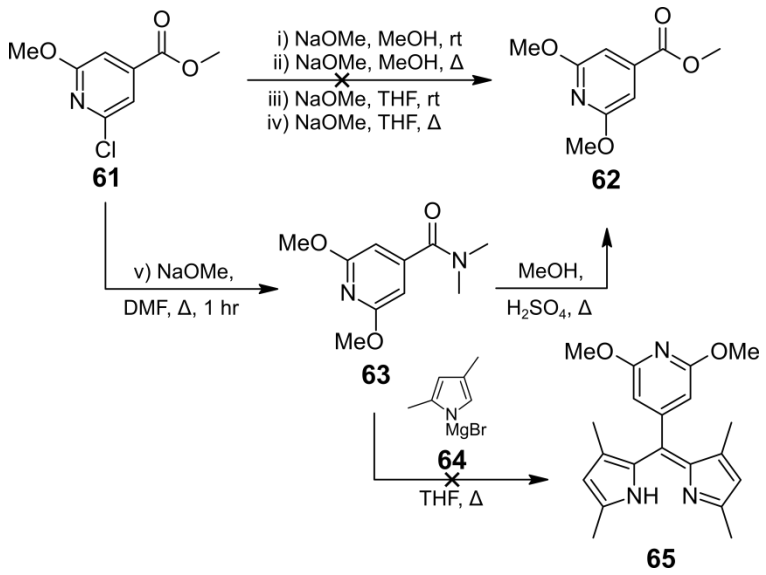

Scheme 3.18. Synthetic scheme for preparation of BODIPY **1C**.

volatile dimethylamine which will leave as a gas resulting in conversion of **63** to **62**. If attempts to prepare series B should be attempted, catalytic hydrohalogenation of **61** can produce the required 2-methoxypyridine ester starting material.

As a means of tuning the solubility of the dyes, the use of different alkylating agents and groups was briefly explored. The results of this are summarized in Table 3.1. The first reagent tested was 2-chloroethanol. Most of the trials exhibited deceptive fluorescence. The green fluorescence of the starting material displayed a bathochromic shift to orange while the reaction was running, but that was the result of the pyridine hydrogen bonding with the alcohol. The hydrogen bonding was strong enough to essentially inhibit the reaction. The N-(2-hydroxyethyl)pyridinium cation was detected by ESI-MS several times (HRMS (ESI): m/z calcd (%) for $C_{20}H_{23}BF_2N_3O$: 369.1933[M*]+; found: 369.1925), but it was never isolatable.

The next alkyl group chosen was an ethylsulfonate to make a zwitter ionic BODIPY. Regardless of the conditions attempted and the multi-week reaction times,

product was never observed by ESI-MS. Upon moving to the small methyl iodide, the reaction proceeded to completion at room temperature in 48-72 hours, but could be completed in 1 hour by refluxing in ACN. Having an additional water-solubilizing group on the dye was still desired so a protected alcohol, 2-bromoethyl benzyl ether, was employed. The reaction went to completion, under reflux, though the rate was decreased by the sterics of the benzyl ether. The benzyl ether is a good choice if the BODIPY has no carbon-halogen bonds, but since the dichloro derivative **3A** does have them, the standard catalytic debenzylation using H_2(g), Pd/C cannot be used so this reagent was not pursued further. It did however provide proof of concept that protected water-solubilizing groups could be used for the alkylation. It is worth noting here that it

Table 3.1. Alkylation reaction conditions explored.

RX	Equiv.	Solvent	Temperature	Yield
2-Chloroethanol	1	DCM	RT	N/A
	1	THF	RT → Δ	N/A
	1	ACN	RT → Δ	N/A
	1	Toluene	RT → Δ	N/A
	N/A	RX	RT → 110°C	N/A
	N/A	1:1 RX/DCM	RT	N/A
	N/A	1:1 RX/ACN	RT	N/A
	1.5*	Acetone	RT	N/A
Sodium 2-Bromo-ethylsulfonate	1	DCM	RT	N/A
	10	DCM	RT	N/A
	10	THF	RT	N/A
	10	ACN	RT → Δ	N/A
Methyl iodide	N/A	RX	RT	100%
	N/A	1:1 RX/ACN	RT → Δ	100%
2-Bromoethyl benzyl ether	1	ACN	RT → Δ	100%

* DIPEA & NaI were included

is preferable that the alkylation be the final step in preparing the desired product. It is not advised that attempts to purify the cationic derivatives over silica be made. These salts precipitated out of methyl iodide and lost some solubility in ACN when the temperature was decreased. If purification of an alkylated derivative is necessary, reverse phase HPLC is strongly recommended.

3.3. Characterization

3.3.1. Photophysical Studies

The photophysical properties of the synthesized BODIPYs are summarized in Figure 3.2 and Table 3.2. The three halogenated derivatives all show similar bathochromic shifts in their absorption spectra. The formyl derivative **6catA** exhibited the expected hypsochromic shift characteristic of 2-formylBODIPYs[13]. The emission spectra show a consistent trend for **1catA**, **3catA**, and **5catA**, but **4catA** and **6catA** both exhibit hypsochromic shifts to about 565 nm. The cationic derivatives all show decreased molar extinction coefficients relative to the neutral analogs.

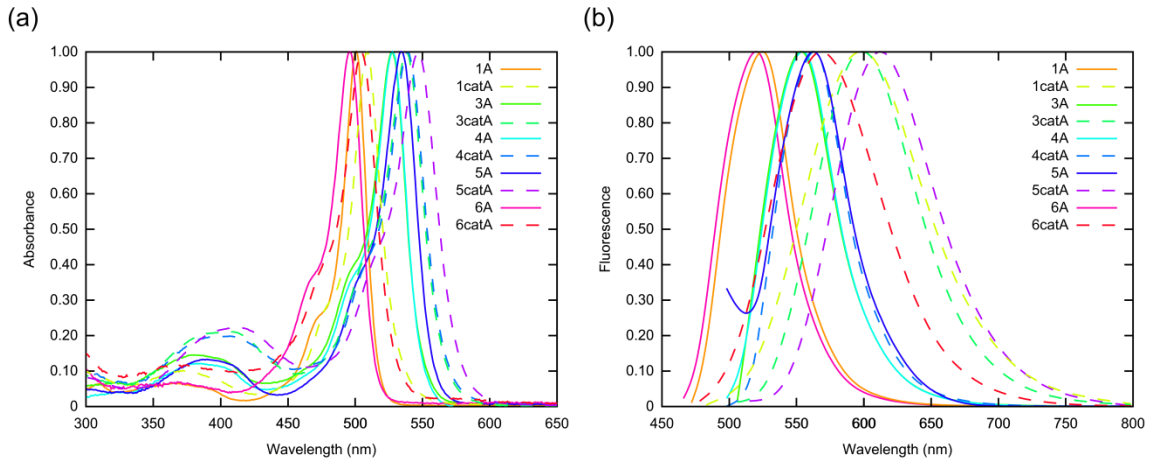

Figure 3.2. Normalized a) absorption and b) emission spectra of neutral and cationic BODIPYs **1A**, **3A**, **4A**, **5A**, and **6A**.

Table 3.2. Photophysical properties of synthesized BODIPYs in ACN.

BODIPY	λ_{max} (nm)		Stokes Shift (nm)	Φ_f*	ε (M^{-1} cm^{-1})
	abs	em			
1A	501	525	28	0.31[a]	78100
1catA	509	596	87	0.058[b]	33100
3A	528	554	26	0.58[a]	53700
3catA	538	598	60	0.103[b]	12600
4A	501	555	54	0.14[a]	58000
4catA	539	560	21	0.021[b]	8500
5A	501	563	62	0.004[a]	55600
5catA	546	611	65	>0.001[b]	26600
6A	495	520	25	0.67[a]	27200
6catA	504	568	64	0.002[b]	4260

*Relative quantum yields determined using: (a) rhodamine-6G (Φ_f = 0.86) in methanol as the standard, λ_{ex} = 473 nm [20] and (b) $Ru(bpy)_3Cl_2$ in water as the standard (Φ_f = 0.028), λ_{ex} = 436 nm.[21]

The fluorescence quantum yields follow the expected trends. The brominated derivative, **4catA**, displays quenched fluorescence compared to both the chlorinated (**3catA**) and unsubstituted (**1catA**) derivatives while the iodinated derivative (**5catA**) is essentially non-fluorescent. The quenching in both cases is due to the heavy atom effect increasing the ISC efficiency. The calculations in Chapter 2 showed that the formyl derivative, **6A**, had a lower oxidation potential than **3A** and so the quantum yield of the cation, **6catA**, was expected to be smaller than that of **3catA** which is reflected in the experimental results.

3.3.2. Biological Studies

The dark toxicity and phototoxicity (Figure 3.3) as well as the cellular uptake (Figure 3.4) were evaluated in HEp-2 cells. Derivatives **4A** and **6A** exhibited some dark toxicity, but all other derivatives had ≥ 90% survival with the cationic monoformyl derivative **6catA** and neutral diiodo **5A** exhibiting the lowest dark toxicities. The dark toxicities of **1A**, **3A**, and **3catA** are equivalent with ~88-89% survival. The dibromo and

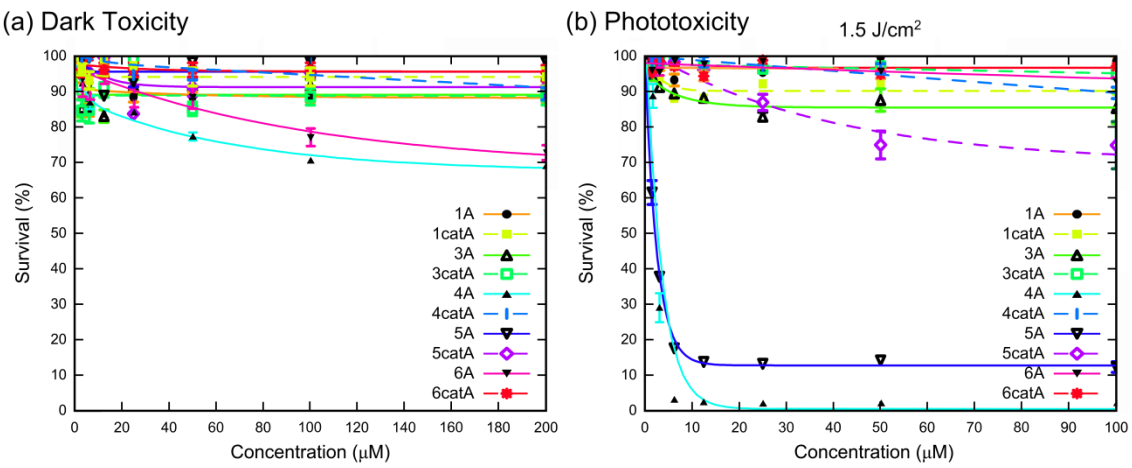

Figure 3.3. Cytotoxicity of synthesized BODIPYs a) in the dark and b) with irradiation.

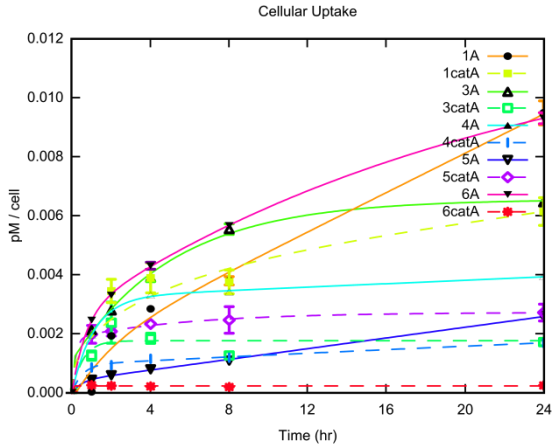

Figure 3.4. Cell uptake of BODIPY derivatives in HEp-2 cells.

diiodo derivatives **4A** and **5A** both displayed high phototoxicity. The diiodo salt **5catA** exhibited phototoxicity analogous to the dark toxicity of **4A** and all other derivatives displayed ≥ 85% survival after exposure to light. The uptake study revealed that the unsubstituted and monoformyl derivatives **1A** and **6A** have the highest cellular uptake followed by **3A** and **1catA**. The ionic monoformyl BODIPY **6catA** however showed almost no uptake. The dark toxicity IC_{50} is > 200 μM for all 12 dyes studied and the phototoxic IC_{50} is > 100 μM for all except **4A** and **5A** which are > 2.5 μM and 2.1 μM, respectively.

3.3.3. Conclusions

In this project so far, six of the meso-pyridyl BODIPYs studied in Chapter 2 have been synthesized, biologically characterized in HEp-2 cells, and the photophysical properties of the ionic derivatives have been measured. The trends in the photophysical data followed the trend predicted in Chapter 2 with the exception of the dibromo- and diiodo- derivatives since the Heavy Atom effect quenches their fluorescence. Both of these were found to be highly phototoxic. The dibromo derivative was found to have greater overall toxicity, both dark and photo, than the diiodo whilethe others had minimal toxicity. The dichloro derivatives **3A** and **3catA**, which exhibited the highest fluorescence quantum yields so far, are both relatively non-toxic with a 90% survival of the cell cultures showing potential for use as a biological label.

3.3.4. **Future Work**

There are two parts left to complete this project. The first is the synthesis of additional dyes. BODIPY **7A**, can be prepared via chlorination of the monoformyl BODIPY **6A** using TCCA in DCM (Scheme 3.19). The proposed routes to the

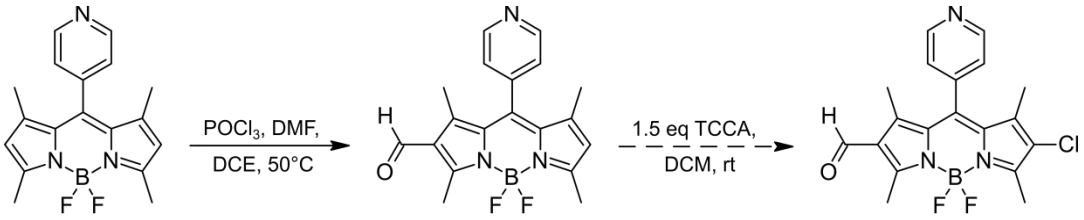

Scheme 3.19: Proposed synthetic scheme for preparing BODIPY **7A**.

dicyanoBODIPYs **12A** and **13A** are shown in Scheme 3.20, Scheme 3.21, and Scheme 3.22, respectively. The aldehyde condensation with cyanopyrrole **60** has already been performed and the oxidation is underway.

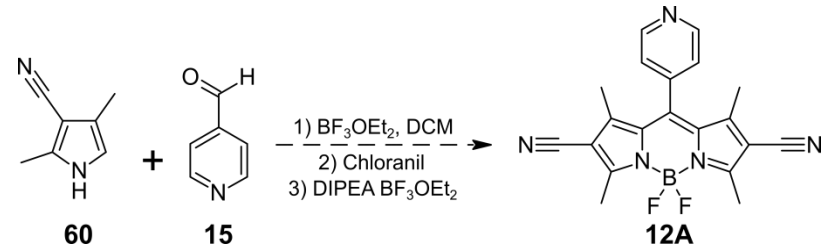

60 **15** **12A**

Scheme 3.20: Proposed synthetic scheme for preparing BODIPY **12A**.

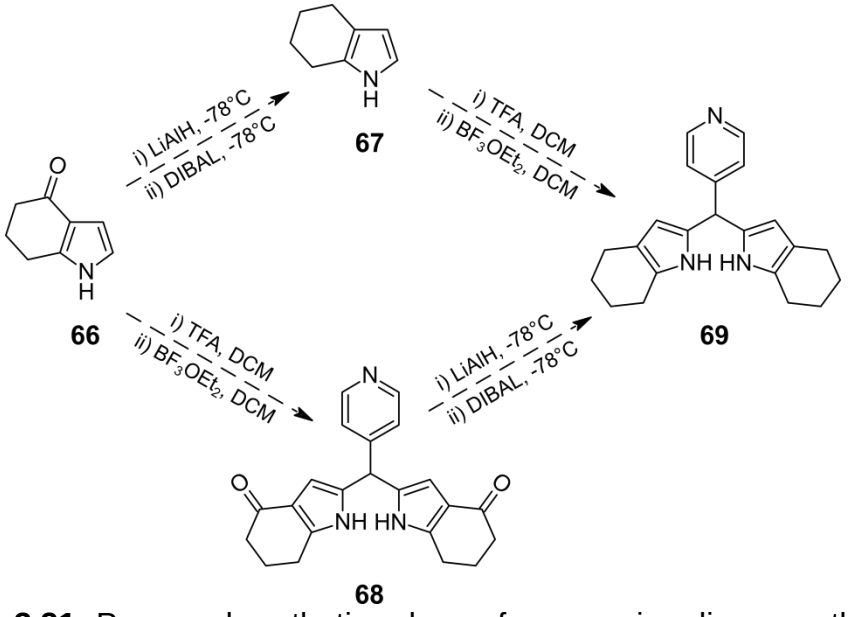

66 **67** **68** **69**

Scheme 3.21: Proposed synthetic scheme for preparing dipyrromethane **69**.

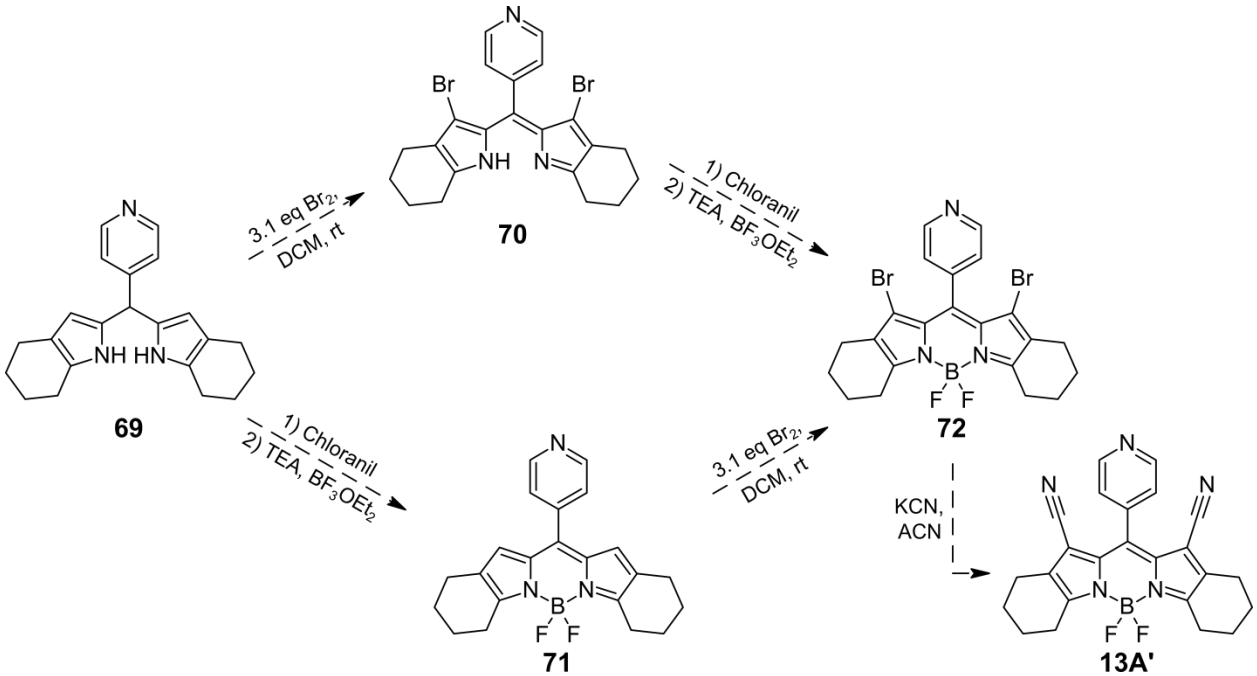

69 **70** **71** **72** **13A'**

Scheme 3.22: Proposed synthetic scheme for preparing BODIPY **13A'**.

The 2,6-dimethoxypyridine derivatives, **1C**, **12C**, and **13C** also need to be synthesized by the proposed routes shown in Scheme 3.23, Scheme 3.24, and Scheme 3.25, respectively. These proposed routes all employ standard methods for the individual transformations, however, in some cases, multiple methods are provided should problems arise with the initial conditions. In preparing **13A'**, the carbonyl reduction is known to be difficult and since α-free, electron-rich pyrroles readily begin to degrade when exposed to air and light, it may be advantageous to prepare dipyrromethane **68** prior to reducing the carbonyl. Two different routes to the 1,7-dibromoBODIPY **72** are proposed since bromine can readily oxidize electron-rich dipyrromethanes to dipyrromethenes, in addition to brominating them, while the use of oxidants such as chloranil and DDQ always results in the formation of meso-free products. Once BODIPY **72** is formed, the 1,7-halogens have been reported to be susceptible to nucleophilic displacement so an S_NAr cyanation is proposed using KCN as the cyanide source and acetonitrile as the solvent. KCN is slightly soluble in acetonitrile, but KBr is insoluble and will precipitate out shifting the equilibrium toward product formation. The proposed preparation of **13C'** has several steps that could be performed in various orders; however the late stage carbonyl reduction is shown. The second part is the photophysical and biological characterization of these additional dyes. The initial photophysical studies on the neutral BODIPYs need to be run and the studies on the ionic derivatives need to be conducted in triplicate to ensure the both the accuracy and reproducibility of the results.

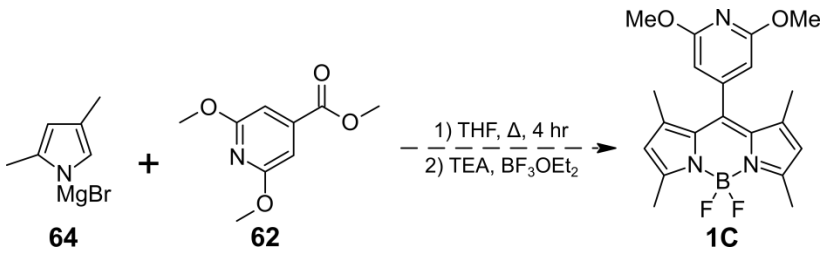

64 **62** **1C**

Scheme 3.23. Proposed synthetic scheme for preparing BODIPY **1C**.

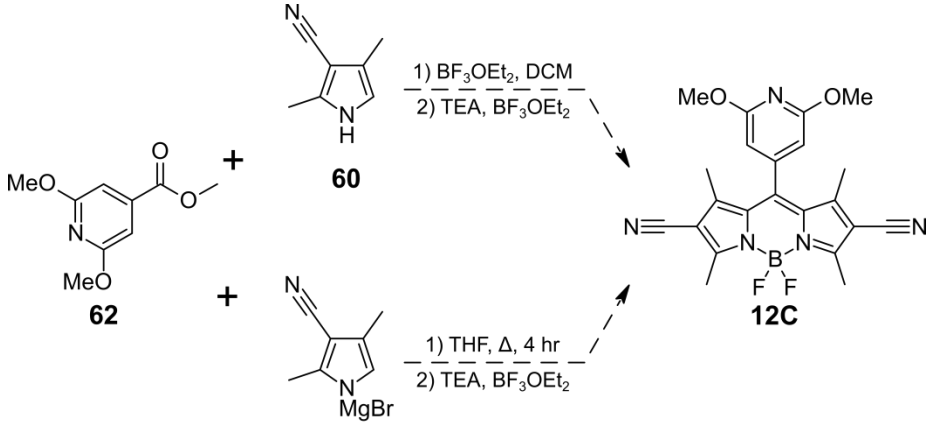

62 **60** **73** **12C**

Scheme 3.24. Proposed synthetic schemes for preparing BODIPY **12C**.

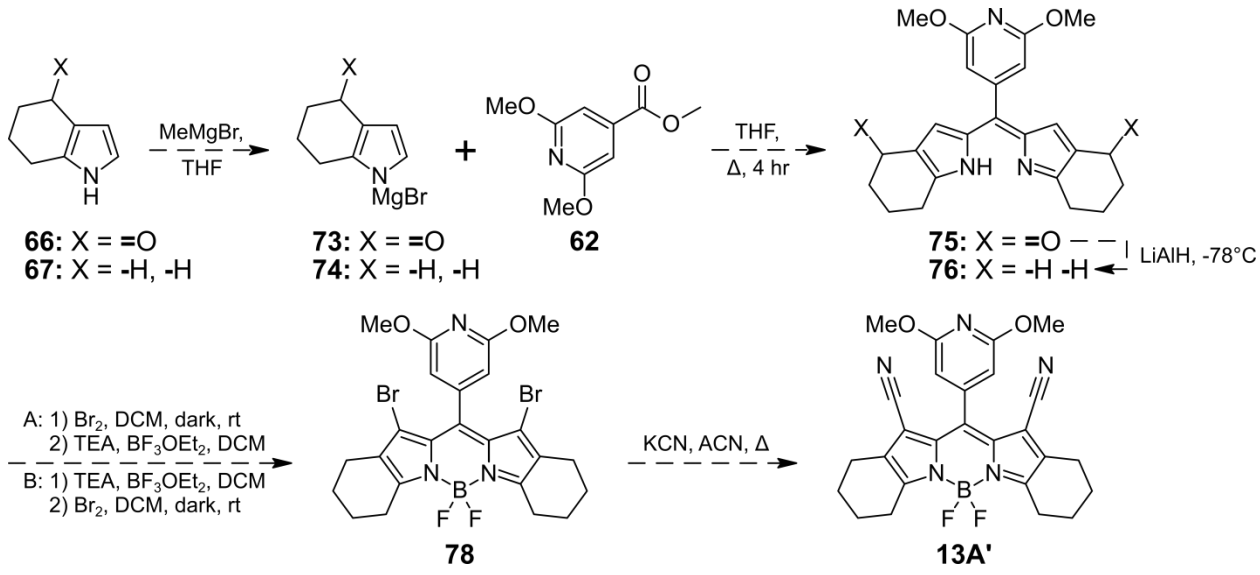

66: X = **=**O
67: X = **-**H, **-**H
73: X = **=**O
74: X = **-**H, **-**H
62
75: X = **=**O
76: X = **-**H **-**H
78
13A'

Scheme 3.25. Proposed synthetic schemes for preparing BODIPY **13C'**.

3.4. Experimental

3.4.1. General

Reactions were monitored using 0.2 mm silica gel plates (with indicator, polyester backed, 60 Å, pre-coated) and UV lamp. Liquid chromatography was performed on preparative TLC plates or via silica gel column chromatography (60 Å, 230−400 mesh) and all solvent systems were buffered with 0.1% triethylamine. NMR spectra were obtained on 400 (^{1}H) and 500 MHz (^{13}C) spectrometers at room temperature for the neutral BODIPYs and at 298.0 or 310.0 K for the ionic BODIPYs depending on whether or not the solution solidified in the NMR tube. Chemical shifts (δ) are given in parts per million (ppm) in CDCl3 (7.27 ppm for ^{1}H NMR, 77.0 ppm for ^{13}C NMR) or C_2D_6SO (2.50 ppm for ^{1}H NMR, 39.5 ppm for ^{13}C NMR) or; coupling constants (J) are given in hertz. High-resolution mass spectra were measured on an ESI-TOF mass spectrometer in positive mode. UV−Vis absorption and emission spectra were recorded at room temperature. Spectroscopic grade solvents and quartz cuvettes (10 mm path length) were used. For the determination of the optical density (ε), solutions with absorbance at λ_{max} between 0.5 and 1 were used. For the determination of quantum yields, dilute solutions with absorbance between 0.03 and 0.05 at the particular excitation wavelength were used and all measurements were taken within XX hours after solution preparation.

3.4.2. Synthesis

8-(4-Pyridyl)-1,3,5,7-tetramethyl-BODIPY (1A). In an oven dried flask, a 14:1 DCM/absolute ethanol solution was degassed with nitrogen for 30 minutes. The flask was then charged with 2,4-dimethylpyrrole (0.13 mL, 1.22 mmol), 4-formylpyridine (55.0 µL, 0.57 mmol, 0.46 eq), and TFA (2 drops). After 24 hours of stirring under a flow of

nitrogen, the solution was neutralized with DIPEA (6 drops) and p-chloranil (0.1422 g, 0.57 mmol, 1.00 eq) was added. The mixture was stirred under a flow of nitrogen for 4 hours after which the solvent was removed under reduced pressure. The residue was then taken up in dry DCM (20 mL), DIPEA (1.00 mL, 5.75 mmol, 10.15 eq) was added and the mixture was stirred for 30 minutes before addition of $BF_3{\cdot}OEt_2$ (0.90 mL, 7.29 mmol, 12.88 eq). When TLC showed disappearance of the dipyrromethene, the solution was filtered to remove the precipitates and purified over silica by column chromatography eluting with 4% EtOAc/DCM and 2% EtOAc/DCM to afford 0.0670 g of product (34% yield). ^{1}H NMR (400 MHz, $CDCl_3$): δ = 8.80-8.79 (d, 2H), 7.32-7.31 (d, 2H), 6.02 (s, 2H), 2.57 (s, 6H), 1.42 (s, 6H); ^{13}C NMR (500 MHz,$CDCl_3$): δ = 156.38, 150.53, 143.50, 142.54, 137.54, 130.24, 123.21, 121.70,14.53, 14.50 ppm; HRMS (ESI): m/z calcd (%) for $C_{18}H_{19}BF_2N_3$: 326.1638 [M+H]+; found: 326.1641; UV/Vis (CH_3CN): λ_{max} = 501, λ_{em} = 515 nm

8-(N-methyl-4-Pyridyl)-1,3,5,7-tetramethyl-BODIPY Iodide (1catA). In a 10 mL round bottom flask wrapped in foil, BODIPY **1A** (6.8 mg, 0.0209 mmol) was dissolved in methyl iodide (2.0 mL). After stirring for 48 hours under a flow of nitrogen, TLC showed consumption of starting material and the excess methyl iodide was removed under reduced pressure. Yield 9.8 mg, 100% (greenish-gray solid): ^{1}H NMR (400 MHz, DMSO-d_6): δ = 9.20-9.18 (d, 2H), 8.42-8.40 (d, 2H), 6.29 (s, 3H), 4.45 (s, 3H), 3.30 (s, 6H), 1.43 (s, 6H); ^{13}C NMR (500 MHz, DMSO-d_6): δ = ppm; HRMS (ESI): m/z calcd (%) for $C_{19}H_{21}BF_2N_3$: 339.1827[M*]+; found: 339.1830; UV/Vis (CH_3CN): λ_{max} = 509, λ_{em} = 596 nm.

2,6-Dichloro-8-(4-pyridyl)-1,3,5,7-tetramethyl-BODIPY (3A). To an oven dried flask charged with BODIPY **1A** (0.0118 g, 0.04 mmol) in dichloromethane (10.0 mL) was dropwise added trichloroisocyanuric acid (0.0076 g, 0.03 mmol, 2.62 eq) in dichloromethane (4.0 mL) and the mixture was stirred at room temperature under a nitrogen atmosphere. After TLC showed consumption of the starting material (about 30 minutes) the solution was purified over silica by column chromatography eluting with 2% methanol/dichloromethane yielding 10 mg, 69% yield (red solid): ^{1}H NMR (400 MHz, $CDCl_3$): δ = 8.85-8.84 (dd, J = 5.9, 1.5 Hz, 2H), 7.31-7.30 (dd, J = 5.9, 1.6 Hz, 2H), 2.61 (s, 6H), 1.42 (s, 6H); ^{13}C NMR (500 MHz,$CDCl_3$): δ = 153.7, 150.9, 142.8, 138.2, 137.5, 128.6, 123.3, 123.1, 12.5, 12.2 ppm; HRMS (ESI): *m/z* calcd (%) for $C_{18}H_{19}BF_2N_3Cl_2$: 393.0891[M+H]+; found: 393.0902; UV/Vis (CH_3CN): λ_{max} = 528, λ_{em} = 554 nm.

2,6-Dichloro-8-(N-methyl-4-Pyridyl)-1,3,5,7-tetramethyl-BODIPY Iodide (3catA). In a 5 mL round bottom flask wrapped in foil, BODIPY **3A** (5.6 mg, 0.014 mmol) was dissolved in anhydrous ACN (1.8 mL) and methyl iodide (1.8 mL). After refluxing for 1 hour, TLC showed consumption of starting material and the solvent was removed under reduced pressure. Yield 7.6 mg, 100% (greenish-gray solid): ^{1}H NMR (400 MHz, DMSO-d_6): δ = 9.24-9.23 (d, J = 6.6 Hz, 2H), 8.44-8.42 (d, J = 6.7 Hz, 2H), 4.47 (s, 3H), 3.32 (s, 6H), 2.55 (s, 6H), 1.30 (s, 6H); ^{13}C NMR (500 MHz,DMSO-d_6): δ = 154.02, 149.59, 147.54, 138.02, 136.71, 128.22, 128.08, 122.98, 49.02, 13.17, 12.89 ppm; HRMS (ESI): m/z calcd (%) for $C_{19}H_{19}BF_2N_3Cl_2$: 407.1048[M*]+; found: 407.1048; UV/Vis (CH_3CN): λ_{max} = 538, λ_{em} = 596 nm.

2,6-Dibromo-8-(4-pyridyl)-1,3,5,7-tetramethyl-BODIPY (4A). To a flask charged with a solution of BODIPY 1A (82.8 mg, 0.25 mmol) in 20 mL of dry DCM was

added dropwise a solution of bromine (0.04 mL, 0.77 mmol) in DCM (5 mL). The mixture was allowed to stir for 2 h, washed with an aqueous solution of sodium thiosulfate, and extracted by DCM. Organic layers were combined, dried over Na_2SO_4, and the solvent was removed under reduced pressure. The residue was purified over silica gel using 1% EA/DCM as eluent, from which the desired product 4A was obtained as red solid in 98% yield (120.8 mg): ^{1}H NMR (400 MHz, $CDCl_3$): δ = 8.86-8.84 (d, J = 5.7, 1.6 Hz, 2H), 7.32-7.30 (dd, J = 5.9, 1.4 Hz, 2H), 2.63 (s, 6H), 1.43 (s, 6H); ^{13}C NMR (500 MHz, $CDCl_3$): δ = 155.22, 151.08, 143.11, 140.26, 138.04, 129.51, 123.19, 112.56, 14.10, 13.95 ppm; HRMS (ESI): m/z calcd (%) for $C_{18}H_{16}BF_2N_3Br_2$: 480.9881[M+H]+; found: 480.9870; UV/Vis (CH_3CN): λ_{max} = 528, λ_{em} = 555 nm.

2,6-Dibromo-8-(N-methyl-4-Pyridyl)-1,3,5,7-tetramethyl-BODIPY Iodide (4catA). In a 5 mL round bottom flask wrapped in foil, BODIPY 4A (10.4 mg, 0.022 mmol) was dissolved in anhydrous ACN (1.8 mL) and methyl iodide (1.8 mL). After refluxing for 1 hour, TLC showed consumption of starting material and the solvent was removed under reduced pressure. Yield 13.5 mg, 100% (greenish-gray solid): ^{1}H NMR (400 MHz, DMSO-d_6): δ = 9.24-9.23 (d, J = 6.6 Hz, 2H), 8.44-8.42 (d, J = 6.7 Hz, 2H), 4.47 (s, 6H), 3.32 (s, 6H), 2.55 (s, 6H), 1.30 (s, 6H) ppm; HRMS (ESI): m/z calcd (%) for $C_{19}H_{19}BF_2N_3Br_2$: 495.0038[M*]+; found: 495.0032; UV/Vis (CH_3CN): λ_{max} = 539, λ_{em} = 560 nm.

2,6-Diiodo-8-(4-pyridyl)-1,3,5,7-tetramethyl-BODIPY (5A). To a flask charged with BODIPY 1A (0.0200 g, 0.062 mmol) in 3:1 MeOH/DCM (8 mL) was dropwise added a solution of iodine monochloride (0.75 mL, 1.0 M) in dichloromethane. When TLC showed consumption of starting material, the mixture was washed with water and

extracted with DCM. The solvent was removed under reduced pressure and the residue was purified by silica gel column chromatography eluting with 2% EA/DCM to give the product as a red solid (16.0 mg, 45%). ^{1}H NMR (400 MHz, $CDCl_3$): δ = 8.83-8.82 (dd, J = 5.8, 1.5 Hz, 2H), 7.29-7.28 (dd, J = 6.0, 1.5 Hz, 2H), 2.65 (s, 6H), 1.43 (s, 6H); ^{13}C NMR (500 MHz, $CDCl_3$): δ = 158.02, 151.10, 146.72, 145.00, 143.47, 131.24, 130.38, 123.21, 17.40, 16.30 ppm; HRMS (ESI): m/z calcd (%) for $C_{18}H_{16}BF_2N_3I_2$: 576.9604[M+H]+; found: 576.9594; UV/Vis (CH_3CN): λ_{max} = 534, λ_{em} = 563 nm.

2,6-Diiodo-8-(N-methyl-4-Pyridyl)-1,3,5,7-tetramethyl-BODIPY Iodide (5catA). In a 3 mL amber vial, BODIPY 5A (4.7 mg, 0.008 mmol) was dissolved in methyl iodide (1.0 mL). After stirring at 35°C for 12 hours, TLC showed consumption of starting material and the solvent was removed under reduced pressure. Yield 7.6 mg, 100% (purpleish-gray solid): ^{1}H NMR (400 MHz, DMSO-d_6): δ = 9.16-9.14 (d, J = 6.3 Hz, 2H), 8.34-8.33 (d, J = 6.5 Hz, 2H), 4.57 (s, 3H), 2.63 (s, 6H), 1.52 (s, 6H) ppm; HRMS (ESI): m/z calcd (%) for $C_{19}H_{19}BF_2N_3I_2$: 590.9760[M*]+; found: 590.9747; UV/Vis (CH_3CN): λ_{max} = 546, λ_{em} = 654 nm.

2-Formyl-1,3,5,7-tetramethyl-BODIPY (6A). To an oven dried flask charged with anhydrous DMF (2.10 mL, 25.61 mmol), under an atmosphere of dry nitrogen, and cooled down to 0°C was dropwise added $POCl_3$ (2.10 mL, 27.18 mmol, 0.94 eq) and the mixture was stirred for 5 minutes before warming to room temperature and stirring for an additional 30 minutes. This solution was then drawn into a syringe and dropwise added to a second oven dried flask charged with a solution of BODIPY **1A** (0.0564 g, 0.17 mmol) in anhydrous dichloroethane (20.00 mL). After the addition was complete, the mixture was heated to 50°C for 2 hours before cooling to room temperature and

slowly pouring into an ice cold solution of saturated $NaHCO_3$(aq). When the mixture warmed to room temperature, the organic layer was separated, dried over anhydrous Na_2SO_4, and the solvent was removed under reduced pressure. The residue was then transferred to another oven dried flask and the process repeated. The second step was heated to 60°C for 5 hours. The crude residue was purified by column chromatography over silica eluting with 12.5% Hexanes/EtOAc, buffered with 0.1% TEA, to yield 0.0114 g of 6A (19%). ^{1}H NMR (400 MHz, $CDCl_3$): δ = 10.03 (s, 1H), 8.83-8.82 (dd, J = 5.9, 1.5 Hz, 2H), 7.29-7.28 (dd, J = 5.9, 1.6 Hz, 2H), 2.59 (1H, s), 1.40 (1H, s); ^{13}C NMR (500 MHz, $CDCl_3$): δ = 185.88, 162.95, 157.41, 151.13, 149.13, 146.76, 142.89, 139.59, 132.05, 126.71, 124.80, 123.13, 77.41, 77.16, 76.91, 29.85, 15.24, 14.27, 13.20, 12.02 ppm; HRMS (ESI): m/z calcd (%) for $C_{19}H_{18}BF_2N_3O$: 353.1620[M+H]+; found: 353.1612; UV/Vis (CH_3CN): λ_{max} = 495, λ_{em} = 511 nm.

2-Formyl-8-(N-methyl-4-Pyridyl)-1,3,5,7-tetramethyl-BODIPY Iodide (6catA). In a 5 mL round bottom flask wrapped in foil, BODIPY 6A (4.7 mg, 0.013 mmol) was dissolved in anhydrous ACN (1.8 mL) and methyl iodide (1.8 mL). After refluxing for 1 hour, TLC showed consumption of starting material and the solvent was removed under reduced pressure. Yield 6.6 mg, 100% (greenish-gray solid): ^{1}H NMR (400 MHz, MeOD): δ = 10.00 (s, 1H), 9.18-9.16 (d, J = 6.4 Hz, 2H), 8.38-8.36 (d, J = 6.3 Hz, 2H), 4.58 (s, 3H), 3.23 (s, 3H), 2.97 (s, 3H), 2.78 (s, 3H), 2.63 (s, 3H) ppm; HRMS (ESI): m/z calcd (%) for $C_{20}H_{21}BF_2N_3O$: 367.1777[M*]+; found: 367.1770; UV/Vis (CH_3CN): λ_{max} = 504, λ_{em} = 653 nm.

N-Benzyl-3-(benzylamino)but-2-enamide (32): To a solution of benzylamine (1.15 mL, 10.63 mmol) in anhydrous o-xylene (1.50 mL) was added 2,2,6-trimethyl-4H-

1,3-dioxin-4-one (0.47 mL, 3.72 mmol) and the mixture was refluxed for 2 h. The mixture was allowed to cool and crystallize. The residue was then taken up in DCM, washed with 11 mL 0.5 M HCl(aq) and filtered to remove excess benzylamine. The solvent was then removed under vacuum and the residue was rinsed with 1:1 EA/Hex (containing 0.1% TEA) and a cream colored solid (0.4429 g, 1.58 mmol, 42% yield) was obtained. TLC of the product showed one spot. Yield: 42%, 0.44 g. ^{1}H NMR(400 MHz, $CDCl_3$): δ = 9.42 (s, 1H), 7.24−7.14 (m, 10H), 4.37−4.35 (d, 2H), 4.33−4.31 (d, 2H), 4.29 (s, 1H), 1.78 (s, 3H) ppm. HRMS (ESI): m/z calcd (%) for $C_{18}H_{20}N_2O$: 281.1648[M+H]+; found 281.1650.

tert-Butyl 3-(N-benzylcarbamoyl)-2,4-dimethylpyrrole-5-carboxylate (34): To a 2-necked flask charged with tert-butyl acetoacetate **22** (0.45 mL, 2.66 mmol) in glacial acetic acid (0.63 mL) and chilled to 0°C was added $NaNO_2$ (0.2046g, 2.88 mmol, 1.08 eq) in water (0.40 mL) dropwise. The mixture was stirred for 30 minutes before being removed from the ice bath and stirred at room temperature for 3 hours. The mixture was then heated to 67°C, N-benzyl-3-(benzylamine)but-2-enamide **32** (0.4405 g, 1.57 mmol, 0.59 eq) in glacial acetic acid (1.00 mL) was added followed by portionwise addition of an intimate mixture of zinc dust (0.3700 g, 5.60 mmol, 3.57 eq) and NaOAc (0.3700 g, 4.47 mmol, 2.84 eq). The mixture was then heated for 1 hr before slowly being poured into 200 mL of ice water and stirring for 5 minutes. The precipitate was collected by filtration and then washed with DCM to separate it from the inorganic solids. The solution was then washed with water, dried over anhydrous sodium sulfate, and purified over silica eluting with DCM to produce 0.3366 g (7%) of the product pyrrole **34**. Note: there was significant product loss due to human error, but the reaction

was not re-run. ^{1}H NMR (400 MHz, $CDCl_3$): δ = 8.85 (s, 1H), 7.37-7.30 (m, 5H), 5.88 (s, 1H), 4.64-4.63 (d, J = Hz, 2 H), 2.49-2.48 (d, 6H), 1.58 (s, 9H); ^{13}C NMR (500 MHz, $CDCl_3$): δ = 165.92, 161.23, 138.76, 134.75, 128.83, 127.81, 127.52, 125.50, 119.18, 118.19, 81.22, 43.72, 28.58, 13.38, 12.02 ppm; HRMS (ESI): m/z calcd (%) for $C_{19}H_{24}N_2O_3$: 329.1860 [M+H]+; found: 329.1863.

N,N-Dibenzylacetoacetamide (35): To a solution of dibenzylamine (2.30 mL, 22.70 mmol) in anhydrous o-xylene (3.20 mL) was added 2,2,6-trimethyl-4H-1,3-dioxin-4-one (1.00 mL, 7.92 mmol) and the mixture was refluxed for 2 h. The mixture was allowed to cool and the residue was then taken up in DCM, washed with 11 mL 0.5 M HCl(aq) and filtered to remove excess dibenzylamine. The solvent was then removed under vacuum and the oil was purified over silica eluting with 1:1 EA/Hex (containing 0.1% TEA) to yield 2.2282 g (7.92 mmol, 100%) of the product. The product is a mixture of the keto-enol tautomers in a 3:1 ratio. ^{1}H NMR (400 MHz, $CDCl_3$): δ = 14.83 (s, 0.3H), 7.42-7.16 (m, 18H), 5.23 (s, 0.3H), 4.66 (s, 3H), 4.44 (s, 3H), 3.66 (s, 2H), 2.31 (s, 3H), 1.97 (s, 1H); ^{13}C NMR (500 MHz, $CDCl_3$): δ = 202.44, 175.96, 172.75, 167.56, 137.31, 136.81, 136.07, 129.60, 129.20, 129.01, 128.86, 128.82, 128.77, 128.25, 128.22, 127.99, 127.66, 126.74, 126.51, 87.02, 50.71, 50.09, 49.82, 48.51, 47.87, 30.51, 22.20 ppm. HRMS (ESI): m/z calcd (%) for $C_{18}H_{19}NO_2$: 282.1489 [M+H]+; found: 282.1487.

Methyl 3,5-dimethylpyrrole-2,4-dicarboxylate benzyl ester(38): To a 2-necked flask charged with benzyl acetoacetate (5.00 mL, 28.11 mmol) in glacial acetic acid (6.50 mL) and chilled to 0°C was added NaNO2 (2.1600g, 30.37 mmol, 1.08 eq) in water (4.25 mL) dropwise. The mixture was stirred for 30 minutes before being

removed from the ice bath and stirred at room temperature for 3 hours. The mixture was then heated to 67°C, methyl acetoacetate (2.00 mL, 18.35 mmol, 0.65 eq) in glacial acetic acid (10.00 mL) was added followed by portion-wise addition of an intimate mixture of zinc dust (4.3000 g, 65.11 mmol, 3.55 eq) and NaOAc (4.3000 g, 51.89 mmol, 2.83 eq). The mixture was then heated for 1 hr before slowly being poured into 200 mL of ice water and stirring for 5 minutes. The precipitate was collected by filtration and then washed with DCM to separate it from the inorganic solids. The solution was then washed with water, dried over anhydrous sodium sulfate, and purified by recrystallization using DCM/Hexanes. The mother liquor was then purified over silica eluting with DCM which collectively yielded 2.2483g (45%) of the product pyrrole. ^{1}H NMR (400 MHz, $CDCl_3$): δ = 8.84 (s, 1H), 7.43-7.32 (m, 5H), 5.31 (s, 2H), 3.82 (s, 3H), 2.57 (s, 3H), 2.49 (s, 3H) ppm; ^{13}C NMR (500 MHz, $CDCl_3$): δ = 165.95, 161.21, 139.18, 136.19, 131.69, 128.79, 128.46, 128.41, 66.17, 50.90, 14.52, 12.18 ppm; HRMS (ESI): m/z calcd (%) for $C_{16}H_{17}NO_4$: 273.1809 [M+H]+; found: 273.1809.

Note: The "recrystallization" was not a true recrystallization using DCM/Hexanes as the two solvents never mixed by Brownian motion. The first recrystallization was left in the freezer overnight and the next morning the vial was still orange on bottom and colorless on top unlike the recrystallization of the 3-acyl derivative in which the entire vial was a light yellow the following morning. I attempted to recrystallize the next bit of material on the bench top which did not crystallize after 8 hours. After moving it to the freezer, crystals formed rather quickly. The last bit was recrystallized by heating to dissolve in a minimal amount of DCM and cooling in the freezer.

3.4.3. Biological Characterization

3.4.3.1. General

The HEp-2 cell line, purchased from ATCC, was used in the biological characterization of the synthesized BODIPYs. All reagents, including the culture medium, were purchased from Life Technologies. HEp-2 cells were cultured in the medium (1:1 Dulbecco's Modified Eagle Medium (DMEM)/Advanced DMEM) containing 10% fetal bovine serum (FBS) and 1% antibiotic (Penicillin-streptomycin). A 32 mM compound stock solution was prepared by dissolving the compound in 5% (v/v) Cremophor in DMSO. The working solutions were prepared by dilution the stock solution with growing medium.

3.4.3.2. Time-Dependent Cellular Uptake

HEp-2 cells were plated at 15,000 cells per well in a Costar 96-well plates (BD biosciences) and grown overnight. The cells were treated by adding 100 μL/well of 10 μM working solution at different time periods of 0, 1, 2, 4, 8, and 24h. The loading medium was removed at the end of the treatments. The cells were washed with 1X PBS and suspended in solution by adding 0.25% Triton X-100 in 1X PBS. A standard curve, 10 μM, 5 μM, 2.5 μM, 1.25 μM, 0.625 μM, 0.3125 μM, for each sample was made by diluting stock solution with 0.25% Triton X-100(Sigma-Aldrich) in 1X PBS. A cell standard curve was prepared using 10000, 20000, 40000, 60000, 80000, and 100000 cell per well. The cells were quantified using a CyQuant Cell Proliferation Assay (Life Technologies). The sample concentration and cell count were determined using a FluoStar Optima micro-plate reader (BMG LRBTEH), with wavelengths 584/650 nm for

the samples and 485/520 nm for the cells. Cellular uptake was expressed in terms of pM/cell.

3.4.3.3. Cytotoxicity

3.4.3.3.1. Dark Toxicity

In a 96-well plate prepared as previously stated, HEp-2 cells were treated with the sample concentration of 0, 6.25, 12.5, 25, 50, 100, and 200 μM and then incubated at 37°C. After 24 hours incubation, the cells were washed with 1X PBS and the media replaced with new the media containing 20 % cell titer blue (CellTiter-Blue® Cell Viability Assay)(Promega). The cells were incubated for an additional 4 hours at 37°C. The viable cell count is measured by fluorescence (570/615 nm) using a FluoStar Optima micro-plate reader. The experiment was run in quintuplicate for each concentration and the dark toxicity was expressed in terms of the percentage of viable cells.

3.4.3.3.2. Phototoxicity

HEp-2 cells in 96-well plates were treated with the samples at 0, 3.125, 6.25, 12.5, 25, 50, and 100 μM concentrations and incubated at 37°C. After 24 hours, the loading media was removed, the cells were washed with 1X PBS, and then suspended in fresh media. The cells were exposed to light for 20 minutes to get a light dose of approximately 1.5 J/cm^2. After exposure to light, the cells were incubated in the dark for an additional 24 hours. The medium was then replaced with media containing 20 % cell titer blue. The cells were incubated for an additional 4 hours before the viable cells were quantified using a FluoStar Optima micro-plate reader. The phototoxicity was expressed in terms of the percentage of viable cells.

3.5. References

1. Caruso, E.; Banfi, S.; Barbieri, P.; Leva, B.; Orlandi, V. T., Synthesis and Antibacterial Activity of Novel Cationic BODIPY Photosensitizers. *J. Photochem. Photobiol., B* **2012,** *114*(3), 44-51.

2. Bartelmess, J.; Weare, W. W.; Latortue, N.; Duong, C.; Jones, D. S., Meso-Pyridyl BODIPYs with Tunable Chemical, Optical and Electrochemical Properties. *New J. Chem.* **2013,** *37*(9), 2663-2668.

3. Lindsey, J. S.; Wagner, R. W., Investigation of the Synthesis of Ortho-Substituted Tetraphenylporphyrins. *J. Org. Chem.* **1989,** *54*(4), 828-836.

4. Huynh, A. M.; Menges, J.; Vester, M.; Dier, T.; Huch, V.; Volmer, D. A.; Jung, G., Monofluorination and Trifluoromethylation of BODIPY Dyes for Prolonged Single-Molecule Detection. *ChemPhysChem* **2016,** *17*(3), 433-442.

5. Heeran, D.; Sandford, G., Fluorination of Pyrrole Derivatives by Selectfluor™. *Tetrahedron* **2016,** *72*(19), 2456-2463.

6. Wiley, R. H.; Borum, O. H., Ethyl Acetamidoacetoacetate. *J. Am. Chem. Soc.* **1948,** *70*(4), 1666-1666.

7. Mataka, S.; Takahashi, K.; Tsuda, Y.; Tashiro, M., Preparation of Ethyl 3,5-Disubstituted Pyrrole-2-Carboxylates from 1,3-Diketones and Ethyl Glycinate Hydrochloride. *Synthesis* **1982,** *1982*(02), 157-159.

8. Banks, R. E.; Lawrence, N. J.; Popplewell, A. L., Efficient Electrophilic Fluorination of β-Dicarbonyl Compounds with the Selectfluor Reagent F-TEDA-BF_4 {1-Chloromethyl-4-Fluoro-1,4-Diazoniabicyclo[2.2.2]Octane Bis(Tetrafluoroborate)}. *J. Chem. Soc., Chem. Commun.* **1994,** (3), 343-344.

9. Zhao, N.; Xuan, S.; Fronczek, F. R.; Smith, K. M.; Vicente, M. G. H., Stepwise Polychlorination of 8-Chloro-BODIPY and Regioselective Functionalization of 2,3,5,6,8-Pentachloro-BODIPY. *J. Org. Chem.* **2015,** *80*(16), 8377-8383.

10. Wallace, D. M.; Leung, S. H.; Senge, M. O.; Smith, K. M., Rational Tetraarylporphyrin Syntheses: Tetraarylporphyrins from the Macdonald Route. *J. Org. Chem.* **1993,** *58*(25), 7245-7257.

11. Thach, O.; Mielczarek, M.; Ma, C.; Kutty, S. K.; Yang, X.; Black, D. S.; Griffith, R.; Lewis, P. J.; Kumar, N., From Indole to Pyrrole, Furan, Thiophene and Pyridine: Search for Novel Small Molecule Inhibitors of Bacterial Transcription Initiation Complex Formation. *Bioorg. Med. Chem.* **2016,** *24*(6), 1171-1182.

12. Bartelmess, J.; Francis, A. J.; El Roz, K. A.; Castellano, F. N.; Weare, W. W.; Sommer, R. D., Light-Driven Hydrogen Evolution by BODIPY-Sensitized Cobaloxime Catalysts. *Inorg. Chem.* **2014,** *53*(9), 4527-4534.

13. Jiao, L.; Yu, C.; Li, J.; Wang, Z.; Wu, M.; Hao, E., β-Formyl-BODIPYs from the Vilsmeier−Haack Reaction. *J. Org. Chem.* **2009,** *74*(19), 7525-7528.

14. Ramírez-Ornelas, D. E.; Alvarado-Martínez, E.; Bañuelos, J.; López Arbeloa, I.; Arbeloa, T.; Mora-Montes, H. M.; Pérez-García, L. A.; Peña-Cabrera, E., FormylBODIPYs: Privileged Building Blocks for Multicomponent Reactions. The Case of the Passerini Reaction. *J. Org. Chem.* **2016,** *81*(7), 2888-2898.

15. Denissen, W.; Rivero, G.; Nicolaÿ, R.; Leibler, L.; Winne, J. M.; Du, P. F. E., Vinylogous Urethane Vitrimers. *Adv. Funct. Mater.* **2015,** *25*(16), 2451-2457.

16. Kremlev, M. M.; Mushta, A. I.; Tyrra, W.; Yagupolskii, Y. L.; Naumann, D.; Möller, A., Me3SiCF3/AgF/Cu—a New Reagents Combination for Selective Trifluoromethylation of Various Organic Halides by Trifluoromethylcopper, CuCF3. *J. Fluorine Chem.* **2012,** *133*, 67-71.

17. Jinadasa, R. G. W. E. Design, Synthesis, and Characterization of Porphyrin Derivatives for Biological Applications. Doctoral Dissertation, Louisiana State University and Agricultural and Mechanical College, Baton Rouge, Louisiana, 2013.

18. Ueno, T.; Urano, Y.; Kojima, H.; Nagano, T., Mechanism-Based Molecular Design of Highly Selective Fluorescence Probes for Nitrative Stress. *J. Am. Chem. Soc.* **2006,** *128*(33), 10640-10641.

19. Ieda, N.; Hotta, Y.; Miyata, N.; Kimura, K.; Nakagawa, H., Photomanipulation of Vasodilation with a Blue-Light-Controllable Nitric Oxide Releaser. *J. Am. Chem. Soc.* **2014,** *136*(19), 7085-7091.

20. Olmsted, J., Calorimetric Determinations of Absolute Fluorescence Quantum Yields. *J. Phys. Chem* **1979,** *83*(20), 2581-2584.

21. Katsumi, N., Synthesis, Luminescence Quantum Yields, and Lifetimes of Trischelated Ruthenium(Ii) Mixed-Ligand Complexes Including 3,3′-Dimethyl-2,2′-Bipyridyl. *Bull. Chem. Soc. Jpn.* **1982,** *55*(9), 2697-2705.

Chapter 4. Photophysical and Biological Properties of meso-Pyridyl BODIPY Isomers: A Family Affair

4.1. Introduction

BODIPYs bearing pyridine moieties are commonly used as metal ion sensors[1,2], organic ligands in metal organic frameworks[3-6] and organometallic complexes[7,8], as well as both heavy-atom induced and heavy-atom free photosensitizers.[9-14] With regard to the BODIPYs bearing pyridines on the meso-position, there are three structural isomers, shown in Figure 4.1, all of which have been reported in the literature. However, a comparative study of the differences in their properties has not been reported. The optical properties of the neutral derivatives have been shown in the literature to be practically identical;[9] however, the same cannot be said for their respective N-methyl salts. Salts of the 4-pyridyl derivative have been used for triplet state sensitization while those of the 2-pyridyl derivative have found use as bio-labels.[15,16] The following study aims to elucidate the structure-property relationship and find a rational explanation for the differences through photophysical characterization, computational analysis of the excited states and electronic structure, as well as characterization of the biological activity of the isomers in human epithelial type-2 (HEp-2) cancer cells.

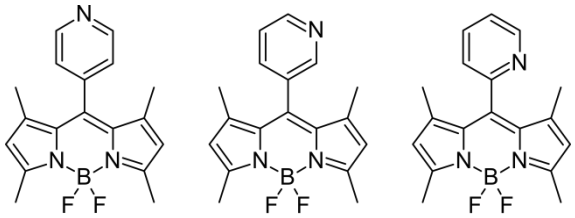

Figure 4.1. Structural isomers of the meso-pyridyl tetramethylBODIPY. The N-methyl salts are denoted with a "$^{+}$".

4.2. Results and Discussion

4.2.1. Synthesis

Derivative **4–Py** was prepared as previously described via the acid catalyzed condensation of 2,4-dimethylpyrrole with pyridine-4-carboxaldehyde in 14:1 DCM/MeOH followed by subsequent oxidation with chloranil and boron complexation. The 3-pyridyl isomer **3–Py** was prepared by reacting the 2,4-dimethylpyrrole Grignard **66** with methyl pyridine-3-carboxylate **67** under reflux in THF for 4 hours followed by BF_3 complexation (Scheme 4.1. The Grignard method for preparing the dipyrromethene yielded a much cleaner transformation than the aldehyde condensation. It is worth noting that the magnesium salts do not need to be removed before boron complexation and the dipyrromethene is quite water soluble. The 2-pyridyl derivative 2–Py was attempted to be prepared by the Grignard method as well, but the reaction always stopped at the pyridylpyrroketone **69** (Scheme 4.2). All attempts to push the transformation to

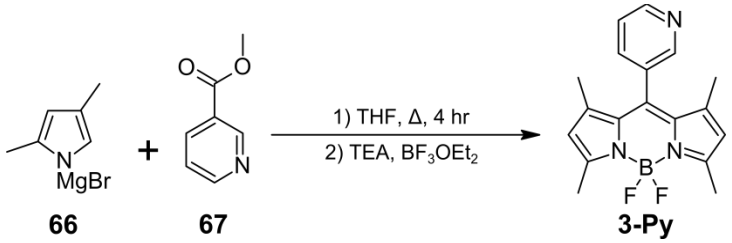

Scheme 4.1. Synthetic route for preparing **3–Py**.

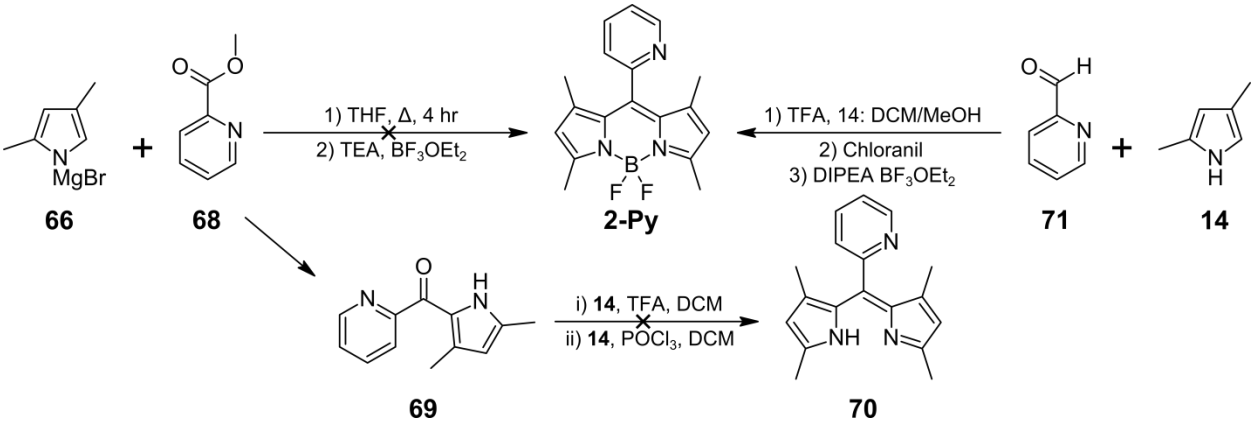

Scheme 4.2. Synthetic scheme for preparing **2–Py**.

completion were unsuccessful so **2–Py** was instead prepared following the same protocol used for **4–Py**. The substrates were methylated as previously described.

4.2.2. Photophysical Studies

The photophysical properties of the three isomers and their N-methyl salts are summarized in Table 4.1 and the spectra are shown in Figure 4.2. The absorption wavelength, molar absorptivity coefficient, and fluorescence quantum yields for **4–Py$^+$** and **3–Py$^+$** are essentially identical, however, there is a dramatic change in the emission wavelength from 596 nm to 537 nm. The **2–Py$^+$** on the other hand, exhibits quite

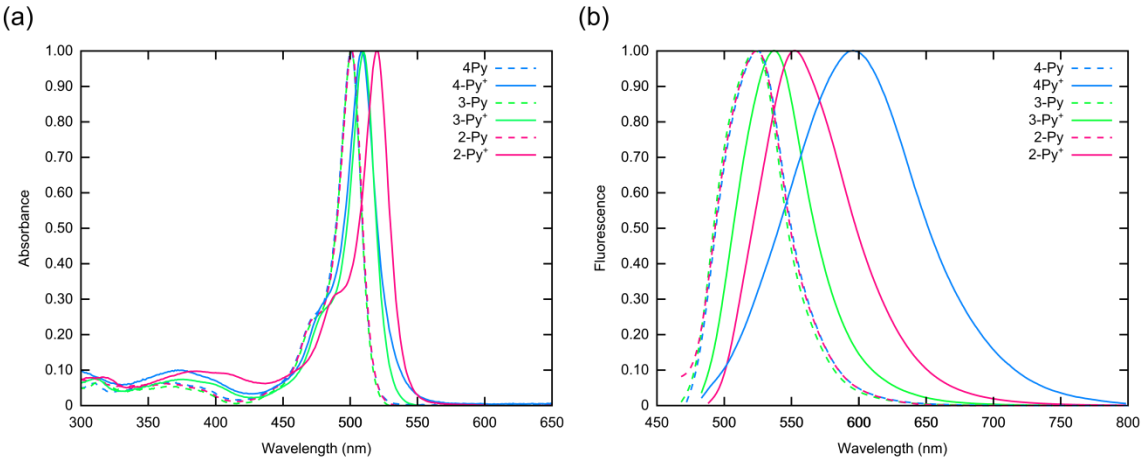

Figure 4.2. Normalized a) Absorption and b) emission spectra of **4–Py** (dashed blue), **4–Py$^+$** (solid blue), **3–Py** (dashed green), **3–Py$^+$** (solid green), **2–Py** (dashed red), and **2–Py$^+$** (solid red) measured in acetonitrile at room temperature.

Table 4.1. Photophysical properties of synthesized BODIPYs in CAN.

BODIPY	λ_{max} (nm)		Stokes Shift (nm)	Φ_f^*	ε (M^{-1} cm^{-1})
	abs	em			
4–Py	501	515	28	0.31[a]	72100
4–Py$^+$	509	596	16/131	0.058[b]	26000
3–Py	501	523	22	0.72	68100
3–Py$^+$	510	537	27	0.032[b]	26600
2–Py	501	525	24	0.08	68500
2–Py$^+$	520	552	32	0.476[b]	26600

*Relative quantum yields determined using: (a) rhodamine-6G (Φ_f = 0.86) in methanol as the standard, λ_{ex} = 473 nm [17] and (b) $Ru(bpy)_3Cl_2$ in water as the standard (Φ_f = 0.028), λ_{ex} = 436 nm.[18]

different photophysical properties. There is a 10 nm bathochromic shift in the absorption and a 15 nm shift in the emission. The molar absorptivity coefficient is consistent with the other two, but the fluorescence quantum yield has an order of magnitude increase. The shift in the absorption can potentially be attributed to the electron-withdrawing strength of the pyridinium. In **4–Py$^+$,** the cationic nitrogen is pulling electron density equally from both the left and right sides of the ring giving the greatest overall minimization of the pull on the density localized on carbon 4. The shift in the nitrogen position in **3–Py$^+$** results in an equivalent increase and decrease of pull from the two halves of the ring since no change in the absorption spectrum is observed. The **2–Py$^+$** isomer on the other hand, has a direct pull on the 2-carbon's electron density which can increase the overall electron withdrawing strength of the pyridinium ring and produce the observed shift.

The hypsochromic shifts in the emission of **3–Py$^+$** and **2–Py$^+$** indicate a change in the charge transfer state, if it still occurs. The quantum yields suggest that **3–Py$^+$** still undergoes d-PeT while **2–Py$^+$** does not, but the emission spectra clearly show that all three cationic derivatives exhibit significantly broadened emission bands, relative to the neutral BODIPYs, which is characteristic of charge recombination luminescence.

4.2.3. Computational

To look at the intersystem crossing (ISC), the cations were optimized along their S_1 excited states and the singlet and triplet excitations were then calculated for these structures. The results are of these calculations are summarized in Table 4.2. The singlet-triplet energy gap increases significantly from **4–Py$^+$** to **2–Py$^+$**, but the overall difference between the two states is still quite small. It is acknowledged that this

method of depicting the ISC is theoretically rather crude and it is only being used since one of the systems is known to undergo ISC. This method only works as a theoretical predictor of ISC when the calculations show the singlet and analogous triplet states to be degenerate.

Table 4.2. Calculated S_1 Singlet-Triplet Charge Transfer State Transitions.

BODIPY	Root	Osc.	Trans. Char.	Population	VEE (eV)	ΔVEE(S-T)
1	S 1	0.00008	HOMO→LUMO	0.9842823	1.4691	0.0003
	T 3	N/A	HOMO→LUMO	0.9842606	1.4688	
2	S 1	0.00126	HOMO→LUMO	0.9715651	1.6335	
	T ?	N/A	HOMO→LUMO			
3	S 1	0.01789	HOMO→LUMO	0.9898658	1.8520	0.0268
	T 2	N/A	HOMO→LUMO	0.9688071	1.8252	

Examining this more closely, the HOMO, LUMO, and LUMO+1 for the all three BODIPYs were plotted and are shown in Figure 4.3. The orbitals do not appear to change from one isomer to the next, however there is one potentially important difference in **2–Py$^+$**. Note the red ring of electron density shown on the pyridinium in the LUMO+1 in all three cases. Upon close inspection of the LUMO+1 from the side, the red ring is now on the pyridinium nitrogen. Since the electron density in the charge transfer state will be largely localized on the cationic nitrogen atom, it could be possible that the pyridinium nitrogen's contribution to the $LUMO_{BDP}$ provides enough orbital overlap with the $LUMO_{Py}$ for the excited electron density to move back to the $LUMO_{BDP}$.

4.2.4. Biological Studies

From the biological characterizations of the three BODIPY isomers and their N-methyl iodide salts (Figure 4.4 and Figure 4.5), it was found that the neutral derivatives had higher cellular uptake than the ionic dyes; however, **4–Py$^+$** is comparable to **3–Py** and **2–Py**. It was interesting to see that **3–Py$^+$** and **2–Py$^+$** had almost no uptake, yet **2–Py$^+$** has been reported as a bio-label for studying mitochondria. Looking at the

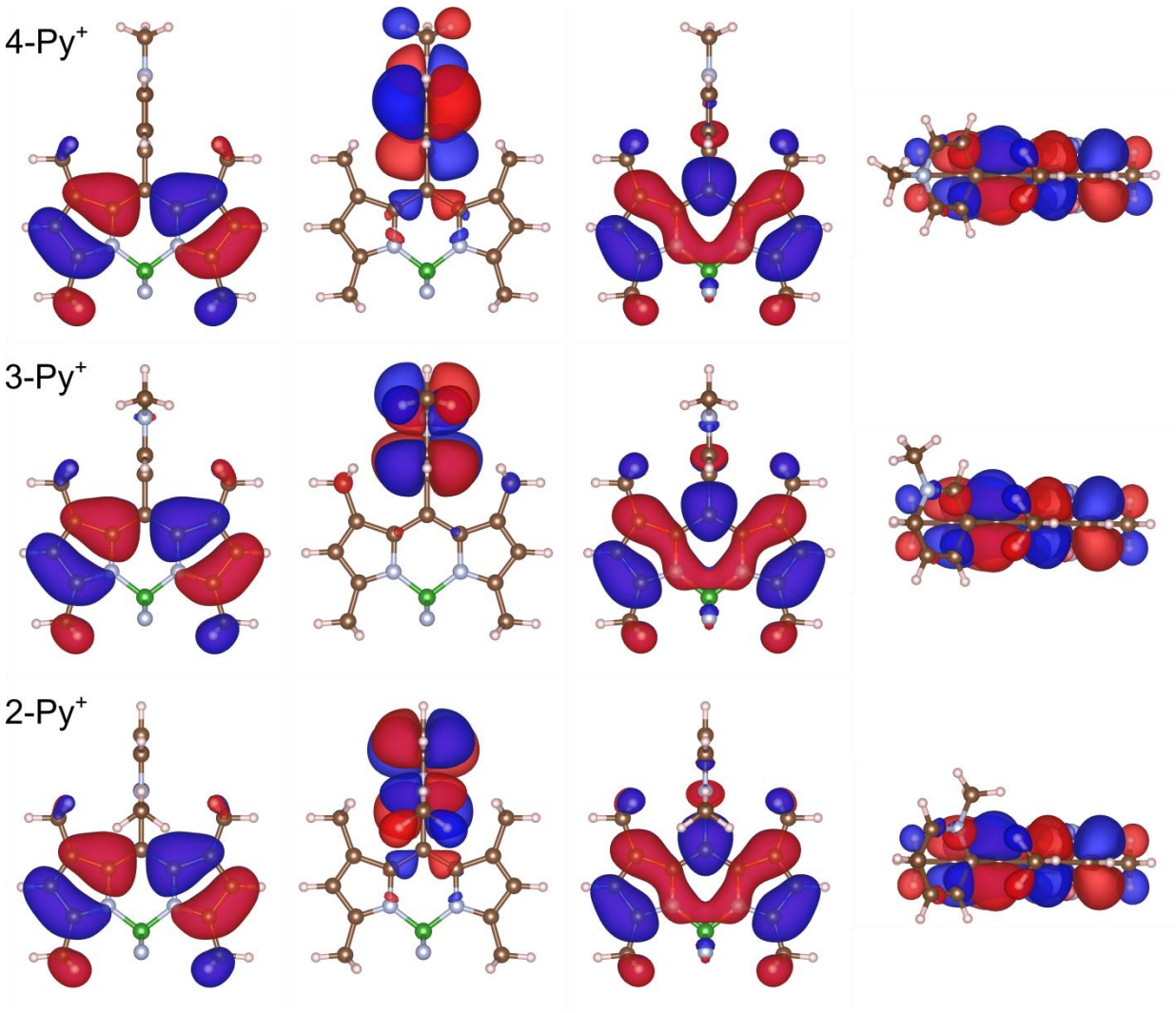

Figure 4.3. MO plots of the HOMO (left), LUMO (middle), and LUMO+1 (right) for **4–Py$^+$**, **3–Py$^+$**, and **2–Py$^+$**. The far right column is the side view of the LUMO+1 shown in the third column. (**Error! Reference source not found.** in Appendix C is an nlarged version of the side view column.)

cytotoxicity, all three ionic derivatives were less toxic in the dark than their neutral counterparts which showed increasing toxicity from **4–Py** < **2–Py** < **3–Py** where **4–Py** is equivalent to **2–Py$^+$**. The phototoxicity reveals a different trend where **4–Py** is the most phototoxic with only 90% of the cell culture surviving while the other five dyes had greater than 95% survival. The phototoxic IC_{50} is > 100 μM and the dark toxicity IC_{50} is > 200 μM for all six dyes in this series.

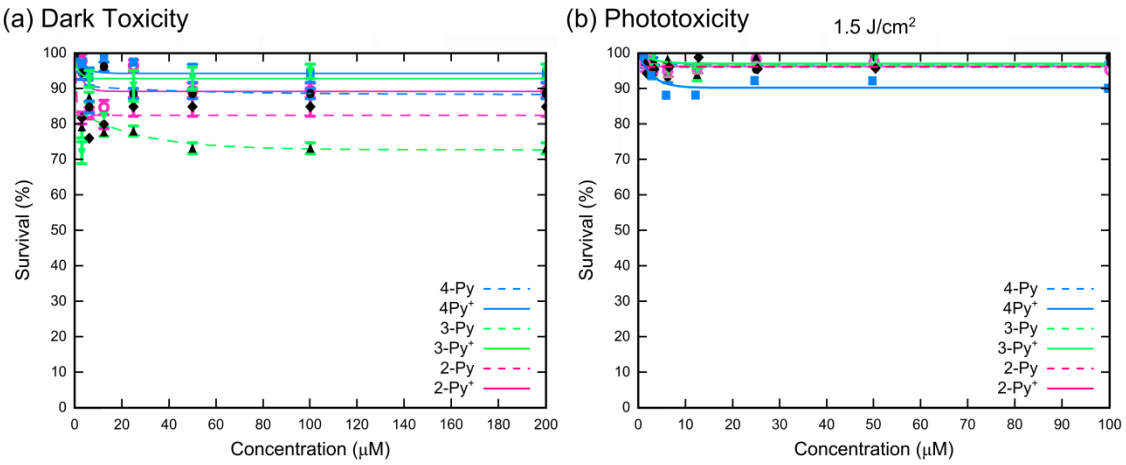

Figure 4.4. Cytotoxicity of neutral and cationic BODIPY isomers a) in the dark and b) with irradiation.

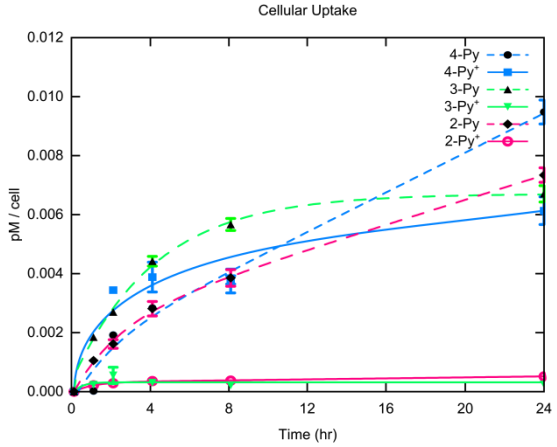

Figure 4.5: Cell uptake of BODIPY derivatives in HEp-2 cells.

4.3. Conclusions

While the optical properties of **2–Py$^+$** are quite different from the other two derivatives, the electronic structure varies only slightly from one isomer to the next. The most noticeable differences are the increase in the singlet-triplet energy gap in the charge transfer state and the pyridinium nitrogen contributing to the $LUMO_{BDP}$ in the S_1 structure of **2–Py$^+$**. Based on the calculations, the differences could be the result of the latter, or potentially have a more dynamic source. When the electron first moves to the pyridinium, it would "arrive" at the closest atom which would be the carbon bonded to the meso-carbon of the BODIPY core. Thinking about electrons as particles is more

useful for synthetic chemists, but looking at them as waves can be a more insightful view in this case. Recalling the Franck-Condon energy well diagram from Chapter 1 section 1.1.7.3.2, as the chromophore follows the potential energy surface (PES) to reach a new equilibrium point, following a vertical excitation, the nuclei and electrons move. In the case of **4–Py$^+$**, the excited electron oscillates back and forth across the pyridinium, as the structure relaxes, traveling both the left and right sides of the ring simultaneously to then recombined at the nitrogen. With the **2–Py$^+$** system, most of the electron goes directly to the nitrogen while a portion of it travels all the way around the ring to then recombine. The time that portion of the electron spends traveling around the ring could potentially keep the system at a higher energy position along the PES and further away from the intersection of the two states.

In considering the work done presented in this dissertation, the next stage of this work would contain two parts. The first would be to finish preparing the libraries designed in Chapter 2, conduct cyclic voltommetry to determine the accuracy of the calculated oxidation potentials, and run photophysical studies to determine if there is a quantifiable relationship between the oxidation potential and the fluorescence quantum yields for the d-PeT systems. The second part would be to apply the results from the presented work to design a new series of dyes with further enhanced properties. On one hand, the calculations have shown that a d-PeT process in cationic meso-pyridinium BODIPYs can be inhibited which should restore the intense BODIPY fluorescence. One the other hand, a combination of calculations and experiment revealed that electron-withdrawing groups on the 2,6- positions can enhance charge recombination luminescence in BODIPYs undergoing d-PeT, collectively demonstrating

two separate methods of fluorescence enhancement. Exploring scopes and limitations of these methods can lead to a series of dyes with a diverse range of properties and combinations.

4.4. Future Work

The use of transient absorption spectroscopy to probe the excited states would provide experimental insight–such as excited state lifetimes and charge recombination energy-that cannot be modelled computationally.

Calculating the ^{13}C NMR will assist in experimental peak assignment as well as potentially provide support for the rationalization of the observed bathochromic shift in the absorption spectrum of **2–Py$^+$**. An upfield shifted signal for the meso-carbon in **2–Py$^+$**, relative to **3–Py$^+$** and **4–Py$^+$**, will support the theory of the nitrogen position altering the electron withdrawing strength of the pyridinium ring.

To obtain a truly accurate comparison of the fluorescence quantum yields of the three isomers, a different set of structural analogs should be used in which structural rigidity is maintained across all three platforms. Figure shows the proposed set of structures. Since the alkylation of **2–Py** introduces a methyl group that protrudes over the BODIPY core, this isomer possesses an intrinsic enhanced structural rigidity which is known to increase fluorescent quantum yields. To account for this, the same rigidity should be applied to all three structures, so using **4–Py$^+$-2** and **3–Py$^+$-2** instead of **4–Py$^+$** and **3–Py$^+$** will provide a more accurate picture of how the position of the pyridinium nitrogen effects the electronic structure and optical properties of the dyes.

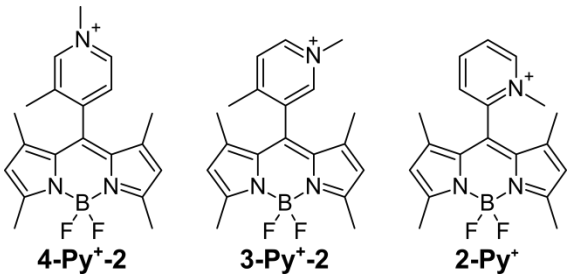

Figure 4.6. Alternative isomer structures proposed for more accurate fluorescence quantum yield comparison.

The lipo-/hydrophilicity of the isomers as well as HPLC retention times and a more comprehensive set of TLC R_f values will be evaluated to help explain differences in the biological characterization, but the uptake and toxicity studies should be repeated since the original data set exhibits discrepancies between the dark and phototoxicities.

4.5. Methodology

4.5.1. Computational

All calculations were performed using the NWChem 6.5 software package.[19] Molecular properties were calculated for gas phase structures at 0 Kelvin. The ground state structures were optimized using density functional theory with the hybrid B3LYP[20,21] functional, the 6-31+G** basis set, and confirmed by subsequent frequency calculations. To evaluate the effect of pyridinium orientation on the excited states, structures were optimized on their first singlet excited state (S_1). This yields the singlet-triplet energy gap involved in the intersystem crossing. Electronic transitions were calculated for each structure using TDDFT with the range-separated CAM-B3LYP[22] functional. Here, the range-separated functional is used to describe the long-range interactions necessary to capture transitions between the BODIPY and the pyridinium ring.

4.5.2. Experimental

All solvents and reagents were obtained from Sigma-Aldrich, Tokyo Chemical Industry, Beantown Chemical, and Honeywell International Incorporated. The solvents were dried over 4Å molecular sieves as needed. The reagents were used as received without purification. Reactions were monitored using 0.2 mm silica gel plates (with indicator, polyester backed, 60 Å, pre-coated) and UV lamp. Liquid chromatography was performed via silica gel column chromatography (60 Å, 230−400 mesh) and all solvent systems were buffered with 0.1% triethylamine. NMR spectra were obtained on 400 (^{1}H) and 500 MHz (^{13}C) spectrometers at room temperature. Chemical shifts (δ) are given in parts per million (ppm) in $CDCl_3$ (7.27 ppm for ^{1}H NMR, 77.0 ppm for ^{13}C NMR) or C_2D_6SO (2.50 ppm for ^{1}H NMR, 39.5 ppm for ^{13}C NMR); coupling constants (J) are given in hertz. High-resolution mass spectra were measured on an ESI-TOF mass spectrometer in positive mode. All absorption spectra were recorded at room temperature on a Varian Cary 50 Bio and emission spectra were recorded on a Perkin Elmer LS 55 Luminescence Spectrophotometer. Spectrophotometric grade solvents and quartz cuvettes (10 mm path length) were used. For the determination of the optical density (ε), solutions with absorbance at λ_{max} between 0.5 and 1 were used. For the determination of quantum yields, dilute solutions with absorbance between 0.03 and 0.05 at the particular excitation wavelength were used and all measurements were taken within 8 hours after solution preparation.[17,23] The external standards employed were rhodamine 6G and $Ru(bpy)_3Cl_2$, both in water.

4.5.3. Synthesis

8-(4-Pyridyl)-1,3,5,7-tetramethyl-BODIPY (1). In an oven dried flask, a 14:1 DCM/absolute ethanol solution was degassed with nitrogen for 30 minutes. The flask was then charged with 2,4-dimethylpyrrole (0.13 mL, 1.22 mmol), 4-formylpyridine (55.0 µL, 0.57 mmol, 0.46 eq), and TFA (2 drops). The solution was neutralized with DIPEA (6 drops), after 24 hours of stirring under a flow of nitrogen, and p-chloranil (0.1422 g, 0.57 mmol, 1.00 eq) was added. The mixture was stirred under a flow of nitrogen for 4 hours after which the solvent was removed under reduced pressure. The residue was then taken up in dry DCM (20 mL), DIPEA (1.00 mL, 5.75 mmol, 10.15 eq) was added and the mixture was stirred for 30 minutes before addition of BF3OEt2 (0.90 mL, 7.29 mmol, 12.88 eq). When TLC showed disappearance of the dipyrromethene, the solution was filtered to remove the precipitates and purified over silica by column chromatography eluting with 4% EtOAc/DCM and 2% EtOAc/DCM to afford 0.0670 g of product (34% yield). ^{1}H NMR (400 MHz, $CDCl_3$): δ = 8.79-8.77 (d, J = 5.9, 1.6 Hz, 1H), 7.39-7.31 (d, J = 5.8, 1.6 Hz, 1H), 6.01 (s, 2H), 2.56 (s, 6H), 1.41 (s, 6H); ^{13}C NMR (500 MHz,$CDCl_3$): δ = 156.38, 150.53, 143.50, 142.54, 137.54, 130.24, 123.21, 121.70,14.53, 14.50 ppm; HRMS (ESI): m/z calcd (%) for C18H19BF2N3: 326.1638 [M+H]+; found: 326.1641; UV/Vis (CH_3CN): λ_{max} = 501, λ_{em} = 515 nm.

8-(N-methyl-4-Pyridyl)-1,3,5,7-tetramethyl-BODIPY Iodide (1cat). In a 5 mL round bottom flask wrapped in foil, BODIPY 1 (6.0 mg, 0.0183 mmol) was dissolved in anhydrous ACN (1.8 mL) and methyl iodide (1.8 mL). After refluxing for 1 hour, TLC showed consumption of starting material and the solvent was removed under reduced pressure. Yield 8.6 mg, 100% (greenish-gray solid): ^{1}H NMR (400 MHz, DMSO-d_6): δ =

9.19-9.17 (d, J = 6.7 Hz, 2H), 8.41-8.39 (d, J = 6.7 Hz, 2H), 6.28 (s, 2H), 4.44 (s, 3H), 2.49 (s, 6H), 1.42 (s, 6H); ^{13}C NMR (500 MHz,DMSO-d_6): δ = 154.02, 149.59, 147.54, 138.02, 136.71, 128.22, 128.08, 122.98, 49.02, 13.17, 12.89 ppm; HRMS (ESI): m/z calcd (%) for $C_{19}H_{21}BF_2N_3$: 339.1827[M*]+; found: 339.1830; UV/Vis (CH_3CN): λ_{max} = 509, λ_{em} = 596 nm.

8-(3-Pyridyl)-1,3,5,7-tetramethyl-BODIPY (2). To an oven dried flask charged with a solution of 2,4-dimethylpyrrole (0.10 mL, 0.94 mmol) in dry THF (1.00 mL) was added a 3.0 M solution of methyl magnesium bromide in THF (0.35 mL, 1.05 mmol, 1.11 eq) and the mixture was allowed to stir under a flow of nitrogen. After 30 minutes, a solution of methyl nicotinate (0.0597 g, 0.44 mmol, 0.46 eq) in dry THF (1.00 mL) was slowly added. The mixture was then heated to reflux for 4 hours before cooling to room temperature and adding TEA (0.70 mL, 5.02 mmol, 11.54 eq) and BF_3OEt_2 (0.70 mL, 5.67 mmol, 13.03 eq). After stirring for 2 hours, the solvent was removed under reduced pressure and the mixture was purified by column chromatography eluting with 4% EA in DCM, 1:3 acetone/Hex to afford the product. Yield was not calculated because of product loss due to degradation during the extensive chromatography. ^{1}H NMR (400 MHz, $CDCl_3$): δ = 8.76-8.75 (dd, J = 4.9, 1.7 Hz, 1H), 8.58-8.57 (d, J = 1.4 Hz, 1H), 7.66-7.63 (dt, J = 7.7, 2.0 Hz, 1H), 7.47-7.44 (dd, J = 7.8, 4.9, 0.9 Hz, 1H), 6.01 (s, 2H), 2.56 (s, 6H), 1.38 (s, 6H); ^{13}C NMR (500 MHz, $CDCl_3$): δ = 156.56, 150.36, 149.58, 148.70, 142.94, 137.43, 136.16, 131.66, 123.87, 121.93, 15.13, 14.77 ppm; HRMS (ESI): m/z calcd (%) for $C_{18}H_{18}BF_2N_3$: 325.1671[M+H]+; found: 325.1672; UV/Vis (CH_3CN): λ_{max}= 501, λ_{em}= 523 nm.

8-(N-methyl-3-Pyridyl)-1,3,5,7-tetramethyl-BODIPY Iodide (2cat). In a 5 mL round bottom flask wrapped in foil, BODIPY 2 (7.7 mg, 0.024 mmol) was dissolved in anhydrous ACN (1.8 mL) and methyl iodide (1.8 mL). After refluxing for 1 hour, TLC showed consumption of starting material and the solvent was removed under reduced pressure. Yield 11.1 mg, 100% (red solid): ^{1}H NMR (500 MHz, DMSO-d_6): δ = 9.34 (s, 1H), 9.21-9.19 (d, J = 6.4 Hz, 1H), 8.85-8.84 (d, J = 8.2 Hz, 1H), 8.35–8.32 (m, 1H), 6.30 (s, 3H), 4.43 (s, 3H), 2.85 (s, 6H), 1.42 (s, 6H); ^{13}C NMR (500 MHz,DMSO-d_6): δ = 156.95, 146.78, 145.62, 144.79, 142.84, 133.25, 132.34, 130.48, 128.30, 122.44, 48.49, 15.41, 14.35 ppm; HRMS (ESI): m/z calcd (%) for $C_{19}H_{21}BF_2N_3$: 339.1827[M*]+; found: 339.1824; UV/Vis (CH_3CN): λ_{max}= 510, λ_{em}= 537 nm.

8-(2-Pyridyl)-1,3,5,7-tetramethyl-BODIPY (3). In a flask with 14:1 DCM/methanol (30 mL) was added 2,4-dimethylpyrrole (0.13 mL, 1.22 mmol), 2-formylpyridine (55.0 μL, 0.56 mmol, 0.46 eq), and TFA (2 drops). The solution was stirred overnight under a flow of nitrogen before being neutralized with DIPEA (6 drops) and adding chloranil (0.1422 g, 0.57 mmol, 1.01 eq). The mixture was stirred under a flow of nitrogen for 3+ hours when TLC showed disappearance of the dipyrromethane (4% EtOAc in DCM, R_f = 0.65). The solvent was then removed under reduced pressure and the residue was then taken up in dry DCM (20 mL). DIPEA (3.00 mL, 17.25 mmol, 30.76 eq) was added and the mixture was stirred for 30 minutes before dropwise addition of BF_3OEt_2 (2.00 mL, 16.21 mmol, 28.89 eq). After 2 hours, TLC showed disappearance of the dipyrromethene and the reaction mixture was directly loaded onto a column and eluted with 4% EtOAc/DCM (R_f = 0.53). The first predominant fluorescent band was collected and further purified over silica by column chromatography eluting

with 2% EtOAc/DCM to afford the product. ^{1}H NMR (400 MHz, $CDCl_3$): δ = 8.78-8.76 (dt, *J* = 4.9, 1.4 Hz, 1H), 7.85-7.81 (td, *J* = 7.7, 1.8 Hz, 1H), 7.44 – 7.40 (m, 2H), 5.98 (s, 2H), 2.55 (s, 6H), 1.31 (s, 6H); ^{13}C NMR (400 MHz,$CDCl_3$): δ = 156.49, 154.15, 150.35, 142.71, 138.75, 136.08, 131.55, 124.53, 123.99, 121.38, 14.79, 13.87 ppm; HRMS (ESI): m/z calcd (%) for $C_{18}H_{19}BF_2N_3$: 326.1638 [M+H]+; found: 326.1642; UV/Vis (CH_3CN): λ_{max}= 501, λ_{em}= 525 nm.

8-(N-methyl-2-Pyridyl)-1,3,5,7-tetramethyl-BODIPY Iodide (3cat). In a 5 mL round bottom flask wrapped in foil, BODIPY 3 (7.5 mg, 0.013 mmol) was dissolved in anhydrous ACN (1.8 mL) and methyl iodide (1.8 mL). The mixture was heated to reflux for several hours until TLC showed consumption of starting material after which the solvent was removed under reduced pressure. It is worth noting that this reaction took considerably longer than methylating the 4- and 3-pyridyl isomers. Yield 10.8 mg, 100% (red solid): ^{1}H NMR (500 MHz, DMSO-d_6) δ = 9.31-9.29 (d, *J* = 6.1 Hz, 1H), 8.85-8.82 (td, *J* = 7.9, 1.4 Hz, 1H), 8.58-8.56 (dd, *J* = 8.0, 1.5 Hz, 1H), 8.45-8.42 (ddd, *J* = 7.9, 6.1, 1.6 Hz, 1H), 6.37 (s, 2H), 4.24 (s, 3H), 2.52 (s, 6H), 1.34 (s, 6H); ^{13}C NMR (500 MHz,DMSO-d_6): δ = 159.11, 148.87, 147.32, 146.96, 142.14, 130.50, 130.40, 129.35, 129.31, 122.98, 45.92, 14.56, 12.74 ppm; HRMS (ESI): m/z calcd (%) for $C_{19}H_{21}BF_2N_3$: 339.1827[M*]+; found: 339.1829; UV/Vis (CH_3CN): λ_{max}= 520, λ_{em}= 552 nm.

4.5.4. Biological Characterization

4.5.4.1. General

The HEp-2 cell line, purchased from ATCC, was used in the biological characterization of the synthesized BODIPYs. All reagents, including the culture medium, were purchased from Life Technologies. HeP-2 cells were cultured in the

medium (1:1 Dulbecco's Modified Eagle Medium (DMEM)/Advanced DMEM) containing 10% fetal bovine serum (FBS) and 1% Penicillin-streptomycin antibiotic. A 32 mM compound stock solution was prepared by dissolving the compound in 5% (v/v) Cremophor in DMSO. The working solutions were prepared by dilution of the stock solution with growing medium.

4.5.4.2. Time-Dependent Cellular Uptake

HEp-2 cells were plated at 15,000 cells per well in a Costar 96-well plates (BD biosciences) and cultivated overnight. The cells were treated by adding 100 μL/well of 10 μM working solution at time periods of 0, 1, 2, 4, 8, and 24 hours. The loading medium was removed after the treatments. The cells were washed with 1X PBS, and solubilized by adding 0.25% Triton X-100 in 1X PBS. A standard curve for the compound was made by diluting the stock solution with 0.25% Triton X-100(Sigma-Aldrich) in 1X PBS to the following concentrations: 0.3125 μM, 0.625 μM, 1.25 μM, 2.5 μM, 5 μM, 10 μM. A standard curve of the cells was prepared using 10000, 20000, 40000, 60000, 80000, and 100000 cells per well. The cells were quantified by CyQuant Cell Proliferation Assay (Life Technologies). The compound and cell number were determined using a FluoStar Optima micro-plate reader (BMG LRBTEH), with wavelengths 584/650 nm for compounds and 485/520 nm for cells. Cellular uptake was expressed in terms of pM/cell.

4.5.4.3. Cytotoxicity

4.5.4.3.1. Dark Toxicity

HEp-2 cells were placed in a 96-well plate again at 15,000 cells per well, with 5 repetitions of each compound concentration of 0, 6.25, 12.5, 25, 50, 100, and 200 μM,

and then incubated at 37°C for 24 hours. The cells were then washed with 1X PBS and the compound was replaced with media containing 20 % cell titer blue (CellTiter-Blue® Cell Viability Assay)(Promega) before an additional 4 hours of incubation at 37°C. Using a FluoStar Optima micro-plate reader, the viable cells were measured fluorescently at 570/615 nm. The dark toxicity was expressed in terms of the percentage of viable cells.

4.5.4.3.2. Phototoxicity

Using a concentration range of 0, 3.125, 6.25, 12.5, 25, 50, and 100 μM, the HEp-2 cells were prepared in a 96-well plate, incubated, and washed as described above. The cells were exposed to light for 20 minutes in order to get the total approximate dose of light of 1.5 J/cm^2. The cells were then incubated for another 24 hours before washing them to replace the media with one containing 20% cell titer blue and incubating them for another 4 hours. Using a FluoStar Optima micro-plate reader, the viable cells were measured fluorescently at 570/615 nm. The phototoxicity was expressed in terms of the percentage of viable cells.

4.6. References

1. Üçüncü, M.; Karakuş, E.; Emrullahoğlu, M., A BODIPY/Pyridine Conjugate for Reversible Fluorescence Detection of Gold(Iii) Ions. *New J. Chem.* **2015,** *39*(11), 8337-8341.

2. Ojida, A.; Sakamoto, T.; Inoue, M.-a.; Fujishima, S.-h.; Lippens, G.; Hamachi, I., Fluorescent BODIPY-Based Zn(Ii) Complex as a Molecular Probe for Selective Detection of Neurofibrillary Tangles in the Brains of Alzheimer's Disease Patients. *J. Am. Chem. Soc.* **2009,** *131*(18), 6543-6548.

3. Gupta, G.; Das, A.; Ghate, N. B.; Kim, T.; Ryu, J. Y.; Lee, J.; Mandal, N.; Lee, C. Y., Novel BODIPY-Based Ru(Ii) and Ir(Iii) Metalla-Rectangles: Cellular Localization of Compounds and Their Antiproliferative Activities. *Chem. Commun.* **2016,** *52*(23), 4274-4277.

4. Gupta, G.; Das, A.; Lee, S. W.; Ryu, J. Y.; Lee, J.; Nagesh, N.; Mandal, N.; Lee, C. Y., BODIPY-Based Ir(Iii) Rectangles Containing Bis-Benzimidazole Ligands with

Highly Selective Toxicity Obtained through Self-Assembly. *J. Organomet. Chem.* **2018,** *868*, 86-94.

5. Gupta, G.; Das, A.; Panja, S.; Ryu, J. Y.; Lee, J.; Mandal, N.; Lee, C. Y., Self-Assembly of Novel Thiophene-Based BODIPY Ruii Rectangles: Potential Antiproliferative Agents Selective against Cancer Cells. *Chem. Eur. J.* **2017,** *23*(68), 17199-17203.

6. Gupta, G.; Das, A.; Park, K. C.; Tron, A.; Kim, H.; Mun, J.; Mandal, N.; Chi, K.-W.; Lee, C. Y., Self-Assembled Novel BODIPY-Based Palladium Supramolecules and Their Cellular Localization. *Inorg. Chem.* **2017,** *56*(8), 4615-4621.

7. Liu, Y.; Li, Z.; Chen, L.; Xie, Z., Near Infrared BODIPY-Platinum Conjugates for Imaging, Photodynamic Therapy and Chemotherapy. *Dyes Pigm.* **2017,** *141*, 5-12.

8. Luo, G.-G.; Fang, K.; Wu, J.-H.; Dai, J.-C.; Zhao, Q.-H., Noble-Metal-Free BODIPY–Cobaloxime Photocatalysts for Visible-Light-Driven Hydrogen Production. *Phys. Chem. Chem. Phys.* **2014,** *16*(43), 23884-23894.

9. Bartelmess, J.; Francis, A. J.; El Roz, K. A.; Castellano, F. N.; Weare, W. W.; Sommer, R. D., Light-Driven Hydrogen Evolution by BODIPY-Sensitized Cobaloxime Catalysts. *Inorg. Chem.* **2014,** *53*(9), 4527-4534.

10. Caruso, E.; Banfi, S.; Barbieri, P.; Leva, B.; Orlandi, V. T., Synthesis and Antibacterial Activity of Novel Cationic BODIPY Photosensitizers. *J. Photochem. Photobiol., B* **2012,** *114*(3), 44-51.

11. Caruso, E.; Gariboldi, M.; Sangion, A.; Gramatica, P.; Banfi, S., Synthesis, Photodynamic Activity, and Quantitative Structure-Activity Relationship Modelling of a Series of BODIPYs. *J. Photochem. Photobiol., B* **2017,** *167*, 269-281.

12. Banfi, S.; Nasini, G.; Zaza, S.; Caruso, E., Synthesis and Photo-Physical Properties of a Series of BODIPY Dyes. *Tetrahedron* **2013,** *69*(24), 4845-4856.

13. Luo, G.-G.; Fang, K.; Wu, J.-H.; Mo, J., Photocatalytic Water Reduction from a Noble-Metal-Free Molecular Dyad Based on a Thienyl-Expanded BODIPY Photosensitizer. *Chem. Commun.* **2015,** *51*(62), 12361-12364.

14. Kolemen, S.; Işık, M.; Kim, G. M.; Kim, D.; Geng, H.; Buyuktemiz, M.; Karatas, T.; Zhang, X. F.; Dede, Y.; Yoon, J.; Akkaya, E. U., Intracellular Modulation of Excited-State Dynamics in a Chromophore Dyad: Differential Enhancement of Photocytotoxicity Targeting Cancer Cells. *Angew. Chem. Int. Ed.* **2015,** *54*(18), 5340-5344.

15. Zhang, S.; Wu, T.; Fan, J.; Li, Z.; Jiang, N.; Wang, J.; Dou, B.; Sun, S.; Song, F.; Peng, X., A BODIPY-Based Fluorescent Dye for Mitochondria in Living Cells, with Low Cytotoxicity and High Photostability. *Org. Biomol. Chem.* **2013,** *11*(4), 555-558.

16. Jiang, N.; Fan, J.; Liu, T.; Cao, J.; Qiao, B.; Wang, J.; Gao, P.; Peng, X., A near-Infrared Dye Based on BODIPY for Tracking Morphology Changes in Mitochondria. *Chem. Commun.* **2013,** *49*(90), 10620-10622.

17. Olmsted, J., Calorimetric Determinations of Absolute Fluorescence Quantum Yields. *J. Phys. Chem* **1979,** *83*(20), 2581-2584.

18. Katsumi, N., Synthesis, Luminescence Quantum Yields, and Lifetimes of Trischelated Ruthenium(Ii) Mixed-Ligand Complexes Including 3,3′-Dimethyl-2,2′-Bipyridyl. *Bull. Chem. Soc. Jpn.* **1982,** *55*(9), 2697-2705.

19. Valiev, M.; Bylaska, E. J.; Govind, N.; Kowalski, K.; Straatsma, T. P.; Van Dam, H. J. J.; Wang, D.; Nieplocha, J.; Apra, E.; Windus, T. L.; de Jong, W. A., Nwchem: A Comprehensive and Scalable Open-Source Solution for Large Scale Molecular Simulations. *Comput. Phys. Commun.* **2010,** *181*(9), 1477-1489.

20. Becke, A. D., Density-Functional Thermochemistry. Iii. The Role of Exact Exchange. *J. Chem. Phys.* **1993,** *98*(7), 5648-5652.

21. Lee, C.; Yang, W.; Parr, R. G., Development of the Colle-Salvetti Correlation-Energy Formula into a Functional of the Electron Density. *Phys. Rev. B* **1988,** *37*(2), 785-789.

22. Yanai, T.; Tew, D. P.; Handy, N. C., A New Hybrid Exchange–Correlation Functional Using the Coulomb-Attenuating Method (Cam-B3lyp). *Chem. Phys. Lett.* **2004,** *393*(1), 51-57.

23. Williams, A. T. R.; Winfield, S. A.; Miller, J. N., Relative Fluorescence Quantum Yields Using a Computer-Controlled Luminescence Spectrometer. *Analyst* **1983,** *108*(1290), 1067-1071.

Appendix A. Supporting Information for Chapter 2

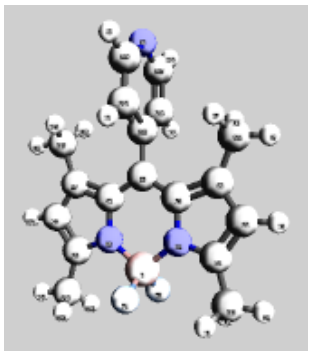

Optimized Cartesian coordinates for modeled BODIPY dyes

BODIPY 1 A **B3LYP/6-31+G****

B	0.0002137500	-2.4131026900	0.0001293200
F	0.0228689800	-3.2209231100	1.1485878800
F	-0.0224033000	-3.2215207800	-1.1479375700
N	1.2475820900	-1.4869717300	-0.0247194800
C	2.5310832900	-1.9008020200	-0.0506691900
C	3.3764494000	-0.7702409500	-0.0645917100
C	2.5866660800	0.3750893700	-0.0465689600
C	1.2255983500	-0.0851433600	-0.0216975000
C	0.0001221100	0.6020794000	0.0022974200
C	-1.2252246600	-0.0852001800	0.0249180500
C	-2.5863670000	0.3749977100	0.0492601400
C	-3.3761113400	-0.7701857500	0.0629364500
C	-2.5308381300	-1.9007186300	0.0471633400
N	-1.2473337600	-1.4870755900	0.0244370400
C	2.9273501100	-3.3409118900	-0.0614528400
H	4.0158453900	-3.4300896300	-0.0846062700
H	2.5456198800	-3.8569342100	0.8255259900
H	2.5083666600	-3.8539582100	-0.9331728100
H	4.4579959700	-0.8023653300	-0.0856844300
C	3.1276893400	1.7756926000	-0.0531411800
H	4.2207155000	1.7451627100	-0.0584770900
H	2.8038160700	2.3407615800	-0.9328037600
H	2.8121987200	2.3463339200	0.8257620900
C	0.0000754000	2.0967639400	0.0020524600
C	0.0104981200	2.8219043200	1.1991711700
H	0.0189568600	2.3105468900	2.1571082300
C	0.0098394300	4.2178624800	1.1435517200
H	0.0178722800	4.8015190000	2.0618998400
N	-0.0007555700	4.9174083600	0.0004842700
C	-0.0108872300	4.2165758400	-1.1417866200
H	-0.0196110600	4.7992059000	-2.0607742500
C	-0.0108053200	2.8206051200	-1.1958247300
H	-0.0192565800	2.3081094500	-2.1531320400
C	-3.1273347300	1.7755632600	0.0591490700
H	-2.8154833400	2.3467833900	-0.8207289100
H	-4.2203071200	1.7449589400	0.0689881600
H	-2.7997896700	2.3401148700	0.9377255200
H	-4.4576465800	-0.8021703700	0.0821831000
C	-2.9273253300	-3.3407390400	0.0525867200
H	-2.5064329100	-3.8578795400	0.9209035100
H	-4.0157192800	-3.4298488400	0.0776913700
H	-2.5477501500	-3.8528952700	-0.8375380900

BODIPY 1cat A

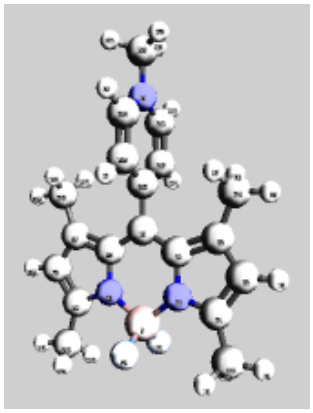

B	-0.0000184700	-2.7392606800	-0.0014264600
F	0.0040666400	-3.5290987500	1.1484356200
F	-0.0039590800	-3.5290233700	-1.1513656800
N	1.2524073700	-1.8049514700	-0.0052143400
C	2.5338354500	-2.2201415700	-0.0060813100
C	3.3826656900	-1.0854372700	-0.0027784700
C	2.5968390500	0.0557535900	0.0000171600
C	1.2316438600	-0.4061292400	-0.0029682400
C	-0.0000804800	0.2665442700	-0.0025410700
C	-1.2318629400	-0.4063124900	-0.0015865200
C	-2.5971814700	0.0554628100	-0.0059551400
C	-3.3829982900	-1.0859458100	-0.0027115100
C	-2.5339091300	-2.2205967600	0.0022688400
N	-1.2524798300	-1.8051000900	0.0022754000
C	2.9302278300	-3.6570996100	-0.0090197000
H	4.0175374800	-3.7491266400	-0.0221523700
H	2.5382342600	-4.1685384500	0.8761722400
H	2.5161176300	-4.1717391400	-0.8819761400
H	4.4637858000	-1.1201682100	-0.0021310800
C	3.1412116300	1.4562443200	0.0068879600
H	4.2330178100	1.4222010500	0.0198474500
H	2.8464778900	2.0253186300	-0.8819397600
H	2.8256693900	2.0244796300	0.8891199200
C	-0.0001270000	1.7571478100	-0.0012865700
C	-0.0236204200	2.4812761800	1.2025980500
H	-0.0421786000	1.9665915100	2.1567866200
C	-0.0222641900	3.8630636400	1.1789489800
H	-0.0389756000	4.4655618100	2.0798675100
N	0.0005216500	4.5397678000	0.0028334300
C	0.0004577200	6.0240198700	0.0253902900
C	0.0227697400	3.8680187600	-1.1733786200
H	0.0399727400	4.4690185500	-2.0744063100
C	0.0233636700	2.4839772100	-1.2006452300
H	0.0416425700	1.9733009800	-2.1569737900
C	-3.1416950000	1.4558983700	-0.0147841300
H	-2.8207424500	2.0250720400	-0.8943715400
H	-4.2334436300	1.4216188600	-0.0343328300
H	-2.8525599300	2.0240777100	0.8765750600
H	-4.4641927400	-1.1208276500	-0.0047471900
C	-2.9300570000	-3.6576822200	0.0052691300
H	-2.5157384900	-4.1722449000	0.8781980600
H	-4.0174127500	-3.7498110000	0.0184140100
H	-2.5380823600	-4.1690559900	-0.8799985500
H	0.0216467500	6.3958501500	-0.9973665500

H	0.8844867700	6.3754539400	0.5602629700
H	-0.9045943700	6.3759851400	0.5235298600

BODIPY 1 B

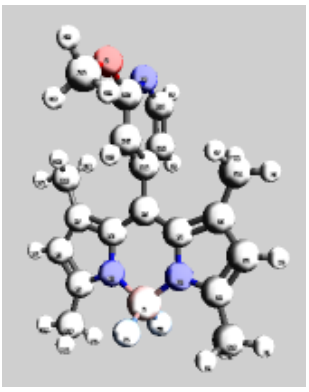

B	-0.0000866500	-2.8082631200	-0.2515651600
F	0.0114163400	-3.5985428500	0.9101655800
F	-0.0109613500	-3.6350694200	-1.3866377500
N	1.2471125700	-1.8825040900	-0.2779885100
C	2.5309288000	-2.2958341200	-0.2944459900
C	3.3759078400	-1.1651697800	-0.3083698700
C	2.5856059900	-0.0199909500	-0.2991836900
C	1.2247293800	-0.4805260000	-0.2795175200
C	-0.0009139000	0.2068139300	-0.2667917100
C	-1.2262594400	-0.4810990700	-0.2572719500
C	-2.5874559400	-0.0211652800	-0.2539732900
C	-3.3772966800	-1.1666688200	-0.2475012400
C	-2.5317133700	-2.2969551000	-0.2469707000
N	-1.2479925300	-1.8830745900	-0.2538553300
C	2.9272169200	-3.7359626100	-0.2960322600
H	4.0159088300	-3.8255335200	-0.3036478100
H	2.5327532100	-4.2498766300	0.5866268100
H	2.5203885700	-4.2513309500	-1.1721881800
H	4.4575692200	-1.1969438700	-0.3248838700
C	3.1243931500	1.3811306800	-0.3132119000
H	4.2174454000	1.3530111800	-0.3273702400
H	2.7903176300	1.9436042500	-1.1906540500
H	2.8137387000	1.9530947900	0.5668111100
C	-0.0012530300	1.7021991100	-0.2609932200
C	-0.0055165200	2.4295137800	-1.4563678800
H	-0.0086944600	1.9278138100	-2.4183553400
C	-0.0053932600	3.8233707300	-1.3741251800
H	-0.0084122100	4.4257531800	-2.2805050100
N	-0.0017001700	4.5047773900	-0.2252514200
C	0.0020938800	3.8054879400	0.9113212400
O	0.0051121200	4.5869388400	2.0189077300
C	0.0079080800	3.9675264400	3.3022581900
H	0.0089741100	4.7862909400	4.0222435900
H	0.9049100300	3.3535532100	3.4493923700
H	-0.8880488800	3.3528749300	3.4529157000
C	0.0027350200	2.3992735400	0.9508484800
H	0.0061186600	1.8521342100	1.8855685900
C	-3.1269773000	1.3797147600	-0.2613474200
H	-2.7998703600	1.9441374500	-1.1401271000
H	-4.2200922400	1.3511208000	-0.2670279000
H	-2.8098828800	1.9500349400	0.6174810600
H	-4.4590644000	-1.1989038100	-0.2450435400
C	-2.9273277100	-3.7372397500	-0.2400895100
H	-2.5130240100	-4.2513019600	0.6333069600

H	-4.0158806200	-3.8272649100	-0.2235365200
H	-2.5399778900	-4.2521184400	-1.1253439700

BODIPY 1cat B

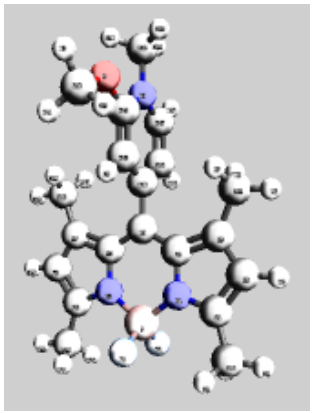

B	0.0001464400	-3.0062391800	0.0432423100
F	0.0018496600	-3.7570482700	1.2214323900
F	-0.0016088600	-3.8378912200	-1.0773334100
N	1.2517780700	-2.0736109300	0.0099976800
C	2.5332619500	-2.4899796900	-0.0019887000
C	3.3827077100	-1.3560849500	-0.0141995500
C	2.5968625200	-0.2136489100	-0.0077206300
C	1.2314568600	-0.6742322700	0.0081506000
C	0.0002872000	0.0005394700	0.0118986600
C	-1.2310195900	-0.6740614100	0.0104671600
C	-2.5964015100	-0.2133910400	-0.0040864700
C	-3.3823470800	-1.3557864900	-0.0088146400
C	-2.5329904200	-2.4897393900	0.0029335200
N	-1.2514430700	-2.0734432100	0.0130736500
C	2.9290277600	-3.9276656100	-0.0007046200
H	4.0166621300	-4.0200529300	-0.0054119500
H	2.5299701700	-4.4392067300	0.8813435800
H	2.5220484900	-4.4425212800	-0.8770225500
H	4.4639317300	-1.3919224700	-0.0285528900
C	3.1424471100	1.1865039700	-0.0234084300
H	4.2344408100	1.1522602300	-0.0407710100
H	2.8215432100	1.7510501000	-0.9058765400
H	2.8500550400	1.7602857100	0.8633265100
C	0.0005015800	1.4931922600	0.0089624600
C	-0.0015586200	2.2003432100	1.2095375300
H	-0.0035896300	1.6689882400	2.1524214700
C	-0.0011372500	3.5994999500	1.1997683000
O	-0.0024097600	4.3968247400	2.2567790200
C	-0.0027345000	3.8317074000	3.5926541600
H	-0.0012222900	4.6930797200	4.2573480500
H	0.8982575900	3.2334307600	3.7485203100
H	-0.9053174400	3.2359984200	3.7492037500
N	0.0008265800	4.2743294900	0.0112294400
C	0.0009695800	5.7569702900	0.0199103600
H	0.0010448800	6.1034740200	-1.0118652200
H	0.8904997000	6.1190975800	0.5371400300
H	-0.8885877300	6.1191723400	0.5369968200
C	0.0029066200	3.5891949400	-1.1674570700
H	0.0047594100	4.1970421100	-2.0638686800
C	0.0029186100	2.2152155500	-1.2019332800
H	0.0048875800	1.7015483900	-2.1560339100
C	-3.1419371800	1.1867801600	-0.0205777800
H	-2.8235635700	1.7497448800	-0.9050236000
H	-4.2339694400	1.1524972500	-0.0347315300

H	-2.8470731900	1.7622023600	0.8642346200
H	-4.4635982600	-1.3915567500	-0.0217960100
C	-2.9288171900	-3.9274482600	0.0039571700
H	-2.5118092900	-4.4447059400	0.8741374300
H	-4.0163439400	-4.0197678800	0.0202543800
H	-2.5400618400	-4.4367136400	-0.8840104600

BODIPY 1 C

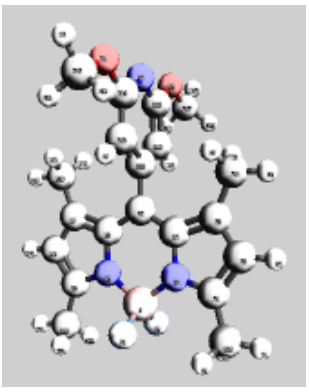

B	-0.0000709700	-3.1472275300	-0.0019678000
F	0.0081961400	-3.9565379400	1.1463301000
F	-0.0083241000	-3.9557581000	-1.1508170600
N	1.2474975400	-2.2217572600	-0.0105924300
C	2.5313928700	-2.6353123400	-0.0196865300
C	3.3766372800	-1.5049197600	-0.0248277200
C	2.5864271200	-0.3594870400	-0.0186621000
C	1.2254007700	-0.8196805000	-0.0096133500
C	-0.0000714200	-0.1319290400	-0.0006306600
C	-1.2255546800	-0.8196983600	0.0075591000
C	-2.5865913600	-0.3595151700	0.0168728700
C	-3.3768086000	-1.5049701900	0.0219726200
C	-2.5315432100	-2.6353602300	0.0159636500
N	-1.2476451700	-2.2217718800	0.0072704200
C	2.9273457600	-4.0755541200	-0.0231181900
H	4.0160326600	-4.1652620400	-0.0316868900
H	2.5336315200	-4.5903124000	0.8593786400
H	2.5197440600	-4.5899843300	-0.8994666500
H	4.4584035500	-1.5369496400	-0.0322498500
C	3.1244278000	1.0417126000	-0.0215289600
H	4.2175958500	1.0152624200	-0.0259666800
H	2.7964154500	1.6077355500	-0.8989782400
H	2.8033837300	1.6087534200	0.8577999300
C	-0.0000584500	1.3642586300	0.0005812700
C	0.0061149900	2.0630447700	1.2105625000
H	0.0108695000	1.5252545600	2.1495536100
C	0.0058850300	3.4683525800	1.1453713100
O	0.0115580300	4.2684024200	2.2391199800
C	0.0183454700	3.6700171000	3.5326365400
H	0.0222729700	4.5008956900	4.2386550300
H	0.9155143400	3.0582605300	3.6865740700
H	-0.8773718900	3.0586170200	3.6961596300
N	0.0000608400	4.1486519800	0.0031986500
C	-0.0058214800	3.4704936100	-1.1402478700
O	-0.0113940800	4.2726235800	-2.2324746100
C	-0.0181209600	3.6767372300	-3.5271373200
H	-0.0218379600	4.5089737300	-4.2315568800
H	0.8775238800	3.0655224700	-3.6917371500
H	-0.9153652100	3.0654163000	-3.6823641400
C	-0.0061806900	2.0653034200	-1.2080883900
H	-0.0109645500	1.5292833800	-2.1480924000
C	-3.1245952100	1.0416862800	0.0207565700
H	-2.8031474500	1.6095029900	-0.8579226700
H	-4.2177682600	1.0152306600	0.0246531500

H	-2.7969752400	1.6069250500	0.8988660200
H	-4.4585817200	-1.5370120000	0.0292369300
C	-2.9274729000	-4.0756182100	0.0183545100
H	-2.5204693800	-4.5904696300	0.8947452500
H	-4.0161668800	-4.1653524100	0.0261562500
H	-2.5331234000	-4.5899259800	-0.8641175100

BODIPY 1cat C

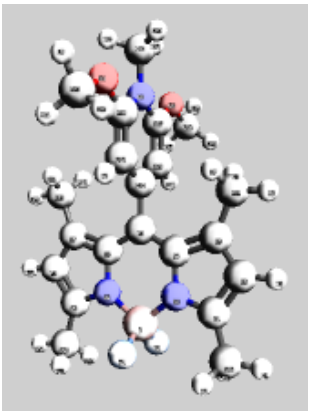

B	0.0000321200	-4.5027753800	0.0031355000
F	0.0028106300	-5.2933253600	1.1547750500
F	-0.0027291100	-5.2974861700	-1.1455876700
N	1.2519153200	-3.5700400500	-0.0009376600
C	2.5339626400	-3.9857244600	-0.0013247000
C	3.3825463400	-2.8519023300	0.0011192900
C	2.5960043400	-1.7094657500	0.0030416500
C	1.2308815000	-2.1703327300	0.0010127200
C	-0.0000859600	-1.4947956400	-0.0006591400
C	-1.2310156800	-2.1703953200	-0.0011922700
C	-2.5961626600	-1.7096427000	-0.0044120500
C	-3.3826275800	-2.8521362400	0.0001911600
C	-2.5339276600	-3.9859055000	0.0053964900
N	-1.2518956000	-3.5700885000	0.0039214900
C	2.9315119400	-5.4232425400	-0.0028275100
H	4.0193097100	-5.5133093600	-0.0151877900
H	2.5405479000	-5.9352266000	0.8826156100
H	2.5194381800	-5.9397010800	-0.8757866100
H	4.4638608900	-2.8869883500	0.0015760600
C	3.1403240600	-0.3092371200	0.0071098000
H	4.2324777100	-0.3414848200	0.0178515100
H	2.8388592600	0.2586383100	-0.8801252800
H	2.8218266400	0.2598372600	0.8874305800
C	-0.0001212500	-0.0006645000	0.0007125400
C	-0.0013313700	0.6995588900	1.2107209200
H	-0.0019169500	0.1660326300	2.1512855700
C	-0.0007945000	2.0895416300	1.1897808800
O	-0.0008115900	2.8922003900	2.2447905900
C	-0.0010335500	2.3251505900	3.5775531000
H	-0.0009327100	3.1843805300	4.2450566300
H	0.9000733300	1.7265368700	3.7330820200
H	-0.9023653600	1.7268400400	3.7329259900
N	-0.0000538000	2.7781533900	0.0006185700
C	0.0000392600	4.2645553100	0.0419389900
H	0.0022869500	4.6399615800	-0.9753185000
H	0.8885212700	4.6043964700	0.5752389900
H	-0.8906538100	4.6047503100	0.5713794800
C	0.0004428200	2.0946394300	-1.1922318500
O	0.0001295900	2.8816708900	-2.2591964600
C	-0.0000140900	2.2981949000	-3.5846544700
H	-0.0005966500	3.1496480800	-4.2621095300
H	0.9015760100	1.6987049300	-3.7335699300
H	-0.9011986000	1.6979529100	-3.7330169000
C	0.0010116100	0.7031835300	-1.2070263700

H	0.0015504700	0.1691309300	-2.1471692400
C	-3.1406299400	-0.3095068900	-0.0121747200
H	-2.8178585800	0.2591279400	-0.8911368400
H	-4.2327380000	-0.3418707100	-0.0283205700
H	-2.8436287700	0.2588604600	0.8763258200
H	-4.4639591500	-2.8873087900	-0.0003971100
C	-2.9313919200	-5.4234433700	0.0104626600
H	-2.5190391400	-5.9377965700	0.8845357400
H	-4.0191997100	-5.5135671800	0.0233719600
H	-2.5406334300	-5.9374820200	-0.8738769300

BODIPY 2 A

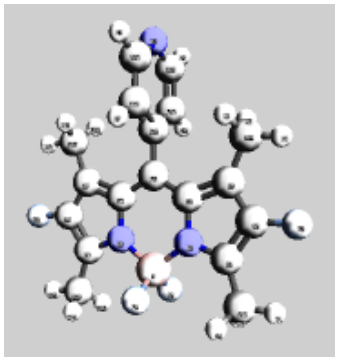

B	-0.0001266200	-2.3467910800	-0.0043112200
F	-0.0001394500	-3.1530242400	1.1415978400
F	-0.0001875100	-3.1462431700	-1.1549875200
N	1.2477630100	-1.4173669300	-0.0015339900
C	2.5283348100	-1.8432772100	-0.0008970100
C	3.3437594000	-0.6956197000	0.0024420900
C	2.5823496600	0.4595758600	0.0037092100
C	1.2260000600	-0.0164380500	0.0009479200
C	0.0000481400	0.6696921600	0.0009383100
C	-1.2259866500	-0.0163075000	-0.0001766300
C	-2.5822819800	0.4598709200	0.0001944800
C	-3.3438357700	-0.6952411200	-0.0006765400
C	-2.5285438800	-1.8430023400	-0.0018626100
N	-1.2479149200	-1.4172346500	-0.0015185100
C	2.9514733300	-3.2720378900	-0.0035859100
H	4.0412318000	-3.3367402000	-0.0021821700
H	2.5589805000	-3.7936520000	0.8752245300
H	2.5616168900	-3.7894727600	-0.8860569100
F	4.6941379000	-0.7439485900	0.0043199900
C	3.1450314400	1.8492587400	0.0078628300
H	4.2364978100	1.7979090900	0.0121597400
H	2.8363501300	2.4199086400	-0.8731796400
H	2.8292505200	2.4174398600	0.8879540100
C	0.0001229100	2.1644089800	0.0016546500
C	-0.0043501900	2.8875319400	1.2000202000
H	-0.0080461900	2.3754994700	2.1576541200
C	-0.0040134800	4.2836302600	1.1450010400
H	-0.0073931300	4.8665716800	2.0636819900
N	0.0002601900	4.9833471700	0.0022908200
C	0.0044601400	4.2841659900	-1.1407473300
H	0.0078925900	4.8675236200	-2.0591644100
C	0.0046590300	2.8880964000	-1.1963908600
H	0.0082860300	2.3764679000	-2.1542417800
C	-3.1448171800	1.8496205100	0.0012052600
H	-2.8309219700	2.4202750100	-0.8779757700
H	-4.2362965300	1.7983884100	-0.0007718100
H	-2.8341225400	2.4177214400	0.8831730900
F	-4.6942224300	-0.7433870800	-0.0004752800
C	-2.9518509100	-3.2717240800	-0.0033587400
H	-2.5618114300	-3.7919095800	0.8774067500
H	-4.0416197100	-3.3363006900	-0.0046865900
H	-2.5596691400	-3.7906891600	-0.8838853400

BODIPY 2cat A

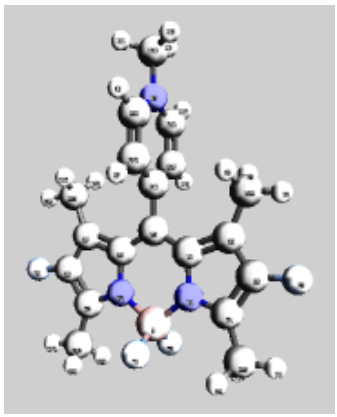

B	-0.0000329900	-2.6510420200	-0.0031942600
F	0.0037810700	-3.4344704200	1.1473709300
F	-0.0037883700	-3.4367533000	-1.1521359500
N	1.2529011300	-1.7131053500	-0.0075526600
C	2.5303882500	-2.1409692400	-0.0077303200
C	3.3505828700	-0.9890573500	-0.0043353000
C	2.5913957400	0.1629687700	-0.0020100400
C	1.2320575000	-0.3137467300	-0.0050811900
C	-0.0000678200	0.3577447300	-0.0036543800
C	-1.2321884800	-0.3138051800	-0.0030457000
C	-2.5915353500	0.1628857100	-0.0066987500
C	-3.3507289200	-0.9891854300	-0.0045686100
C	-2.5304833300	-2.1410776400	-0.0009546000
N	-1.2529836400	-1.7131525800	-0.0005987500
C	2.9554188900	-3.5665175800	-0.0100313000
H	4.0443328900	-3.6319651100	-0.0232282200
H	2.5743503000	-4.0832248200	0.8767925100
H	2.5517678800	-4.0875591100	-0.8839978200
F	4.6935181700	-1.0365756700	-0.0031857200
C	3.1624847500	1.5501383600	0.0042293200
H	4.2528882900	1.4894039700	0.0191014100
H	2.8808367700	2.1210505600	-0.8871546300
H	2.8565702900	2.1227994000	0.8864104400
C	-0.0000620400	1.8498264900	0.0005045500
C	-0.0222560100	2.5710125000	1.2058782400
H	-0.0397407200	2.0554481300	2.1596462100
C	-0.0209777600	3.9531774700	1.1852078100
H	-0.0367751600	4.5533255800	2.0877459100
N	0.0004618200	4.6324878200	0.0107197700
C	0.0001088700	6.1174006100	0.0365842300
H	0.0212218400	6.4917012400	-0.9853286500
H	0.8841562700	6.4671220600	0.5724272200
H	-0.9050899200	6.4674137000	0.5356962900
C	0.0214992500	3.9633862900	-1.1667118900
H	0.0375796500	4.5659512900	-2.0667417000
C	0.0221942000	2.5789499000	-1.1971231400
H	0.0395107300	2.0717661900	-2.1553478300
C	-3.1625931500	1.5500616600	-0.0145968600
H	-2.8541646400	2.1225702400	-0.8959308600
H	-4.2529632000	1.4893254400	-0.0324604700
H	-2.8834791800	2.1211146000	0.8775737100
F	-4.6936734100	-1.0367316400	-0.0066228600
C	-2.9554729600	-3.5666498600	0.0009747600
H	-2.5515089100	-4.0880116800	0.8746095600

H	-4.0443973300	-3.6320898100	0.0145051000
H	-2.5747108000	-4.0830224000	-0.8861848600

BODIPY 3 A

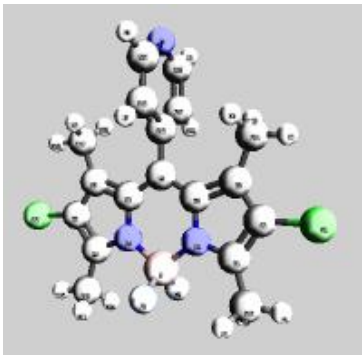

B	-0.0001174800	-2.2848305700	-0.0027566100
F	0.0006744900	-3.0870276600	1.1447233100
F	-0.0009786500	-3.0837066200	-1.1525087600
N	1.2487098000	-1.3545166300	-0.0015888000
C	2.5267044800	-1.7796935300	-0.0009794100
C	3.3606179700	-0.6366817200	0.0024117000
C	2.5828554000	0.5174675500	0.0038545300
C	1.2266102200	0.0455925400	0.0011691600
C	0.0000602600	0.7329875400	0.0012785900
C	-1.2265704500	0.0457261000	0.0000688700
C	-2.5827652000	0.5177708500	-0.0006255400
C	-3.3606656800	-0.6362875700	-0.0022642100
C	-2.5268920700	-1.7794044000	-0.0026635600
N	-1.2488442100	-1.3543840300	-0.0010963700
C	2.9210292700	-3.2169643400	-0.0024541700
H	4.0076190300	-3.3095507700	-0.0165183300
H	2.5284850900	-3.7238463600	0.8848103300
H	2.5041971200	-3.7290545100	-0.8752638800
Cl	5.0986589800	-0.7022545900	0.0046622700
C	3.1142158300	1.9185001400	0.0079093900
H	4.2056963400	1.8976843200	0.0127931600
H	2.7902943600	2.4806082900	-0.8729042500
H	2.7823455900	2.4785361800	0.8870301900
C	0.0001335300	2.2278553900	0.0018258600
C	-0.0041756800	2.9510985800	1.1997169200
H	-0.0076984500	2.4397075300	2.1576081800
C	-0.0039074600	4.3468416000	1.1444886400
H	-0.0072082100	4.9294657200	2.0631916200
N	0.0001876000	5.0466690800	0.0020484600
C	0.0042607700	4.3470445100	-1.1405136100
H	0.0075680500	4.9298117600	-2.0591266600
C	0.0044806700	2.9513154500	-1.1959529600
H	0.0079596300	2.4400508500	-2.1539137600
C	-3.1139586000	1.9188774100	0.0002147800
H	-2.7844048000	2.4810485600	-0.8784468700
H	-4.2054513000	1.8982132500	-0.0017224300
H	-2.7875635700	2.4787567000	0.8815044500
Cl	-5.0987148500	-0.7016384800	-0.0037727200
C	-2.9214127900	-3.2166244200	-0.0062052600
H	-2.5002573300	-3.7331435500	0.8618569100
H	-4.0079372700	-3.3091448400	0.0126409900
H	-2.5334638300	-3.7191076900	-0.8980318100

BODIPY 3cat A

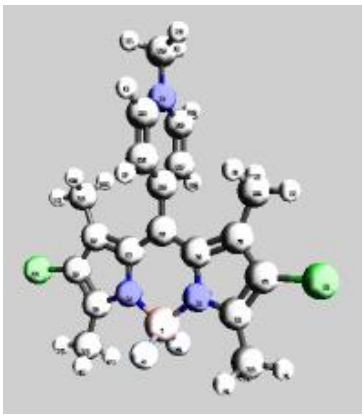

B	-0.0001174600	-2.5677731400	-0.0025760300
F	0.0036798300	-3.3505638900	1.1484376400
F	-0.0038716500	-3.3524481400	-1.1522504300
N	1.2534002600	-1.6301895000	-0.0067336900
C	2.5291652900	-2.0566020300	-0.0069474600
C	3.3694034800	-0.9096743100	-0.0036528600
C	2.5918386700	0.2401552500	-0.0012544900
C	1.2327247100	-0.2323481300	-0.0043146900
C	-0.0000045200	0.4402212800	-0.0034053300
C	-1.2328586300	-0.2323224800	-0.0030155200
C	-2.5919979200	0.2402698100	-0.0067937600
C	-3.3697375600	-0.9096273000	-0.0037401200
C	-2.5294095100	-2.0565924800	0.0003241100
N	-1.2535777900	-1.6301270400	0.0000979600
C	2.9235116000	-3.4915511900	-0.0088720700
H	4.0092490900	-3.5871233900	-0.0237366000
H	2.5296490900	-3.9974985000	0.8785844100
H	2.5039250000	-4.0028766600	-0.8810117500
Cl	5.0989868000	-0.9761839400	-0.0024082200
C	3.1283307200	1.6408556600	0.0048379500
H	4.2193459400	1.6132317100	0.0199559300
H	2.8301658200	2.2033608400	-0.8864377800
H	2.8053636000	2.2049003800	0.8863790100
C	0.0000380900	1.9319813800	0.0003746700
C	-0.0222549000	2.6532045400	1.2057167400
H	-0.0398638000	2.1376111400	2.1595432400
C	-0.0209926900	4.0350186900	1.1846076000
H	-0.0369865900	4.6357272600	2.0867070900
N	0.0006631300	4.7136705900	0.0097284100
C	0.0005434100	6.1981286500	0.0352382600
H	0.0212407700	6.5718028600	-0.9868703700
H	0.8849719500	6.5475657700	0.5705060700
H	-0.9044642600	6.5481106800	0.5345740900
C	0.0217998600	4.0445087600	-1.1676500400
H	0.0381503600	4.6471604100	-2.0675661400
C	0.0223652700	2.6603967600	-1.1976672200
H	0.0397891500	2.1526192600	-2.1556613900
C	-3.1284169300	1.6409499900	-0.0150204700
H	-2.8008964200	2.2053120500	-0.8945922600
H	-4.2193819900	1.6132932400	-0.0356677800
H	-2.8348098000	2.2030608500	0.8781291500
Cl	-5.0992719200	-0.9761025600	-0.0056463700
C	-2.9237413400	-3.4915599000	0.0029811100
H	-2.5041140100	-4.0024151600	0.8754220000

H	-4.0095334500	-3.5870138600	0.0179633200
H	-2.5298807300	-3.9979398900	-0.8842237500

BODIPY 4 A

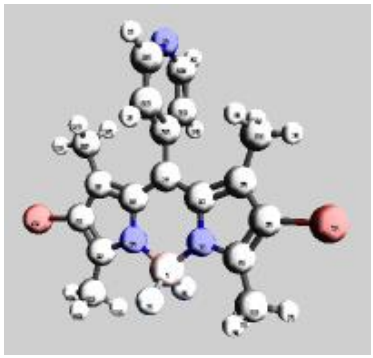

B	0.00016855	-2.17290391	-0.09008794
F	-0.00061203	-2.90555148	-1.28509145
F	0.00105523	-3.03789716	1.00864548
N	1.24915805	-1.24396508	-0.03929653
C	2.52697413	-1.66952267	-0.03474995
C	3.36258989	-0.52739234	-0.00380880
C	2.58401140	0.62693133	0.00871484
C	1.22692937	0.15569525	-0.01271040
C	-0.00012840	0.84292828	-0.00247975
C	-1.22702932	0.15540147	-0.01063585
C	-2.58418809	0.62631946	0.01342587
C	-3.36250938	-0.52817035	0.00215894
C	-2.52668510	-1.67010598	-0.03049058
N	-1.24898631	-1.24427016	-0.03737117
C	2.91450618	-3.10889531	-0.04321153
H	2.31710719	-3.66677464	-0.76809075
H	3.97318767	-3.21333194	-0.28453369
H	2.73507008	-3.55784954	0.94042307
Br	5.25703914	-0.60461393	0.02158454
C	3.10733721	2.03066185	0.03926160
H	4.19870581	2.01652319	0.03310004
H	2.77123702	2.61057432	-0.82500558
H	2.78158910	2.56838804	0.93454326
C	-0.00027554	2.33757720	0.02349611
C	0.00147641	3.04085333	1.23313527
H	0.00299987	2.51354498	2.18230461
C	0.00120981	4.43727439	1.20112483
H	0.00249615	5.00455048	2.12931948
N	-0.00057106	5.15594518	0.07042891
C	-0.00218934	4.47533824	-1.08361502
H	-0.00358753	5.07319570	-1.99239593
C	-0.00215912	3.08074214	-1.16216152
H	-0.00354879	2.58523997	-2.12830479
C	-3.10773934	2.02993386	0.04526068
H	-4.19912012	2.01554530	0.04334218
H	-2.77516807	2.60942444	-0.82067344
H	-2.77858369	2.56825392	0.93891793
Br	-5.25687559	-0.60598446	0.03113887
C	-2.91409388	-3.10951761	-0.03802748
H	-2.31418808	-3.66863287	-0.75980472
H	-3.97196434	-3.21436381	-0.28280328
H	-2.73837741	-3.55676573	0.94708743

BODIPY 4cat A

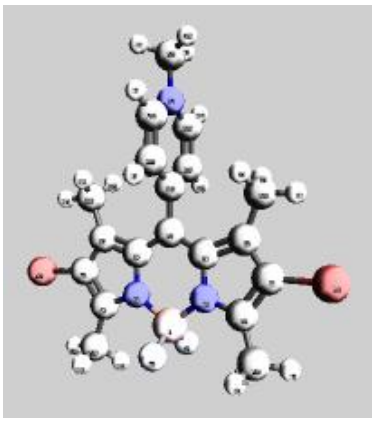

B	-0.0000450500	-2.4192531400	-0.0310192500
F	-0.0010476500	-3.1626964500	-1.2100322900
F	0.0009085100	-3.2429692300	1.0891614200
N	1.2534499300	-1.4822255000	-0.0018818900
C	2.5290230000	-1.9088354300	0.0174607100
C	3.3719653900	-0.7630881800	0.0168497800
C	2.5934256200	0.3867175400	-0.0056485000
C	1.2331382100	-0.0843785100	-0.0163899400
C	-0.0000233600	0.5887472200	-0.0250088900
C	-1.2331340400	-0.0843195500	-0.0127337300
C	-2.5934063300	0.3868195500	-0.0038105300
C	-3.3719860400	-0.7629260600	0.0178222500
C	-2.5290932600	-1.9087236600	0.0185648900
N	-1.2535111700	-1.4821851700	0.0004979700
C	2.9165725700	-3.3451730800	0.0517340600
H	2.3184881800	-3.9261647800	-0.6541878000
H	3.9750141400	-3.4583029900	-0.1845672400
H	2.7355848700	-3.7613899100	1.0497014400
Br	5.2588039600	-0.8413003800	0.0472872500
C	3.1225806200	1.7901267000	-0.0136933500
H	4.2137062200	1.7682311900	-0.0062201800
H	2.8150656400	2.3440799700	-0.9070297100
H	2.8033809400	2.3589786600	0.8663377600
C	0.0000017100	2.0805046500	-0.0408437900
C	-0.0205670400	2.8191400800	1.1539402900
H	-0.0370860000	2.3173710600	2.1150684400
C	-0.0196512500	4.2005397200	1.1132336300
H	-0.0349954900	4.8137888800	2.0068954400
N	0.0004964700	4.8626452700	-0.0710908800
C	-0.0000401500	6.3475004900	-0.0667115300
H	0.0209990000	6.7069005200	-1.0939461500
H	0.8839865400	6.7049810100	0.4639868600
H	-0.9052836500	6.7045354500	0.4273067200
C	0.0203162100	4.1765561000	-1.2388070800
H	0.0358607800	4.7659763400	-2.1474786800
C	0.0207271900	2.7921106800	-1.2489974300
H	0.0371304200	2.2706636100	-2.1996012200
C	-3.1225119100	1.7902181900	-0.0142899600
H	-4.2136479400	1.7682687000	-0.0206477500
H	-2.8033205100	2.3470856300	-0.9017213600
H	-2.8149775800	2.3561556800	0.8717207100
Br	-5.2588093000	-0.8411141400	0.0463827900
C	-2.9169732400	-3.3449748500	0.0516316700
H	-2.3143738500	-3.9266558600	-0.6497644600

H	-3.9739005700	-3.4581036500	-0.1914835500
H	-2.7429785700	-3.7602697300	1.0512571100

BODIPY 5 A

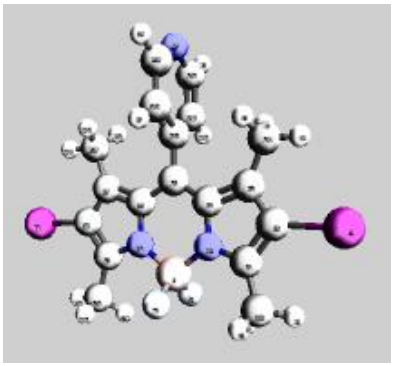

B	0.0000555500	-2.0898117200	-0.0366956000
F	0.0002298200	-2.8560375100	-1.2113205500
F	-0.0002760400	-2.9242833800	1.0859668100
N	1.2492178600	-1.1606750400	-0.0109808400
C	2.5268650200	-1.5863943500	0.0072948200
C	3.3696936400	-0.4455401300	0.0061370300
C	2.5854689900	0.7088525400	-0.0151313500
C	1.2275262900	0.2388392300	-0.0244050000
C	-0.0000198400	0.9269447800	-0.0352974800
C	-1.2274408800	0.2389377800	-0.0247747600
C	-2.5854726800	0.7089043900	-0.0154540400
C	-3.3695602400	-0.4453352000	0.0058820300
C	-2.5267532300	-1.5862159800	0.0069730700
N	-1.2491664800	-1.1606421500	-0.0113622600
C	2.8995864200	-3.0302250900	0.0424859800
H	2.2891564500	-3.6047483500	-0.6581263300
H	3.9547206900	-3.1573635100	-0.2040717800
H	2.7238674300	-3.4441764000	1.0422088200
I	5.4765319900	-0.5319376100	0.0415395100
C	3.0955330200	2.1181778900	-0.0251182000
H	4.1872290600	2.1178579300	-0.0235714900
H	2.7598016900	2.6672217600	-0.9096686600
H	2.7580166000	2.6806752200	0.8503841800
C	-0.0000505700	2.4215308500	-0.0515791800
C	0.0014249000	3.1584619500	1.1382264000
H	0.0027613500	2.6579026500	2.1019409400
C	0.0011895700	4.5537157000	1.0669712400
H	0.0023732100	5.1471343000	1.9789051100
N	-0.0004428100	5.2400236900	-0.0838527100
C	-0.0017682200	4.5275364100	-1.2186626200
H	-0.0031850400	5.0998971700	-2.1439380700
C	-0.0015372000	3.1309698500	-1.2580183200
H	-0.0027638100	2.6084067900	-2.2099681800
C	-3.0954111300	2.1182450200	-0.0252857200
H	-4.1870806500	2.1179286100	-0.0264189400
H	-2.7574690000	2.6682065900	-0.9083343700
H	-2.7600713800	2.6797294700	0.8517385600
I	-5.4763698800	-0.5318886000	0.0417436300
C	-2.8997602800	-3.0299370700	0.0425517900
H	-2.2848127600	-3.6059574500	-0.6527156200
H	-3.9532680400	-3.1575083100	-0.2106407100
H	-2.7310499500	-3.4417201000	1.0443694700

BODIPY 5cat A

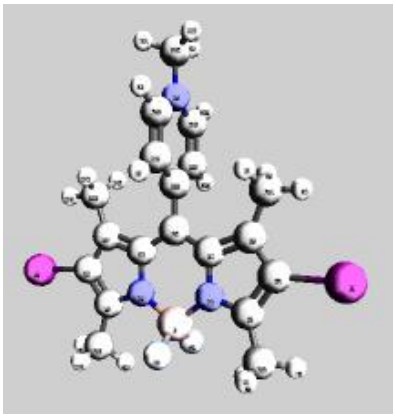

B	-0.0005546700	-2.3081221200	-0.0496145300
F	-0.0023009600	-3.0518477400	-1.2296826000
F	0.0005213400	-3.1332574000	1.0701364700
N	1.2538605600	-1.3730607200	-0.0198312300
C	2.5292688700	-1.7994606900	0.0010058200
C	3.3797460800	-0.6557568500	0.0111634900
C	2.5958632000	0.4938245400	-0.0081645400
C	1.2342377800	0.0248501000	-0.0264440400
C	0.0006259500	0.6987509800	-0.0359866400
C	-1.2335001100	0.0257899900	-0.0254069900
C	-2.5947720400	0.4957898800	-0.0097656200
C	-3.3795030500	-0.6531440400	0.0122330300
C	-2.5299158400	-1.7974874200	0.0045850900
N	-1.2541747900	-1.3720977500	-0.0168727700
C	2.9098801200	-3.2388982500	0.0334940000
H	2.1993277000	-3.8471442700	-0.5279445100
H	3.9126849100	-3.3764479200	-0.3749805200
H	2.9136594800	-3.6035182100	1.0683467600
I	5.4805348900	-0.7523531100	0.0638353700
C	3.1117990800	1.9028293500	-0.0065669500
H	4.2033464900	1.8941414700	0.0025135200
H	2.8001374100	2.4596225300	-0.8968087100
H	2.7860694000	2.4630240300	0.8767073400
C	0.0011546700	2.1907061300	-0.0521835900
C	-0.0110064400	2.9309788500	1.1420330200
H	-0.0207104200	2.4301741600	2.1039446900
C	-0.0096263400	4.3126677800	1.0995872400
H	-0.0183219900	4.9271208500	1.9927027800
N	0.0028760800	4.9735513800	-0.0858468400
C	-0.0035327700	6.4584832700	-0.0836542100
H	0.0575938200	6.8168586500	-1.1098688300
H	0.8574895400	6.8202617300	0.4809669500
H	-0.9290600200	6.8133275800	0.3737930100
C	0.0143436400	4.2858024700	-1.2531751500
H	0.0236562100	4.8743288000	-2.1627149500
C	0.0141846700	2.9011125500	-1.2616642700
H	0.0241136700	2.3781643500	-2.2117354600
C	-3.1097605700	1.9051288100	-0.0141531500
H	-4.2012381300	1.8971372800	-0.0301751700
H	-2.7771629900	2.4654994100	-0.8943474500
H	-2.8043412000	2.4612638600	0.8790540400
I	-5.4803591900	-0.7478547900	0.0654323500
C	-2.9116204300	-3.2365755100	0.0394808000
H	-2.2021024100	-3.8461352400	-0.5218430200

H	-3.9149187600	-3.3739060700	-0.3678372300
H	-2.9146529300	-3.5998273700	1.0748093000

BODIPY 6 A

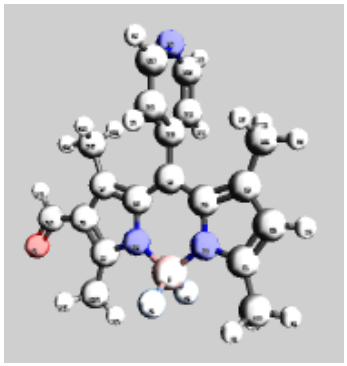

B	-0.0000000000	-3.0203279327	-0.0000000000
F	0.0055454200	-3.8176304868	1.1505646703
F	0.0055470221	-3.8205080690	-1.1483824623
N	1.2441987632	-2.0883832913	-0.0003040334
C	2.5253834515	-2.5005253399	0.0035555040
C	3.3722891709	-1.3676420100	0.0099918859
C	2.5858812804	-0.2245706076	0.0103884548
C	1.2200781753	-0.6857716035	0.0030388766
C	0.0000000000	0.0000000000	0.0000000000
C	-1.2336003132	-0.6871194155	-0.0045814524
C	-2.5812763088	-0.2227535012	-0.0126229364
C	-3.3924846483	-1.3751898862	-0.0131959862
C	-2.5313025825	-2.5161723043	-0.0063903941
N	-1.2593120960	-2.0949047272	-0.0019074276
C	2.9244678476	-3.9389821954	0.0030199054
H	4.0127647179	-4.0271778616	-0.0068652154
H	2.5319876391	-4.4509711312	0.8876725786
H	2.5148060699	-4.4557154008	-0.8708109592
H	4.4536756154	-1.4011444989	0.0143176451
C	3.1282004836	1.1746897956	0.0178739037
H	4.2205900947	1.1410173270	0.0379157722
H	2.8249851791	1.7404221473	-0.8685350365
H	2.7921730609	1.7442025010	0.8898166948
C	0.0085401342	1.4951267109	0.0033335918
C	-0.0103091366	2.2158413680	1.2028357475
H	-0.0311903526	1.7018534349	2.1591830684
C	-0.0027803172	3.6117118478	1.1511505837
H	-0.0187519296	4.1920132944	2.0711927622
N	0.0224981910	4.3143082081	0.0106367659
C	0.0433487156	3.6173981793	-1.1334603043
H	0.0648320393	4.2022431367	-2.0504957174
C	0.0383444089	2.2217927516	-1.1923578080
H	0.0564269606	1.7125598790	-2.1513000585
C	-3.0793805940	1.1943715386	-0.0202943945
H	-2.7086420906	1.7491465383	-0.8867030436
H	-4.1690721871	1.2257552994	-0.0500710080
H	-2.7570734759	1.7413878152	0.8704272320
C	-4.8492736130	-1.4245586360	-0.0189980799
H	-5.3631385053	-0.4429091629	-0.0203553891
O	-5.5185658272	-2.4515915687	-0.0218978162
C	-2.9339522227	-3.9512791774	-0.0057076378
H	-2.0718648357	-4.6139331269	0.0277411680
H	-3.5895008790	-4.1507932675	0.8474383352
H	-3.5309814129	-4.1679599531	-0.8974127627

BODIPY 6cat A

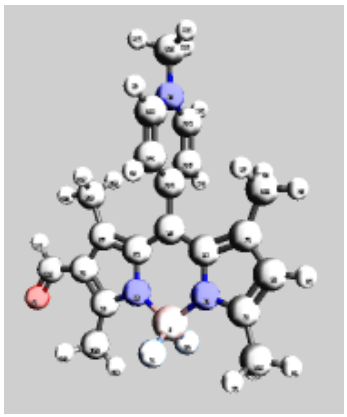

B	0.0174059200	-3.0205459000	0.0065112700
F	0.0321152800	-3.7992255600	1.1600990300
F	0.0238996600	-3.8064072200	-1.1420924500
N	1.2611156800	-2.0739634900	-0.0000119700
C	2.5426001000	-2.4815923200	0.0005706600
C	3.3871402500	-1.3398662700	0.0014778000
C	2.5980657500	-0.2045548200	0.0014656000
C	1.2310025200	-0.6744435500	-0.0005384100
C	-0.0002412100	-0.0100359400	-0.0005574400
C	-1.2345559900	-0.6910848500	0.0015220800
C	-2.5903978100	-0.2337804100	-0.0030077200
C	-3.3897165600	-1.3856847700	0.0016899500
C	-2.5189947500	-2.5254027800	0.0081152000
N	-1.2499568000	-2.0949041200	0.0073282700
C	2.9495036200	-3.9147250900	0.0016735700
H	4.0372045600	-3.9994762500	-0.0107965700
H	2.5596106800	-4.4258760100	0.8881094700
H	2.5380089000	-4.4343893500	-0.8696824800
H	4.4683504800	-1.3708967800	0.0025352800
C	3.1369476800	1.1976071200	0.0042686400
H	4.2287327900	1.1676384900	0.0204405400
H	2.8423960500	1.7610041900	-0.8880305800
H	2.8162743000	1.7675796600	0.8832494500
C	-0.0005261100	1.4818157000	0.0007541500
C	-0.0190438900	2.2054923500	1.2048357900
H	-0.0361454400	1.6915423700	2.1595619400
C	-0.0154749500	3.5872736700	1.1813429000
H	-0.0292991200	4.1894545200	2.0825281200
N	0.0056374700	4.2641156100	0.0052878700
C	0.0071419300	5.7487212000	0.0282070300
H	0.0292955400	6.1207224200	-0.9944879100
H	0.8913622700	6.0981363400	0.5638263900
H	-0.8978895300	6.1008154300	0.5260980800
C	0.0257349100	3.5926623100	-1.1709403600
H	0.0425697900	4.1934971000	-2.0720875600
C	0.0240931400	2.2085069500	-1.1984809400
H	0.0402882100	1.6988830800	-2.1555133600
C	-3.1020733000	1.1805939000	-0.0124729100
H	-2.7544227000	1.7369899500	-0.8890079200
H	-4.1917453700	1.1994982800	-0.0381126100
H	-2.7960911800	1.7338485400	0.8817964100
C	-4.8531390800	-1.4503945600	0.0005113500
H	-5.3830991800	-0.4773381200	-0.0012170800
O	-5.4965264500	-2.4881960900	0.0016355400

C	-2.9121398600	-3.9604494300	0.0132873800
H	-2.0479410700	-4.6200799400	0.0443101500
H	-3.5647948400	-4.1603532600	0.8688447200
H	-3.5137498500	-4.1803777100	-0.8748103200

BODIPY 7 A

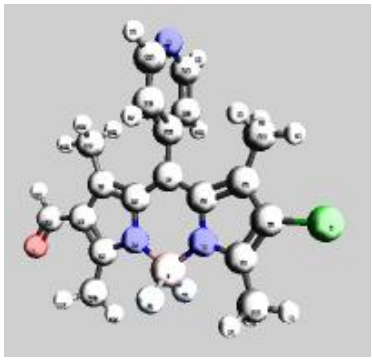

B	-0.0428372600	-2.2598411800	-0.0012920600
F	-0.0299548800	-3.0544836100	1.1488777000
F	-0.0375668900	-3.0556398800	-1.1506082800
N	1.2039042500	-1.3242484600	-0.0051198100
C	2.4796336600	-1.7486064900	-0.0054850500
C	3.3156475600	-0.6038943300	-0.0024264600
C	2.5401392600	0.5490948200	0.0004739900
C	1.1808293300	0.0770777600	-0.0019657700
C	-0.0434200500	0.7618835900	-0.0008187600
C	-1.2743222800	0.0735317100	-0.0012564500
C	-2.6245201600	0.5368944600	-0.0047549600
C	-3.4337802700	-0.6155324300	-0.0027121800
C	-2.5714596500	-1.7563487400	0.0012509600
N	-1.3000008900	-1.3342152700	0.0014745800
C	2.8754136600	-3.1849137900	-0.0069941100
H	3.9618809400	-3.2772367900	-0.0223703300
H	2.4831756800	-3.6911509200	0.8807701000
H	2.4565390500	-3.6971046700	-0.8787338200
Cl	5.0525224500	-0.6737578800	-0.0019902900
C	3.0736111700	1.9491588800	0.0055141500
H	4.1648103100	1.9265455600	0.0246016900
H	2.7629362300	2.5074756600	-0.8823942600
H	2.7313090700	2.5137085600	0.8774740800
C	-0.0392748200	2.2571486700	0.0029068800
C	-0.0552077400	2.9765127000	1.2030655200
H	-0.0726683500	2.4620326500	2.1591630900
C	-0.0479657300	4.3723568300	1.1520764000
H	-0.0599174500	4.9522783100	2.0724000500
N	-0.0264607600	5.0753898400	0.0118251000
C	-0.0100453300	4.3793943400	-1.1328315800
H	0.0087084200	4.9650302700	-2.0494278000
C	-0.0149924200	2.9838944400	-1.1926891900
H	-0.0003395000	2.4753840500	-2.1520155500
C	-3.1251844600	1.9529303300	-0.0105573300
H	-2.7593787500	2.5085201100	-0.8785902600
H	-4.2150385800	1.9814327000	-0.0358063200
H	-2.8003100000	2.5007427800	0.8788015500
C	-4.8915532500	-0.6673922500	-0.0038243900
H	-5.4077553000	0.3127535600	-0.0033981200
O	-5.5567929100	-1.6965777300	-0.0047354300
C	-2.9730644300	-3.1914454400	0.0036944700
H	-2.1106974800	-3.8539037100	0.0314669900
H	-3.6231206000	-3.3915518500	0.8609872300
H	-3.5761583300	-3.4076891500	-0.8840517300

BODIPY 7cat A

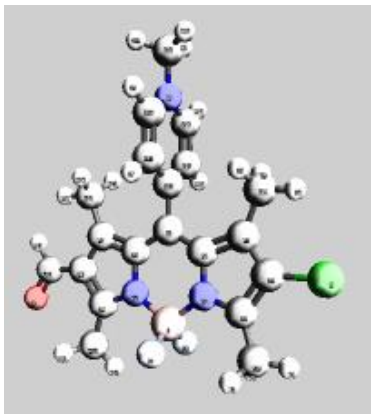

B	-0.0335718000	-2.5449541700	0.0037983000
F	-0.0166243300	-3.3209836400	1.1573477600
F	-0.0246058800	-3.3276461800	-1.1452372800
N	1.2158810100	-1.5981962100	-0.0024532400
C	2.4904195300	-2.0199453200	-0.0017911100
C	3.3294222600	-0.8683896000	-0.0019272000
C	2.5503877100	0.2777809700	-0.0024875200
C	1.1896889800	-0.1991564300	-0.0038763700
C	-0.0429870300	0.4669645100	-0.0040648100
C	-1.2770792200	-0.2123420700	-0.0015895900
C	-2.6333625500	0.2477355400	-0.0065290600
C	-3.4344547400	-0.9019620300	-0.0015712700
C	-2.5662226200	-2.0438669600	0.0051817400
N	-1.2962027500	-1.6160830300	0.0046395300
C	2.8907011000	-3.4524249900	0.0002835900
H	3.9766516700	-3.5442575700	-0.0151167600
H	2.4979049800	-3.9566578400	0.8892605900
H	2.4707796900	-3.9675575900	-0.8695262800
Cl	5.0577257300	-0.9334934200	-0.0010811300
C	3.0851209500	1.6788673200	-0.0011497000
H	4.1760041400	1.6517467100	0.0198204700
H	2.7917458700	2.2356641000	-0.8974918800
H	2.7573608700	2.2474600200	0.8755021300
C	-0.0435721700	1.9594412900	-0.0040444000
C	-0.0645889800	2.6838603300	1.1994459600
H	-0.0823165200	2.1708882000	2.1547137100
C	-0.0618168300	4.0657502600	1.1747802900
H	-0.0773562700	4.6684592000	2.0755771000
N	-0.0392254000	4.7415410500	-0.0017721900
C	-0.0383366400	6.2264575300	0.0197664900
H	-0.0191236300	6.5974859000	-1.0033378800
H	0.8471225100	6.5766975100	0.5528259400
H	-0.9423016200	6.5783296500	0.5197150800
C	-0.0168517100	4.0691853000	-1.1773308600
H	0.0012623100	4.6691697200	-2.0790077000
C	-0.0175900500	2.6848480200	-1.2038591600
H	0.0008676400	2.1747435000	-2.1606212500
C	-3.1432210700	1.6624996600	-0.0163240700
H	-2.7952287200	2.2181844600	-0.8930296600
H	-4.2328478100	1.6824487500	-0.0416550800
H	-2.8362875000	2.2154751900	0.8775885300
C	-4.8986950200	-0.9637601600	-0.0031798400
H	-5.4268806500	0.0100828500	-0.0052903700
O	-5.5429232500	-2.0007119600	-0.0019226600

C	-2.9631507500	-3.4774944400	0.0108099000
H	-2.1013321700	-4.1403134300	0.0384626000
H	-3.6137207400	-3.6756604500	0.8683606900
H	-3.5689524800	-3.6943783000	-0.8751665000

BODIPY 8 A

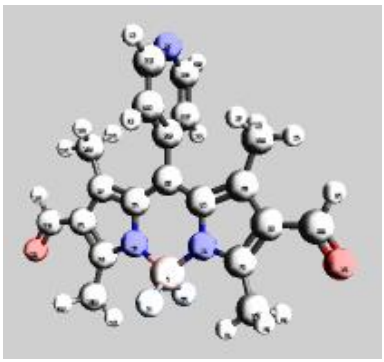

B	-0.0003686800	-2.2349022100	0.0056844400
F	0.0013447800	-3.0236230800	1.1574369100
F	0.0004707500	-3.0266354400	-1.1437957000
N	1.2535738000	-1.3038687200	0.0034104700
C	2.5235525600	-1.7250082200	0.0003504100
C	3.3865436500	-0.5819486600	-0.0060030100
C	2.5795147700	0.5684997500	-0.0058644700
C	1.2261095400	0.1037602300	0.0003192200
C	-0.0018753300	0.7893651200	0.0026522300
C	-1.2298787800	0.1033442400	0.0016137400
C	-2.5834144300	0.5678076800	-0.0056390000
C	-3.3905047900	-0.5826054200	-0.0060533900
C	-2.5275459400	-1.7259376100	0.0005127100
N	-1.2572548000	-1.3049122100	0.0042502000
C	2.9271281100	-3.1594559900	0.0020894000
H	2.0663476300	-3.8234393300	0.0350726600
H	3.5825012800	-3.3572873700	0.8559026900
H	3.5259845200	-3.3751792800	-0.8887965600
C	4.8454914000	-0.6338118800	-0.0109068800
H	5.3617642600	0.3460380400	-0.0115589300
O	5.5090020100	-1.6633374700	-0.0137031500
C	3.0793277800	1.9841343200	-0.0133794800
H	2.7114821800	2.5374501600	-0.8815427400
H	4.1689476100	2.0139220700	-0.0405719800
H	2.7535138800	2.5322194400	0.8755066800
C	0.0003498700	2.2854369900	0.0073681300
C	-0.0197396300	3.0046577100	1.2077332700
H	-0.0396871300	2.4911970500	2.1643408300
C	-0.0134959100	4.4009606100	1.1569516500
H	-0.0295429400	4.9809088200	2.0772197900
N	0.0114966400	5.1039301900	0.0169308200
C	0.0317344100	4.4084084000	-1.1279190300
H	0.0536589400	4.9942592200	-2.0442268300
C	0.0271856900	3.0127691300	-1.1879309700
H	0.0472925500	2.5050045400	-2.1475862600
C	-3.0832987700	1.9836606400	-0.0139709000
H	-2.7147108900	2.5372840000	-0.8819189100
H	-4.1729326400	2.0134078400	-0.0417471300
H	-2.7591818100	2.5315610700	0.8754015400
C	-4.8497131400	-0.6341737100	-0.0109363900
H	-5.3659925900	0.3457638400	-0.0114958700
O	-5.5135835300	-1.6634859500	-0.0136136600
C	-2.9324711500	-3.1599473800	0.0021443500
H	-2.0722877100	-3.8246812200	0.0350977400

H	-3.5880573800	-3.3573082400	0.8559398100
H	-3.5316530500	-3.3752369000	-0.8886245500

BODIPY 8cat A

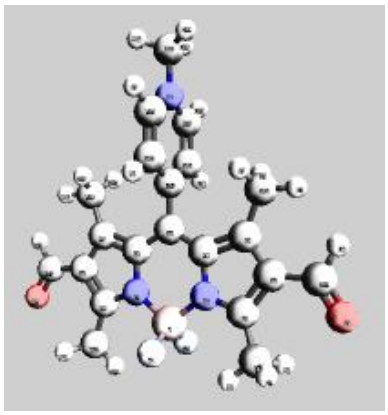

B	-0.0022731700	-2.5244412400	0.0037903800
F	-0.0015529300	-3.2932444600	1.1601822700
F	-0.0036787500	-3.3054452800	-1.1440838400
N	1.2571245900	-1.5867687100	-0.0026143000
C	2.5263725500	-2.0108325600	-0.0045793300
C	3.3933349400	-0.8649551800	-0.0096847800
C	2.5919201500	0.2812347500	-0.0098712800
C	1.2330325200	-0.1823629700	-0.0059356100
C	-0.0007205800	0.4911789900	-0.0036217300
C	-1.2350056800	-0.1811459200	-0.0023076200
C	-2.5932074200	0.2842059600	-0.0078369200
C	-3.3961003400	-0.8608857300	-0.0082784200
C	-2.5305602900	-2.0079003400	-0.0031778700
N	-1.2607791300	-1.5854672500	-0.0002070900
C	2.9285856400	-3.4421469300	-0.0027457100
H	2.0698771300	-4.1085267800	0.0265765900
H	3.5833594400	-3.6384631300	0.8520924000
H	3.5324986300	-3.6544326700	-0.8912342100
C	4.8591650900	-0.9243200800	-0.0140101800
H	5.3860072100	0.0497990100	-0.0132532100
O	5.5035329600	-1.9605368500	-0.0181465000
C	3.1006563800	1.6959363800	-0.0148065900
H	2.7674718800	2.2485414700	-0.8991055700
H	4.1904239600	1.7154775300	-0.0223829500
H	2.7787893300	2.2508595100	0.8726055900
C	0.0004233700	1.9843634200	0.0032074500
C	-0.0191648000	2.7025095200	1.2104053400
H	-0.0370165700	2.1850439800	2.1632851200
C	-0.0152467500	4.0848443000	1.1936072600
H	-0.0295398600	4.6824094000	2.0980473300
N	0.0069880400	4.7674759300	0.0209994700
C	0.0100462300	6.2528284600	0.0511264200
H	0.0333961000	6.6299123400	-0.9697207200
H	0.8942181000	6.5984868900	0.5893721600
H	-0.8950677100	6.6029740100	0.5502988100
C	0.0253630700	4.1013510700	-1.1582543300
H	0.0426986100	4.7061847900	-2.0568779400
C	0.0225681700	2.7169199300	-1.1923009900
H	0.0380758500	2.2129608900	-2.1523966900
C	-3.0991842600	1.6999139200	-0.0145964900
H	-2.7510384300	2.2557938300	-0.8910735600
H	-4.1886593200	1.7218237800	-0.0386553900
H	-2.7899408200	2.2503358400	0.8800768000
C	-4.8620448000	-0.9182185900	-0.0141336500

H	-5.3874509000	0.0566310300	-0.0137996000
O	-5.5076162600	-1.9537084000	-0.0190566400
C	-2.9345188800	-3.4387344400	-0.0027477900
H	-2.0765496200	-4.1060293400	0.0266408600
H	-3.5902558000	-3.6351859900	0.8513040300
H	-3.5377993700	-3.6496049300	-0.8920022600

BODIPY 9 A

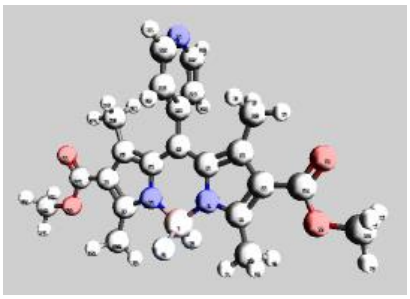

B	-0.0004132000	-3.0318675200	-0.0101413500
F	0.0094051100	-3.8304877400	1.1394052500
F	-0.0114350100	-3.8271103800	-1.1619102200
N	1.2552719200	-2.1070545300	-0.0188722500
C	2.5279324400	-2.5303801000	-0.0264904400
C	3.3916091900	-1.3890583900	-0.0261212900
C	2.5838124800	-0.2364940100	-0.0170677100
C	1.2302149600	-0.7031424700	-0.0133053200
C	0.0018201700	-0.0155870400	-0.0052797000
C	-1.2275825000	-0.7013351600	0.0008012800
C	-2.5804846000	-0.2327091400	0.0078969000
C	-3.3899451600	-1.3840978600	0.0136628700
C	-2.5279964500	-2.5266818700	0.0085126200
N	-1.2547127400	-2.1052222300	0.0015038500
C	2.8871017200	-3.9809697000	-0.0338312600
H	2.0004359800	-4.6096978100	-0.0464721500
H	3.4890448400	-4.2223919500	0.8470373600
H	3.5059136500	-4.2096196700	-0.9061094600
C	4.8667756200	-1.4031467200	-0.0330577100
O	5.5909336100	-0.4204988900	-0.0474579900
O	5.3733699400	-2.6616321500	-0.0212681200
C	6.8105563600	-2.7561492400	-0.0278375000
H	7.0278548900	-3.8240859200	-0.0210913100
H	7.2291868700	-2.2706750600	0.8568176700
H	7.2204429900	-2.2834286800	-0.9234035300
C	3.0708552900	1.1827082800	-0.0103050500
H	2.7310496500	1.7224764800	-0.8994303500
H	4.1578330700	1.2016380500	0.0123785300
H	2.6893373000	1.7296702800	0.8565611300
C	0.0029641200	1.4798499300	-0.0029140200
C	-0.0099302700	2.2006921400	1.1958539100
H	-0.0209543700	1.6882363900	2.1531062600
C	-0.0075079600	3.5962783700	1.1426492700
H	-0.0165654000	4.1773395900	2.0622380300
N	0.0054214500	4.2976381700	0.0013870500
C	0.0170955600	3.5997548800	-1.1420401200
H	0.0272028500	4.1836201300	-2.0598408100
C	0.0170708900	2.2043570800	-1.1995061600
H	0.0272301000	1.6947990900	-2.1583170400
C	-3.0655129900	1.1871874500	0.0057439700
H	-2.6781349300	1.7383743700	-0.8557096600
H	-4.1523525000	1.2078007800	-0.0219876100
H	-2.7303311000	1.7215694900	0.8999789700
C	-4.8650995900	-1.3959768200	0.0233610700

O	-5.5875356700	-0.4126217100	0.0594587000
O	-5.3737764400	-2.6531361300	-0.0133641500
C	-6.8110895500	-2.7455401400	-0.0045864500
H	-7.0301237500	-3.8127889600	-0.0320715600
H	-7.2177318200	-2.2901322500	0.9013725400
H	-7.2313971800	-2.2418917300	-0.8782138100
C	-2.8893889500	-3.9767312900	0.0106753600
H	-2.0038095000	-4.6068114200	0.0306166100
H	-3.5168550400	-4.2056695300	0.8765865300
H	-3.4832163500	-4.2160260900	-0.8763444400

BODIPY 9cat A

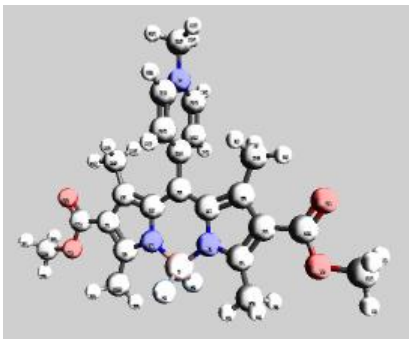

B	0.0000936900	-3.0243116600	0.0000151200
F	0.0040123500	-3.8058615100	1.1521750200
F	-0.0038756100	-3.8063079800	-1.1517295600
N	1.2586055100	-2.0906297200	-0.0031580600
C	2.5317425600	-2.5124779400	-0.0028922400
C	3.3961834400	-1.3664909300	0.0006760000
C	2.5908756700	-0.2206350600	0.0032512100
C	1.2339661500	-0.6899365300	-0.0002661000
C	0.0003262000	-0.0159406200	-0.0000678500
C	-1.2335083500	-0.6898658300	0.0003577500
C	-2.5904121700	-0.2203728700	-0.0015971000
C	-3.3960105700	-1.3663021400	0.0013948300
C	-2.5315110600	-2.5123857600	0.0033493800
N	-1.2583097300	-2.0904954500	0.0030537500
C	2.8970555000	-3.9581647200	-0.0059163700
H	2.0162214900	-4.5945706800	-0.0229778600
H	3.4969322200	-4.1920429800	0.8784778400
H	3.5245996400	-4.1818699400	-0.8732633400
C	4.8778802800	-1.3743554600	0.0025290700
O	5.5815679800	-0.3772337000	-0.0090582100
O	5.3843648800	-2.6213768900	0.0190811400
C	6.8273696600	-2.7219272000	0.0215573700
H	7.0373395500	-3.7902624200	0.0321648400
H	7.2371452200	-2.2355834500	0.9089021200
H	7.2391926500	-2.2526535100	-0.8739828400
C	3.0800641400	1.2002168600	0.0107962000
H	2.7626191800	1.7406453600	-0.8876830200
H	4.1679181700	1.2103765700	0.0393217400
H	2.7114986600	1.7497756200	0.8833406500
C	0.0006273900	1.4771942000	0.0013256600
C	-0.0217834700	2.2008029600	1.2048190700
H	-0.0399991000	1.6877287700	2.1598984400
C	-0.0189792700	3.5821977100	1.1812199600
H	-0.0341977600	4.1838629000	2.0826914700
N	0.0037299000	4.2592039100	0.0054893200
C	0.0050833300	5.7440377000	0.0283361800
H	0.0293745000	6.1162215500	-0.9943586700
H	0.8883973800	6.0937227900	0.5655529800
H	-0.9011591000	6.0961375300	0.5242455200
C	0.0243174700	3.5872753200	-1.1703179100
H	0.0411790700	4.1874844500	-2.0718543100
C	0.0238495300	2.2034934600	-1.1975933500
H	0.0409978900	1.6945282300	-2.1548773800
C	-3.0794880300	1.2005111300	-0.0093986400

H	-2.7081610000	1.7508054900	-0.8802212100
H	-4.1673482500	1.2107753800	-0.0400311200
H	-2.7646633400	1.7399428200	0.8907300900
C	-4.8777222500	-1.3739669000	0.0020783100
O	-5.5812449100	-0.3770784400	0.0312528700
O	-5.3842083800	-2.6206389300	-0.0341234800
C	-6.8271608200	-2.7212215600	-0.0347162500
H	-7.0370876000	-3.7892775600	-0.0628657500
H	-7.2367620200	-2.2671508500	0.8696717900
H	-7.2391476100	-2.2200043600	-0.9127355800
C	-2.8969180900	-3.9581177100	0.0057237600
H	-2.0162818200	-4.5945396100	0.0323819500
H	-3.5331415700	-4.1800561500	0.8671369500
H	-3.4879948400	-4.1934976500	-0.8843448200

BODIPY 10 A

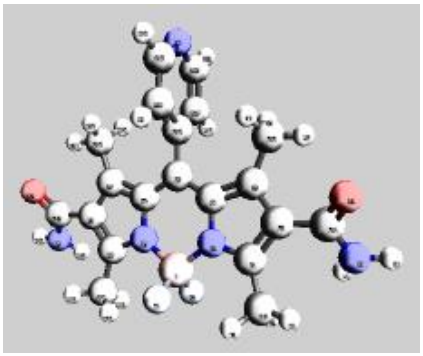

B	0.0005501800	-3.0374001700	0.1007894600
F	0.0009327700	-3.7682934900	1.2991768100
F	-0.0005213500	-3.9123304300	-0.9950404500
N	1.2497011200	-2.1140838200	0.0398486000
C	2.5268247300	-2.5359215900	0.0229415000
C	3.3875960200	-1.4023049300	-0.0036189700
C	2.5854107100	-0.2498998800	0.0127584100
C	1.2289151100	-0.7125135200	0.0238319700
C	0.0019112700	-0.0227597200	0.0186152100
C	-1.2257413500	-0.7113877100	0.0225141600
C	-2.5817997500	-0.2475924800	0.0076882200
C	-3.3850280700	-1.3993076100	-0.0065366100
C	-2.5252950000	-2.5336394500	0.0236624300
N	-1.2478333700	-2.1129202300	0.0411066600
C	2.8823425400	-3.9892525100	0.0720742000
H	3.9004660100	-4.1242891700	0.4395663400
H	2.8077985900	-4.4430518200	-0.9243789800
H	2.1898765400	-4.5305501700	0.7191748500
C	4.8776572600	-1.4075306400	-0.0113445700
O	5.5499857600	-0.5859010500	0.6093763100
N	5.4772823500	-2.4014696300	-0.7478207600
H	6.4839133700	-2.3555226600	-0.8278315300
H	4.9717033000	-2.9079408700	-1.4584744300
C	3.0942431200	1.1614478800	-0.0051162100
H	2.7307683900	1.7106887200	-0.8786592800
H	4.1833346400	1.1630374300	-0.0052035500
H	2.7633337800	1.7141186100	0.8794154700
C	0.0026631500	1.4722073700	0.0099079100
C	-0.0071934700	2.2005388800	1.2044387200
H	-0.0158570000	1.6939917500	2.1648695400
C	-0.0056004100	3.5963447100	1.1419890200
H	-0.0130044500	4.1836506500	2.0577268700
N	0.0046458300	4.2900448200	-0.0041532400
C	0.0138389800	3.5851936300	-1.1435275800
H	0.0221544400	4.1638353800	-2.0649501100
C	0.0134413400	2.1891981900	-1.1919367900
H	0.0214419700	1.6733197000	-2.1475754700
C	-3.0891237900	1.1641435200	-0.0161125300
H	-2.7070876600	1.7162032500	-0.8797338800
H	-4.1779911800	1.1670694400	-0.0380500800
H	-2.7766317300	1.7131748200	0.8774622100
C	-4.8749551400	-1.4026340500	-0.0157316400
O	-5.5465248800	-0.5766028600	0.5999821600
N	-5.4755214700	-2.3996494500	-0.7473125700

H	-6.4820104000	-2.3524054400	-0.8283457700
H	-4.9703287700	-2.9103677000	-1.4551935000
C	-2.8822758300	-3.9865176800	0.0753386800
H	-3.8991207600	-4.1199303900	0.4469661400
H	-2.8125011600	-4.4411499800	-0.9210991000
H	-2.1879211000	-4.5282289200	0.7200035800

BODIPY 10cat A

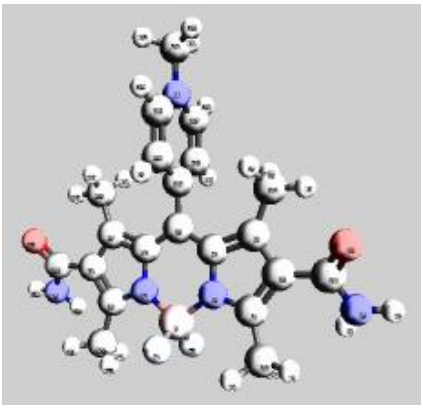

B	0.0005128200	-3.0169073400	0.0595138000
F	0.0021910100	-3.6949874300	1.2804672900
F	-0.0011962800	-3.9095347200	-1.0107358700
N	1.2538973600	-2.0878390800	-0.0289497800
C	2.5313700000	-2.5076156100	-0.0265945300
C	3.3940345100	-1.3694838100	-0.0703773600
C	2.5920436100	-0.2237868600	-0.0805938200
C	1.2332572300	-0.6897176400	-0.0662191400
C	0.0010648100	-0.0139051600	-0.0732597700
C	-1.2313417000	-0.6893668000	-0.0672719900
C	-2.5898116500	-0.2229334100	-0.0868560500
C	-3.3923816300	-1.3681697400	-0.0713763500
C	-2.5303479800	-2.5065036200	-0.0224160000
N	-1.2526772700	-2.0873392800	-0.0256595100
C	2.8909486100	-3.9560581200	0.0525366500
H	3.8913535600	-4.0828046100	0.4684598700
H	2.8650010100	-4.4166602000	-0.9435926100
H	2.1735534300	-4.4980115800	0.6707476100
C	4.8888050900	-1.3565824600	-0.0445607500
O	5.5150649500	-0.4819879000	0.5519090100
N	5.5244580400	-2.3684407400	-0.7078955000
H	6.5348902200	-2.3370473200	-0.7334927100
H	5.0514245800	-2.9669017700	-1.3671483900
C	3.0982368700	1.1901133300	-0.1239192300
H	2.7476678900	1.7228578500	-1.0143998700
H	4.1874939100	1.1887376500	-0.1220103900
H	2.7822030900	1.7584653000	0.7577993200
C	0.0008055300	1.4786721100	-0.0387044400
C	-0.0160172700	2.1615563400	1.1890630700
H	-0.0285074200	1.6163517300	2.1265018700
C	-0.0159597100	3.5434194300	1.2114138700
H	-0.0281324200	4.1150435500	2.1324763400
N	-0.0005196100	4.2587405900	0.0582358600
C	-0.0045424700	5.7417736900	0.1311380500
H	0.0287088600	6.1487624500	-0.8780706700
H	0.8721592400	6.0756839400	0.6889543100
H	-0.9168393000	6.0738901400	0.6300873700
C	0.0155081600	3.6264808800	-1.1397217500
H	0.0269718300	4.2570516000	-2.0205286100
C	0.0169423100	2.2439501600	-1.2133560300
H	0.0301465700	1.7674515400	-2.1873586900
C	-3.0950060000	1.1908776600	-0.1410353800
H	-2.7121688600	1.7288379900	-1.0146453600
H	-4.1835705200	1.1901468100	-0.1781821900

H	-2.8125828400	1.7540153200	0.7555701200
C	-4.8869023700	-1.3527375900	-0.0453527400
O	-5.5108344200	-0.4714757700	0.5437850900
N	-5.5251913100	-2.3691360900	-0.6991584900
H	-6.5355555700	-2.3352369000	-0.7245445000
H	-5.0542443000	-2.9732869700	-1.3547129200
C	-2.8905163000	-3.9544825700	0.0619664500
H	-3.8902811900	-4.0793723900	0.4799730700
H	-2.8664764200	-4.4182271700	-0.9327655400
H	-2.1723269900	-4.4948127200	0.6806375300

BODIPY 11 A

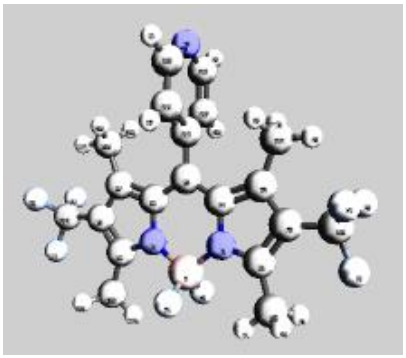

B	0.0000448100	-3.0455448100	-0.0013774500
F	0.0011453200	-3.8403203500	1.1495433100
F	-0.0011375300	-3.8425484100	-1.1505015200
N	1.2542314400	-2.1172114900	-0.0034464400
C	2.5304081700	-2.5399078400	-0.0041348300
C	3.3766287900	-1.3969774300	-0.0029373500
C	2.5811277200	-0.2472870100	-0.0011917400
C	1.2270048700	-0.7159904100	-0.0017332200
C	0.0001347000	-0.0277169100	-0.0003465300
C	-1.2267692900	-0.7158644900	-0.0020104300
C	-2.5808447900	-0.2471010000	-0.0050981000
C	-3.3764058600	-1.3967132100	-0.0046760900
C	-2.5302902400	-2.5396734500	-0.0020012500
N	-1.2540780500	-2.1171144800	-0.0011260200
C	2.9077393000	-3.9872091800	-0.0072304300
H	2.0273060700	-4.6250374600	0.0107276900
H	3.5318192900	-4.2190476600	0.8610451800
H	3.4976040100	-4.2234768400	-0.8984344400
C	4.8687703000	-1.3962084400	-0.0058304800
F	5.3957348600	-2.6431526500	-0.0010096300
F	5.3879118300	-0.7509672800	1.0776776500
F	5.3831937900	-0.7612753300	-1.0977288000
C	3.0900684700	1.1653636300	-0.0004509500
H	2.7528139600	1.7129573500	-0.8849869600
H	4.1792582500	1.1853816600	0.0094037800
H	2.7365625800	1.7184645000	0.8741859900
C	0.0005152200	1.4672531500	0.0063654500
C	-0.0137586700	2.1823696800	1.2093050900
H	-0.0260553100	1.6655043700	2.1643334900
C	-0.0115892100	3.5788321200	1.1617948900
H	-0.0222986500	4.1566772300	2.0835258300
N	0.0031429300	4.2842133600	0.0228752900
C	0.0163603200	3.5921022100	-1.1242066300
H	0.0283421100	4.1807397500	-2.0390656800
C	0.0158560900	2.1962874800	-1.1881277200
H	0.0273979500	1.6907908900	-2.1492261300
C	-3.0895529600	1.1656151200	-0.0085882900
H	-2.7242751900	1.7213078900	-0.8765455900
H	-4.1785119400	1.1858006100	-0.0330132000
H	-2.7642394000	1.7105430500	0.8822135700
C	-4.8685631200	-1.3957156500	-0.0077218600
F	-5.3955455300	-2.6426608600	-0.0019191500
F	-5.3831562400	-0.7618788100	-1.1001975400
F	-5.3873226900	-0.7496611200	1.0754349600

C	-2.9076995900	-3.9869472900	-0.0013161500
H	-2.0272800700	-4.6248193600	0.0157465700
H	-3.5293547700	-4.2169684800	0.8692284500
H	-3.5000852300	-4.2250963700	-0.8902772700

BODIPY 11cat A

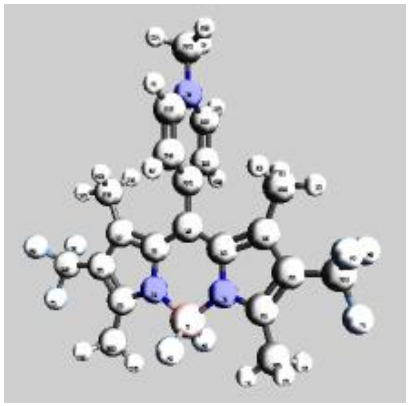

B	0.0010141300	-3.0244022500	0.0089697700
F	0.0159587100	-3.8011819300	1.1623113800
F	-0.0143514700	-3.8069199900	-1.1404671900
N	1.2592995700	-2.0881340200	-0.0098924700
C	2.5344983700	-2.5117810700	-0.0257883800
C	3.3838230100	-1.3646691500	-0.0374051800
C	2.5916423700	-0.2199532300	-0.0275667200
C	1.2336747800	-0.6894842800	-0.0109604100
C	0.0018588800	-0.0139012500	0.0026380000
C	-1.2303566800	-0.6887460800	0.0185697300
C	-2.5880770500	-0.2184055600	0.0319288100
C	-3.3809051400	-1.3626315300	0.0451893100
C	-2.5322233700	-2.5102442600	0.0391607500
N	-1.2567665400	-2.0873724700	0.0230537100
C	2.9149633400	-3.9552046400	-0.0295618400
H	2.0386177100	-4.5984914200	-0.0140393300
H	3.5395555200	-4.1833225000	0.8398071100
H	3.5102774700	-4.1862879700	-0.9185364800
C	4.8809612000	-1.3591082100	-0.0566212800
F	5.4083240500	-2.5986716700	-0.0693595700
F	5.3950909200	-0.7162190100	1.0281565900
F	5.3667381600	-0.7059013600	-1.1482226800
C	3.1036842500	1.1935410700	-0.0333838600
H	2.7747241000	1.7406888900	-0.9228934400
H	4.1926984100	1.2096265600	-0.0321192800
H	2.7727137500	1.7488238700	0.8501427900
C	0.0020938600	1.4796097500	0.0010371100
C	0.0058698600	2.2051933100	1.2040653100
H	0.0092663700	1.6943405600	2.1608650200
C	0.0057153400	3.5875675700	1.1772329400
H	0.0086379900	4.1913112200	2.0777260400
N	0.0016026000	4.2618428900	-0.0005303000
C	-0.0015001500	5.7475480600	0.0190415000
H	0.0134040300	6.1174584900	-1.0047436100
H	0.8850606900	6.1008371200	0.5486011900
H	-0.9048351900	6.0976141000	0.5219785100
C	-0.0021402900	3.5878347100	-1.1755330800
H	-0.0054751500	4.1863727300	-2.0786188100
C	-0.0016877500	2.2029524500	-1.2003536800
H	-0.0046541200	1.6923403700	-2.1572610600
C	-3.0994376900	1.1953631700	0.0313087700
H	-2.7711778700	1.7453009500	-0.8565687100
H	-4.1884367300	1.2119630700	0.0337558400
H	-2.7672629500	1.7475563400	0.9164847600

C	-4.8780668400	-1.3561441200	0.0618840100
F	-5.4061987700	-2.5953468900	0.0770864300
F	-5.3899330800	-0.7159108800	-1.0255095300
F	-5.3653808600	-0.6996649700	1.1508724500
C	-2.9134838700	-3.9534351700	0.0482366600
H	-2.0374421900	-4.5972476300	0.0386116100
H	-3.5120210600	-4.1801466900	0.9361456700
H	-3.5351519200	-4.1852126700	-0.8222813500

BODIPY 12 A

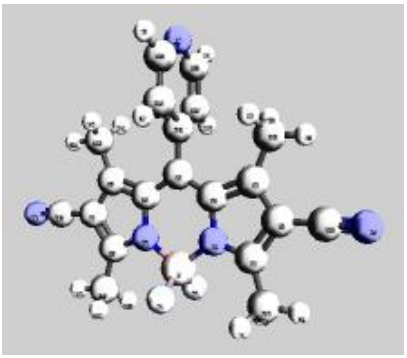

B	-0.0009540000	-3.0211768600	-0.0215591800
F	-0.0000913600	-3.8223063400	1.1222070600
F	-0.0034669000	-3.8066803700	-1.1760906000
N	1.2500879700	-2.0882261700	-0.0170835700
C	2.5217203800	-2.5116947300	-0.0224899100
C	3.3729949700	-1.3710152900	-0.0163672900
C	2.5781977600	-0.2154323500	-0.0069607100
C	1.2268812200	-0.6834066600	-0.0073382900
C	0.0021359800	0.0070255900	-0.0001454400
C	-1.2240150600	-0.6809075700	-0.0028505700
C	-2.5743709500	-0.2102319200	0.0034946800
C	-3.3715004200	-1.3641917700	-0.0036789100
C	-2.5225743800	-2.5065707600	-0.0139428700
N	-1.2500826200	-2.0856822900	-0.0132699100
C	2.9244035300	-3.9465699700	-0.0333379800
H	2.5221449200	-4.4646715500	0.8428284200
H	4.0121058900	-4.0339551200	-0.0341375400
H	2.5220743500	-4.4512699200	-0.9172949600
C	4.7926643900	-1.4163576800	-0.0194091800
N	5.9573335300	-1.4507202100	-0.0218320400
C	3.1214063400	1.1805234100	0.0012456000
H	2.7911773800	1.7505900900	-0.8719772100
H	4.2132886300	1.1531772400	-0.0048919700
H	2.8009211000	1.7363067400	0.8872649400
C	0.0037241500	1.5015842100	0.0105842500
C	0.0105440800	2.2145122300	1.2145792500
H	0.0148227600	1.6968350100	2.1690729400
C	0.0117451000	3.6108482600	1.1686781000
H	0.0169608200	4.1871920600	2.0911090600
N	0.0068407800	4.3174761700	0.0308076100
C	0.0003993800	3.6272771700	-1.1170929800
H	-0.0034984400	4.2168194900	-2.0311517000
C	-0.0014847400	2.2317433900	-1.1830446100
H	-0.0068209300	1.7278411300	-2.1448761600
C	-3.1147094000	1.1868011800	0.0153061700
H	-2.7935996800	1.7543485800	-0.8630009300
H	-4.2066373900	1.1616239200	0.0217077700
H	-2.7828027200	1.7438441300	0.8962514900
C	-4.7912431600	-1.4067014100	-0.0011325900
N	-5.9559709600	-1.4387393600	0.0009837400
C	-2.9281649700	-3.9406255300	-0.0237204800
H	-2.5261109500	-4.4590242800	0.8523884900
H	-4.0160345400	-4.0258471400	-0.0232919400
H	-2.5276791500	-4.4466513300	-0.9077235400

BODIPY 12cat A

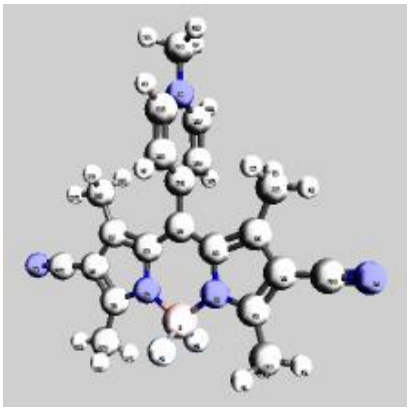

B	0.0001359400	-3.0320890900	0.0007365400
F	0.0002842700	-3.8098010200	1.1521058900
F	-0.0003545100	-3.8112401100	-1.1496202000
N	1.2540912200	-2.0910109700	-0.0000246200
C	2.5253546500	-2.5157783200	0.0003720400
C	3.3791521100	-1.3703690100	0.0017240900
C	2.5869206500	-0.2193802900	0.0019925300
C	1.2317412200	-0.6888042600	0.0004994300
C	0.0008471900	-0.0120574300	-0.0004228700
C	-1.2303932100	-0.6882662700	-0.0009798200
C	-2.5853663200	-0.2182311700	-0.0028717500
C	-3.3781453500	-1.3688917200	-0.0020503900
C	-2.5248461500	-2.5146778500	-0.0000661500
N	-1.2533862900	-2.0904495500	0.0003918400
C	2.9292546800	-3.9479449200	-0.0004647000
H	2.5258925400	-4.4597490200	0.8794407000
H	4.0165594000	-4.0369613200	-0.0011426900
H	2.5248050300	-4.4590327500	-0.8802634600
C	4.7993681000	-1.4070011000	0.0027928300
N	5.9637369300	-1.4165303200	0.0037408600
C	3.1354408900	1.1768480300	0.0039048000
H	2.8317373900	1.7410070700	-0.8843535400
H	4.2271439600	1.1432524000	0.0092331000
H	2.8231103400	1.7419920600	0.8885311300
C	0.0009726800	1.4815166100	0.0002849800
C	-0.0050976200	2.2050928400	1.2044710900
H	-0.0095997200	1.6933168300	2.1607888100
C	-0.0050996800	3.5878352300	1.1795713900
H	-0.0096954400	4.1901391100	2.0810558500
N	0.0006187800	4.2637246100	0.0028961700
C	-0.0038969500	5.7498625700	0.0246275200
H	0.0305756800	6.1212705100	-0.9981326700
H	0.8721496200	6.1025750900	0.5716791700
H	-0.9170294600	6.0982970000	0.5107847600
C	0.0065118400	3.5916666500	-1.1730482500
H	0.0108167000	4.1914752100	-2.0753175400
C	0.0069793400	2.2064829500	-1.2000956400
H	0.0120355500	1.6978154400	-2.1580429700
C	-3.1333907500	1.1782082500	-0.0057936600
H	-2.8223943000	1.7419303100	-0.8917786300
H	-4.2251189100	1.1449702600	-0.0090821500
H	-2.8279555400	1.7435352000	0.8811506100
C	-4.7983961700	-1.4048283600	-0.0031852400
N	-5.9627773700	-1.4137354000	-0.0040783600

C	-2.9293751800	-3.9466795000	0.0010459800
H	-2.5236069000	-4.4582865500	0.8799222500
H	-4.0167259400	-4.0351911400	0.0034952100
H	-2.5277932900	-4.4583086400	-0.8797957500

BODIPY 12 B

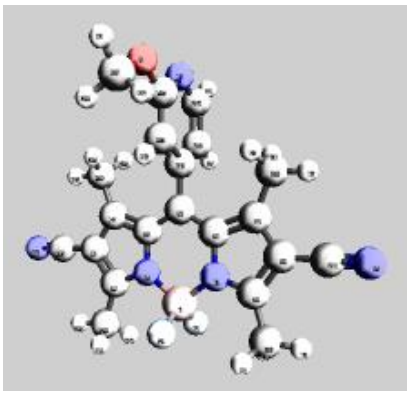

B	0.0001177900	-4.5237349100	0.0188886000
F	0.0001529800	-5.2978609700	1.1826395500
F	0.0001895100	-5.3384476200	-1.1157963500
N	1.2496106800	-3.5903796200	0.0030258800
C	2.5218899700	-4.0128057800	-0.0010848200
C	3.3721542700	-2.8712819700	-0.0086336700
C	2.5758317700	-1.7160136900	-0.0083911300
C	1.2251629900	-2.1853367700	-0.0000928700
C	-0.0000890700	-1.4954457200	0.0015386800
C	-1.2252450900	-2.1855127000	-0.0001654000
C	-2.5759837100	-1.7163651900	-0.0084551600
C	-3.3721476200	-2.8717478800	-0.0085988800
C	-2.5217227600	-4.0131533500	-0.0009877800
N	-1.2495024700	-3.5905545000	0.0030259400
C	2.9252310200	-5.4478627100	0.0019753300
H	2.5156361600	-5.9600562900	0.8783584300
H	4.0131085600	-5.5349722900	0.0104842200
H	2.5302588200	-5.9592034400	-0.8816905600
C	4.7918783400	-2.9154204500	-0.0146669900
N	5.9566521800	-2.9490274900	-0.0184218700
C	3.1161780600	-0.3190065600	-0.0200047300
H	2.7780603500	0.2394046000	-0.8978635500
H	4.2082376900	-0.3432323900	-0.0315351800
H	2.7975002100	0.2471349400	0.8602836000
C	-0.0002260800	-0.0003830200	0.0068510700
C	-0.0007374600	0.7219465700	-1.1909269000
H	-0.0009951100	0.2200905100	-2.1528402000
C	-0.0009795600	2.1168250800	-1.1093390800
H	-0.0014602800	2.7181151500	-2.0162106100
N	-0.0006593800	2.7975758100	0.0385268800
C	-0.0000784000	2.1020749500	1.1782455800
O	0.0003225900	2.8841327600	2.2807862300
C	0.0013085100	2.2720801600	3.5693303300
H	0.0017441600	3.0956632200	4.2832697100
H	0.8986854100	1.6600273600	3.7204357600
H	-0.8957203800	1.6598406900	3.7217408900
C	0.0000955100	0.6948538700	1.2196536100
H	0.0004607700	0.1500384600	2.1558375500
C	-3.1165256000	-0.3194341300	-0.0201729800
H	-2.7786108600	0.2388851100	-0.8981645600
H	-4.2085842400	-0.3438149800	-0.0315639800
H	-2.7977908200	0.2468882400	0.8599839100
C	-4.7918686600	-2.9161023500	-0.0146075400
N	-5.9566376900	-2.9499102800	-0.0183531900

C	-2.9248867700	-5.4482590000	0.0023843900
H	-2.5164611300	-5.9598191100	0.8796961600
H	-4.0127664400	-5.5354882700	0.0095004500
H	-2.5286148900	-5.9601402400	-0.8803736300

BODIPY 12cat B

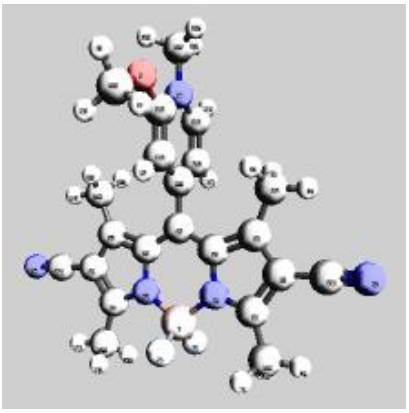

B	-0.0001537100	-3.0267826900	0.0173043200
F	0.0010424300	-3.7841549000	1.1836888600
F	-0.0014172500	-3.8283613500	-1.1175139400
N	1.2531441500	-2.0862271900	-0.0003198900
C	2.5245515000	-2.5107391800	-0.0043692500
C	3.3777544900	-1.3655902700	-0.0056772900
C	2.5848974000	-0.2143225300	-0.0034041800
C	1.2302234400	-0.6837019600	0.0016686700
C	-0.0000533800	-0.0057185300	0.0055457000
C	-1.2303870500	-0.6836007100	0.0028039600
C	-2.5850409100	-0.2141106400	-0.0014872700
C	-3.3779963200	-1.3652972200	-0.0014497300
C	-2.5248879000	-2.5104966000	0.0002032800
N	-1.2534320300	-2.0861163200	0.0021398100
C	2.9285804800	-3.9430474500	-0.0070895100
H	2.5239502600	-4.4571599500	0.8708377500
H	4.0159409000	-4.0318320100	-0.0064748700
H	2.5257487100	-4.4521031200	-0.8887390200
C	4.7979479400	-1.4018440200	-0.0046910000
N	5.9623798800	-1.4111323900	0.0001072800
C	3.1327723500	1.1819581700	-0.0126592100
H	2.8182687300	1.7413835100	-0.8999941000
H	4.2244873200	1.1493840100	-0.0169223100
H	2.8256573900	1.7515506400	0.8708104100
C	-0.0000168500	1.4893561100	0.0080485700
C	-0.0003873800	2.1917768600	1.2106937300
H	-0.0006722100	1.6609254400	2.1539961300
C	-0.0001785100	3.5925294800	1.2041227600
O	-0.0002700700	4.3859147800	2.2606865700
C	-0.0002616200	3.8249006400	3.6004148100
H	-0.0001658900	4.6894604700	4.2607247100
H	0.9023305900	3.2296854500	3.7583755300
H	-0.9029101700	3.2298049100	3.7584850600
N	0.0002247400	4.2687476400	0.0157822900
C	0.0004134500	5.7527890700	0.0275725900
H	0.0013925600	6.1014505000	-1.0034150100
H	0.8898033100	6.1124386900	0.5466990700
H	-0.8898041400	6.1126547200	0.5451297000
C	0.0004405000	3.5867274700	-1.1634716000
H	0.0006793100	4.1954406500	-2.0593548400
C	0.0003993500	2.2120326800	-1.2018817400
H	0.0006627200	1.7027481600	-2.1584498800
C	-3.1327393200	1.1821854400	-0.0120651700
H	-2.8152331900	1.7419338200	-0.8980760600

H	-4.2244311800	1.1497348400	-0.0198983100
H	-2.8284561100	1.7513811600	0.8726668100
C	-4.7982104900	-1.4014188000	0.0013042500
N	-5.9626352800	-1.4105420700	0.0076078000
C	-2.9289979400	-3.9427612200	-0.0004242600
H	-2.5191381000	-4.4571834900	0.8748489300
H	-4.0163387800	-4.0314084200	0.0064721300
H	-2.5314982300	-4.4515818500	-0.8846727400

BODIPY 12 C

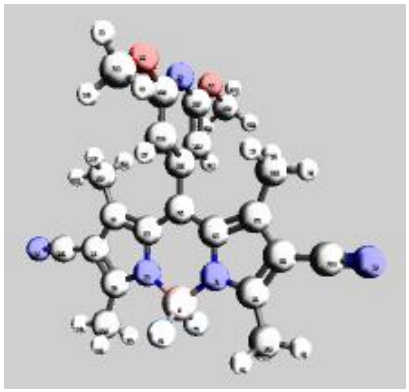

B	-0.0001132700	-3.0274807500	0.0280211000
F	-0.0004990000	-3.7989226800	1.1934799300
F	0.0003277100	-3.8453232500	-1.1049135500
N	1.2494114500	-2.0943653400	0.0096430800
C	2.5216074600	-2.5172259300	0.0074011700
C	3.3721196300	-1.3761105900	-0.0040893300
C	2.5761631600	-0.2204168600	-0.0083019700
C	1.2252418800	-0.6890829600	0.0011058700
C	0.0000378400	0.0011952700	-0.0003114300
C	-1.2252652000	-0.6890763700	0.0001916700
C	-2.5761170000	-0.2202973300	-0.0101408400
C	-3.3722158000	-1.3760002300	-0.0063799700
C	-2.5218134500	-2.5171276600	0.0057546800
N	-1.2495319800	-2.0943508100	0.0087825000
C	2.9247046300	-3.9524145200	0.0156863600
H	2.5149628200	-4.4614264900	0.8938268500
H	4.0125886300	-4.0396610700	0.0248171800
H	2.5300923200	-4.4669324500	-0.8662773700
C	4.7917941500	-1.4204700200	-0.0094083600
N	5.9565811800	-1.4543057800	-0.0129929000
C	3.1169475000	1.1761307500	-0.0237802200
H	2.7779888200	1.7314432200	-0.9031717500
H	4.2090177400	1.1518869200	-0.0352691800
H	2.7962205100	1.7447672800	0.8541264400
C	0.0000914600	1.4973536500	-0.0007462400
C	0.0000480400	2.1934923500	1.2104515300
H	0.0000016900	1.6579617600	2.1508014600
C	0.0001023000	3.6004435000	1.1439499000
O	0.0002241900	4.3991125900	2.2341616500
C	0.0004246500	3.8044287900	3.5310228700
H	0.0007622100	4.6376973800	4.2336782900
H	0.8974027400	3.1941800900	3.6902049300
H	-0.8967081100	3.1945204700	3.6906434700
N	0.0000940500	4.2777679300	0.0001211100
C	0.0000406900	3.6010369500	-1.1440244000
O	0.0000006100	4.4001763300	-2.2339807300
C	-0.0001478800	3.8055788700	-3.5308431900
H	-0.0002852800	4.6387332600	-4.2335929200
H	0.8968974700	3.1954769500	-3.6903768800
H	-0.8971782300	3.1953921700	-3.6901267800
C	0.0000593100	2.1942431100	-1.2113289300
H	0.0000198000	1.6590295400	-2.1518345500
C	-3.1168120600	1.1763115300	-0.0260875400
H	-2.7774253100	1.7315472000	-0.9053640100

H	-4.2088798600	1.1520411900	-0.0381719300
H	-2.7965860400	1.7451307800	0.8518915900
C	-4.7919308700	-1.4202877900	-0.0126517300
N	-5.9567255700	-1.4540503700	-0.0170291100
C	-2.9249350400	-3.9523441600	0.0140663700
H	-2.5170388200	-4.4608674700	0.8933807100
H	-4.0128377700	-4.0395306700	0.0210667500
H	-2.5285020200	-4.4675283000	-0.8666976500

BODIPY 12cat C

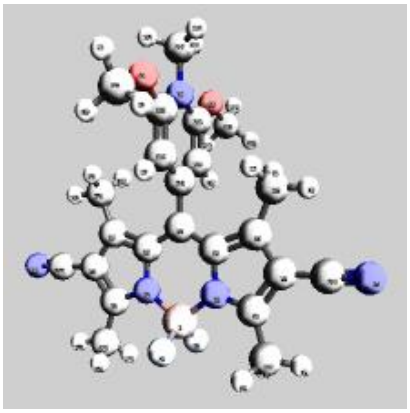

B	-0.0004329100	-3.0189278700	0.0024992000
F	0.0003798200	-3.7981386700	1.1541929100
F	-0.0015149400	-3.8007390200	-1.1474031700
N	1.2534020200	-2.0790709600	0.0006041500
C	2.5248888900	-2.5037602800	0.0005356800
C	3.3779567800	-1.3591299500	0.0008840700
C	2.5851712700	-0.2071050200	0.0010793200
C	1.2302911500	-0.6763525300	0.0006146500
C	-0.0000871400	0.0015017200	-0.0001062700
C	-1.2306036100	-0.6760067600	0.0002296000
C	-2.5853818100	-0.2064255500	-0.0009245000
C	-3.3784141600	-1.3582065800	0.0008941300
C	-2.5256352100	-2.5030812000	0.0029040300
N	-1.2540595100	-2.0787281700	0.0023415300
C	2.9287121200	-3.9363517300	0.0002072800
H	2.5261310100	-4.4477993700	0.8805707600
H	4.0160848100	-4.0250792300	-0.0010199100
H	2.5240529700	-4.4479418500	-0.8790932900
C	4.7982533800	-1.3950146100	0.0011844200
N	5.9627562300	-1.4041705400	0.0014862500
C	3.1353973000	1.1883081500	0.0019578600
H	2.8277398900	1.7523521200	-0.8845505700
H	4.2272284500	1.1542232100	0.0065945900
H	2.8202626600	1.7540425800	0.8846758200
C	0.0000126800	1.4969194300	0.0001505700
C	-0.0008293900	2.1952045900	1.2101869600
H	-0.0015413000	1.6647700400	2.1525992700
C	-0.0004038100	3.5866264300	1.1878005900
O	-0.0004221200	4.3877411800	2.2403606600
C	-0.0004294500	3.8236229500	3.5763972100
H	-0.0001784600	4.6850902100	4.2408284700
H	0.9012595100	3.2262689500	3.7321266800
H	-0.9023446800	3.2266587000	3.7322539300
N	0.0001237900	4.2729025000	-0.0026535900
C	0.0002764300	5.7603630500	0.0372026800
H	0.0023816900	6.1340214200	-0.9805637000
H	0.8892147100	6.0992423200	0.5701506400
H	-0.8906805500	6.0996285400	0.5665680900
C	0.0004051700	3.5894461300	-1.1954273900
O	0.0001054300	4.3729614400	-2.2613897000
C	-0.0002593100	3.7898650700	-3.5890753300
H	-0.0009508300	4.6422694900	-4.2651399300
H	0.9018971200	3.1913774300	-3.7373654800
H	-0.9020572200	3.1906260000	-3.7365437400

C	0.0008445600	2.1964893400	-1.2089969500
H	0.0014207000	1.6637986100	-2.1500300700
C	-3.1352921900	1.1891003500	-0.0040109600
H	-2.8214997000	1.7528247000	-0.8884989500
H	-4.2271325700	1.1552787500	-0.0067702100
H	-2.8259942300	1.7550193300	0.8807231800
C	-4.7986943000	-1.3936714200	0.0005826800
N	-5.9631782000	-1.4024232100	0.0003245900
C	-2.9298382100	-3.9355427500	0.0049032800
H	-2.5237794700	-4.4467687900	0.8837451200
H	-4.0172336900	-4.0239647500	0.0080209700
H	-2.5289784100	-4.4475663400	-0.8759171600

BODIPY 13 A

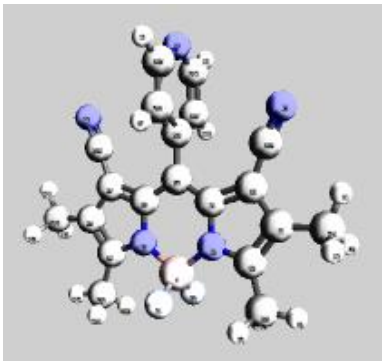

B	-0.0001175500	-3.0090849700	-0.0012861300
F	0.0010476000	-3.8025839600	1.1483286500
F	-0.0013896800	-3.8024855100	-1.1509715700
N	1.2529751700	-2.0756486900	-0.0024371500
C	2.5406719300	-2.4891280500	-0.0029511500
C	3.4039912000	-1.3631849000	-0.0015551200
C	2.5751148400	-0.2335839600	-0.0003017400
C	1.2158273300	-0.6873993500	-0.0012354300
C	-0.0000404000	0.0138391000	-0.0007948700
C	-1.2159357300	-0.6874530200	-0.0004133200
C	-2.5752132300	-0.2334534600	-0.0012547300
C	-3.4042531300	-1.3630789800	-0.0010393500
C	-2.5409402000	-2.4891010800	-0.0005442000
N	-1.2532120700	-2.0756156100	-0.0000817900
C	2.9288990600	-3.9306329200	-0.0046279600
H	4.0153993200	-4.0325202100	-0.0072377400
H	2.5271978900	-4.4422361300	0.8760113700
H	2.5230791400	-4.4412520500	-0.8839084900
C	4.9019019800	-1.3897457600	-0.0020913500
H	5.3081153500	-0.3757399700	0.0139646000
H	5.2933761100	-1.8932117800	-0.8937296900
H	5.2936430000	-1.9217325000	0.8725388400
C	3.0576945500	1.1022510100	0.0027047700
N	3.5374536000	2.1639335100	0.0055316300
C	-0.0001539000	1.5066721700	-0.0017920700
C	-0.0114455800	2.2257440300	1.1980724100
H	-0.0203747500	1.7161534800	2.1566418800
C	-0.0111275700	3.6208060400	1.1390472900
H	-0.0200745000	4.2048156900	2.0564851200
N	-0.0006388700	4.3159672400	-0.0044552200
C	0.0101231800	3.6186748200	-1.1466624500
H	0.0187953000	4.2009456900	-2.0652129400
C	0.0109281500	2.2235206200	-1.2030343800
H	0.0200530600	1.7121133300	-2.1606411800
C	-3.0576509000	1.1024388000	-0.0028978300
N	-3.5375016700	2.1641306900	-0.0044730700
C	-4.9021182600	-1.3894728800	-0.0024331300
H	-5.3082159100	-0.3753573100	0.0135954900
H	-5.2930356500	-1.8927877900	-0.8944211600
H	-5.2942280100	-1.9216735100	0.8719192200
C	-2.9292235000	-3.9305196200	-0.0013070900
H	-2.5213879600	-4.4432802600	0.8757607000
H	-4.0157974400	-4.0322838900	0.0032272400
H	-2.5294875900	-4.4398127600	-0.8841903500

BODIPY 13cat A

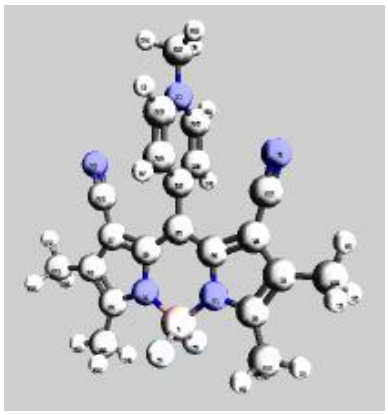

B	-0.0001570700	-3.0242141400	-0.0027242100
F	0.0006127200	-3.8001025800	1.1484106000
F	-0.0009364200	-3.7988146800	-1.1546843400
N	1.2607161000	-2.0816374500	-0.0027747200
C	2.5491459700	-2.4901558500	-0.0030106000
C	3.4137389400	-1.3544372500	-0.0008537700
C	2.5800967400	-0.2337027400	0.0004107700
C	1.2200595200	-0.6966503500	-0.0010931100
C	0.0002584600	-0.0091436400	-0.0008165600
C	-1.2198512700	-0.6964969400	-0.0011170300
C	-2.5798477400	-0.2331684600	-0.0009399400
C	-3.4138632000	-1.3541144300	-0.0008966800
C	-2.5492518100	-2.4899772900	-0.0014263800
N	-1.2607256200	-2.0813444600	-0.0014595900
C	2.9419982600	-3.9276660700	-0.0052249900
H	4.0277823000	-4.0302284000	-0.0071707400
H	2.5386644300	-4.4398841200	0.8746549000
H	2.5356906300	-4.4379368300	-0.8848283000
C	4.9100673800	-1.3787225300	-0.0005223600
H	5.3193710300	-0.3660332000	0.0117839600
H	5.2998237600	-1.8877910500	-0.8892489400
H	5.2992582900	-1.9092439800	0.8756816900
C	2.9981383900	1.1224375800	0.0041118200
N	3.3155331200	2.2438409500	0.0077748100
C	0.0000425100	1.4847763800	0.0004722500
C	-0.0049690600	2.2011502400	1.2056584100
H	-0.0084786900	1.6902126800	2.1616114900
C	-0.0055303200	3.5821793800	1.1797028700
H	-0.0096146900	4.1850787500	2.0800093900
N	-0.0012176900	4.2548519700	0.0038729200
C	-0.0067573100	5.7385068100	0.0272319700
H	0.0285129600	6.1107096700	-0.9950317400
H	0.8700188000	6.0889553500	0.5744120900
H	-0.9219455100	6.0833118900	0.5119594700
C	0.0037588300	3.5869124800	-1.1716135000
H	0.0071823800	4.1878508400	-2.0723392300
C	0.0045176700	2.2032802700	-1.2004659400
H	0.0087065000	1.6960077300	-2.1583407600
C	-2.9980616400	1.1230445500	-0.0005367700
N	-3.3149498500	2.2446899800	0.0001304400
C	-4.9103215400	-1.3781169800	-0.0009800400
H	-5.3193877500	-0.3652910500	0.0110917300
H	-5.2997608800	-1.8873112700	-0.8898581300
H	-5.2996313000	-1.9085094900	0.8753390000

C	-2.9423745000	-3.9275730900	-0.0023832100
H	-2.5329591700	-4.4407355000	0.8741164700
H	-4.0282567400	-4.0297871500	0.0028913100
H	-2.5423023100	-4.4366629000	-0.8856454100

BODIPY 13 B

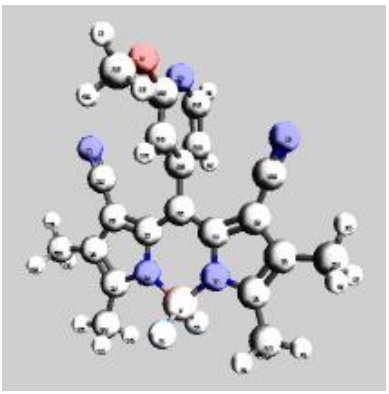

B	-0.0003025900	-4.5189086700	-0.0147696400
F	-0.0000810200	-5.3230618800	1.1282458700
F	-0.0006802500	-5.3026261800	-1.1710762400
N	1.2525355100	-3.5859251100	-0.0054221200
C	2.5398949200	-4.0003691800	-0.0094795800
C	3.4037331900	-2.8752521700	0.0058485900
C	2.5753816200	-1.7448331400	0.0185550100
C	1.2158453000	-2.1976067300	0.0103978100
C	0.0000009100	-1.4958758300	0.0145272100
C	-1.2159811800	-2.1973546300	0.0101738600
C	-2.5754182000	-1.7442956900	0.0178115800
C	-3.4039998500	-2.8745286600	0.0054787900
C	-2.5404088000	-3.9998340100	-0.0091773300
N	-1.2529613900	-3.5856766800	-0.0050740100
C	2.9257357700	-5.4424528500	-0.0283631100
H	4.0120259200	-5.5467748200	-0.0235240800
H	2.5152382200	-5.9659109200	0.8412026400
H	2.5260315200	-5.9395994900	-0.9182529400
C	4.9017689000	-2.9024056600	0.0081941600
H	5.3082573200	-1.8884094500	0.0185955600
H	5.2945102200	-3.4117006400	-0.8794718200
H	5.2918799300	-3.4291118100	0.8868566100
C	3.0599550300	-0.4099762900	0.0447810900
N	3.5444450200	0.6491968400	0.0721121200
C	0.0001366300	-0.0023540000	0.0095047400
C	0.0000068200	0.7014924400	-1.1984979600
H	-0.0002286000	0.1882099200	-2.1539142900
C	0.0001329700	2.0964433800	-1.1333405800
H	0.0000392400	2.6856336900	-2.0477629000
N	0.0003006100	2.7895344600	0.0052616200
C	0.0003423800	2.1100285700	1.1527055100
O	0.0003548700	2.9068858300	2.2460939800
C	-0.0004844600	2.3077276700	3.5380056100
H	-0.0010813700	3.1374290600	4.2453630400
H	0.8973163800	1.6974063000	3.6958222000
H	-0.8983950500	1.6972370000	3.6945211800
C	0.0003350900	0.7047941300	1.2144948100
H	0.0005270000	0.1730043700	2.1576208400
C	-3.0597144100	-0.4093271900	0.0429967000
N	-3.5440100000	0.6499590600	0.0692721600
C	-4.9020384900	-2.9013553200	0.0074017400
H	-5.3083044400	-1.8872872600	0.0191410700
H	-5.2946792300	-3.4092841500	-0.8810925100
H	-5.2924923300	-3.4292312500	0.8852008700

C	-2.9265730600	-5.4418268300	-0.0280765100
H	-2.5096169900	-5.9672158800	0.8371646600
H	-4.0128111500	-5.5460220500	-0.0155389700
H	-2.5336725000	-5.9370947400	-0.9220993800

BODIPY 13cat B

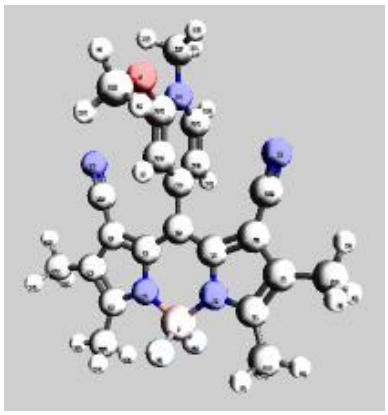

B	-0.0000993700	-3.0094949300	0.0094962700
F	0.0005046300	-3.7716836300	1.1713247200
F	-0.0006561500	-3.8001636400	-1.1315445100
N	1.2600166800	-2.0678809200	-0.0006594000
C	2.5481798000	-2.4768187800	-0.0015008200
C	3.4126515600	-1.3420356000	0.0000152200
C	2.5795141000	-0.2201707100	0.0027555000
C	1.2194905800	-0.6827473300	0.0023565000
C	-0.0000839300	0.0051442100	0.0047291800
C	-1.2197509800	-0.6828282900	0.0020362700
C	-2.5797595200	-0.2201767700	0.0014914800
C	-3.4130313600	-1.3422852100	-0.0000485500
C	-2.5484364400	-2.4770151500	-0.0001748400
N	-1.2602379100	-2.0678462200	0.0002893800
C	2.9405024500	-3.9145143200	-0.0008605500
H	4.0262764400	-4.0168962700	-0.0013789500
H	2.5361135500	-4.4250826400	0.8795443600
H	2.5349226200	-4.4263523400	-0.8798359700
C	4.9088764800	-1.3675293200	-0.0003051800
H	5.3192415400	-0.3552145900	0.0109061900
H	5.2977313200	-1.8775362600	-0.8887866100
H	5.2975222400	-1.8980007800	0.8761354400
C	3.0041738400	1.1342261500	0.0108507700
N	3.3371673300	2.2510263200	0.0234048800
C	-0.0001813900	1.4993719300	0.0027420100
C	-0.0012506700	2.1989365400	1.2041931200
H	-0.0020981500	1.6713195800	2.1488268900
C	-0.0010027100	3.5976099400	1.1901749800
O	-0.0017079200	4.3949761400	2.2447111100
C	-0.0026005200	3.8316575600	3.5790791700
H	-0.0029127000	4.6929572700	4.2439856100
H	0.9004385700	3.2360725100	3.7350278900
H	-0.9059713300	3.2362765600	3.7339328000
N	0.0001497900	4.2666898800	0.0010573400
C	0.0003309600	5.7486827800	0.0112296700
H	0.0017683900	6.0952912300	-1.0201977100
H	0.8909034200	6.1057701600	0.5299087700
H	-0.8915464200	6.1059526300	0.5275250500
C	0.0011058800	3.5845290400	-1.1749390100
H	0.0020632500	4.1914613000	-2.0713805300
C	0.0009931700	2.2109944300	-1.2102241800
H	0.0018248200	1.6982255200	-2.1643883300
C	-3.0046469100	1.1341981300	0.0069819600
N	-3.3375877000	2.2511505100	0.0170029200

C	-4.9092240200	-1.3677327200	-0.0006540200
H	-5.3194521100	-0.3553319400	0.0102002700
H	-5.2977438200	-1.8780583400	-0.8891446400
H	-5.2978601800	-1.8980071500	0.8759545600
C	-2.9406538000	-3.9147470400	0.0015765100
H	-2.5298171100	-4.4262824300	0.8783988700
H	-4.0264701700	-4.0169454600	0.0084908600
H	-2.5413231200	-4.4252084500	-0.8811713600

BODIPY 13 C

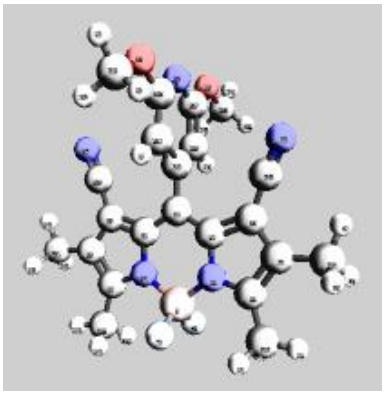

B	-0.0000337600	-3.0197954600	-0.0442154400
F	0.0000531200	-3.8342485600	1.0913054000
F	-0.0001619300	-3.7935694000	-1.2077440300
N	1.2526096900	-2.0868392400	-0.0272802500
C	2.5400938300	-2.5011013100	-0.0317598600
C	3.4036372500	-1.3760515400	-0.0125375500
C	2.5752367000	-0.2456393900	0.0029840000
C	1.2158888000	-0.6984758600	-0.0072122900
C	-0.0000002600	0.0030334700	-0.0009015100
C	-1.2159048900	-0.6984688500	-0.0077283800
C	-2.5752021800	-0.2455716200	0.0016430500
C	-3.4037130300	-1.3759860200	-0.0138211900
C	-2.5401310900	-2.5010747600	-0.0322323100
N	-1.2526691900	-2.0867756400	-0.0273301500
C	2.9256083400	-3.9431008500	-0.0547046700
H	4.0118533200	-4.0477775900	-0.0504147000
H	2.5151246500	-4.4686098400	0.8135932400
H	2.5253469200	-4.4377896800	-0.9457103300
C	4.9016766800	-1.4034952500	-0.0092191000
H	5.3085431800	-0.3896945300	0.0045721100
H	5.2949271800	-1.9104329100	-0.8979945300
H	5.2910747700	-1.9328207200	0.8681667800
C	3.0604126300	1.0890070700	0.0307954400
N	3.5489789200	2.1463048200	0.0562357300
C	-0.0000351300	1.4972534000	0.0034427900
C	-0.0000057800	2.1903866600	1.2150042000
H	-0.0000647600	1.6556690300	2.1553512400
C	0.0001086200	3.5963675700	1.1452079400
O	0.0002141100	4.3966557600	2.2356681500
C	0.0004700700	3.8011530100	3.5297608100
H	0.0006979300	4.6336075100	4.2339740500
H	0.8982407700	3.1913273100	3.6886248300
H	-0.8973315800	3.1914726300	3.6890605500
N	0.0001007600	4.2707443000	0.0015554100
C	0.0000645100	3.5952340300	-1.1413566900
O	0.0000092500	4.3943614600	-2.2330610400
C	-0.0001656300	3.7978718000	-3.5266942700
H	-0.0002706200	4.6297863000	-4.2315553500
H	0.8975151600	3.1879015400	-3.6858244100
H	-0.8978940700	3.1878975800	-3.6855709100
C	0.0000725800	2.1894581700	-1.2093176700
H	0.0000878000	1.6533414000	-2.1489343200
C	-3.0605403000	1.0889888000	0.0284514600
N	-3.5488340200	2.1464949900	0.0528582800

C	-4.9017367100	-1.4033457300	-0.0113348100
H	-5.3085420700	-0.3895229500	0.0036337800
H	-5.2944024300	-1.9090543200	-0.9010849000
H	-5.2914821500	-1.9339009800	0.8651612600
C	-2.9257389500	-3.9430251200	-0.0554377800
H	-2.5088881600	-4.4703222700	0.8086592100
H	-4.0119505100	-4.0477322200	-0.0437653400
H	-2.5318740400	-4.4355342300	-0.9505593600

BODIPY 13cat C

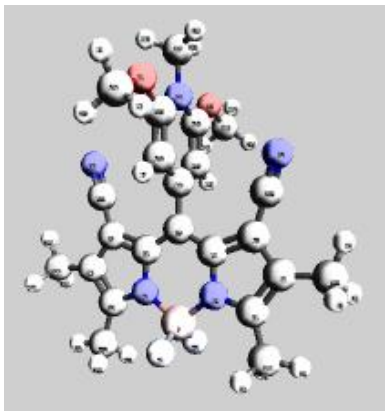

B	0.0000549400	-3.0109618600	-0.0010998800
F	0.0006632300	-3.7886721400	1.1501752700
F	-0.0004864000	-3.7880947700	-1.1527000500
N	1.2598662600	-2.0695221000	-0.0012004900
C	2.5481947900	-2.4787659600	-0.0009925200
C	3.4122850800	-1.3443534100	0.0008359600
C	2.5789101900	-0.2220216000	0.0015945700
C	1.2190257900	-0.6840082500	0.0001545300
C	-0.0001788900	0.0050917500	0.0002327900
C	-1.2192705300	-0.6841810600	-0.0001745400
C	-2.5792117100	-0.2223990700	0.0003835400
C	-3.4124224500	-1.3448367500	0.0007738300
C	-2.5481594400	-2.4791243700	0.0002855700
N	-1.2599166200	-2.0696855300	-0.0002848100
C	2.9409206500	-3.9167526300	-0.0022177900
H	4.0268717300	-4.0187447300	-0.0038304200
H	2.5378086200	-4.4286510600	0.8779055200
H	2.5352266900	-4.4279117700	-0.8815478600
C	4.9088972300	-1.3688050300	0.0015011700
H	5.3178214800	-0.3558878600	0.0119801400
H	5.2991900300	-1.8794145000	-0.8861320500
H	5.2982163200	-1.8974824800	0.8788217200
C	3.0077947200	1.1310067500	0.0046025200
N	3.3530001700	2.2441693500	0.0077191500
C	-0.0002763700	1.5004557200	0.0018779400
C	-0.0008502100	2.1923479900	1.2129658600
H	-0.0012976000	1.6631214000	2.1552494500
C	-0.0007368300	3.5827135400	1.1891864500
O	-0.0010561100	4.3844596000	2.2422819100
C	-0.0009198400	3.8203770100	3.5745979500
H	-0.0007477700	4.6809655900	4.2405305200
H	0.9015891000	3.2238608400	3.7304573400
H	-0.9034846500	3.2240158600	3.7307313200
N	-0.0002868500	4.2669615200	0.0008794400
C	-0.0002419400	5.7526219600	0.0429540000
H	0.0016724100	6.1282313400	-0.9739711700
H	0.8900521700	6.0885999800	0.5754863200
H	-0.8924307000	6.0888368600	0.5722025700
C	-0.0000111200	3.5873119500	-1.1906125400
O	-0.0000171600	4.3726296100	-2.2563150000
C	-0.0005077300	3.7905844300	-3.5806990100
H	-0.0011787800	4.6425871200	-4.2576326000
H	0.9023105600	3.1928058500	-3.7297488500
H	-0.9030661400	3.1921734400	-3.7287726500

C	0.0002260600	2.1953530800	-1.2073265700
H	0.0006548600	1.6649938700	-2.1488551800
C	-3.0083276300	1.1305445900	0.0008470700
N	-3.3536028100	2.2436743600	0.0014242100
C	-4.9090105000	-1.3694699500	0.0011516300
H	-5.3180752300	-0.3566094200	0.0113016000
H	-5.2990442500	-1.8803751200	-0.8864164700
H	-5.2983737900	-1.8979803800	0.8785465700
C	-2.9406934900	-3.9171568300	0.0001231400
H	-2.5311940200	-4.4301826600	0.8765645200
H	-4.0266131900	-4.0192763900	0.0059176200
H	-2.5412512000	-4.4270090000	-0.8828873000

BODIPY 1cat A S_1

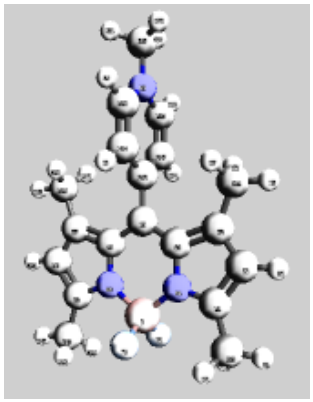

B	0.0000080300	-2.7654107400	-0.0012167100
F	0.0040838200	-3.5433553100	1.1440795200
F	-0.0040441000	-3.5467067400	-1.1441731900
N	1.2365766700	-1.8216777000	-0.0064081300
C	2.5095854500	-2.2247762700	-0.0079406500
C	3.3679937700	-1.0792028200	-0.0027840600
C	2.5943919100	0.0431981800	0.0035777700
C	1.2052524100	-0.4289344700	0.0004556600
C	-0.0001306300	0.2816139300	0.0014897500
C	-1.2054682300	-0.4290129500	-0.0008842100
C	-2.5946458900	0.0430079400	-0.0056701500
C	-3.3681395600	-1.0794784200	-0.0041047600
C	-2.5096210200	-2.2249955100	0.0003076100
N	-1.2366606000	-1.8217664700	0.0010761200
C	2.9074895400	-3.6481153600	-0.0111958600
H	3.9919061000	-3.7478288600	-0.0236357300
H	2.5018213600	-4.1525267300	0.8719855900
H	2.4799695500	-4.1564545700	-0.8814340400
H	4.4478533000	-1.1240813400	-0.0025728900
C	3.0988282400	1.4448558200	0.0132711100
H	4.1897983600	1.4411780000	0.0224613400
H	2.7605757900	1.9977562700	-0.8652929200
H	2.7454545300	1.9910294500	0.8899742600
C	-0.0001750600	1.7633025200	0.0012451200
C	-0.0197097200	2.5125251100	1.2104973400
H	-0.0355062500	2.0150606100	2.1738092900
C	-0.0188506600	3.8717714100	1.1932221200
H	-0.0333376700	4.4687663500	2.0953693000
N	0.0011704900	4.5790363200	-0.0021574900
C	0.0000306100	6.0317150400	0.0262682300
C	0.0195217700	3.8725609800	-1.1923949000
H	0.0340622000	4.4662656400	-2.0964881900
C	0.0194733200	2.5134893700	-1.2117167900
H	0.0346102700	2.0172546200	-2.1752664400
C	-3.0992406300	1.4446405500	-0.0130380500
H	-2.7414170300	1.9938639500	-0.8860484300
H	-4.1901534900	1.4408030600	-0.0277085900
H	-2.7657312600	1.9945889200	0.8691532700
H	-4.4479921800	-1.1244812500	-0.0066229200
C	-2.9073944800	-3.6483683100	0.0024505200
H	-2.4785326400	-4.1575599900	0.8715148100
H	-3.9917785900	-3.7482154100	0.0164073100
H	-2.5029555300	-4.1518318600	-0.8818533100
H	0.0214710600	6.4135462800	-0.9938483700

H	0.8797219000	6.4088259000	0.5562608900
H	-0.9011296400	6.4087234500	0.5190537300

BODIPY 12cat A S_1

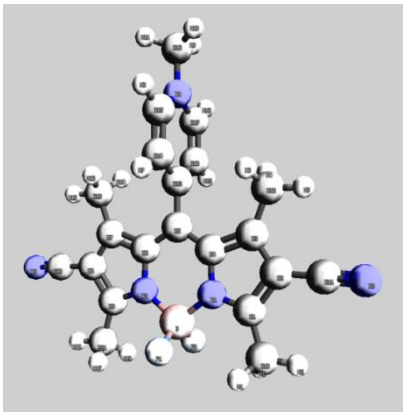

B	-0.0000335400	-3.0585871400	0.0008240100
F	-0.0015591500	-3.8174720300	1.1519888800
F	0.0012636000	-3.8358816400	-1.1378594400
N	1.2396146300	-2.1088111800	-0.0048953600
C	2.5031603500	-2.5200695000	-0.0072106900
C	3.3622018600	-1.3604646000	-0.0080127500
C	2.5842266000	-0.2308715400	-0.0054844100
C	1.2059639900	-0.7119614000	-0.0033093200
C	0.0003736300	0.0003515000	-0.0018506000
C	-1.2054013900	-0.7115909200	-0.0035534400
C	-2.5835801900	-0.2301786600	-0.0037716600
C	-3.3618572000	-1.3595901500	-0.0083822200
C	-2.5030532700	-2.5194184200	-0.0101546000
N	-1.2394208300	-2.1084640400	-0.0079267700
C	2.9139167300	-3.9368552100	-0.0074007500
H	2.5006175600	-4.4442413500	0.8707889700
H	3.9992235100	-4.0290436700	-0.0086293700
H	2.4983433900	-4.4449449000	-0.8840359900
C	4.7828403800	-1.4226852600	-0.0110748000
N	5.9379146500	-1.4818796300	-0.0136096100
C	3.0907290500	1.1668454800	-0.0053200500
H	2.7329623600	1.7157334600	-0.8785704000
H	4.1814056200	1.1663336300	-0.0135341600
H	2.7469002600	1.7102371600	0.8770536700
C	0.0008549200	1.4798692400	-0.0034093400
C	0.0042223500	2.2307566300	1.2064110400
H	0.0060024000	1.7372961400	2.1717573100
C	0.0048497400	3.5901714600	1.1840506900
H	0.0062876500	4.1889836400	2.0852795600
N	0.0038268600	4.2944325000	-0.0118898900
C	0.0024038800	5.7489299200	0.0135391000
H	0.0276726100	6.1289659700	-1.0068278300
H	0.8805276600	6.1250599100	0.5457856200
H	-0.8997471800	6.1266202900	0.5034185500
C	-0.0030226300	3.5869546800	-1.2000673700
H	-0.0072835800	4.1790674900	-2.1054779300
C	-0.0040152500	2.2274429900	-1.2196771300
H	-0.0085838000	1.7316357700	-2.1833952200
C	-3.0897246700	1.1676650400	-0.0000920500
H	-2.7397792400	1.7155244800	-0.8772681200
H	-4.1804411200	1.1674445400	0.0012335800
H	-2.7377045900	1.7119497000	0.8783921600
C	-4.7825379300	-1.4213337200	-0.0105175400
N	-5.9376217900	-1.4802030200	-0.0122978500
C	-2.9141596000	-3.9361223900	-0.0129003100

H	-2.4980359700	-4.4462784600	0.8623200100
H	-3.9995021000	-4.0280527500	-0.0110086600
H	-2.5016606800	-4.4416704200	-0.8925045600

Table A1. Neutral BODIPY S_1 & S_2 vertical excitation energies (eV), oscillator strengths (*f*, arbitrary units), and predominant transition character.

BODIPY	S_1			S_2		
	VEE	*f*	Trans.	VEE	*f*	Trans.
1 A	2.9516	0.54521	H → L	3.8194	0.04981	H-1 → L
2 A	2.8528	0.46647	H → L	3.7053	0.11664	H-1 → L
3 A	2.8410	0.56555	H → L	3.6804	0.10418	H-1 → L
4 A	2.8391	0.60547	H → L	3.6723	0.10265	H-1 → L
5 A	2.8184	0.67417	H → L	3.6347	0.10608	H-2 → L
6 A	2.9702	0.65842	H → L	3.8638	0.03097	H-1 → L
7 A	2.9112	0.67590	H → L	3.7393	0.06654	H-1 → L
8 A	2.9556	0.78414	H → L	3.7924	0.00000	H-1 → L/L+2, H-3 → L+4 *
9 A	2.9747	0.80393	H → L	3.9064	0.01036	H-1 → L
10 A	2.9554	0.68269	H → L	3.7612	0.03511	H-1 → L
11 A	3.0202	0.66837	H → L	3.9379	0.02004	H-1 → L
12 A	2.9337	0.71577	H → L	3.7914	0.04127	H-1 → L

* 24%/44% carbonyl transition to pyridinium and 27% BODIPY H-1 to virtual carbonyl orbital.

Table A2. Calculated TDDFT/B3LYP vertical excitation energies (eV), oscillator strengths (*f*, x10-4 arbitrary units), and predominant transition character for specified BODIPYs.

	S_1			S_2			S_3		
	VEE	*f*	Trans.	VEE	*f*	Trans.	VEE	*F*	Trans.
1cat A	1.0987	1.0	H → L	2.1117	1.1	H → L+1	2.2840	0.0	H-1 → L
2cat A	1.1536	1.0	H → L	2.1661	201.4	H → L+1	2.2547	0.0	H-1 → L
3cat A	1.1409	1.1	H → L	2.1489	173.7	H → L+2	2.1611	0.3	H-1 → L
11cat A	1.4391	0.5	H → L	2.4435	133.8	H → L+2	2.6446	0.1	H-1 → L
12cat A	1.4672	0.5	H → L	2.4681	143.9	H → L+2	2.4733	0.1	H-1 → L

Table A2. Continued

	S_4			S_5		
	VEE	*f*	Trans.	VEE	*f*	Trans.
1cat A	2.4704	0.1	H-2 → L	2.9076	4837.8	H → **L+2**
2cat A	2.3991	0.5	H-2 → L	2.7386	3313.0	H → **L+2**
3cat A	2.2459	0.8	H-2 → L	2.6388	3810.0	H → **L+1**
11cat A	2.8138	0.1	H-2 → L	2.9465	6299.7	H → **L+1**
12cat A	2.5965	0.1	H-2 → L	2.7484	5555.1	H → **L+1**

Orbitals in **red** indicate the $LUMO_{BDP}$.

Table A3. Pyridinium Orbital Energies (eV).

Compound	ε_{HOMO}	ε_{LUMO}
N-MePy$^+$	-14.217	-5.567
2-OMe-N-MePy$^+$	-13.013	-5.058
2,6-DiOMe-N-MePy$^+$	-12.269	-4.570

Table A4. Calculated Cationic Py'-BODIPY S_1 & S_2 excitation energies (eV), oscillator strengths (*f*, arbitrary units), and predominant transition character.

BODIPY	S_1			S_2		
	VEE	*f*	Trans.	VEE	*f*	Trans.
1cat A	1.9148	0.00024	H → L	2.8746	0.55350	H → L+1
1cat B	2.2445	0.00093	H → L	2.8766	0.54686	H → L+1
1cat C	2.5725	0.00019	H → L	2.8823	0.54100	H → L+1
12cat A	2.3255	0.00008	H → L	2.8084	0.72367	H → L+1
12cat B	2.6684	0.00105	H → L	2.8169	0.71620	H → L+1
12cat C	2.8280	0.71071	H → L	3.0143	0.00026	H → L+1
13cat A	2.5747	0.62108	H → L	2.9304	0.00008	H → L+1
13cat B	2.5793	0.61379	H → L	3.2421	0.00099	H → L+1
13cat C	2.5832	0.60579	H → L	3.5514	0.00099	H → L+1

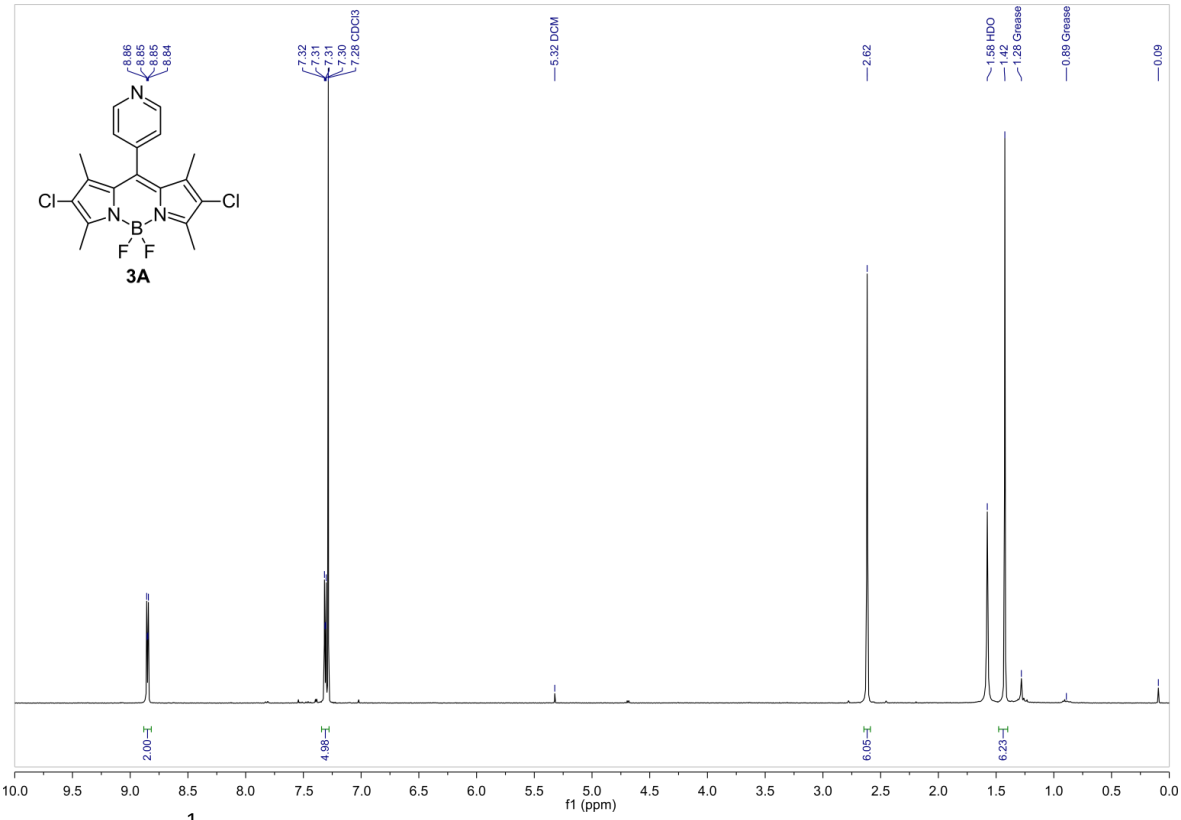

Figure A.1. ^{1}H NMR spectra of **3A** in $CDCl_3$.

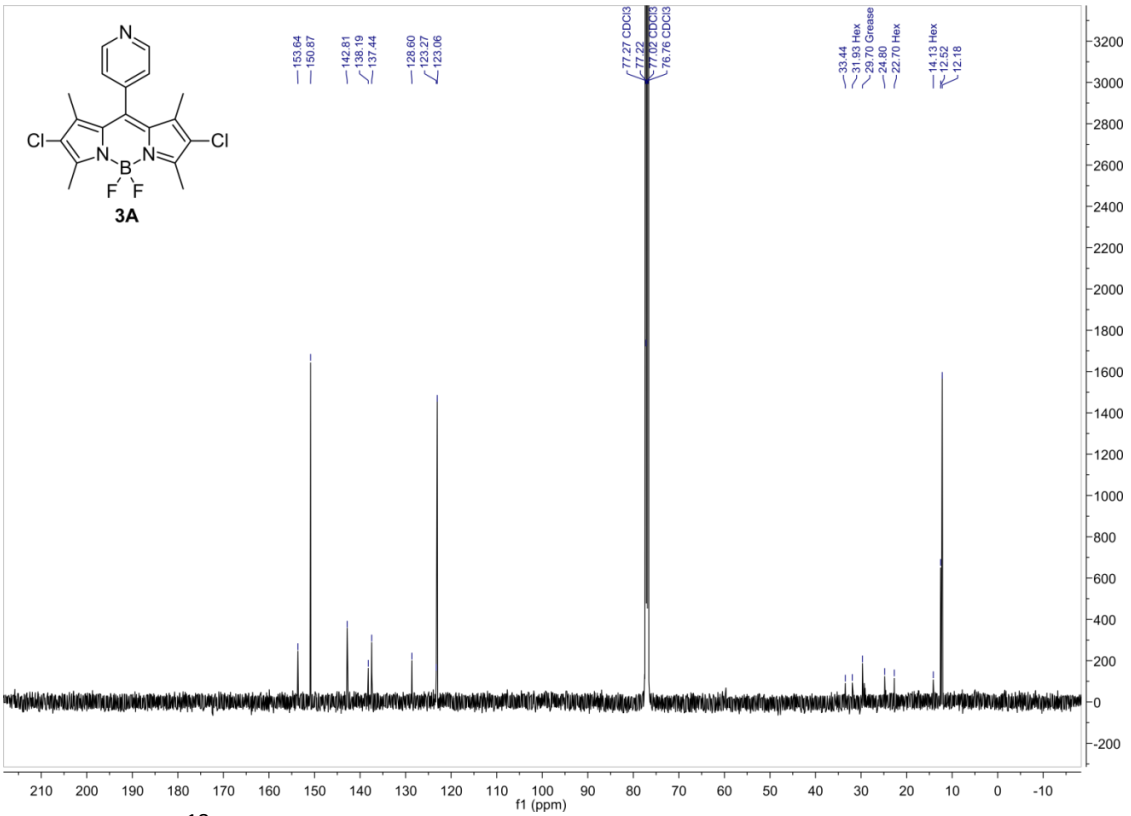

Figure A.2. ^{13}C NMR spectra of **3A** in $CDCl_3$.

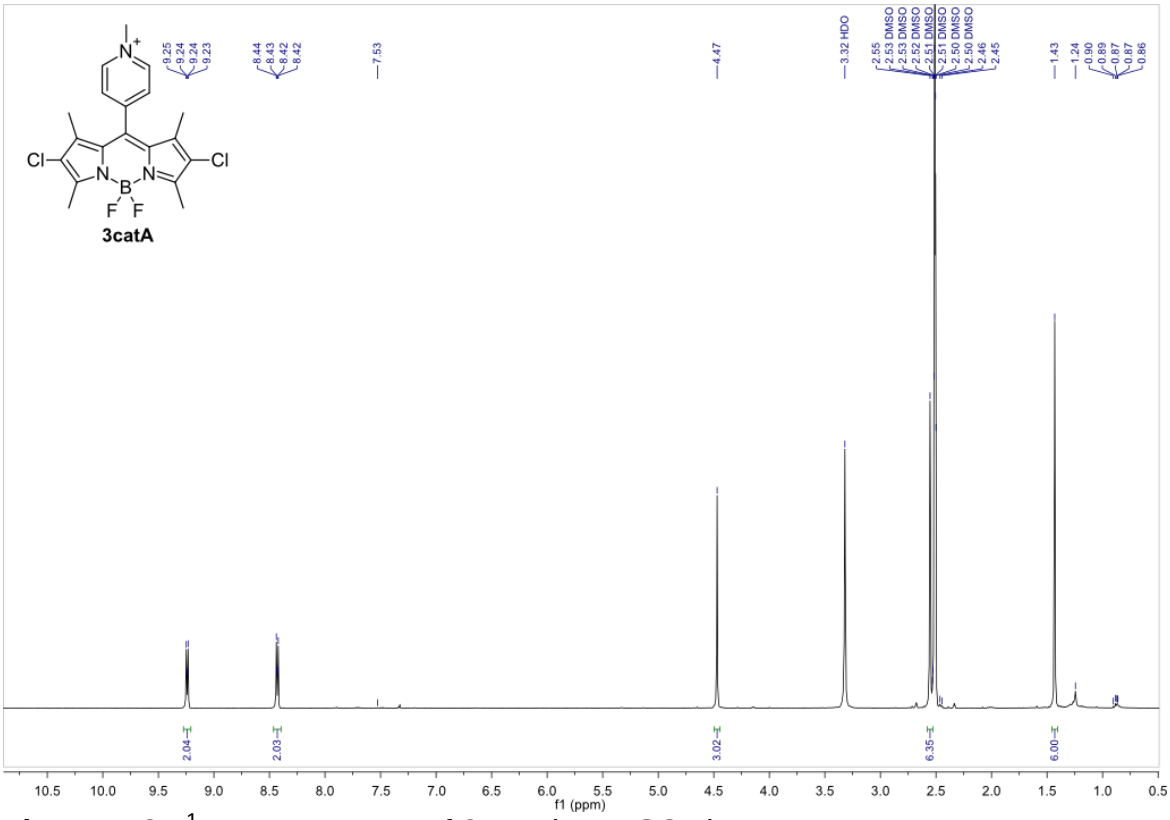

Figure A.3. ^{1}H NMR spectra of 3catA in DMSO-d_6.

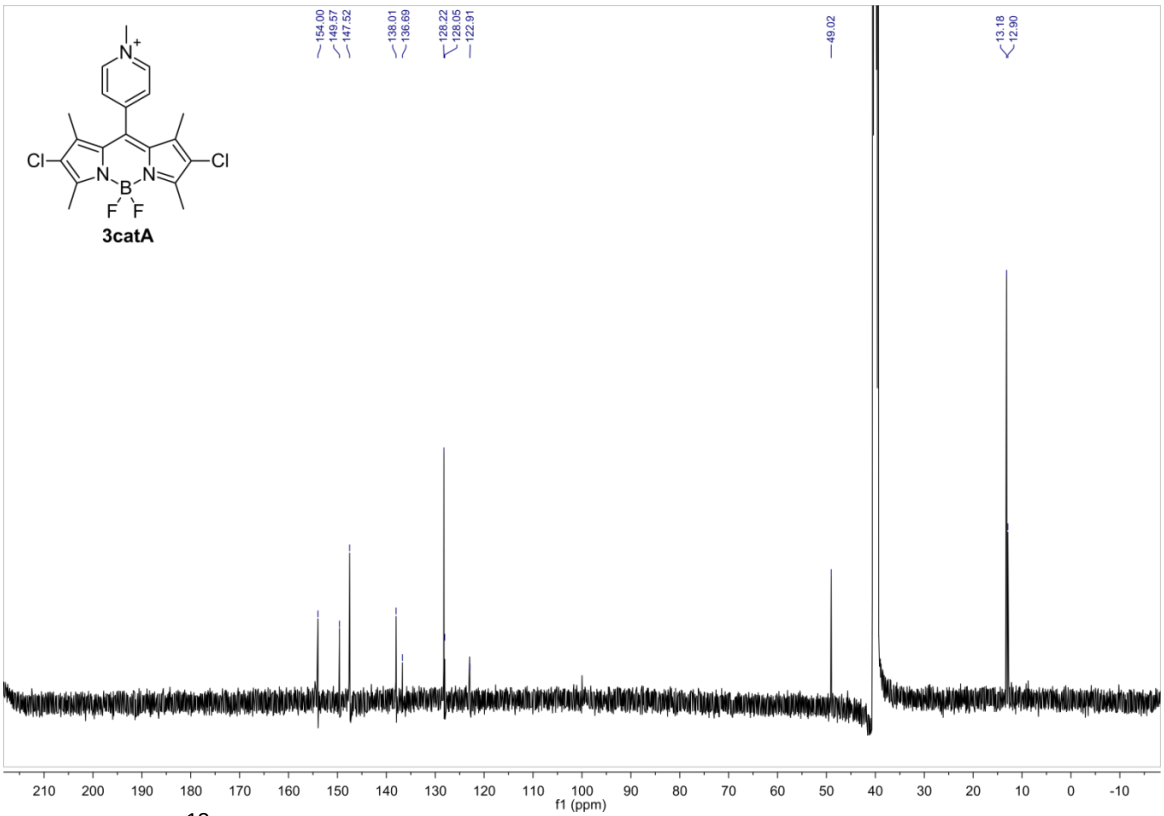

Figure A.1. ^{13}C NMR spectra of 3catA in DMSO-d_6.

Appendix B. Supporting Information for Chapter 3

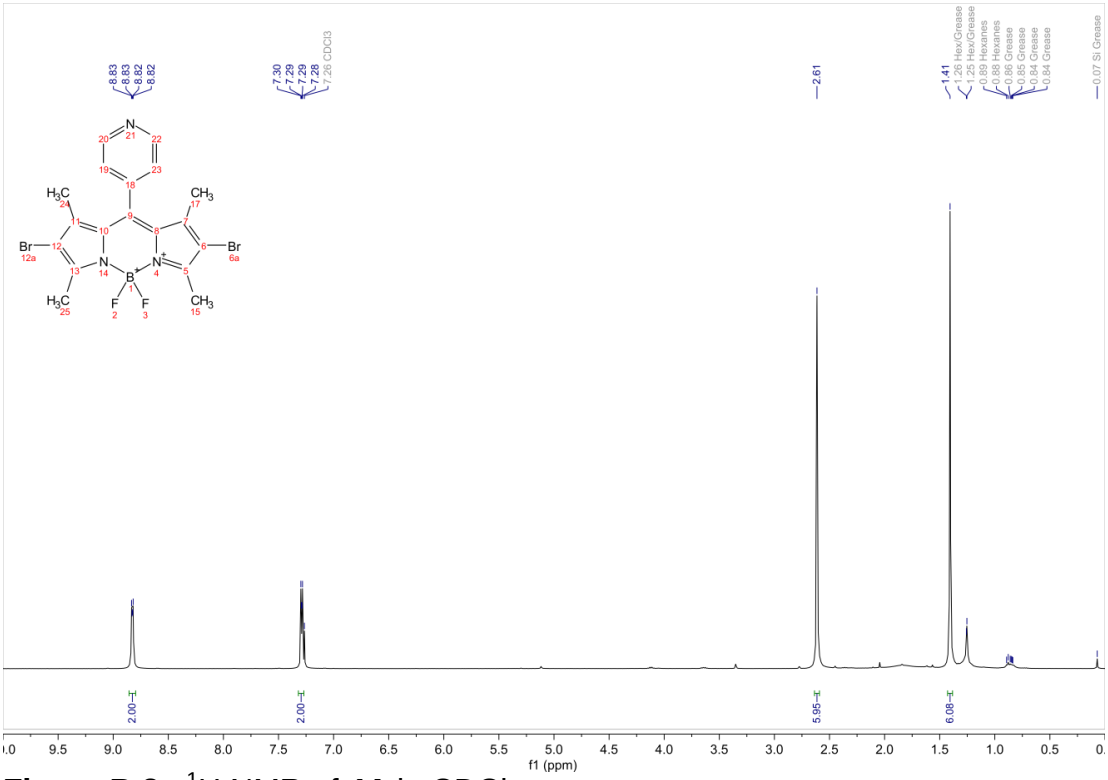

Figure B.2. ^{1}H NMR of **4A** in $CDCl_3$.

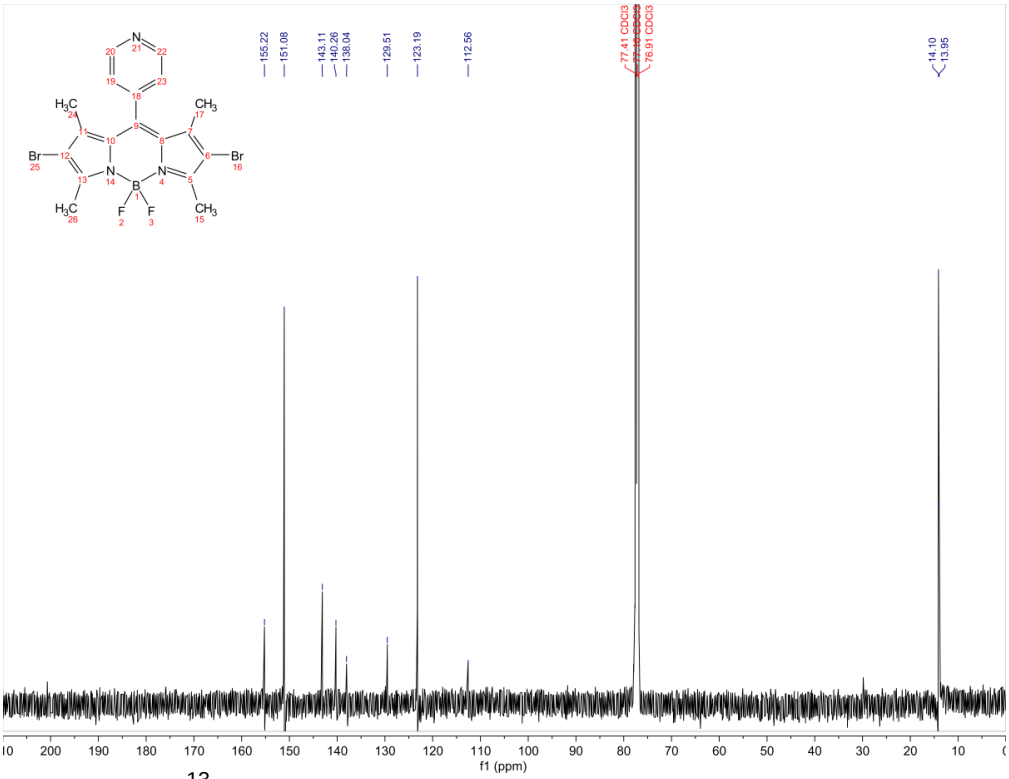

Figure B.3. ^{13}C NMR of **4A** in $CDCl_3$.

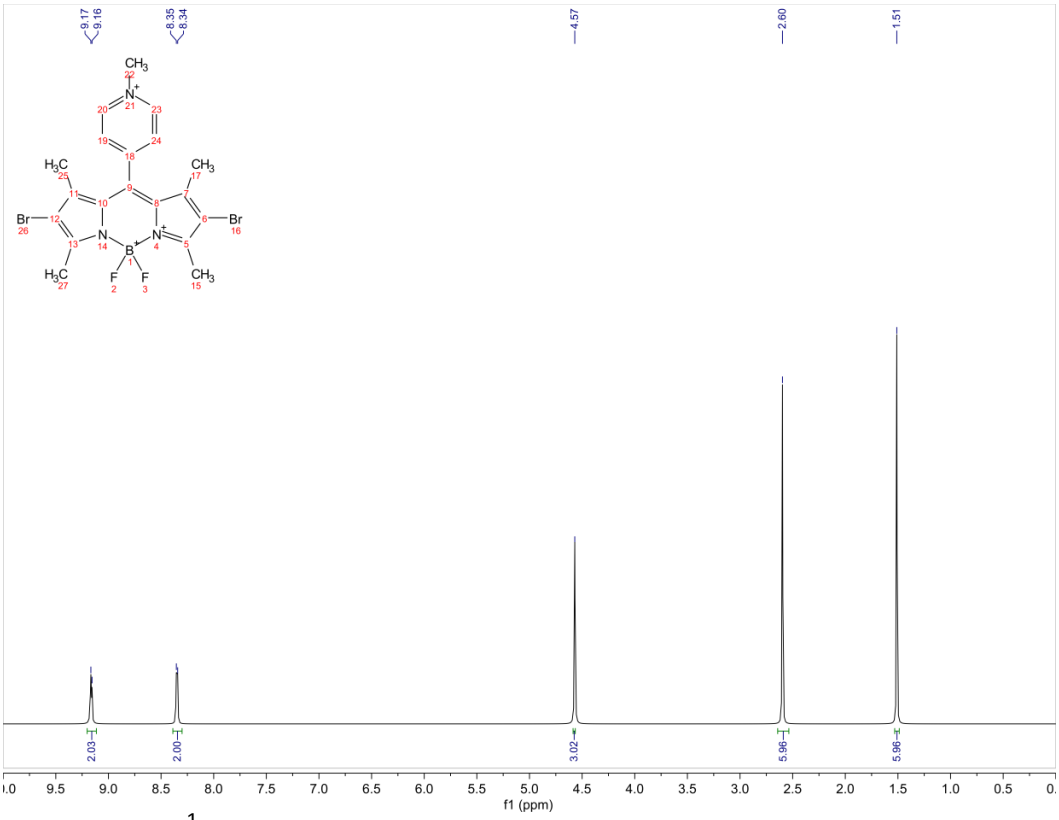

Figure B.4. ^{1}H NMR of **4catA** in MeOD.

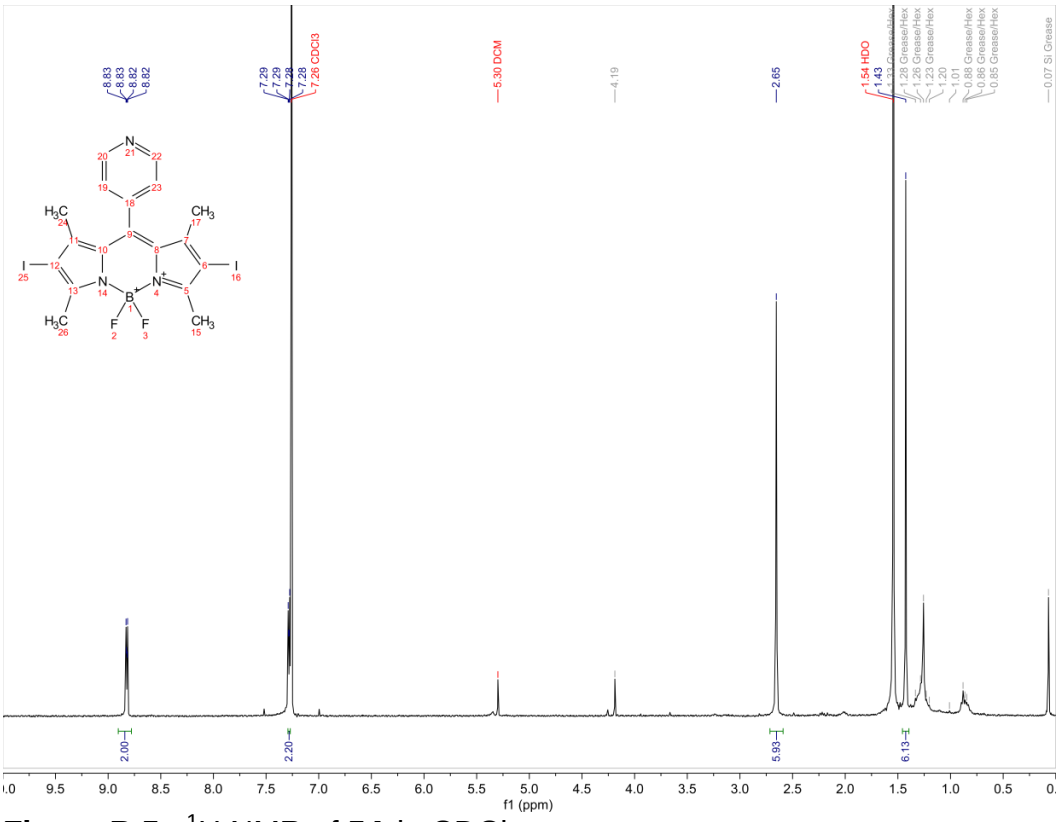

Figure B.5. ^{1}H NMR of **5A** in $CDCl_3$.

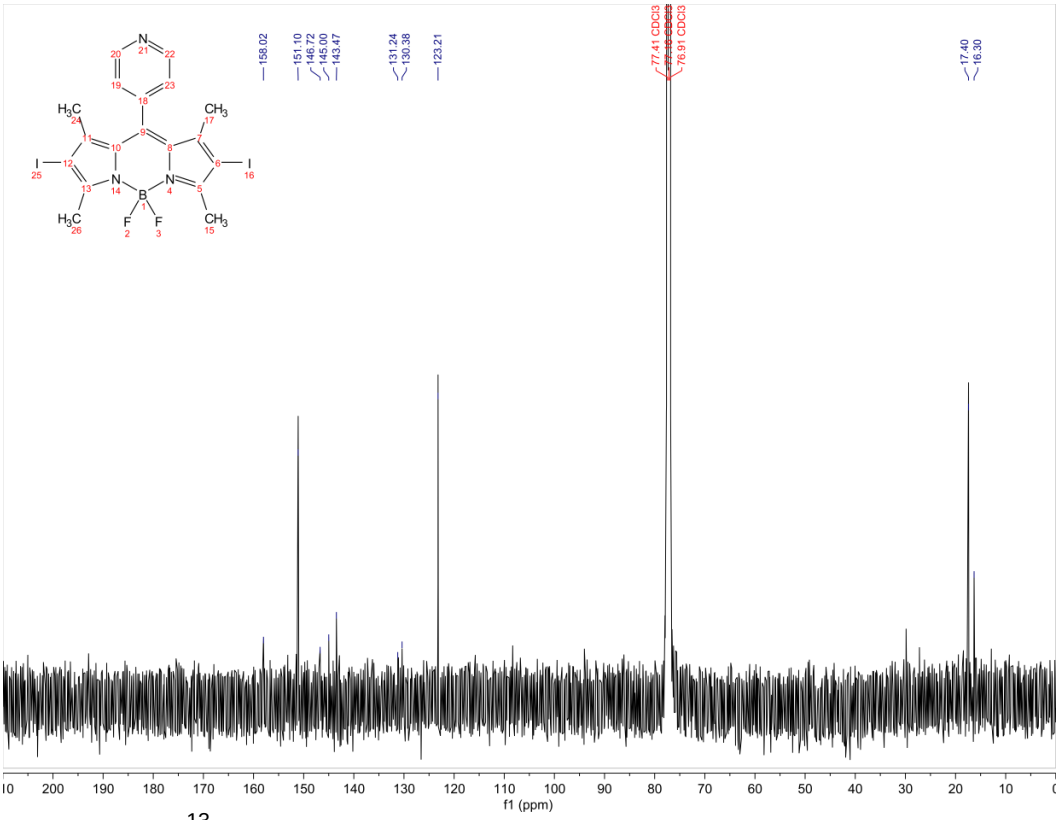

Figure B.6. ^{13}C NMR of **5A** in $CDCl_3$.

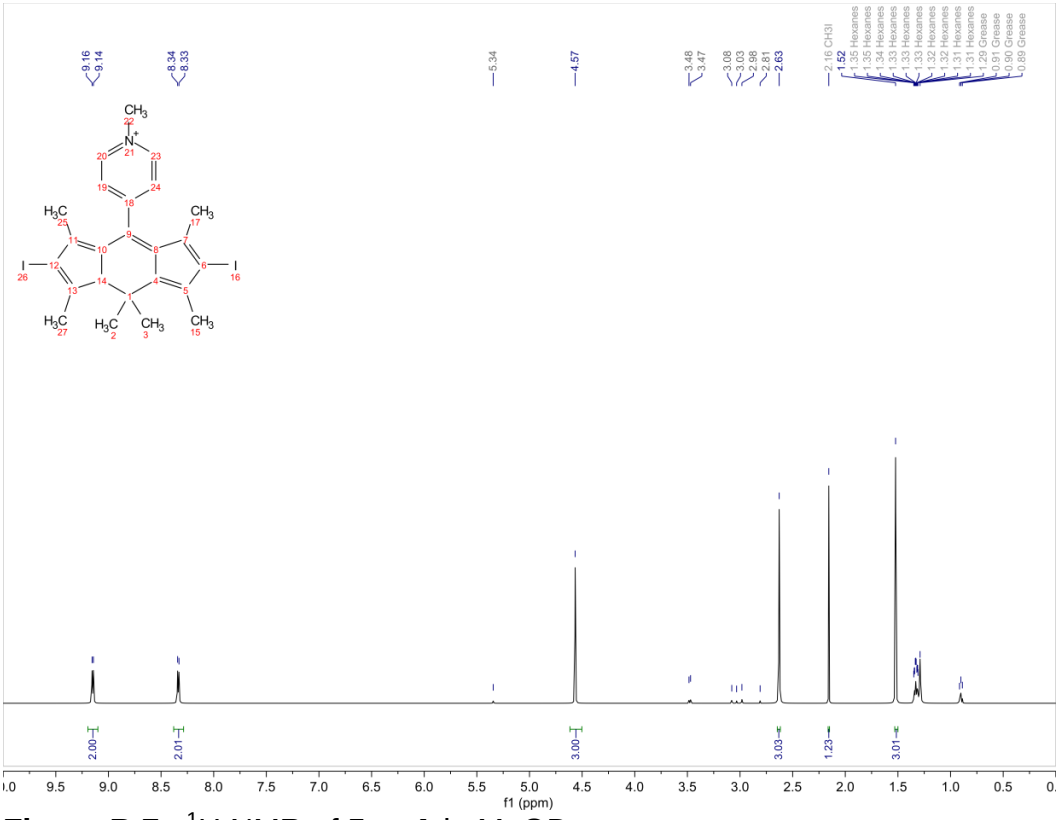

Figure B.7. ^{1}H NMR of **5catA** in MeOD.

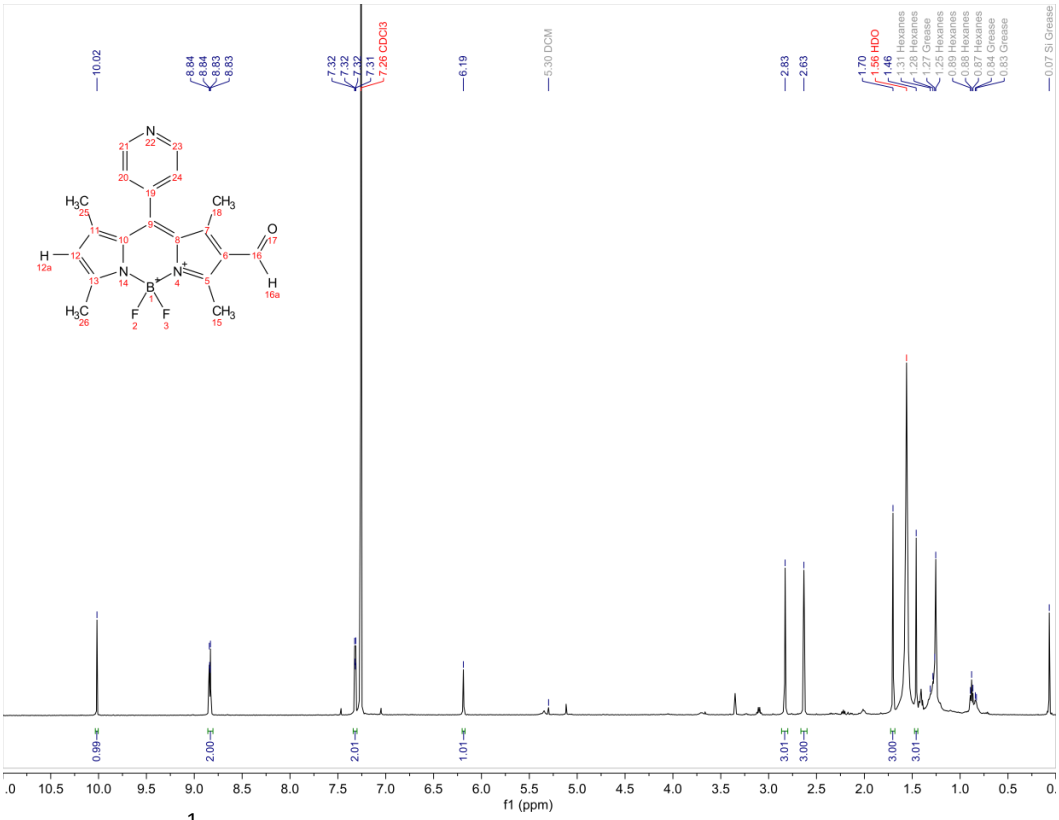

Figure B.8. ^{1}H NMR of **6A** in $CDCl_3$.

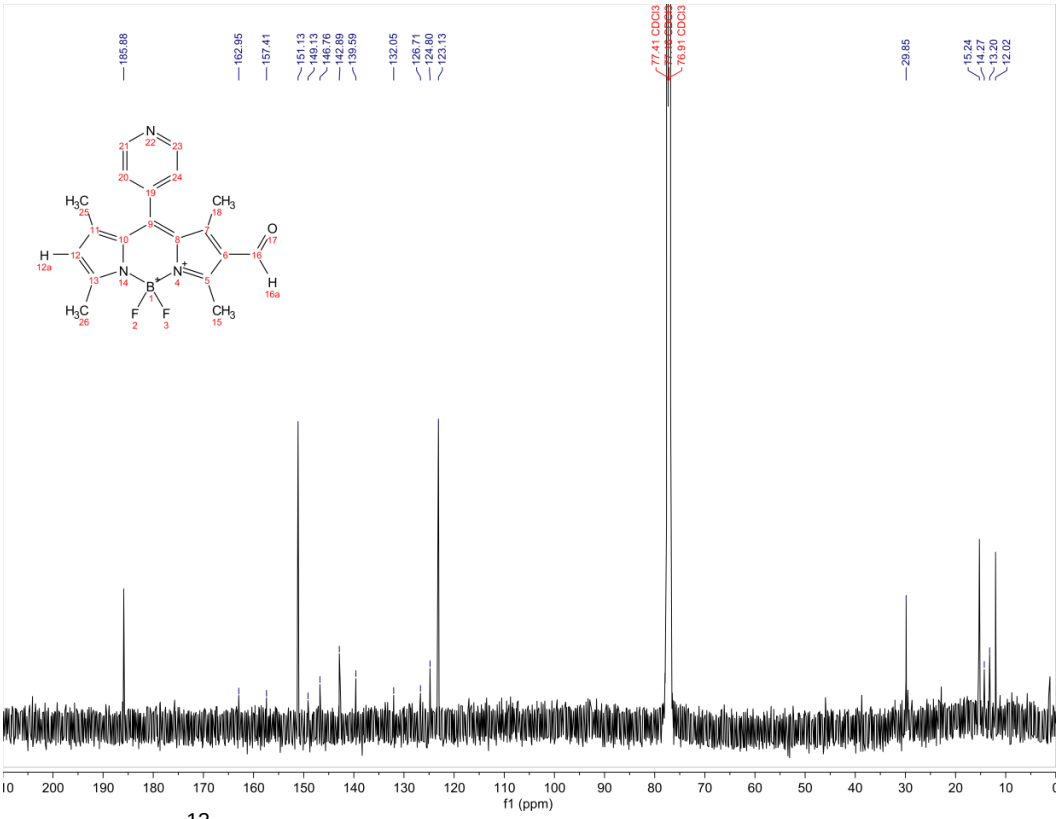

Figure B.9. ^{13}C NMR of **6A** in $CDCl_3$.

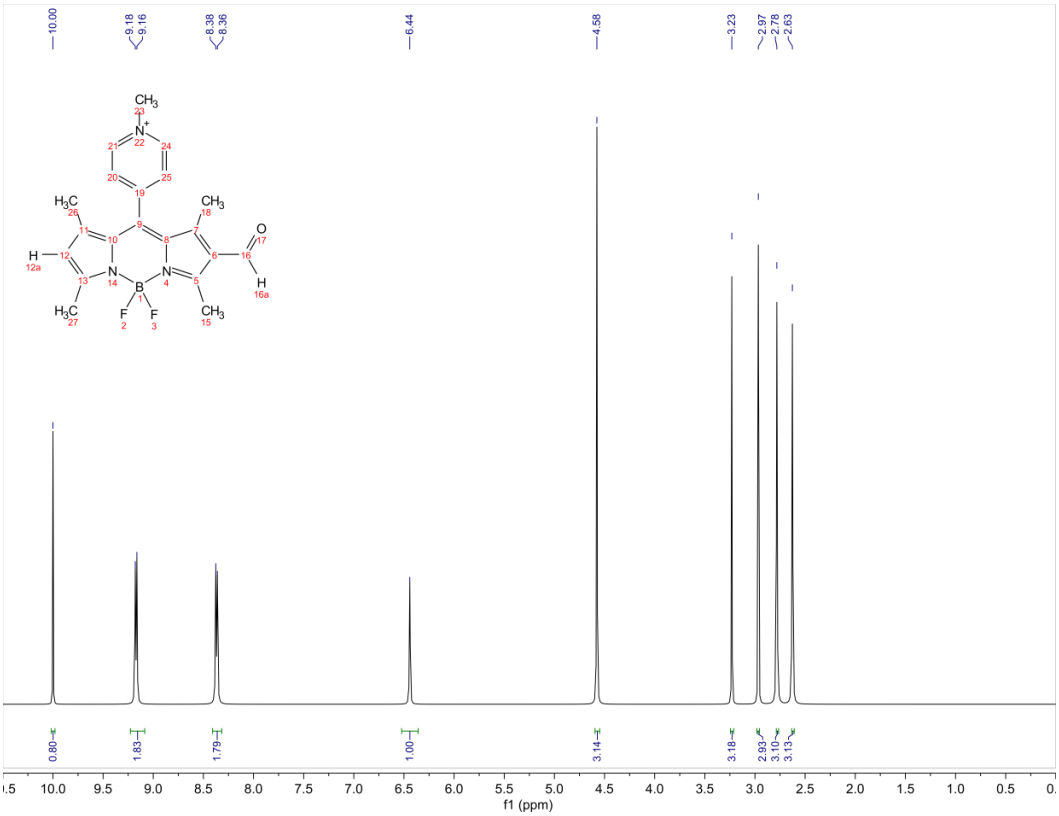

Figure B.10. 1H NMR of **6catA** in MeOD.

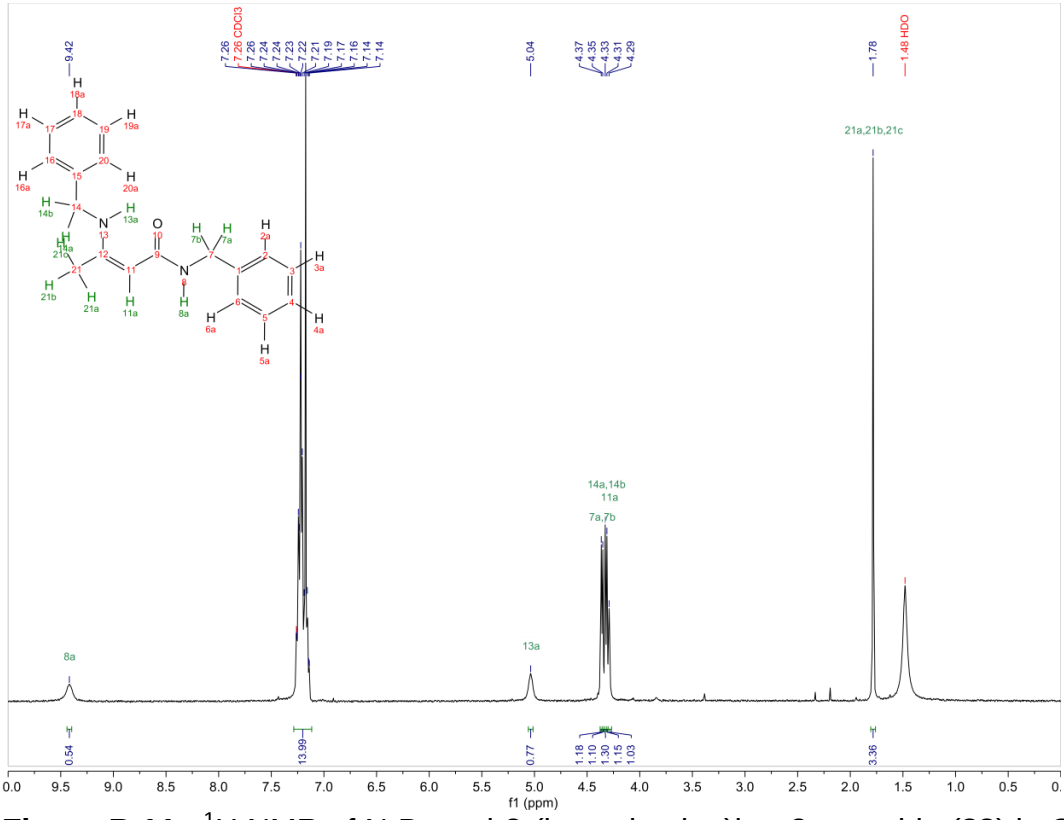

Figure B.11. ^{1}H NMR of N-Benzyl-3-(benzylamino)but-2-enamide (**32**) in $CDCl_3$.

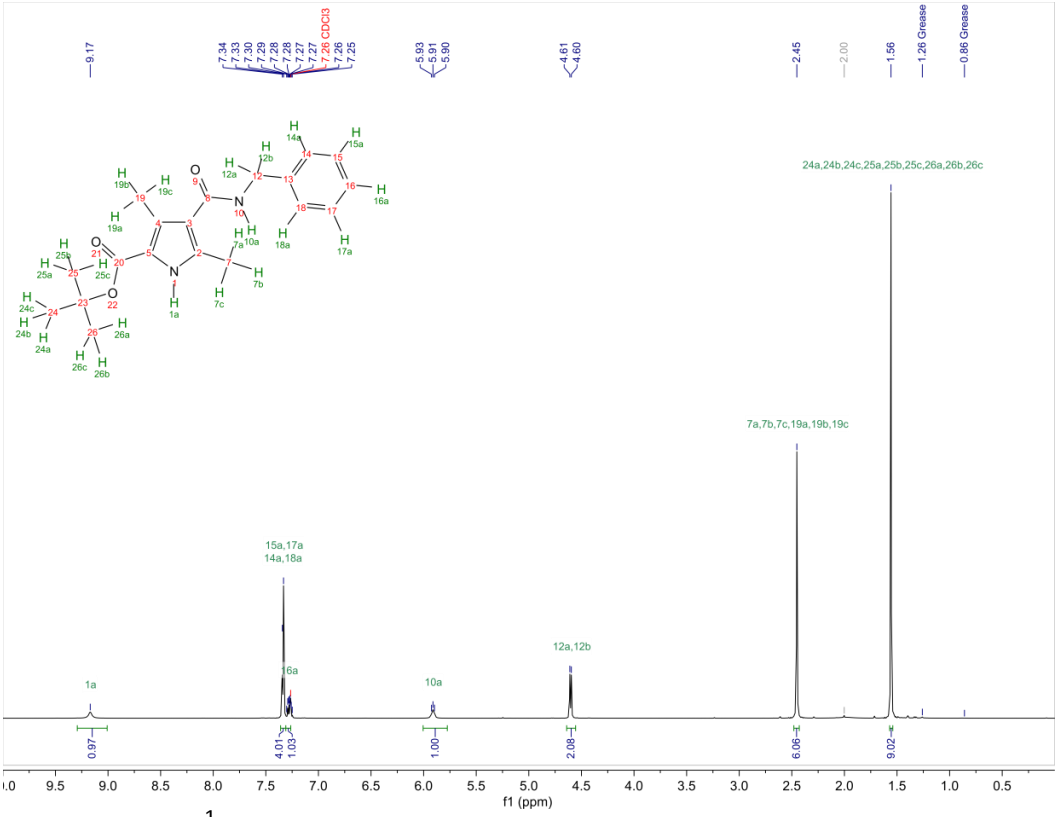

Figure B.12. ^{1}H NMR of 3-benzylamidepyrrole (**34**) in $CDCl_3$.

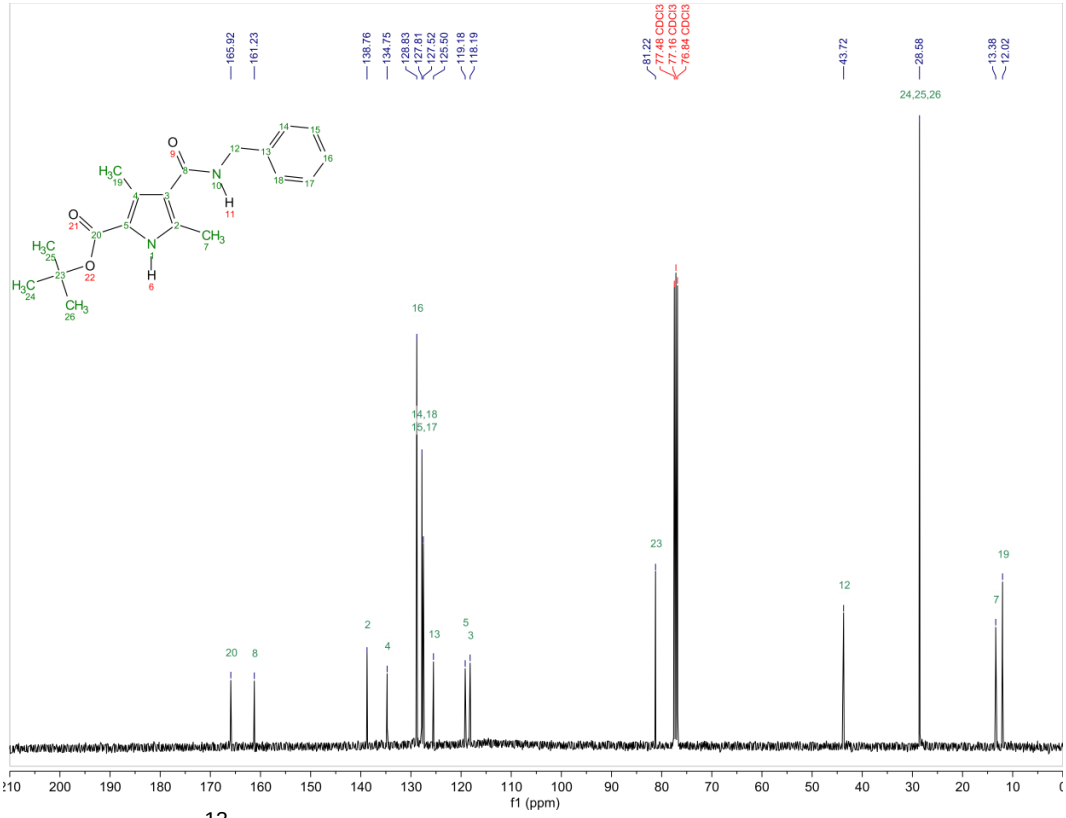

Figure B.13. ^{13}C NMR of 3-benzylamidepyrrole (**34**) in $CDCl_3$.

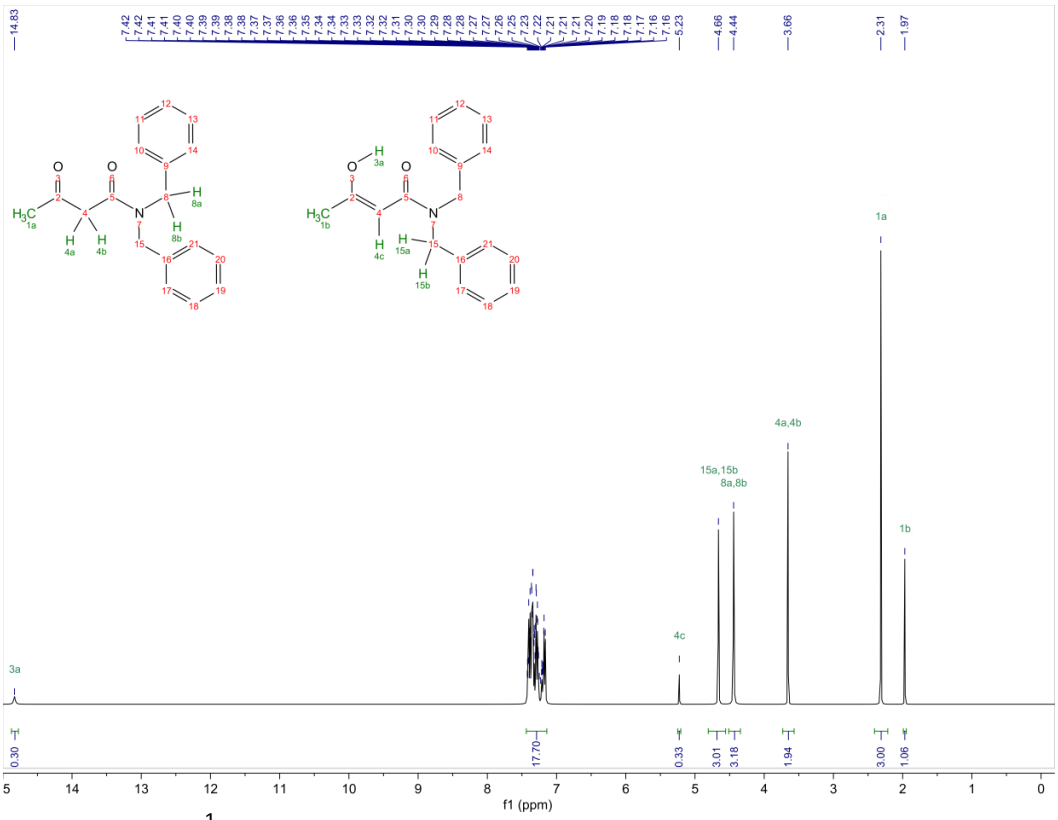

Figure B.14. ^{1}H NMR of N,N-dibenzylacetoacetamide (**35**) in $CDCl_3$.

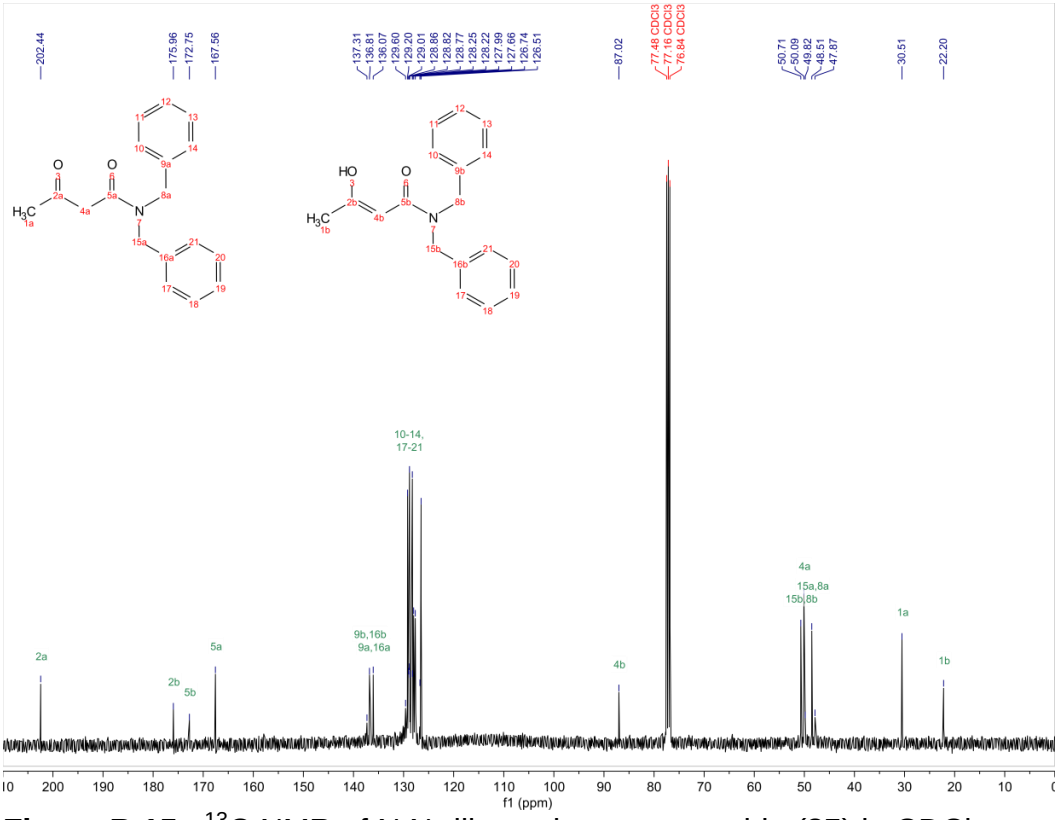

Figure B.15. ^{13}C NMR of N,N-dibenzylacetoacetamide (**35**) in $CDCl_3$.

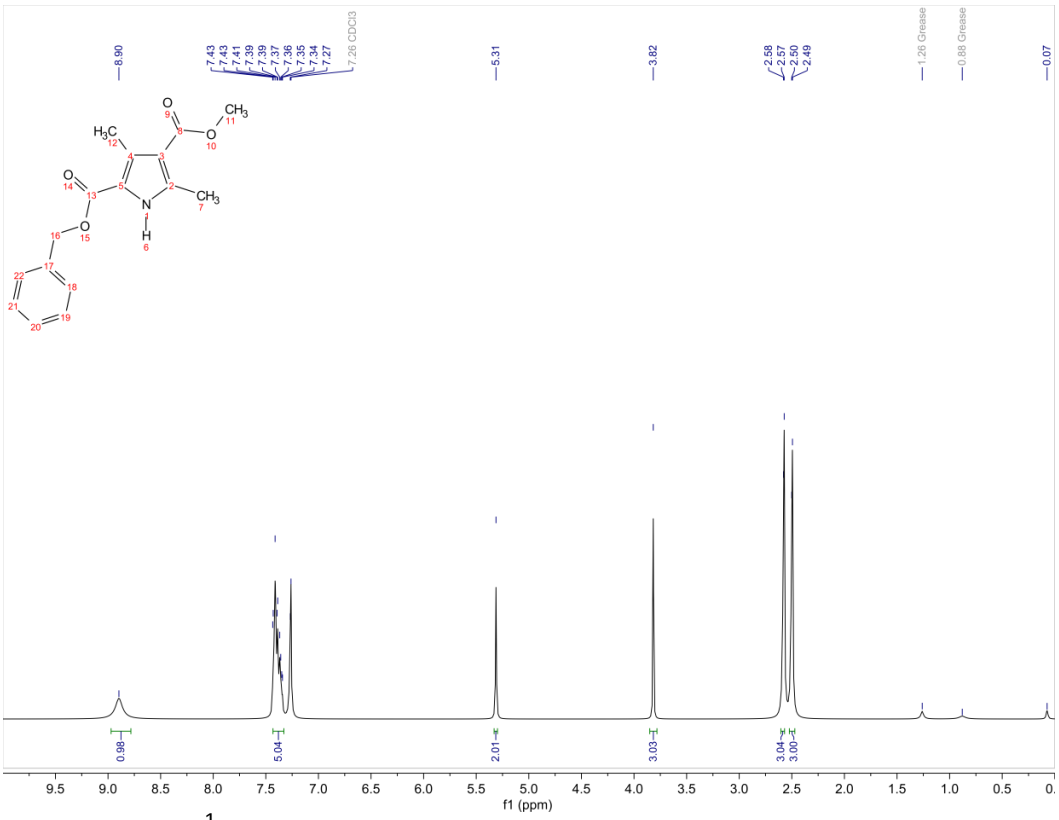

Figure B.16. ^{1}H NMR of orthogonally protected diester pyrrole **38** in $CDCl_3$.

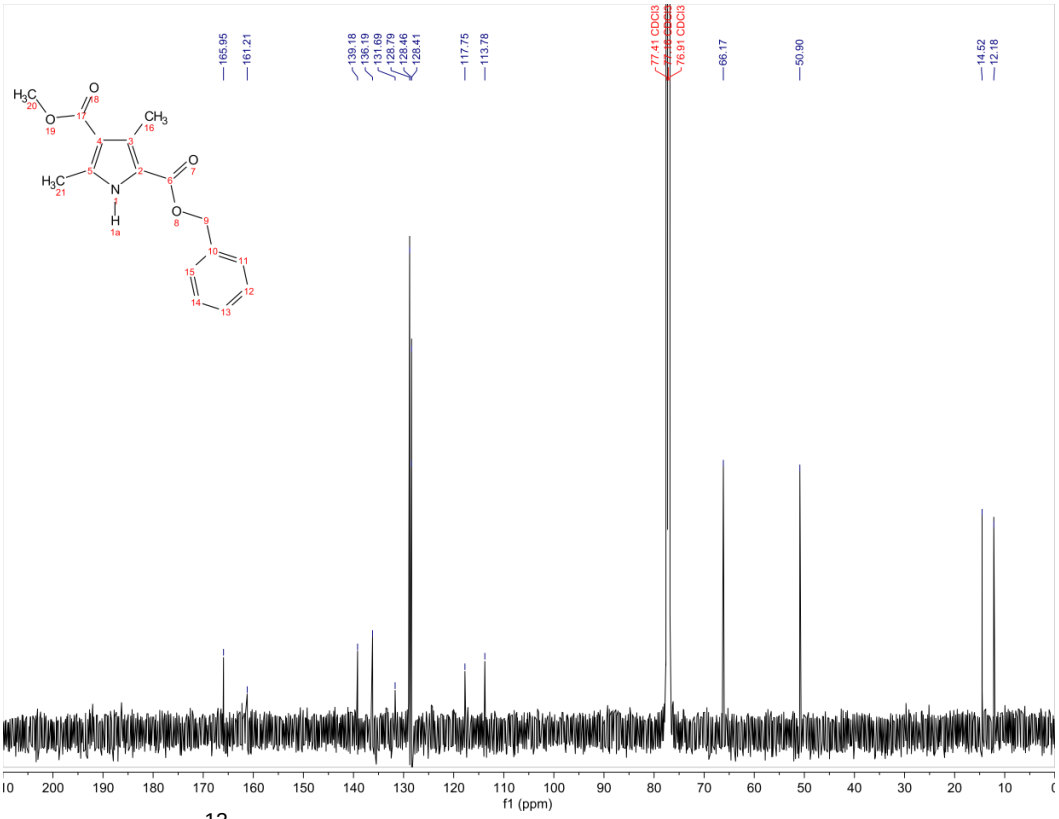

Figure B.17. ^{13}C NMR of orthogonally protected diester pyrrole **38** in $CDCl_3$.

Appendix C. Supporting Information for Chapter 4

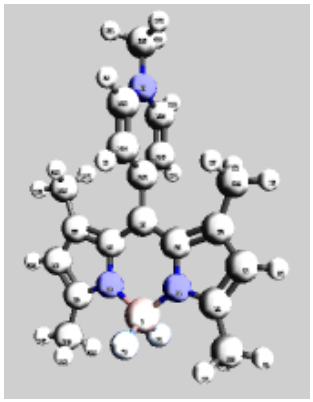

Optimized Cartesian coordinates for modeled BODIPY dyes
BODIPY 4–Py^{+} S_1 CAM-B3LYP/6-31+G**

B	0.0000080300	-2.7654107400	-0.0012167100
F	0.0040838200	-3.5433553100	1.1440795200
F	-0.0040441000	-3.5467067400	-1.1441731900
N	1.2365766700	-1.8216777000	-0.0064081300
C	2.5095854500	-2.2247762700	-0.0079406500
C	3.3679937700	-1.0792028200	-0.0027840600
C	2.5943919100	0.0431981800	0.0035777700
C	1.2052524100	-0.4289344700	0.0004556600
C	-0.0001306300	0.2816139300	0.0014897500
C	-1.2054682300	-0.4290129500	-0.0008842100
C	-2.5946458900	0.0430079400	-0.0056701500
C	-3.3681395600	-1.0794784200	-0.0041047600
C	-2.5096210200	-2.2249955100	0.0003076100
N	-1.2366606000	-1.8217664700	0.0010761200
C	2.9074895400	-3.6481153600	-0.0111958600
H	3.9919061000	-3.7478288600	-0.0236357300
H	2.5018213600	-4.1525267300	0.8719855900
H	2.4799695500	-4.1564545700	-0.8814340400
H	4.4478533000	-1.1240813400	-0.0025728900
C	3.0988282400	1.4448558200	0.0132711100
H	4.1897983600	1.4411780000	0.0224613400
H	2.7605757900	1.9977562700	-0.8652929200
H	2.7454545300	1.9910294500	0.8899742600
C	-0.0001750600	1.7633025200	0.0012451200
C	-0.0197097200	2.5125251100	1.2104973400
H	-0.0355062500	2.0150606100	2.1738092900
C	-0.0188506600	3.8717714100	1.1932221200
H	-0.0333376700	4.4687663500	2.0953693000
N	0.0011704900	4.5790363200	-0.0021574900
C	0.0000306100	6.0317150400	0.0262682300
C	0.0195217700	3.8725609800	-1.1923949000
H	0.0340622000	4.4662656400	-2.0964881900
C	0.0194733200	2.5134893700	-1.2117167900
H	0.0346102700	2.0172546200	-2.1752664400
C	-3.0992406300	1.4446405500	-0.0130380500
H	-2.7414170300	1.9938639500	-0.8860484300
H	-4.1901534900	1.4408030600	-0.0277085900
H	-2.7657312600	1.9945889200	0.8691532700
H	-4.4479921800	-1.1244812500	-0.0066229200
C	-2.9073944800	-3.6483683100	0.0024505200
H	-2.4785326400	-4.1575599900	0.8715148100
H	-3.9917785900	-3.7482154100	0.0164073100

H	-2.5029555300	-4.1518318600	-0.8818533100
H	0.0214710600	6.4135462800	-0.9938483700
H	0.8797219000	6.4088259000	0.5562608900
H	-0.9011296400	6.4087234500	0.5190537300

BODIPY 3–Py^{+} S_1

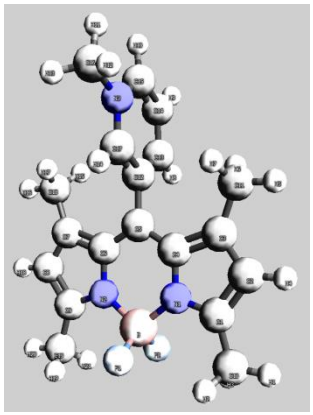

B	0.0000688000	-3.0468874600	-0.0054786700
F	0.0006099600	-3.8230138100	1.1412442900
F	-0.0005384500	-3.8310272300	-1.1466549000
N	1.2347063600	-2.1025204400	-0.0106910200
C	2.5102802500	-2.5081588200	-0.0349732200
C	3.3678113400	-1.3663255500	-0.0357981400
C	2.5939187000	-0.2425410000	-0.0088919300
C	1.2065108500	-0.7127226700	0.0083405600
C	0.0001445000	-0.0037278500	0.0253022400
C	-1.2062489400	-0.7126705300	0.0087953400
C	-2.5936260800	-0.2423933500	-0.0085777900
C	-3.3675940700	-1.3661153800	-0.0360804800
C	-2.5101148500	-2.5080239200	-0.0354275600
N	-1.2345346000	-2.1024740800	-0.0102868900
C	2.9096425300	-3.9312624600	-0.0580412200
H	3.9946617400	-4.0235406200	-0.0751230400
H	2.5103234700	-4.4518187000	0.8187288800
H	2.4840615100	-4.4301399800	-0.9347151200
H	4.4472857500	-1.4125352700	-0.0581187500
C	3.0814240100	1.1608674900	-0.0101018100
H	4.1719955000	1.1784821000	-0.0201938600
H	2.7105015700	1.7057044900	-0.8821174900
H	2.7300143200	1.7022149800	0.8714342500
C	0.0000752900	1.4969042000	0.0004811100
C	0.0004386600	2.1761652200	-1.2370415600
H	0.0008655800	1.6413887200	-2.1755206300
C	0.0000516600	3.5994535000	-1.1971484200
H	0.0003126600	4.1771443800	-2.1136799600
C	-0.0005997600	4.2629036000	-0.0130580000
H	-0.0008609100	5.3426120400	0.0550021800
N	-0.0007199200	3.5795852200	1.1946516400
C	-0.0026088300	4.2836083300	2.4650079900
H	0.0003463900	5.3570275800	2.2801527900
H	0.8856990900	4.0317869600	3.0521841900
H	-0.8950670700	4.0358476500	3.0476562700
C	-0.0005957700	2.1913020800	1.1801448800
H	-0.0010967100	1.7115600300	2.1507382400
C	-3.0809825400	1.1610602600	-0.0093897300
H	-2.7096032500	1.7061977800	-0.8810143900
H	-4.1715463400	1.1788376700	-0.0199428200
H	-2.7298360400	1.7019979200	0.8725136600
H	-4.4470814900	-1.4122151000	-0.0584973300
C	-2.9095552100	-3.9310523200	-0.0618370500
H	-2.4884518300	-4.4611102600	0.7986491400

H	-3.9946705200	-4.0235983900	-0.0546899100
H	-2.5059125300	-4.4199636900	-0.9546183300

BODIPY 2–Py^{+} S_1

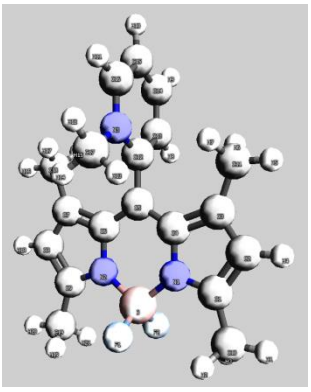

B	-0.0001309000	-3.0590185000	-0.0023945400
F	-0.0005208000	-3.8267526300	1.1491140000
F	0.0001901500	-3.8453640000	-1.1395836900
N	1.2382038400	-2.1138838500	-0.0070570600
C	2.5128474900	-2.5134237400	-0.0170884000
C	3.3692556500	-1.3642453800	-0.0040312000
C	2.5935767700	-0.2440750400	0.0106963700
C	1.2058571700	-0.7222492700	0.0071037800
C	-0.0001039800	-0.0174035300	0.0164310700
C	-1.2060523000	-0.7222109400	0.0056279600
C	-2.5938511600	-0.2440133000	0.0068008200
C	-3.3695143500	-1.3642242000	-0.0098063900
C	-2.5130356600	-2.5134241300	-0.0216169900
N	-1.2384368600	-2.1138724200	-0.0087149100
C	2.9137805600	-3.9350380200	-0.0368982500
H	3.9983594800	-4.0334895100	-0.0409056600
H	2.4996376300	-4.4539967200	0.8340675200
H	2.4952948700	-4.4306551800	-0.9191864000
H	4.4493473200	-1.4070696900	-0.0077869700
C	3.0849989400	1.1623714600	0.0266552500
H	4.1750852000	1.1703984000	0.0664678300
H	2.7657003000	1.7063426600	-0.8645789100
H	2.7039532300	1.7143340600	0.8882354800
C	-0.0001425400	1.4691200700	0.0092457200
C	0.0005068700	2.1878142900	-1.1670746800
H	0.0011847900	1.6330238400	-2.0999781900
C	0.0002082200	3.5777130800	-1.1870916400
H	0.0007459400	4.1272491700	-2.1173235000
C	-0.0010248100	4.2476636200	0.0750513900
H	-0.0015769600	5.3292461900	0.1318546400
C	-0.0015804300	3.5399315100	1.2304074200
H	-0.0025585500	4.0138689600	2.2030379300
N	-0.0007686900	2.1477460500	1.2476184100
C	-0.0023206800	1.4342786600	2.5090613500
H	-0.0010928400	2.1569732100	3.3240065500
H	0.8845035200	0.8019240000	2.6202515300
H	-0.8914699100	0.8050559700	2.6200376200
C	-3.0853789100	1.1624343900	0.0224782200
H	-2.7642288400	1.7068939200	-0.8677995300
H	-4.1755587400	1.1703777800	0.0600481500
H	-2.7061430900	1.7139241100	0.8851821800
H	-4.4496161800	-1.4070317200	-0.0155459400
C	-2.9139664100	-3.9349846200	-0.0455923000
H	-2.4795882900	-4.4636868600	0.8092086300

H	-3.9983775800	-4.0338043500	-0.0271855600
H	-2.5161194600	-4.4202418000	-0.9433481000

4-Py$^+$

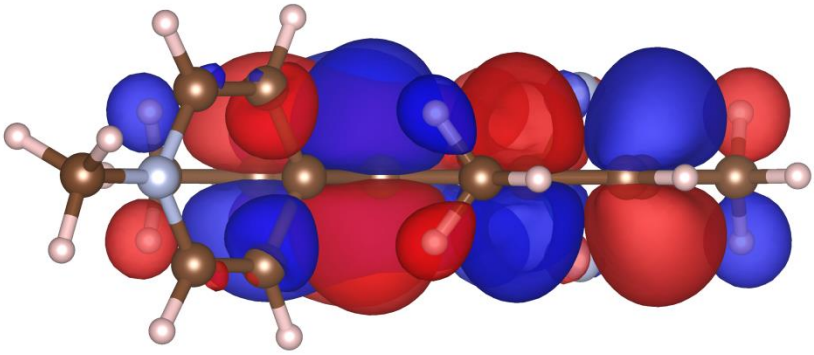

3-Py$^+$

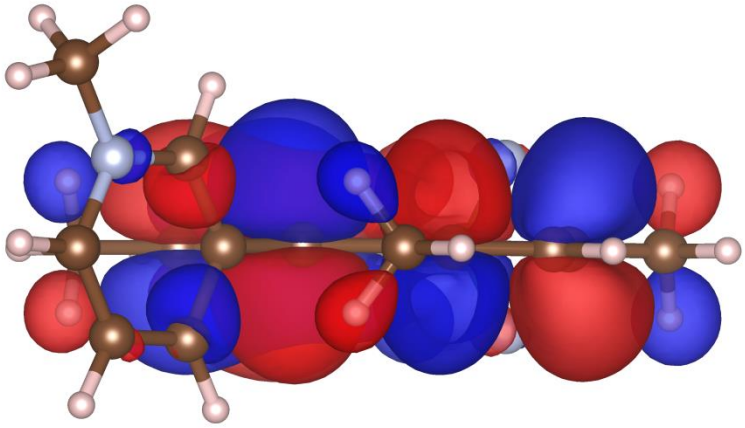

2-Py$^+$

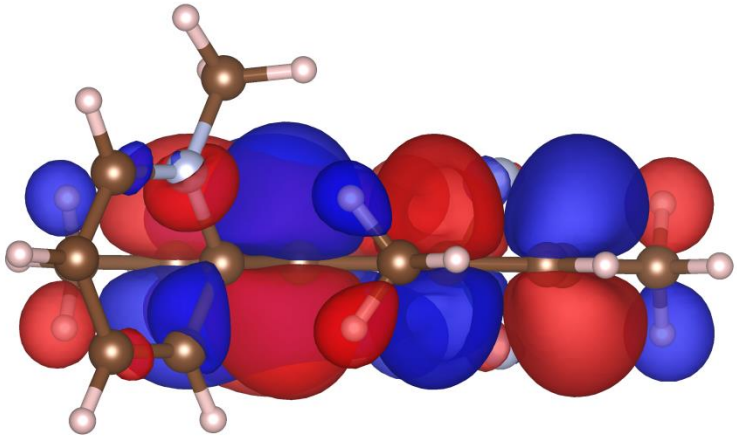

Figure C.1: Enlarged side view of S_1 optimized structures LUMO+1.

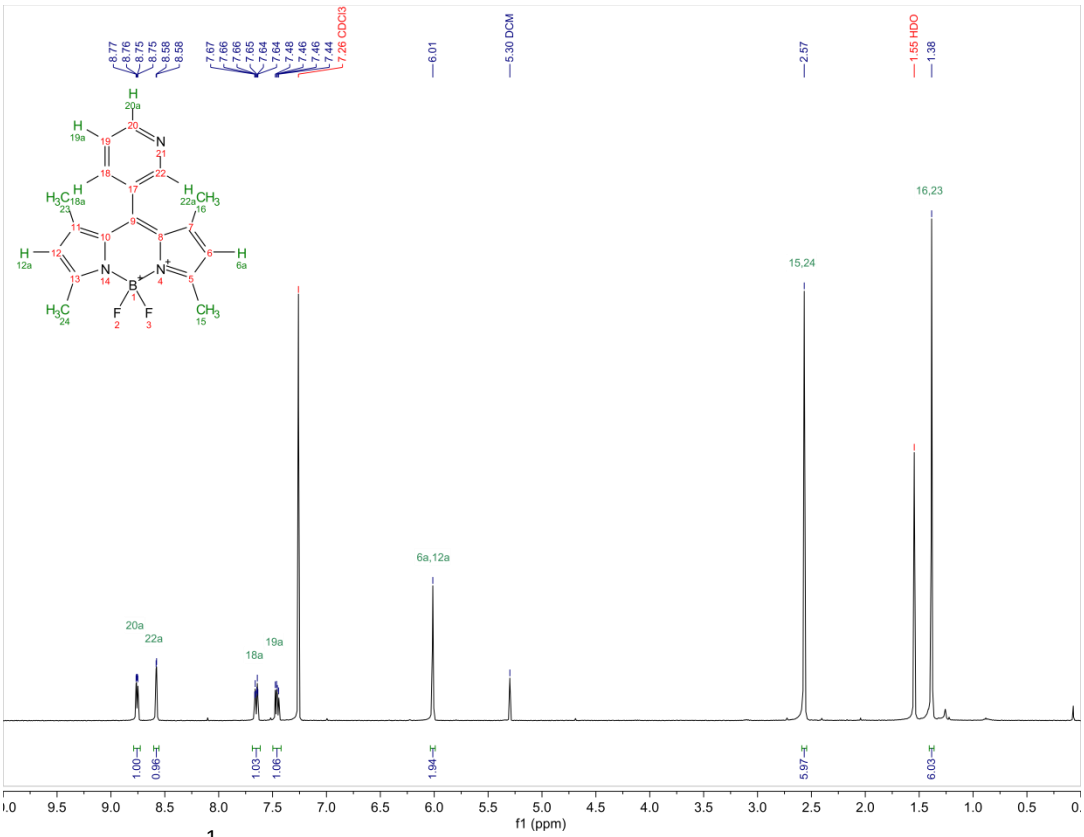

Figure C.18: ^{1}H NMR of **3-Py** in $CDCl_3$.

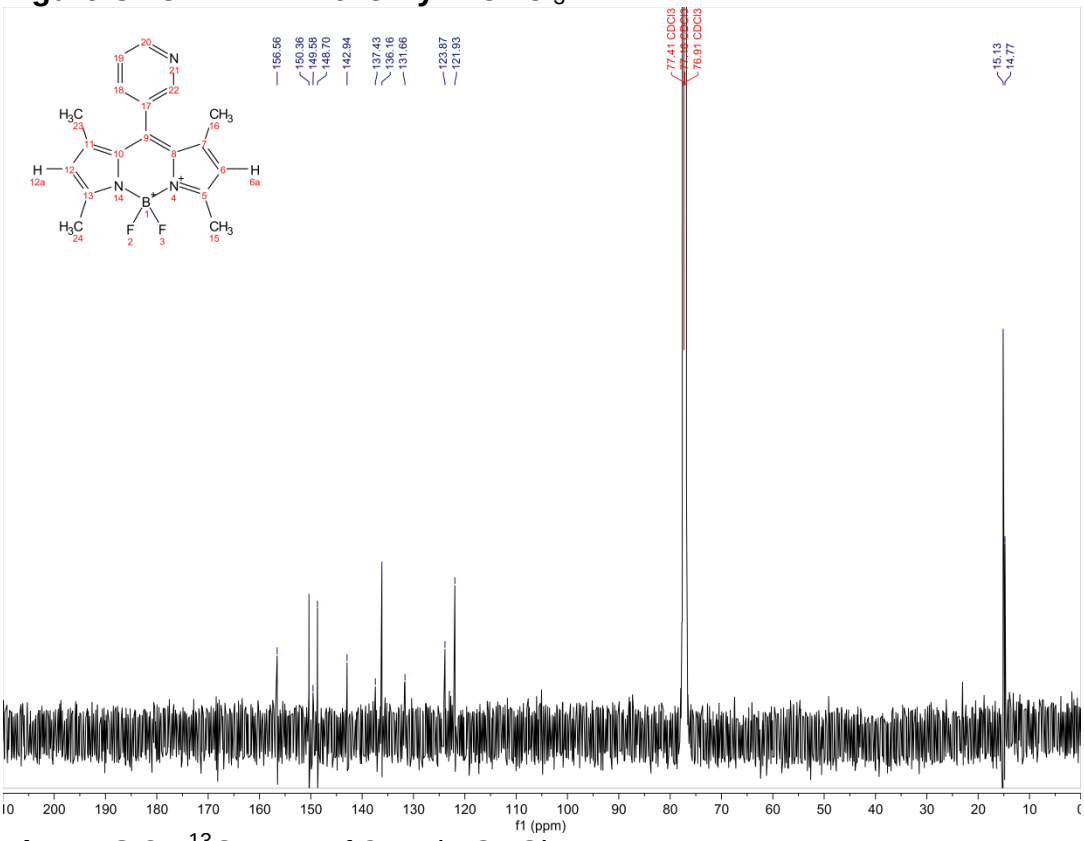

Figure C.3: ^{13}C NMR of **3-Py** in $CDCl_3$.

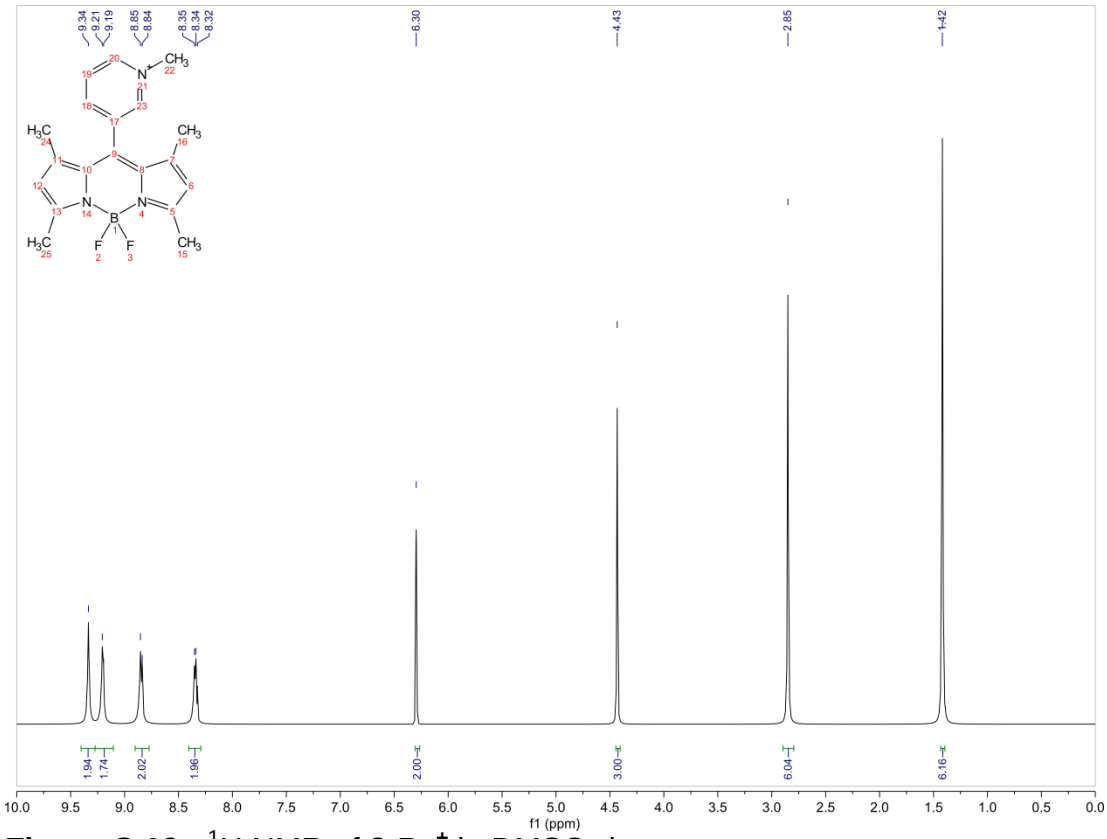

Figure C.19: ^{1}H NMR of **3-Py^{+}** in DMSO-d$_6$.

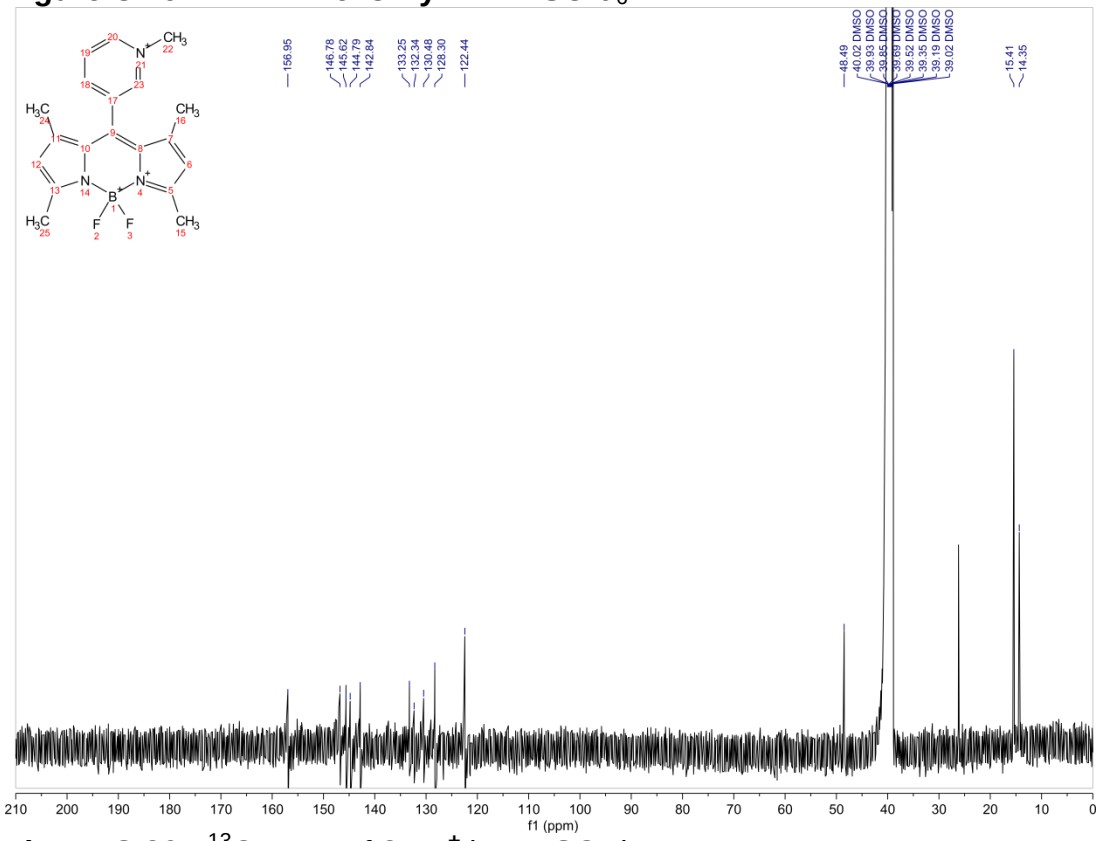

Figure C.20: ^{13}C NMR of **3-Py^{+}** in DMSO-d$_6$.

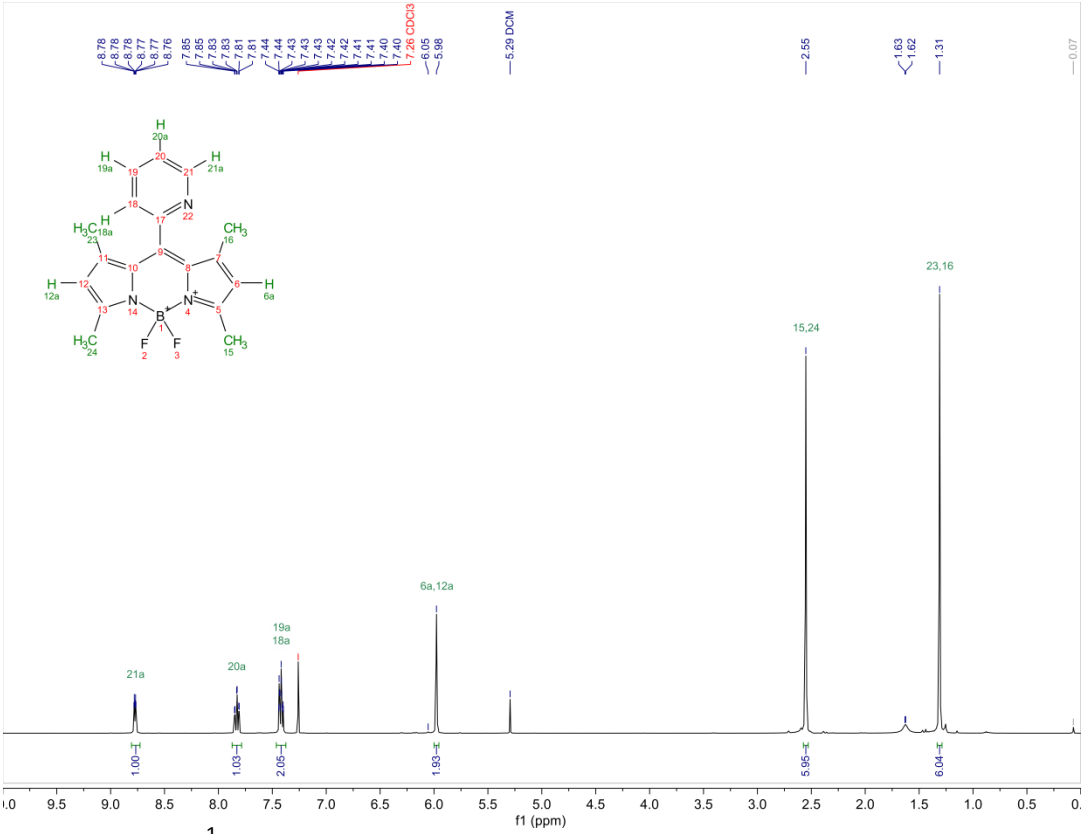

Figure C.21: ^{1}H NMR of **2-Py** in $CDCl_3$.

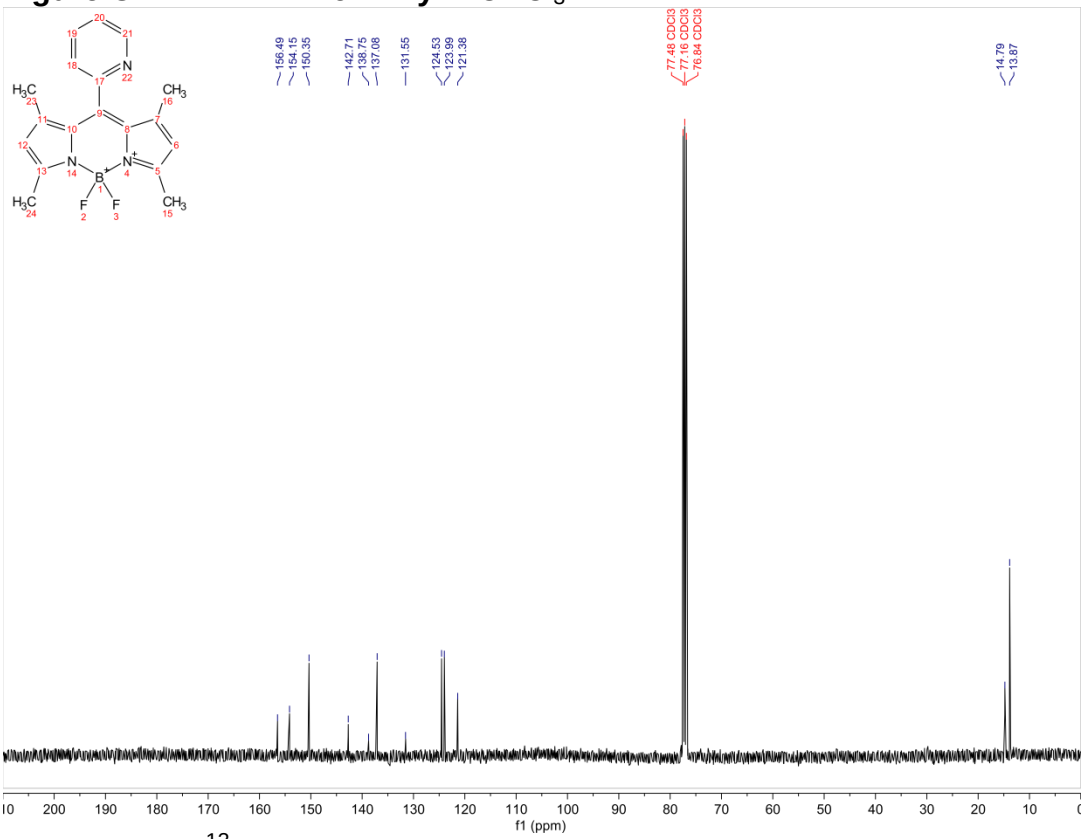

Figure C.22: ^{13}C NMR of **2-Py** in $CDCl_3$.

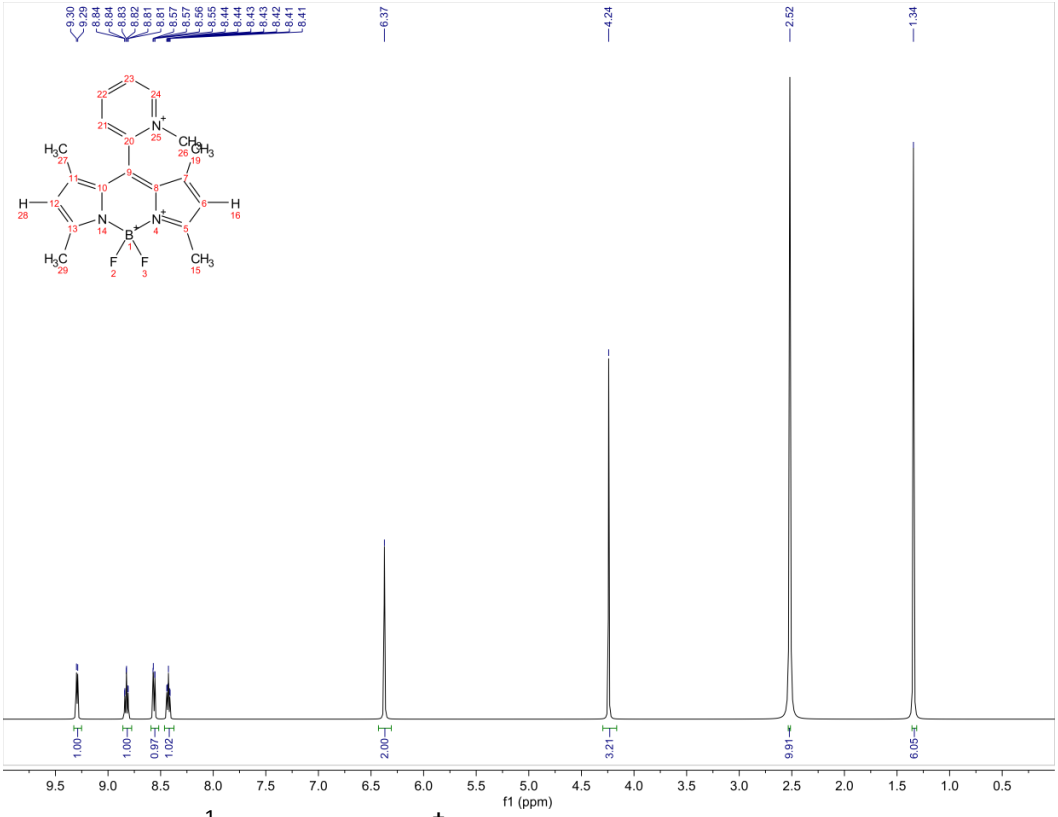

Figure C.23. ^{1}H NMR of **2-Py^{+}** in DMSO-d$_6$.

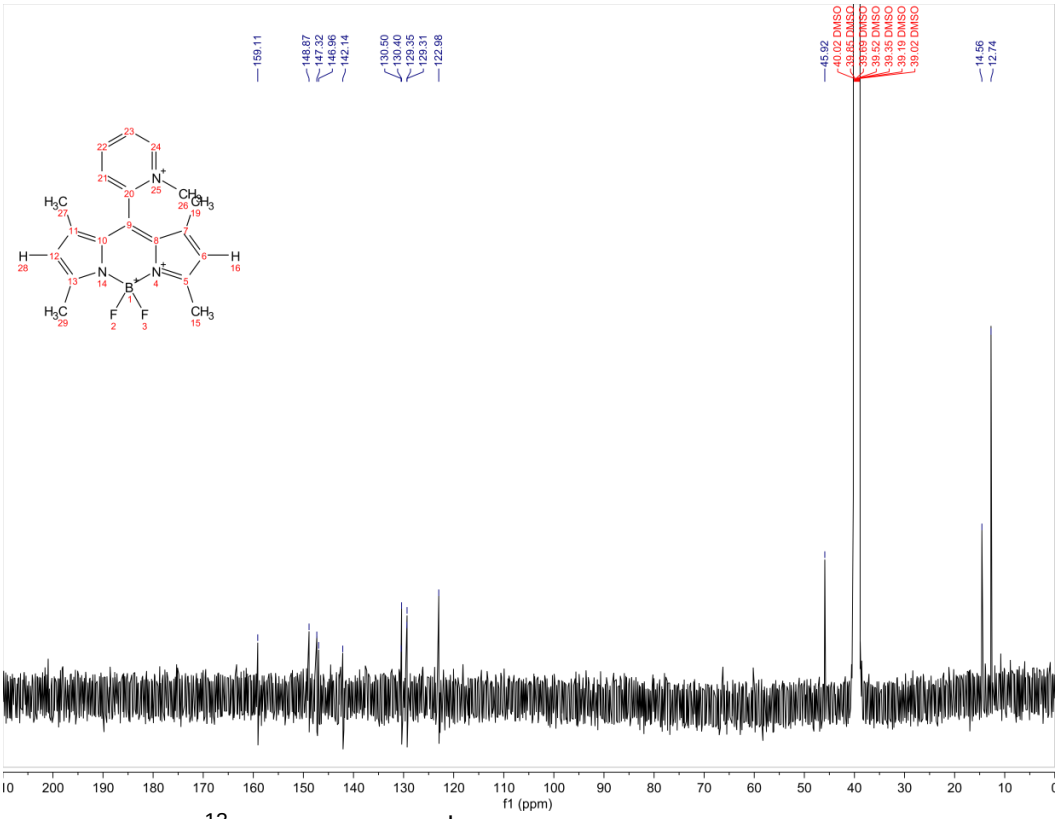

Figure C.24. ^{13}C NMR of **2-Py^{+}** in DMSO-d$_6$.

Appendix D. Copyright Release

Title: Structure Based Modulation of Electron Dynamics in meso-(4-Pyridyl)-BODIPYs: A Computational and Synthetic Approach

Author: Daniel J. LaMaster, Nichole E. M. Kaufman, Adam S. Bruner, et al

Publication: The Journal of Physical Chemistry A

Publisher: American Chemical Society

Date: Aug 1, 2018

LOGIN

If you're a copyright.com user, you can login to RightsLink using your copyright.com credentials.

Already **a RightsLink user** or want to learn more?

PERMISSION/LICENSE IS GRANTED FOR YOUR ORDER AT NO CHARGE

This type of permission/license, instead of the standard Terms & Conditions, is sent to you because no fee is being charged for your order. Please note the following:

- Permission is granted for your request in both print and electronic formats, and translations.
- If figures and/or tables were requested, they may be adapted or used in part.
- Please print this page for your records and send a copy of it to your publisher/graduate school.
- Appropriate credit for the requested material should be given as follows: "Reprinted (adapted) with permission from (COMPLETE REFERENCE CITATION). Copyright (YEAR) American Chemical Society." Insert appropriate information in place of the capitalized words.
- One-time permission is granted only for the use specified in your request. No additional uses are granted (such as derivative works or other editions). For any other uses, please submit a new request.

BACK CLOSE WINDOW

Vita

Hailing from O'Fallon, Illinois, Daniel J. LaMaster received his bachelor's degree at McKendree University in 2013. That fall, he began his doctoral studies in the Department of Chemistry at Louisiana State University. He will receive his doctoral degree in December 2018 and plans to pursue a post-doctoral fellowship and subsequent career in academia after graduation.